

ENERGY BALANCE CLIMATE OF MEIGHEN ICE CAP: VOLUME I

THE ENERGY BALANCE CLIMATE
OF MEIGHEN ICE CAP, N.W.T.

by

BEA TAYLOR

A thesis submitted to the Faculty of Graduate Studies
and Research in partial fulfillment of the requirements
for the degree of Doctor of Philosophy.

Department of Meteorology
McGill University
Montréal, Canada

August 1974

VOLUME I

ABSTRACT

Data obtained during the summers of 1968 to 1970 on Meighen Island N. W. T. were combined with three years of existing observations to investigate the climate and synoptic regime of the area, and to obtain values of the energy balance components for Meighen Ice Cap. Creation of a Synoptic Energy-Balance Diagram permitted analysis of the interaction of meso and synoptic scale influences with the energy balance and hence mass balance of the Ice Cap.

The existence of Meighen Ice Cap, although precarious, stems from the Island's small size and its position on the edge of the Polar Ocean surrounded by expanses of ice covered sea. The Ice Cap is maintained by suppression of melt resulting from advection of cool thin cloud and fog from the Polar Ocean, and by the spring and summer accumulation associated with Cyclonic System Conditions. There is evidence that it originated following the Climatic Optimum during a period dominated by such Cyclonic System Conditions.

RESUME

Des données obtenues durant les étés 1968, 1969 et 1970 sur l'île de Meighen, dans les Territoires du Nord-Ouest, ont été réunies avec des observations déjà existantes effectuées sur une période de trois ans afin de permettre une investigation du régime climatique et synoptique de la région, et une évaluation des composantes du bilan énergétique de la calotte glaciaire Meighen. La création d'un Diagramme du Bilan Energétique Synoptique a permis l'étude des interactions entre les influences d'échelle méso et synoptique et le bilan énergétique ou la variation de la masse de la calotte glaciaire.

L'existence, même précaire, de la calotte glaciaire Meighen résulte de la petitesse de l'île et de sa position à la limite de l'océan Arctique, où elle est encerclée par la surface océanique en grande partie gelée. La calotte glaciaire est protégée de la fonte par l'advection de nuages froids de faible épaisseur de l'océan Arctique, et par des accumulations nivales printanières et estivales associées à des Conditions Cycloniques. Tout porte à croire que la calotte s'est formée après l'Optimum Climatique, pendant une période où ces Conditions Cycloniques dominaient.

PREFACE

Since the existence of Meighen Ice Cap was first suspected in 1916 it has tantalized Arctic researchers. In 1959 the Polar Continental Shelf Project of the Federal Department of Energy, Mines and Resources, under Dr. E. F. Roots, began a glaciological program on Meighen Island. The present study was supported by PCSP as part of this ongoing research. The field program and initial analysis undertaken by the author was conducted along the lines of previous glacial-meteorological studies, but in order to solve the problem of Meighen Ice Cap it was necessary to carry the investigation further. Development of a diagram relating mass balance to the synoptic situation, through climate and energy balance, allowed analysis of the factors governing the delicate balance of conditions responsible for maintaining the ice cap on Meighen Island. It is hoped that this method of approach will be of use in future studies and that the answers it provides have solved the problem of the existence of Meighen Ice Cap.

The study is presented in two volumes. Volume II contains the detailed analysis of the observed climate, energy balance and synoptic regime of Meighen Island and outlines the computer model used to extend the two years of energy budget observations to the six years of climate data. In Volume I the results of these analyses and energy balance calculations are used to develop the Synoptic Energy Balance Diagram and discuss its implications regarding the synoptic-mass balance regime of Meighen Ice Cap.

ACKNOWLEDGEMENTS

In addition to the financial support mentioned previously the Polar Continental Shelf Project extended complete logistic support to the field program on Meighen Island. This program could not have existed without the patient assistance of Dr. W.S.B. Paterson, head of the PCSP Ice Physics section and the help provided by the PCSP support personnel who handled all manner of logistic problems created by the field program and its green author. Special thanks are due Eddie Chapman, the Resolute Bay Base Manager, and Harold Mordy, "our" pilot. I am also indebted to the students who assisted me so ably in the field; to G. Schram, L. Wilson, S. Peck, S. Hurum and D. Goodall who spent a summer on Meighen; to D. Findlay and D. Crossley who weathered two seasons and to D. Petzold who survived three summers in the fog (leading the field party in 1971).

The Meteorological Branch of the Department of Transport generously lent the program Stevenson screens and basic meteorological equipment while their counterparts at the High Arctic Weather Stations provided encouragement and advice on taking and coding meteorological observations.

I would like to acknowledge the help and cooperation given by K. C. Arnold, particularly in the initial stages of the study. He also generously made available three summers of meteorological data collected by his party. Dr. W.S.B. Paterson provided access to the mass balance data and valuable advice and criticism throughout the study. Dr. E. F. Roots, then Coordinator of PCSP, was a constant source of encouragement mixed with constructive criticism. Prof. E. Vowinckel of the Department

of Meteorology of McGill University whose computer program "EBBA" was used in the study, not only provided invaluable assistance during this phase of the work but engaged the author in many constructive discussions on all aspects of the work.

Chul-Un Ro and L. Taylor assisted in various stages of data reduction and plotting. In preparation of the text, I am indebted to my parents who prepared the tables for typing and proofread the manuscript; to P. Herman, M. McAllister and B. Perkins who drafted the bulk of the diagrams; and to Dallas Wells who undertook the mammoth job of preparing the typescript.

Finally I would like to acknowledge the wise counsel, assistance and encouragement provided throughout the study by Professor Sverre Orvig of the Department of Meteorology of McGill University, whose patience during his many years as my adviser was limitless and without whose backing I would not have been involved in field work.

to

OSCAR HOTEL DELTA

LIMA ALPHA PAPP

MIKE ECHO SIERRA

ALPHA LIMA TANGO

TABLE OF CONTENTS

VOLUME I

	Page
Abstract	iii
Résumé	iv
Preface	v
Acknowledgements	vi
Table of Contents	ix
List of Figures Volume I	xv
List of Tables Volume I	xviii
Chapter 1 INTRODUCTION	1
1: 1 Meighen Island	1
1: 1.1 The History	1
1: 1.2 The Mysteries	2
1: 1.3 The Approach	5
1: 2 Energy Balance Climate of Polar Ocean and Island Years	10
1: 2.1 Mean Summer Climate	10
1: 2.2 Wind Roses of Climatic Elements	11
1: 2.3 Summer Means of Energy Balance Components	12
1: 2.4 Wind Roses of Energy Balance Components	12
1: 3 Circulation Types and Energy Balance Climate	14
1: 3.1 Type I Polar Ocean Circulation	15
1: 3.2 Type II Cyclonic System Circulation	15
1: 3.3 Type III Island Circulation	15
1: 3.4 Type IV	16
1: 3.5 Circulation Types and the Mean Pressure Pattern	16
1: 3.6 Relationship of Wind Direction to Circula- tion Type	17
1: 3.7 Type and Energy Balance Climate	18
1: 4 Origin of Meighen Island Fog	
Chapter 2 THE SYNOPTIC ENERGY BALANCE DIAGRAM	25
2: 1 Basis for Further Breakdown	25
2: 2 Creating the Synoptic Energy Balance Diagram	27

	Page
2: 3 Energy Balance Regimes of the Classes	32
2: 3.1 Polar Ocean Climate	32
2: 3.2 Modified Island Climate	34
2: 3.3 Cyclonic Activity Climate	35
2: 3.4 Island Climate	37
Chapter 3 CHARACTERISTICS OF THE SIX SUMMER SEASONS	41
3: 1 Introduction	41
3: 2 1968	41
3: 3 1969	42
3: 4 1961	43
3: 5 1970	44
3: 6 1962	45
3: 7 1960	46
3: 8 Governing Factors	47
3: 9 Intervening Years	48
Chapter 4 THE EXISTENCE OF MEIGHEN ICE CAP	49
4: 1 Mass Balance	49
4: 1.1 Net Mass Balance	49
4: 1.2 Prediction of Mass Balance	51
4: 2 Factors Governing Mass Balance of Meighen Ice Cap	53
4: 2.1 Melt	54
4: 2.2 Suppression of Melt	54
4: 2.3 Spring and Summer Accumulation	56
4: 3 The Existence of Meighen Ice Cap	56
4: 3.1 Origin and Maintenance	56
4: 3.2 The Shape	58
4: 3.3 The Geographical Position	58
4: 3.4 Conclusions	59
Appendix I LEGEND FOR SEB DIAGRAM	60
References	61

VOLUME II

	Page
Table of Contents	iii
List of Figures Volume II	ix
List of Tables Volume II	xiv
Chapter 1 FIELD PROGRAM AND AVAILABLE DATA	1
1: 1 Introduction	1
1: 2 Meighen Island Stations	3
1: 2.1 Main Ice Station (Mi)	3
1: 2.2 Bore Hole Station (Bh)	3
1: 2.3 North Land Station (Nl)	3
1: 2.4 West Land Station (Wl)	3
1: 2.5 North Ocean Station (No)	3
1: 2.6 North Ice Station (Ni)	4
1: 2.7 South Ice	4
1: 3 Meteorological Data	4
1: 3.1 Screen Temperatures	4
1: 3.2 Humidity	5
1: 3.3 Atmospheric Pressure	6
1: 3.4 Wind	6
1: 3.5 Radiation	6
1: 3.6 Precipitation	8
1: 3.7 Cloud	8
1: 3.8 Other Observations	8
1: 4 Measurements in Snow, Ice and Ground During the Summer Season	8
1: 4.1 Surface Temperature and Condition	8
1: 4.2 Temperature at Depth	9
1: 4.3 Properties of Snow and Mud	7
1: 4.4 Surface Lowering	9
1: 4.5 Permanent Meteorological Station Data	9
1: 5 Glaciological Data	10
1: 5.1 Maps	10
1: 5.2 Mass Budget and Flow	10
1: 5.3 Bore Hole	10
Chapter 2 CLIMATIC ELEMENTS	11
2: 1 Surface Air Temperature	11
2: 1.1 Summer and Monthly Means	11
2: 1.2 Daily Temperature Range	14
2: 1.3 Melting Degree Days	15
2: 2 Humidity	15
2: 3 Pressure	16

	Page
2: 4 Wind Speed and Direction	17
2: 5 Cloud and Fog	20
2: 5.1 Mean Patterns	20
2: 5.2 Seasonal Variations	21
2: 5.3 Daily Variations	24
2: 6 Weather and Obstructions to Vision	25
2: 7 Precipitation	25
2: 8 Temperature in the Troposphere	28
Chapter 3 SYNOPTIC CLIMATOLOGY	31
3: 1 Introduction	31
3: 2 Type I	32
3: 2.1 Type I Case a	32
3: 2.2 Type I Case b	33
3: 2.3 General Characteristics of Type I	33
3: 3 Type II	36
3: 3.1 Type II Case a	36
3: 3.2 Type II Case b	36
3: 3.3 General Characteristics of Type II	37
3: 4 Type III	38
3: 4.1 Type III Case a	38
3: 4.2 Type III Case b	39
3: 4.3 Type III Case c	40
3: 4.4 General Characteristics of Type III	40
3: 5 Type IV	42
3: 6 Ten-Day Climate and Synoptic Situation	42
3: 6.1 1960	43
3: 6.2 1961	43
3: 6.3 1962	43
3: 6.4 1968	44
3: 6.5 1969	44
3: 6.6 1970	45
3: 7 Frequency of Circulation Types and Their Relationship to Climate	45
3: 8 Wind Direction and Synoptic Conditions	47
3: 8.1 1960	48
3: 8.2 1961	48
3: 8.3 1962	48
3: 8.4 1968	49
3: 8.5 1969	49
3: 8.6 1970	49
Chapter 4 MEASURED RADIATION COMPONENTS	50
4: 1 Diurnal Variations of the Radiation Components	50
4: 2 Daily Totals of Radiation Components	50

	Page
4: 3 The Influence of Weather on the Radiation Components	51
4: 3.1 Percent Solar and Long Wave Incoming	53
4: 3.2 Radiation Components and Sky Cover	53
4: 3.3 Radiation Components and Sky Conditions over Sun	57
4: 3.4 Solar Incoming Radiation and Sun's Visibility	57
4: 3.5 Radiation Components and Precipitation Type	58
4: 4 Radiation Component Wind Roses	58
4: 5 Surface Albedo	60
 Chapter 5 SENSIBLE AND LATENT HEAT FLUXES	 62
5: 1 Temperature, Humidity and Wind Speed Profiles-Theory	62
5: 2 Measured Profiles	65
5: 2.1 Calculations of R ₁ for 30-90 cm	67
5: 2.2 Profile Slopes	70
5: 2.3 Surface Roughness Z ₀	74
5: 3 Sensible and Latent Heat - Theory	77
5: 4 Sensible and Latent Heat from Measured Profiles	77
5: 4.1 Relationship of Sensible to Latent Heat	79
5: 4.2 Diurnal Variation of Sensible and Latent Heat Flux	79
5: 4.3 Relationship to Temperature and Wind Direction	80
 Chapter 6 CALCULATED ENERGY BALANCE COMPONENTS	 81
6: 1 EBBA	81
6: 2 MIEBA	82
6: 3 Comparison of Measured and Calculated Radiation Components	84
6: 4 Errors in Ablation Measurements	85
6: 5 Modeling Run Off	86
6: 6 Comparison of Measured and Calculated Melt	87
6: 6.1 1970	88
6: 6.2 1969	88
6: 6.3 1968	89
6: 6.4 1962	89
6: 6.5 1961	90
6: 6.6 1960	90
6: 7 Calculated Surface Temperature	90

Appendix I

Page
92

Appendix II

93

Appendix III

94

References

95

LIST OF FIGURES VOLUME I

Figure		Facing Page
1: 1. 1a	Map of Queen Elizabeth Islands	1
1: 1. 1b	Profile of Meighen Ice Cap from North	2
1: 1. 3	Rime Deposited in Three Hours on Mini Screen	7
1: 2. 2	Roses of Climatic Elements for Polar Ocean and Island Years	10, 11
1: 2. 4	Roses of Energy Balance Components for Polar Ocean and Island Years	12, 13, 14
1: 3	Examples of Circulation Types	15
1: 3. 5	Circulation Types and Mean Pressure Pattern	16
1: 3. 6	Wind Roses for Circulation Types	18*
1: 3. 7a	Roses of Climatic Elements for Types	18
1: 3. 7b	Roses of Energy Balance Components for Types	19, 20
1: 4a	Mean Frequencies of Cloud Type	21
1: 4b	Satellite Photograph	22*
1: 4c	N Coast of Ellesmere Island Looking NE with Low Cloud Cover to N and W	23
1: 4d	Approaching Nansen Sound and N Axel Heiberg Island	23
1: 4e	E Sverdrup Channel Looking W: Holes Burned by Meighen Island and Fay Islands	24
2: 2a	Wind Roses for each class of SEB Diagram and Legend for SEB Diagram	28
2: 2b	Synoptic Energy Balance (SEB) Diagram of Melt	29
2: 2c	Frequency Distribution of Melt, Short Wave Incoming Radiation and Long Wave Incoming Radiation for Classes of SEB Diagram	30*
2: 2d	Occurrence of Classes and Percent Occurrence of Classes in Circulation Types	31

* Figure is on the page indicated rather than facing it.

Figure		Facing Page
2: 3a	SEB Diagrams of Climatic Elements	32
2: 3b	SEB Diagrams of Radiation Components	33
2: 3c	SEB Diagrams of Other Energy Balance Components	34
3: 1a	Ten-day Means of Climatic Elements	39*
3: 1b	Ten-day Means of Radiation Components	40
3: 1c	Ten-day Means of Other Components	40*
3: 2	Energy and Mass Balance of 1968	41
3: 3	Energy and Mass Balance of 1969	42
3: 4	Energy and Mass Balance of 1961	43
3: 5	Energy and Mass Balance of 1970	44
3: 6	Energy and Mass Balance of 1962	45
3: 7	Energy and Mass Balance of 1960	46
4: 1. 1a	Net Mass Balance from: 1) Stakes in Vicinity of Mi and 2) Calculated Summer Mass Balance and Measured Winter Accumulation	49
4: 1. 1b	Net Mass Balance of: 1) Stakes in Vicinity of Mi and 2) Whole Ice Cap	51
4: 1. 2a	Prediction of net Mass Balance or Summer Net Mass Balance from Melting Degree Days at IC and M ₁	52*
4: 1. 2b	SEB Diagram Frequencies Used to Estimate Mass Balance	53
4: 2. 1	Summary of Climate, Energy Balance and Mass Balance Characteristics of Six Years of Mi Data	54
4: 3. 2	Comparison of Height Contours and Equal Ablation Contours, with Roses of Melt and Warm Air Advection	58
4: 3. 3	Geographical Position of Meighen Island in Comparison to other Queen Elizabeth Islands and to Islands of the Soviet Arctic	59

Figure		Facing Page
A: 1	Legend for SEB Diagram: Mean Daily Melt	60*

Back Pocket Removable Copies of Figures

4: 2.1	Summary of Climate, Energy and Mass Balance Characteristics of Six Years of Mi Data	
2: 3a,b,c	SEB Diagrams of Climatic and Energy Balance Components	

LIST OF TABLES VOLUME I

Table		Facing Page
1: 1.2	Net Mass Balance of Meighen Ice Cap 1961-1971	5
1: 2.1	Summer Means of Climatic Elements of Polar Ocean and Island Years	10*
1: 2.3	Summer Means of Energy Balance Components of Polar Ocean and Island Years	12*
1: 3.7	Mean Values of Calculated Energy Balance Components for Three Circulation Types	19*
3: 1	Summer Season Means of Climatic and Energy Balance Components	39

* Table is on the page indicated rather than facing it.

CHAPTER 1

INTRODUCTION

1: 1 Meighen Island

1: 1.1 The History

In the spring of 1916 a three man sledge party lead by Vilhjalmur Stefansson made its way along the NW edge of the Canadian Arctic Archipelago in search of uncharted land among what are now know as the Queen Elizabeth Islands. On leaving the north tip of Ellef Ringnes Island the party travelled in a NE'ly direction along an open lead, to the NW of which lay the moving ice of the polar pack. " The first premonitions of land ahead were peculiarities in the sea currents." (Stefansson, 1939). The excitement at the possibility of new land ahead grew as both Noice and Andersen thought they spied land to the NE, from the tops of pressure ridges. When the party was about 20 miles from the intersection of the 80th latitude and the 100th longitude Stefansson writes, "from the top of a hummock I saw indubitable land to the northeast. . . . This land, first seen, was barely visible against the clouded sky. The top of it was snow-covered, with a smooth and oval skyline such as I have never seen on any land. It occured to me that it might be covered with a glacier." (Stefansson, 1944)

On 15 June the party landed on the SW corner of the new land and, mapping as they went, sledged the 20 miles to the N end of the island and then 35 miles S along the E coast to the southern tip of the pear shaped island. The island was subsequently named Meighen Island and the existence of Meighen Ice Cap was confirmed 30 years later when

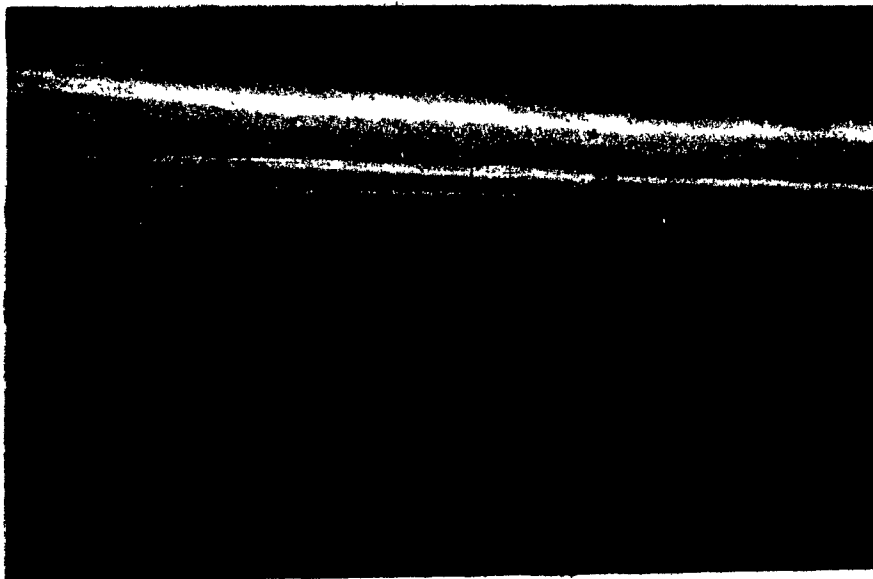


Figure 1: 1.1b Profile of Meighen Ice Cap from North

air photographs were taken of the island (Dunbar and Greenaway, 1956). The ice cap was first visited by Thorsteinsson in 1957 who also comments on the lack of relief of the island. " The land surface is dome-shaped, a feature accentuated by the ice cap. . . . (The Island) exhibits a uniform landscape of rounded hills, subdued rolling plains and intervening valleys." (Thorsteinsson, 1961, p. 13)

The Polar Continental Shelf Project began a research program on Meighen Island Ice Cap in 1959. The investigations included survey and mapping (Arnold 1966); mass balance and flow measurements of the glacier (Arnold 1965, Paterson 1969); gravity measurements of the glacier depth (Hornal unpublished); the drilling of a bore hole through the ice cap (Paterson 1968, Koerner 1969) and the collection of meteorological data (Arnold 1965, Arnold and MacKay 1964, MacKay and Arnold 1965). Further details of these programs are given in Volume II Chapter 1. These studies showed the oval shaped ice cap to occupy 85 km² of the north central portion of the island, to have a maximum thickness of approximately 120 meters and to reach 268 m amsl at its summit which was also the highest point on the island. There are no obvious signs of past or present movement, no crevasses and particularly at the north end of the ice cap the edges are thin and gently sloping. Figures 1: 1.1b* and II 1:2a** illustrate the gentle profile of the ice cap and surrounding island.

1: 1.2 The Mysteries

Though Stefansson is credited with the discovery of Meighen Island, a Chicago newspaper of 1909 carried a story and map describing Cook's alleged journey to the North Pole which showed an island of almost identi-

* References to Volume I have no volume indicators

** References to Volume II are preceded by " II"

cal size, shape and position to Meighen Island as mapped by Stefansson in 1916. Cook, however, denied ever seeing the island. Stefansson discusses the problem at length including accounts of other parties which might have had an opportunity to see the island only to conclude:

" 1) It is impossible to believe that Stefansson was the discoverer of Meighen Island.

2) It is difficult to believe that Cook did not discover it - either on such a journey as Peary describes or on such a journey as he himself describes;

3) But it is difficult to believe, and seemingly impossible to explain, that Cook discovered Meighen Island and then refused to acknowledge the discovery.

It is one of these problems where every answer seems wrong." Stefansson (1939).

The second problem surrounding Meighen Island, to which it is hoped a more satisfactory set of solutions can be found, is to explain the existence of the ice cap. The elevation of Meighen Ice Cap is anomalously low even for a glacier at 80° N. On Axel Heiberg Island, 40 miles to the east, the snowline (i. e., the elevation above which there is net annual accumulation and below which net ablation) ranges from 700 to 1000 m amsl (Ommanney, 1969). Similar snowlines are found on the other heavily glacierized, mountainous islands of the eastern Queen Elizabeth group. In other words, to the east of Meighen the glaciers are fed by accumulation zones well above 1000 m amsl while on Meighen Island the accumulation area of the ice cap does not reach 260 m amsl. The Western Queen Elizabeth Islands, though they resemble Meighen Island topographically, do reach elevations up to 500 m amsl. With the exception of three small ice caps on Melville Island, where elevations over 1000 m amsl are encountered, the islands to the west and south of Meighen Island are devoid of glacier ice.

The western Queen Elizabeth Islands including Meighen Island are shown on the Glacier map of Canada as unglaciated because no evidence

of erosion or deposition by moving ice can be seen in the unconsolidated sands and gravels which dominate the geology of Meighen Island. From studies of the flora of the region, Savile (1961) feels that the area could not have been free from permanent snow or ice cover during the last ice age. On the basis of core studies, Koerner (1968) found no evidence that Meighen Ice Cap was ever more than 15 meters thicker than today and no evidence of past or present ice movement, and he feels that the ice cap has probably developed since the Climatic Optimum (approximately 3000 years ago).

Paterson studying the annual ablation, accumulation and flow from seven years of Meighen Ice Cap data points out that: " precipitation on Meighen Ice Cap, though greater than on Ellef Ringnes Island, is not abnormally high compared with that on other ice caps in the region. . . . Ablation on the Meighen Ice Cap is only about 30% of that at similar elevations on White Glacier*. Low ablation, perhaps resulting from the high frequency of fog during summer, is probably the main reason for the existence of the Meighen Ice Cap."

Meteorological observation performed by K.C. Arnold during the summers of 1960-1962 confirm that " freezing temperatures and obstruction to vision are more common at Meighen Island than at Isachsen during the "summer" months. . . . During early June and late August obstruction to vision at Isachsen and Meighen Island is mainly caused by blowing snow. Fog is frequent at Meighen Island throughout June, July and August. " (MacKay and Arnold, 1965, 196). Regarding the problems of access by air to Meighen Island, MacKay and Arnold conclude: " It is evident from the 1961 and 1962 records, rep-

* on Axel Heiberg Island

Table 1: 1.2

Net Mass Balance of Meighen Ice Cap (cm we).*

1960-61	-26
1961-62	-108
1962-63	-24
1963-64	25
1964-65	6
1965-66	-7
1966-67	0
1967-68	5
1968-69	6
1969-70	-1
1970-71	-50

(after Paterson, various dates)

* cm of water equivalent

representing colder and warmer than average conditions respectively, that the Meighen Island ice cap station has consistently poorer weather than Isachsen. . . . Fog is the chief hazard, but is hard to predict. . . ." (MacKay and Arnold, 1965, p. 198).

Table 1: 1.2 shows the measured net mass balance for the years 1961 to 1971 (Arnold 1965; Paterson, various dates). Both Paterson and Arnold note that, based on the assumption that these mass balance conditions continue, the ice cap would disappear in a few hundred years. There is however, during the period of record, a stretch of seven years during which the ice cap succeeded in maintaining itself.

The unanswered questions emerging from previous investigations can be summarized, for the purpose of the present study, as follows:

How and when did Meighen Ice Cap originate?

How has it been maintained?

Assuming that fog is in some manner connected with the existence of the ice cap:

What causes the persistent fog?

By what mechanisms does it suppress negative mass balance?

Is the influence of fog sufficient to account for the observed mass balance regime on Meighen Ice Cap?

1: 1.3 The Approach

The relationship of glacier mass balance to meteorological phenomena is most effectively studied through surface energy balance determinations. The birth of traditional glacial meteorology occurred in the 1930's with the work of Alhman (various dates) and Sverdrup (various dates) in Spitsbergen, Scandinavia, Iceland and Greenland. Wallen

followed these early investigations with his, now classic, study of glacier-climate interaction on Karsa Glacier. Glacial-meteorology in the Canadian Arctic Archipelago was first performed by Orvig, whose investigations of the Penny and Barnes ice caps on Baffin Island began in 1950 (Orvig 1951, 1954).

Instrumentation was constantly improved, but a similar approach was used by Liljequist on the Norwegian-British-Swedish Antarctic Expedition, (Liljequist, various dates); by Hubley and others in Alaska (Hubley, various dates); by Dalrymple et al at the South Pole (Dalrymple et al, 1966); by Lister on Ward Hunt Island (Lister 1962); and by Muller (various dates), Havens (various dates) Adams (1965) and Keeler (1964) on the glaciers of Axel Heiberg and Devon Islands. The most recent comprehensive micro-meteorological investigation of glacier-climatic-interaction in the Canadian Arctic is Holmgren's six volume study of climate and energy exchange on Devon Ice Cap. (Holmgren, 1971). Though instrumentation and theoretical formulation of processes have developed constantly over the years, the basic method of approach has remained the micro-meteorological measurement and calculation of each of the surface energy budget terms and evaluation from these of the energy and, hence, mass balance of the site being investigated. Reference should be made to the aforementioned authors for detailed discussion of these methods.

A second approach to snow-ice-atmosphere interaction emerged with the advent of computers and with the increase in data from arctic regions following the International Geophysical Year. Computer programmes, modelling the energy balance processes and often requiring only standard meteorological data as input, permitted the study of energy terms



———— Ca. Scm.

Figure 1: 1.3 Rime Deposited in Three Hours on Mini Screen.

over large areas and the examination of the way in which the processes interact to produce observed changes in ice or snow. Of particular interest to the study of Meighen Ice Cap are the Polar Ocean studies of Maykut and Untersteiner (Maykut and Untersteiner, 1969; Untersteiner, various dates) and of Vowinckel and Orvig (various dates).

Meighen Ice Cap presents a combination of problems not experienced in previous glacial meteorology investigations.

The six summers of meteorological and surface lowering measurements indicate that the melt season on Meighen Ice Cap can begin as early as May or as late as August and can end as early as July or as late as September. Even more critical is the fact that the melt season is frequently interrupted by periods of freezing temperatures and/or snow accumulation. In addition mass turnover in the average summer is very small and difficult to measure. Unlike other high arctic accumulation areas, which experience this type of broken ablation season, on Meighen Ice Cap in some seasons the snow is lost over the complete glacier, significantly altering the surface albedo and the drainage characteristics of the "accumulation" area.

Frequent strong winds accompanied by snow, blowing snow, freezing precipitation and rime deposits play havoc with delicate micro-meteorological instruments. Figure 1: 1.3 shows a three-hour deposit of rime. These conditions and the isolation of the station due to distance from the Polar Shelf Base Camp and the poor weather conditions on Meighen Island necessitate use of basic, tough instrumentation and as little dependence as possible on machinery such as generators.

The seeming uniqueness of Meighen Ice Cap climate requires expansion of the investigations from a site study to meso- or synoptic

scale study. This requires the establishment of other stations on the island and close examination of the synoptic situation in an effort to determine the origin of the Meighen Island weather. The seasonal variability of high arctic climate demands the use of many seasons' data, if results are to be representative.

In order, therefore, to isolate the processes responsible for the creation and maintenance of this fragile patch of ice, and to determine the forces behind these processes, a combination of the traditional and computer model approaches is needed. The emphasis in the case of Meighen Ice Cap must be on the interaction of the meso- and synoptic scale processes which control the health of the ice cap via surface energy balance. Whereas previous studies were concerned with the mechanisms and amount of glacier melt, the Meighen Ice Cap study must be centred on the reasons for the lack of net summer ablation.

The steps involved in implementing the present study are discussed in the following paragraphs. Discussion of the results of the initial phases of the work are presented in Volume II.

The field program initiated in 1968 by the author, with the support of Polar Continental Shelf Project, is outlined in II 1 and had as its objective to obtain estimates of the energy balance components, using basic instrumentation, in order to augment the existing 1960 to 1962 observations.

The climate of the six years of Meighen Island data from up to 5 stations and of Isachsen and Eureka for the years 1961 through 1970 was analysed in detail (II 2).

Synoptic conditions were studied for the six years of Meighen Island record, using weather charts, satellite photographs, upper air data and results of the climate analysis (II 3).

The measured energy budget components from the 1969 and 1970 field season were scrutinized to discover the relative importance of the various terms and the variation of the terms with climate and synoptic conditions (II 4 and 5). These measured values were also used in adapting EBBA - the energy balance program of Vowinckel and Orvig (1972) to the Meighen Island problem. MIEBA, the model, was developed to allow calculation of the energy balance from the years where only climate records existed (II 6). Daily totals of the energy balance components, along with mass balance and climate terms, were then available for 6 years for the months of June, July and August. Equation 1: 1.3 shows the form of the energy balance equation used in MIEBA.

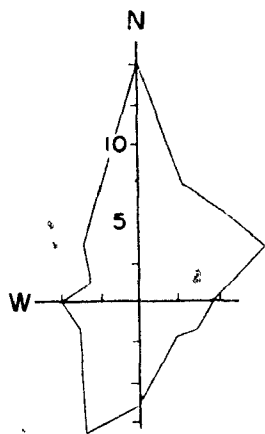
$$SGI (1 - ALB) + DFL - RLU + QL + QS + QI = QM \quad 1: 1.3$$

where SGI is solar incoming radiation, ALB is surface albedo, DFL is long wave incoming radiation, RLU is longwave outgoing radiation, QL is latent heat flux, QS is sensible heat flux, QI is heat from the ice and QM is the heat available for melting. QM was converted to runoff, which was treated as discussed in II 6. Comparison of the measured and calculated values of the energy and mass balance components are found in II 6.

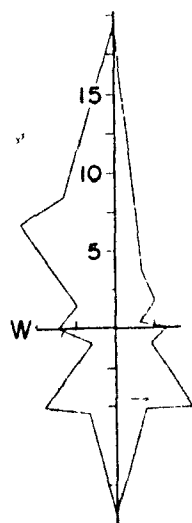
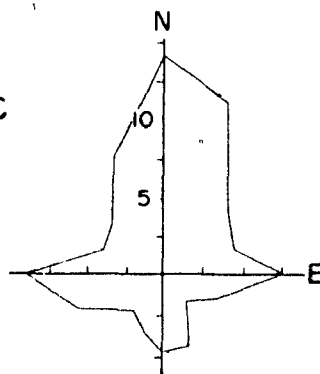
The calculated daily totals of the energy and mass balance components were manipulated in various ways as discussed in Volume I, in order to study the interaction of energy balance components and atmosphere in creating the mass balance conditions existing on Meighen Ice Cap.

ISLAND YEARS

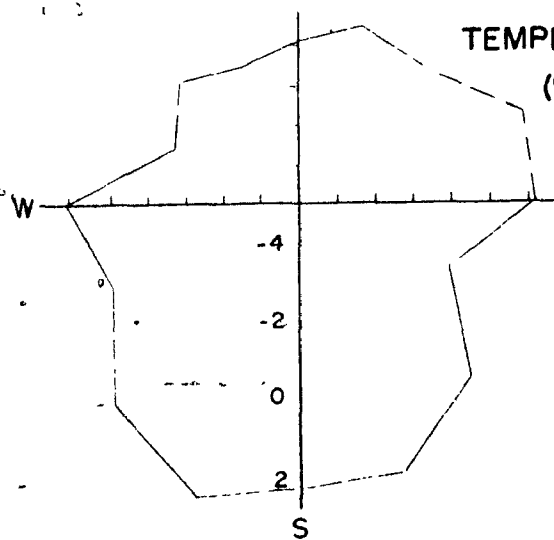
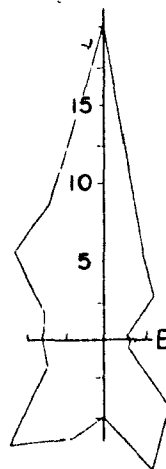
POLAR OCEAN YEARS



GEOSTROPHIC WIND (%)



MAIN ICE WIND (%)



TEMPERATURE (°C)

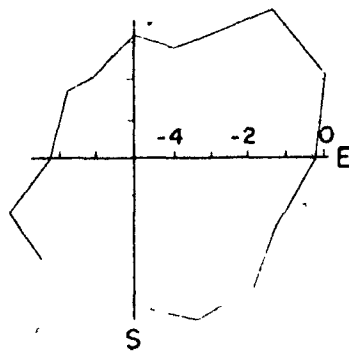


Figure 1: 2.2

1: 2 Energy Balance Climate of Polar Ocean and Island Years

Analysis of the monthly and summer ~~season~~ means of the climatic elements from the Meighen Island stations (II 2) showed that in general the climate of Meighen Island is similar to that of the Polar Ocean floating ice island stations. At times however the climate of the islands to the south spreads N to the edge of the Polar Ocean enveloping Meighen Island. The Island conditions dominated the summer season in two of the 11 years examined (II 2). In the following discussion of the summer energy balance climate of Meighen Ice Cap, the six years of Main Ice climate data have been divided into Polar Ocean years (1961, 1968, 1969 and 1970) and Island years (1960 and 1962).

Table 1: 2.1

	Polar Ocean	Island
Temperature ($^{\circ}$ C)	-1.8	0.6
Relative Humidity (%)	95.7	93.8
Pressure (mb)	982.7	984.5
Wind Speed (m/sec)	6.0	4.9
Cloud Amount (tenths)	8.2	7.1
Melting Degree Days	37	125
Precipitation (cm)	4.9	1.6
<u>Precip. with density of .3 gm/cc</u>	18.6	9.6

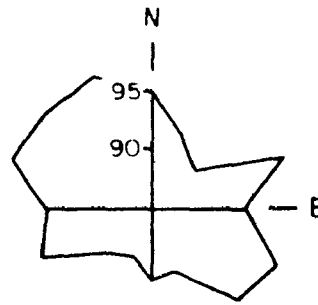
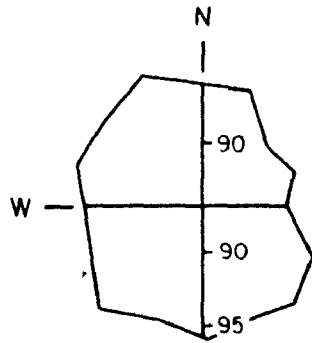
1: 2.1 Mean Summer Climate

Means of the various climatic elements for the Polar Ocean and Island years are shown in Table 1: 2.1. The Polar Ocean years are colder, more humid, cloudier, windier and experience considerably more precipitation than the Island years.

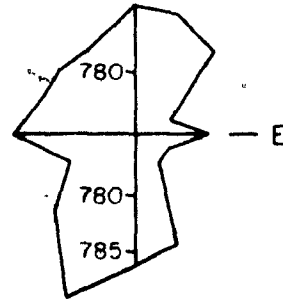
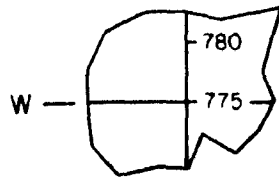
POLAR OCEAN YEARS

ISLAND YEARS

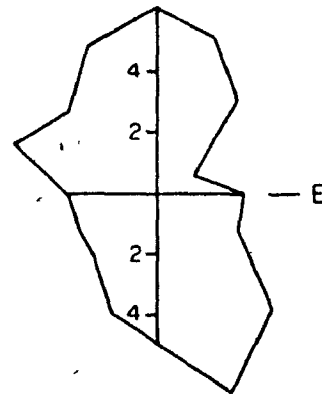
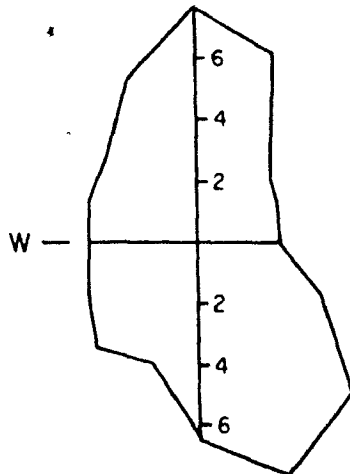
RELATIVE HUMIDITY



PRESSURE (MB)



WIND SPEED (M/SEC)



— CLOUD
--- FOG
AMOUNT (TENTHS)

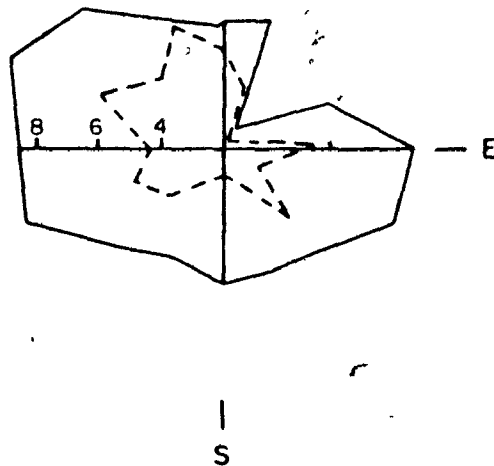
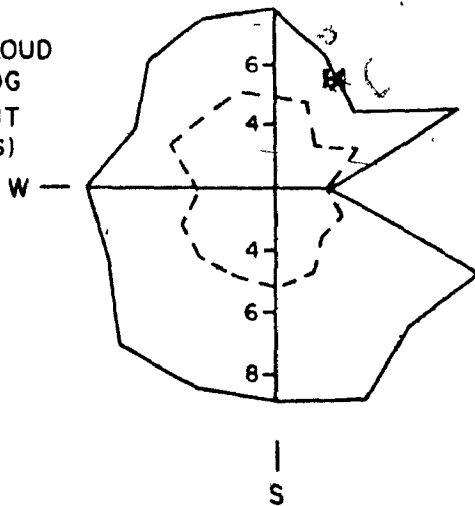


Figure 1: 2.2 cont'd

1: 2.2 Wind Roses of Climatic Elements

Some insight into the reasons for the observed climate at Main Ice can be obtained by examining wind roses of the various elements for Polar Ocean and Island years shown in Figure 1: 2.2.

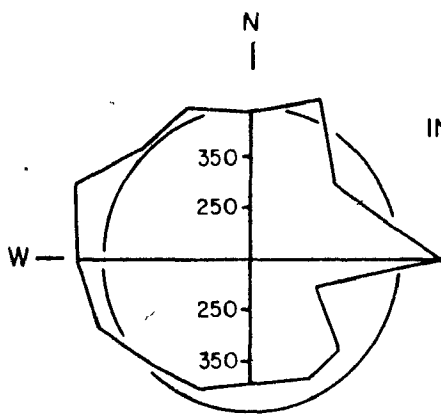
Comparing roses of geostrophic wind direction (II 3:8) with Main Ice surface wind direction, it can be seen that the E'ly flow of the Polar Ocean years is deflected S around Axel Heiberg Island producing SE'lies at Main Ice while ENE'ly flow of the Island years is deflected N around Axel Heiberg Island producing N'lies at Main Ice.

In the four Polar Ocean years cold N'lies are most frequent, followed by the relatively warm prefrontal SSE winds and cool post frontal SW winds of cyclonic passages. During these years, only NE'ly surface winds accompanied by S'ly flow in the lower troposphere result in mean temperatures above freezing. In warm years N'lies dominate but temperatures accompanying these are somewhat higher due partially to the effect of land heated ENE'ly flow deflected around Axel Heiberg. SSW'ly flow gives a secondary maximum of warm S'lies at the surface.

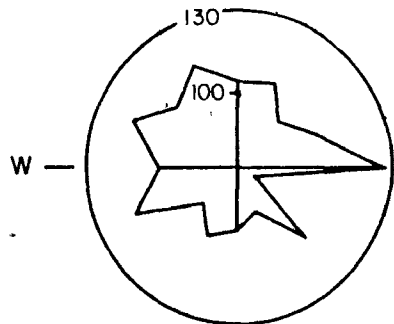
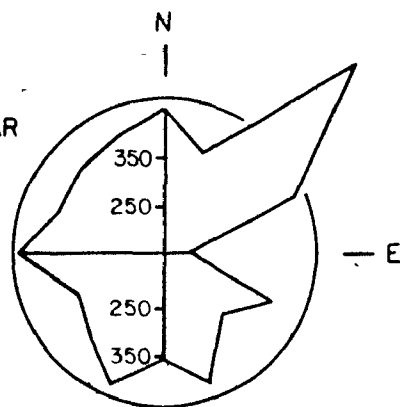
Relative humidity is low with NE'lies in all years and with S'ly sector Island flow. Pressures tend to follow the same pattern being high with NE'lies and S'ly sector Island flow. Wind speeds are high with N'ly and SW'ly sector flow in all years. Cloud and fog cover are low with NE'lies in all years and S'ly sector Island flow once again follows having low cloud and very low fog amounts. There is a tendency, with Island flow, for low cloud amounts with N'lies though the fog amounts remain high.

POLAR OCEAN YEARS

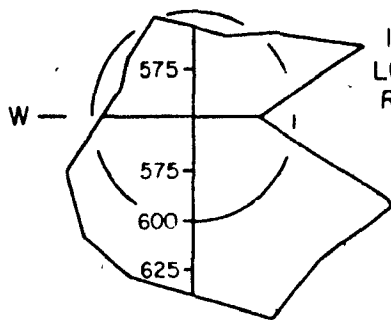
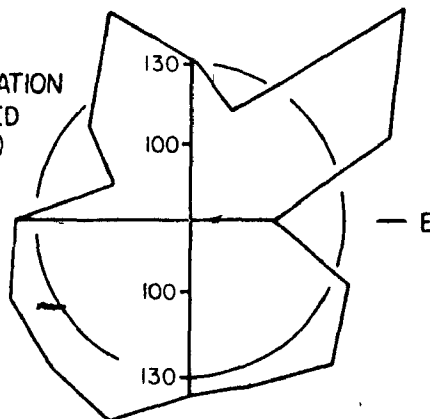
ISLAND YEARS



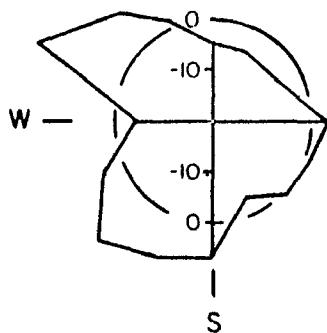
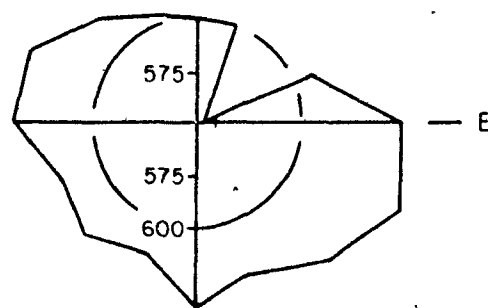
INCOMING SOLAR RADIATION (LY/DAY)



SOLAR RADIATION ABSORBED (LY/DAY)



INCOMING LONG WAVE RADIATION (LY/DAY)



Δ TEMPERATURE SURFACE TO 850 MB ($^{\circ}$ C)

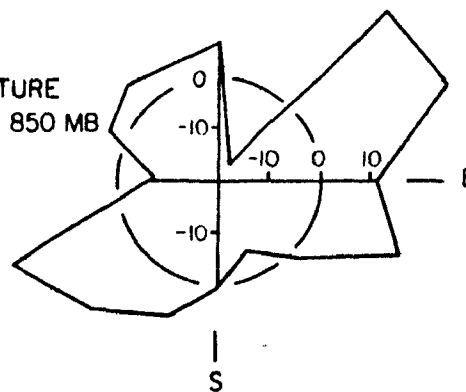


Figure 1: 2.4

1: 2.3 Summer Means of Energy Balance Components

Table 1: 2.3 shows the season means of energy balance components for the Polar Ocean and Island years. The components exhibit the expected differences, melt in the Polar Ocean years being less than half that experienced in the Island years.

Table 1: 2.3

(ly/day)	Polar Ocean	Island
Incoming solar	438.	392
Absorbed solar	101.	138
Incoming long wave	617.	620
Sensible heat	-12.	3.
Latent heat	-11	-.8
Heat from ice	-19	-27
Melt (cm)	-45	1.08
Snow (cm)	.06	.01
Rain (cm)	.05	.02
Net summer mass balance	.39	1.07

1: 2.4 Wind Roses of Energy Balance Components

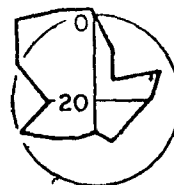
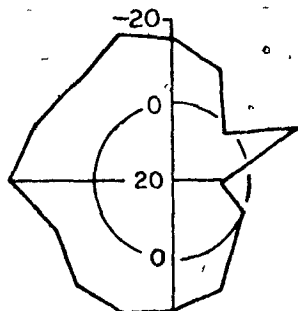
Roses of the energy balance components show the effects of the variation of climatic elements on the surface energy balance and thus on the mass balance of the Ice Cap. (see Figure 1: 2.4)

Solar incoming radiation is consistently greater with Polar Ocean flow than with flow off the Islands, as the cloud and fog accompanying this flow is colder and thinner than the frontal cloud or the warm Island cloud and fog experienced with flow from the other sectors. The solar radiation absorbed at the ground on the other hand is much greater in warm years, as in these years all the snow melts and the

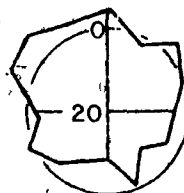
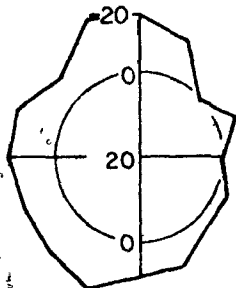
POLAR OCEAN YEARS

ISLAND YEARS

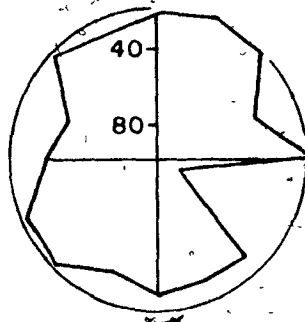
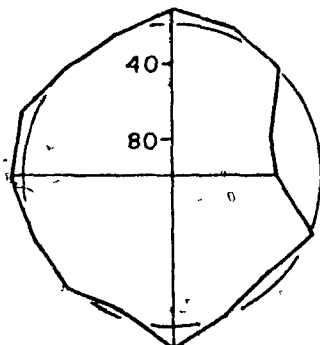
SENSIBLE
HEAT
(LY/DAY)



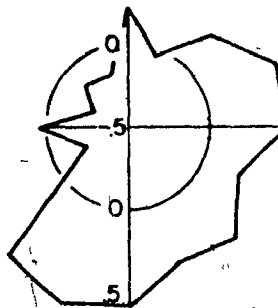
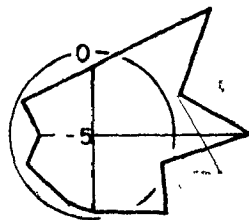
LATENT
HEAT
(LY/DAY)



HEAT INTO
ICE
(LY/DAY)



SLOPE OF
TEMPERATURE
PROFILE (°C)



SURFACE
ROUGHNESS
 $\ln z_0$ (cm)

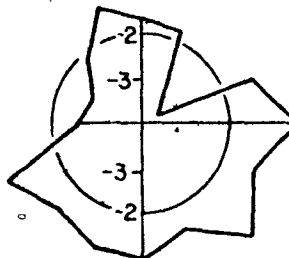
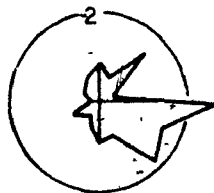


Figure 1: 2.4 cont'd

glacier ice is exposed, causing a 20% decrease in surface albedo. The NE'ly maximum of the Island years and the E'ly maximum of the Polar Ocean years result from low cloud amounts.

The cold thin cloud of the Polar Ocean flow results in considerably lower values of long wave incoming radiation than are experienced with warmer thicker cloud from the Islands. The relatively clear NE'lies of the Island years and E'lies of Polar Ocean years give low values of incoming long wave. The temperature inversion in the lower troposphere accompanying SE'lies produces slightly higher values of long wave incoming radiation than the strong lapse conditions of SW'ly flow. (Though in Polar Ocean years, due to the persistent fog, this may be more a reflection of screen temperature.)

Turbulent heat transfer is consistently negative in Polar Ocean years as a result of the lapse conditions (temperature and humidity) in the lowest meter experienced in cold fog (II 5: 2). Sensible and latent heat fluxes are least negative with NE'ly and E'ly winds which are accompanied by lower cloud and fog amounts and warmer temperatures. In the Island years sensible heat is negative only with winds from the NW sector off the Polar Ocean, while latent heat transfer is negative also in the dry clear NE'ly flow. Surface roughness is largest in Island years due to greater deterioration of the surface in these years.

As a result of high values of absorbed solar and incoming long wave radiation and positive turbulent heat fluxes, the mean surface temperatures are close to freezing with all types of flow in the Island years. The cold thin Polar Ocean fog and cloud hold surface temperatures well below freezing in the cold years. Mean surface temperatures higher than -1°C are experienced only with E'lies and ESE'lies (turbulent fluxes

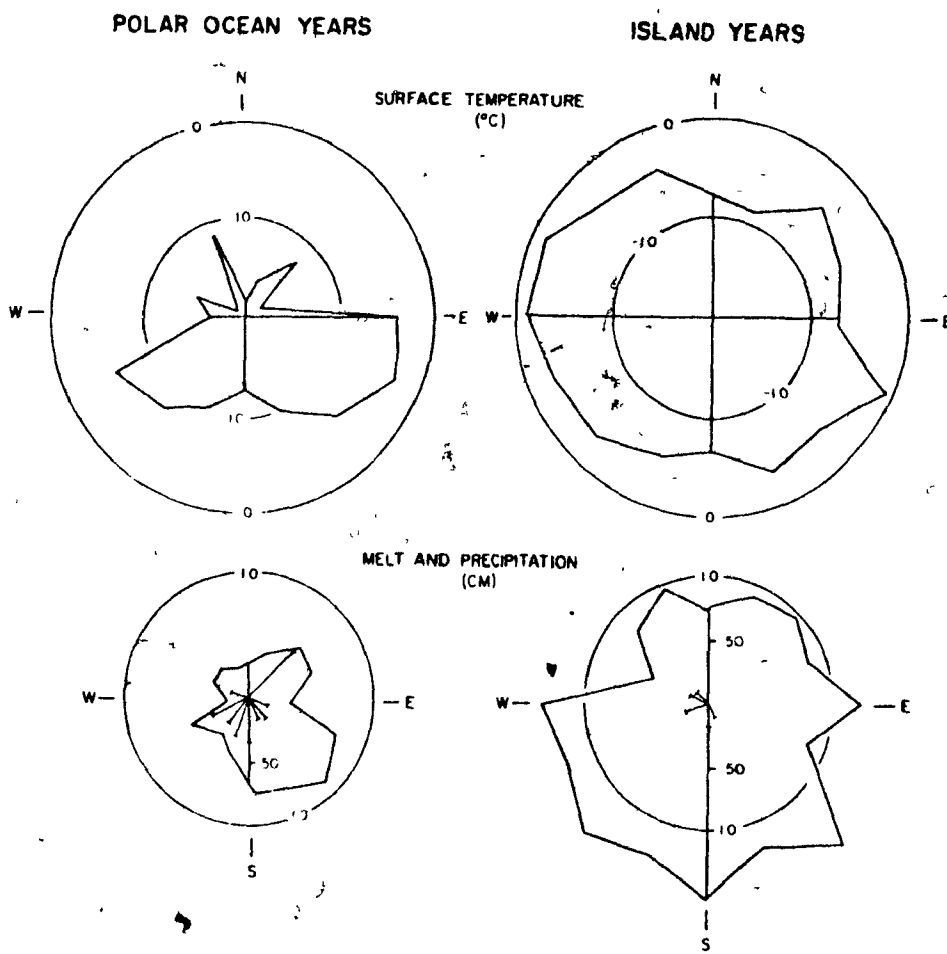


Figure 1: 2.4 cont'd

not negative) and with WSW'lies (long wave incoming and solar absorbed radiation combine) but the occurrence wind roses show that these directions are infrequent at Main Ice.

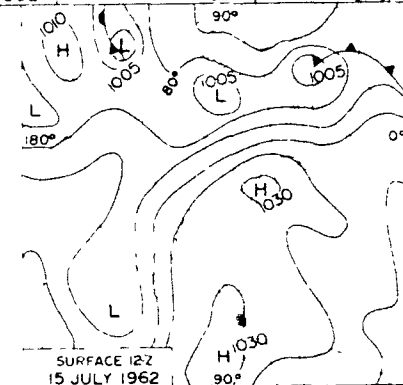
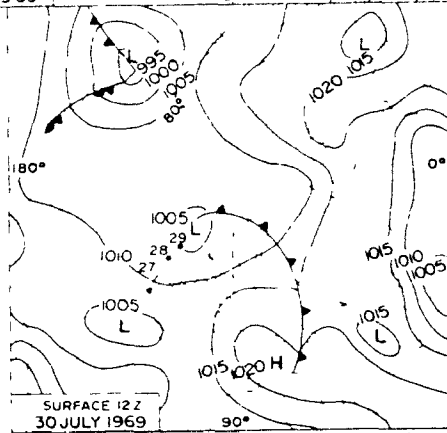
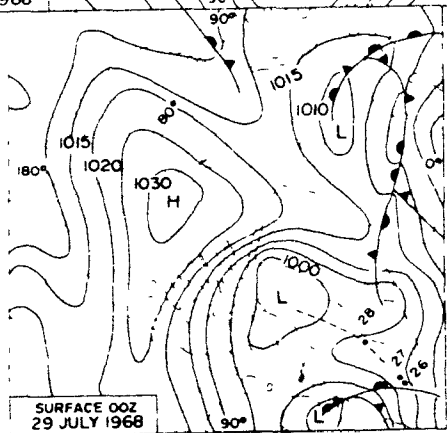
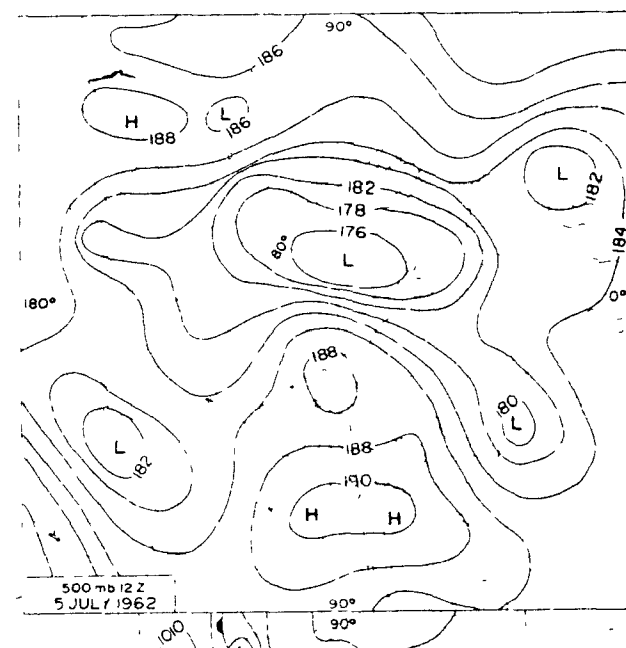
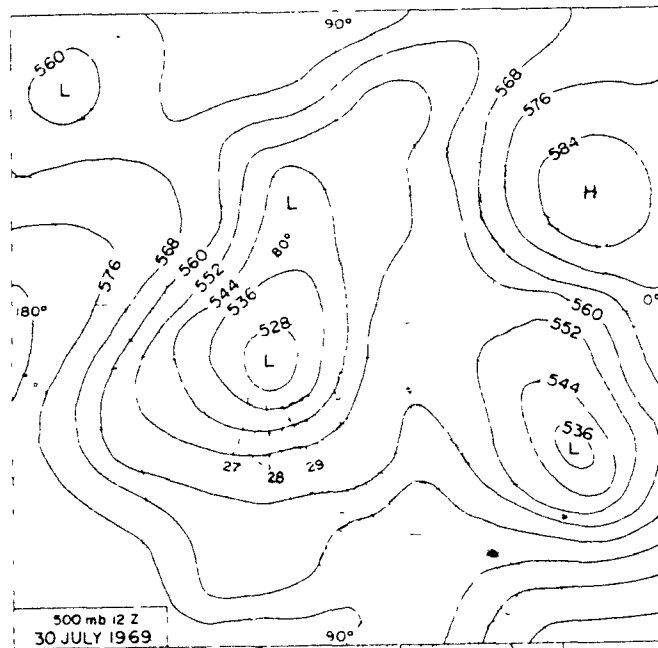
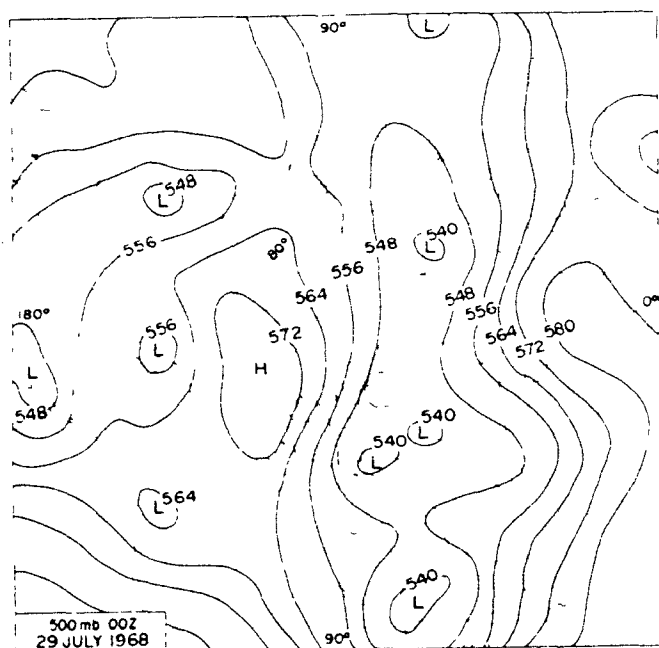
Melt in the Polar Ocean years is consistently lower than in the Island years with the lowest melt values accompanying NW sector flow. The lowest summer mass balance (melt - precipitation) results from SW sector flow in Polar Ocean years. The greatest ablation occurs in Polar Ocean years with NE'lies and SE'lies and in Island years with S sector flow.

1:3 Circulation Types and Energy Balance Climate

The warm and cold year wind roses show that there is a strong relationship between wind direction and energy balance climate and that with the exception of the angle subtended by Axel Heiberg Island the surface wind direction at Main Ice is representative of the geostrophic wind direction and thus related to the synoptic pattern. As discussed in detail in II 3, four distinct circulation configurations were isolated such that variations in the relative importance of those circulation Types, during a period, adequately accounted for the observed climatic characteristics of that period.

The most important characteristics of each Type will be outlined here but reference should be made to II 3 for examples of the Types and justification of their validity as indicators of climate.

Surface and 500 mb charts illustrating the three major Types are reproduced here from II 3. (Figure 1:3)



TYPE III CASE A

TYPE I CASE A

TYPE II CASE A

Figure 1: 3 Examples of Circulation Types I, II and III

1: 3.1 Type I Polar Ocean Circulation

This Type is characterized, at the surface, by a high pressure area west of Meighen Island in the Polar Ocean, and a low in Baffin Bay. The dominant feature of the 500 mb map is a cold low in the Hudson Bay area. The position of the upper cold low in this circulation Type results in a predominance of storm tracks along the northern coast of mainland Canada and into Baffin Bay.

When the Polar Ocean high dominates the Meighen Island region, a strong subsidence inversion results. This subsidence inversion may be enhanced by an advection inversion caused by the intrusion of cold Polar Ocean air into the islands in the lowest levels.

1: 3.2 Type II Cyclonic System Circulation

Circulation of Type II features a 500 mb cold low in the Polar Ocean north of Alaska. Lows, developing in the strongly baroclinic zone between the radiationally heated land of Siberia and Alaska and the cold Polar Ocean, pick up moisture over the ice-free areas of the peripheral seas. They travel around the upper cold low in a short wave trough. This results in tracking of surface lows and well-developed baroclinic zones NE along the NW edge of the Archipelago. The temperature sounding shows the sharp tropopause associated with the arctic jet. The lowest layers are unstable, though there is a slight suggestion of subsidence around 850 mb.

1: 3.3 Type III Island Circulation

A complete development of Type III involves positioning of a cold low on the Siberian side of the Polar Ocean and a ridge over the eastern

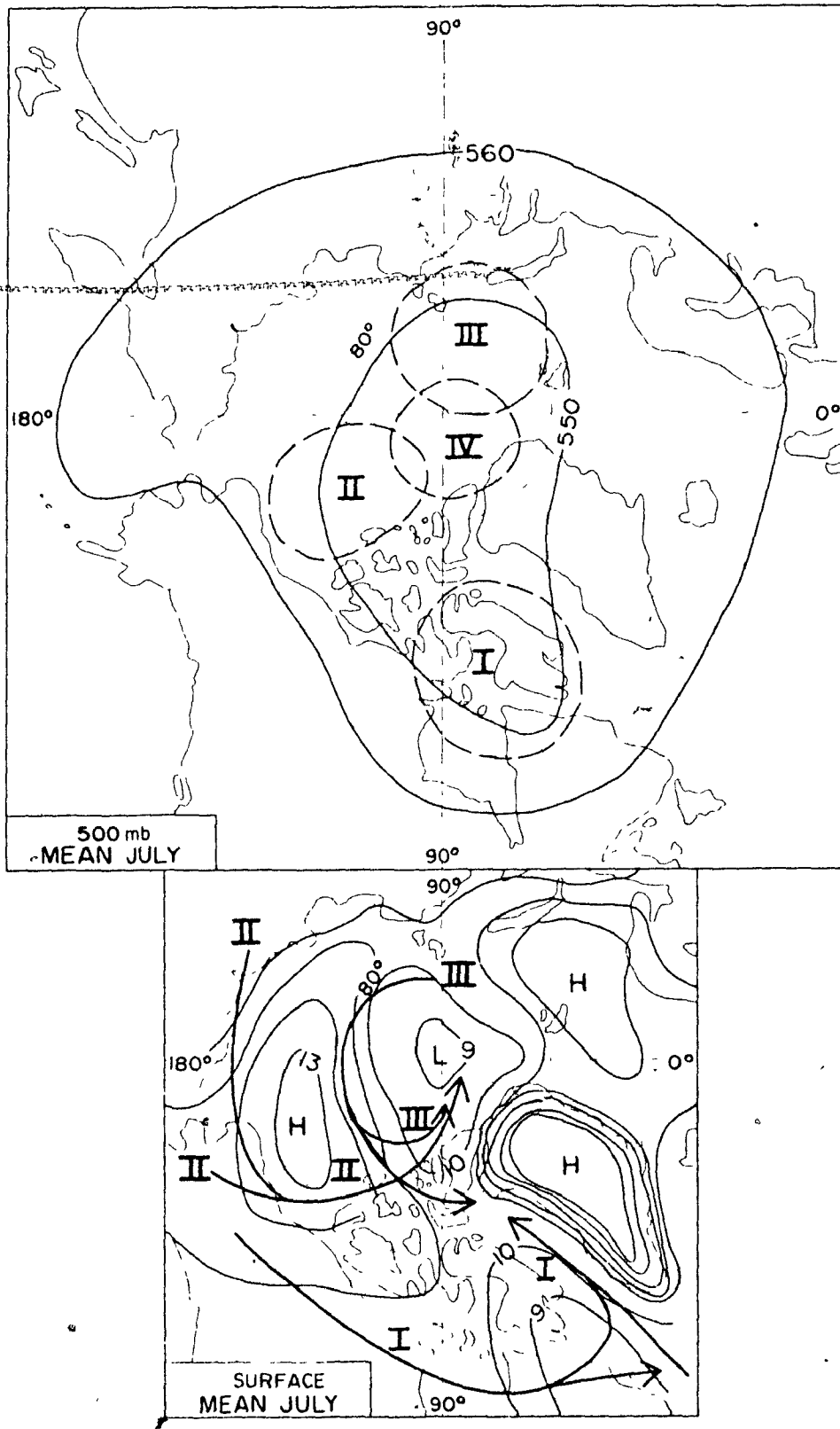


Figure 1: 3.5 Circulation Types and Mean Pressure Pattern

Canadian Arctic and Greenland. Surface lows track around the central Polar Ocean, occasionally penetrating the Queen Elizabeth Islands from the west but more often being deflected along the edge of the Islands to die near the Pole. Partial development of this Type is more common. The essential feature of this modified form is the intrusion of a ridge over the eastern Islands or Greenland at some level in the lower troposphere, resulting in southerly flow at that level over Meighen Island. This southerly flow combined with subsidence blocks the advance of Polar Ocean stratus into the Meighen Island region.

1: 3.4 Type IV

A fourth classification is needed to account for occasions when the 500 mb cold low is centred over the Pole. Under these circumstances there is a rapid alteration between the other three types producing a variety of surface weather conditions. (Type IV was significantly frequent only in 1970.)

1: 3.5 Circulation Types and the Mean Pressure Pattern

Schematized lows representing the 500 mb flow for the four Types are plotted on the mean July 500 mb chart in Figure 1: 3.5. The Types do appear to correspond to the mean pressure pattern. Examination of the January 500 mb pattern suggests that Type I could be considered a variation of the winter situation. At the surface the Baffin low and Polar Ocean high of Type I are evident in the mean pattern. The tendency for travelling cyclones to track into the central Polar Ocean and die there, is reflected in a mean surface low near the North Pole. The trough over N Ellesmere and Axel Heiberg results from the combined

effect of lows tracking along the edge of the Islands and of the Baffin Bay low.

Based on the six years considered in this study the major storm tracks affecting Meighen Island are included in Figure 1: 3.5. The tracks typical of Types I and III are found on most representations of Arctic storm tracks (e.g. U.S. Navy, 1952; Hare and Orvig, 1958; McKay, 1969) but that of Type II does not generally appear. During the six years of the present study this track was of considerable importance as it was responsible for a large part of the summer precipitation on Meighen Island. Considering the strong temperature gradient between the snow free land and the ice covered Polar Ocean it seems reasonable to find a cyclone track in this position. That these cyclonic disturbances are accompanied by baroclinic zones and considerable moisture should be expected, due to this temperature gradient and the availability of moisture from the ice free areas along the coast.

1: 3.6 Relationship of Wind Direction to Circulation Type

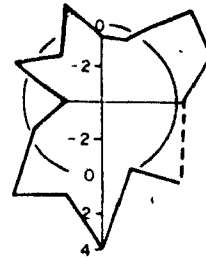
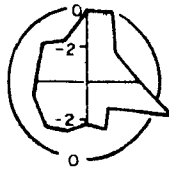
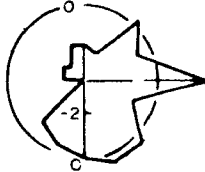
Figure 1: 3.6 shows the distribution of daily resultant wind direction for each circulation Type. The Polar Ocean Type is accompanied almost entirely by N'ly and NW'ly winds. The Cyclonic System Type shows a dominance of SSE'lies but also a significant number of SW'lies and a few NW'lies and NE'lies (the latter resulting from pre- and post-frontal situations or from passage of systems south of the station.) S'ly sector winds, tending to be SW'lies, represent complete development of Type III, the Island Type, while N'ly sector winds tending to be NE'lies represent the modified Island circulation.

TYPE I

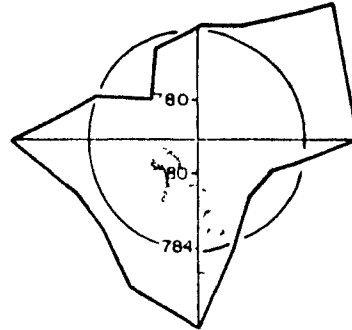
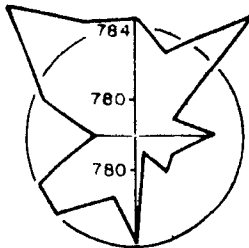
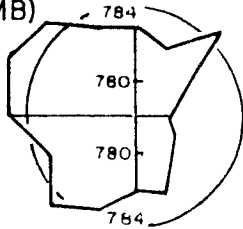
TYPE II

TYPE III

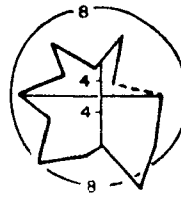
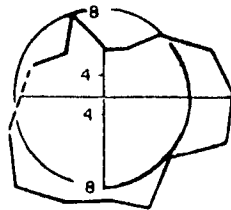
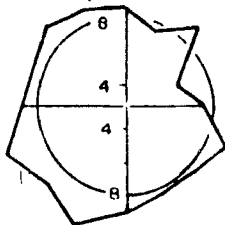
TEMPERATURE
(°C)



STATION PRESSURE
(MB)



CLOUD AMOUNT
(TENTHS)



FOG FREQUENCY
(%)

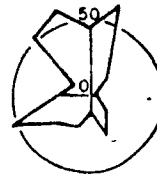
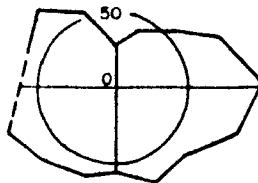
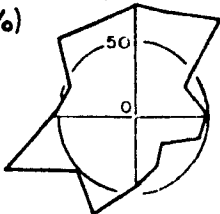


Figure 1: 3.7a

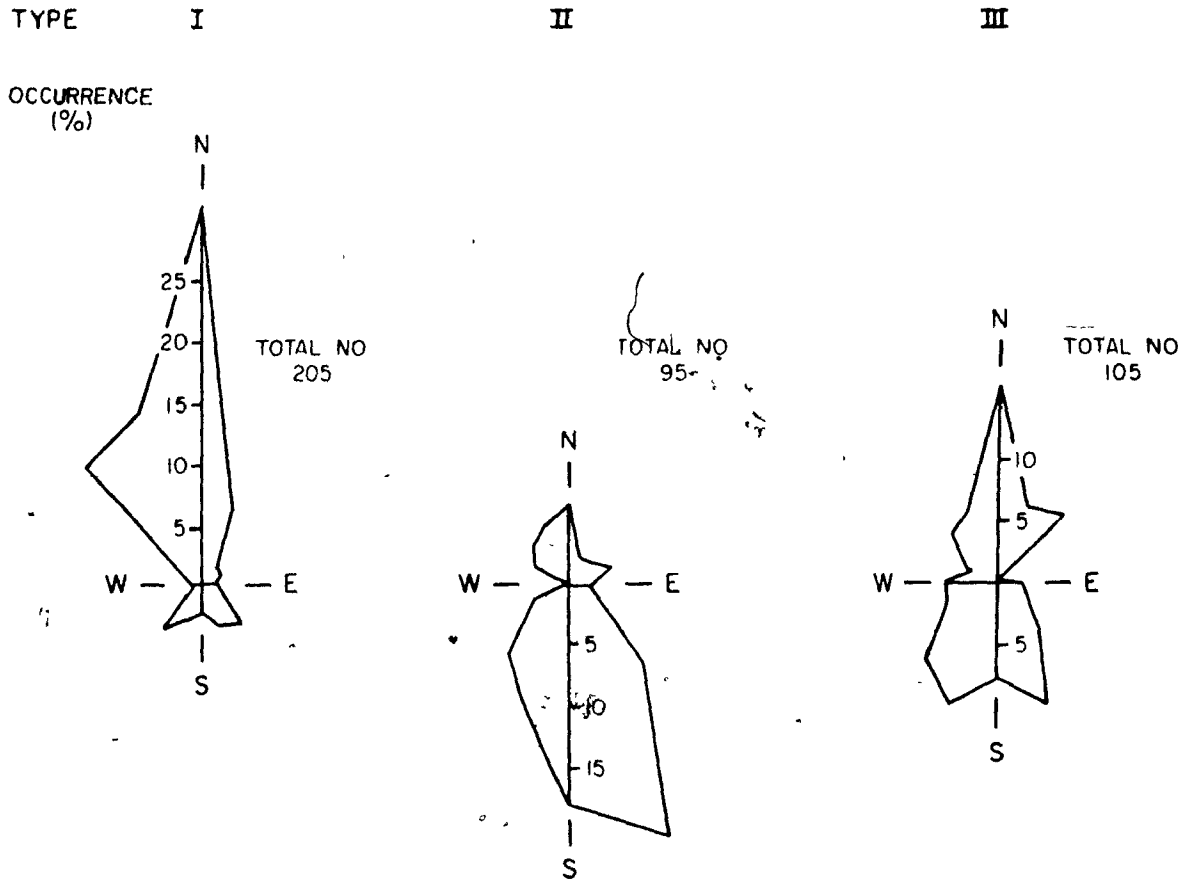


Figure 1: 3.6 Wind Roses for Circulation Types

1: 3.7 Type and Energy Balance Climate

Wind roses of the climate elements for each circulation Type are shown in Figure 1: 3.7a. The cold NW sector flow is primarily associated with Type I circulation. With the Cyclonic passage Type II temperatures remain below freezing with all wind directions. The warm NE'lies and SW sector flow are associated with Type III Island circulation.

The roses of pressure show Island flow to have generally higher pressures. NW'lies show high pressures while SE sector flow has the lowest pressures.

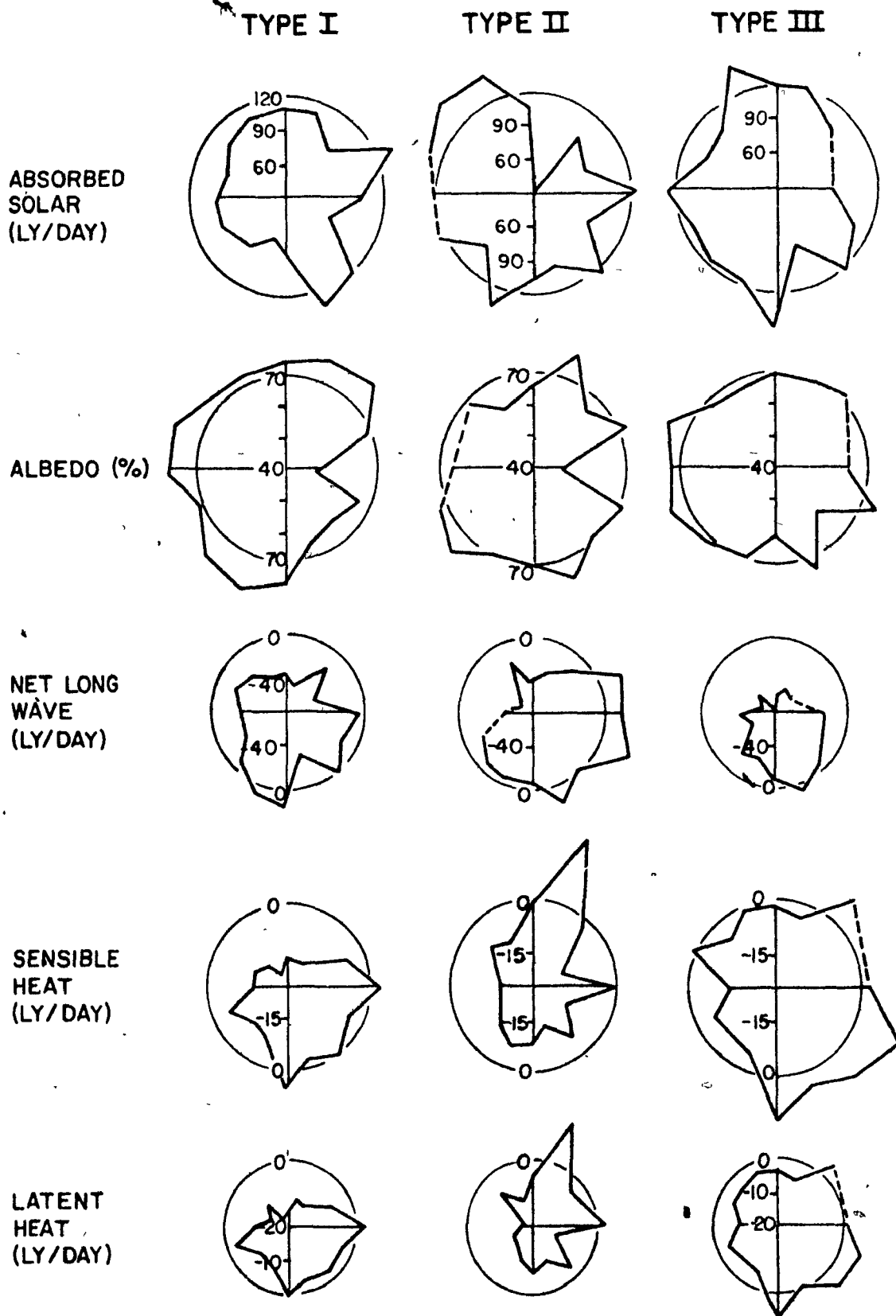


Figure 1: 3.7b

With Island circulation, cloud amounts and fog frequencies are considerably lower than in the case of Type I and II circulation where cloud amounts and fog frequencies are high for the prevailing wind directions.

Table 1: 3.7

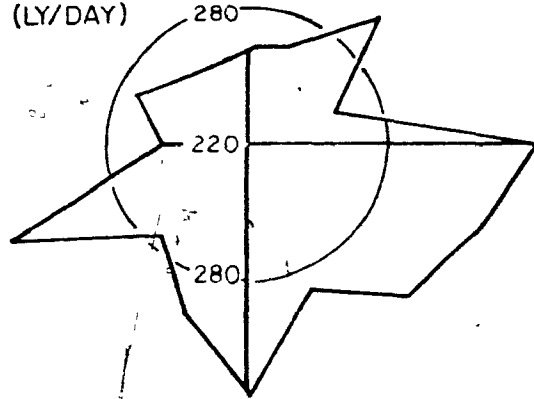
Type	I	II	III
Absorbed solar	117	112	117
Albedo	74	72	70
Net long wave	-27	-7	-34
Sensible heat	-14	-8	2
Latent heat	-12	-8	-2
Melt (cm)	.429	.753	.793
Snow (cm)	.083	.261	.039
Summer net mass balance (cm)	.346	.531	.716

Table 1: 3.7 gives the mean values of the calculated energy balance components for the three Types.

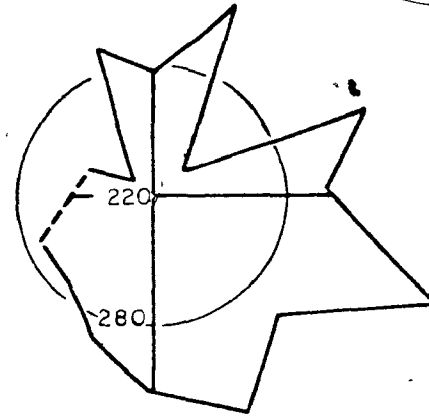
The mean values of absorbed solar radiation differ rather little between the Types, the thick frontal cloud of Type II producing the lowest values. The mean net long wave radiation and turbulent fluxes on the other hand show considerable variation. Type III (Island) circulation has the most negative net long wave radiation balance but nearly positive turbulent fluxes while Type I (Polar Ocean) circulation shows strongly negative net long wave radiation and turbulent fluxes. With Type II (Cyclonic System) circulation the net long wave balance approaches positive values and the turbulent fluxes are only moderately negative. These combinations of components result in considerably lower values of melt for Polar Ocean circulation while Island Cyclonic System circulation has similar mean melt values, but for different reasons. When precipitation

TYPE I

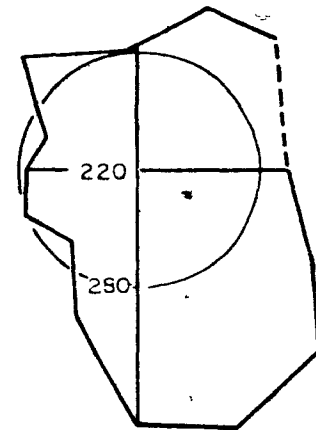
WARM AIR ADVECTION
(LY/DAY)



TYPE II



TYPE III



MELT & PRECIPITATION
(cm)

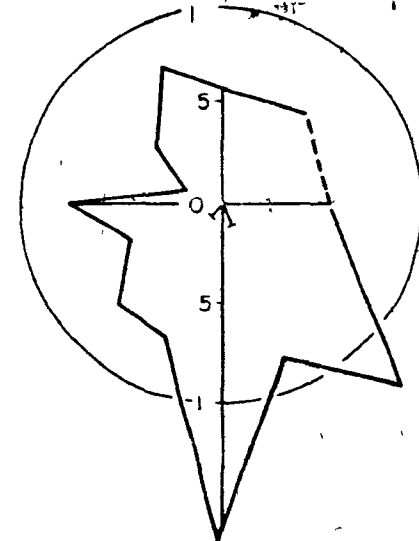
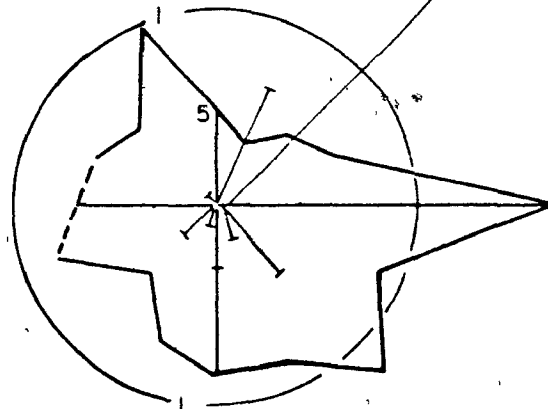
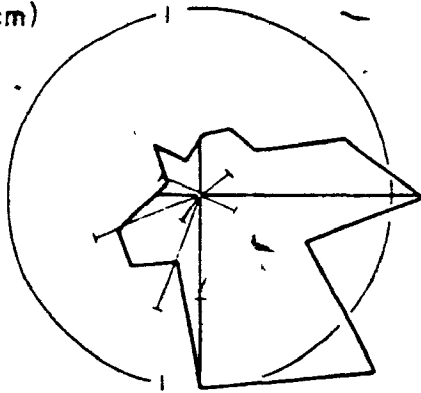


Figure 1: 3.7b cont'd

is considered, the effective melt power of Type II is significantly decreased.

Figure 1: 3.7b shows wind roses of the energy balance components for the three Types. These roses largely reflect the mean values but there are some significant variations with wind direction within the Types.

Positive net long wave radiation balances are experienced with Cyclonic System flow from the E and SE and with Polar Ocean circulation from the SSW. The most negative values of net long wave radiation occur with Polar Ocean NW sector flow.

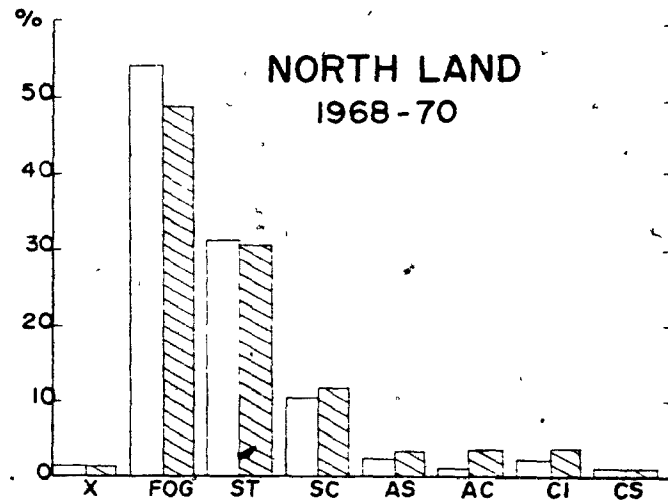
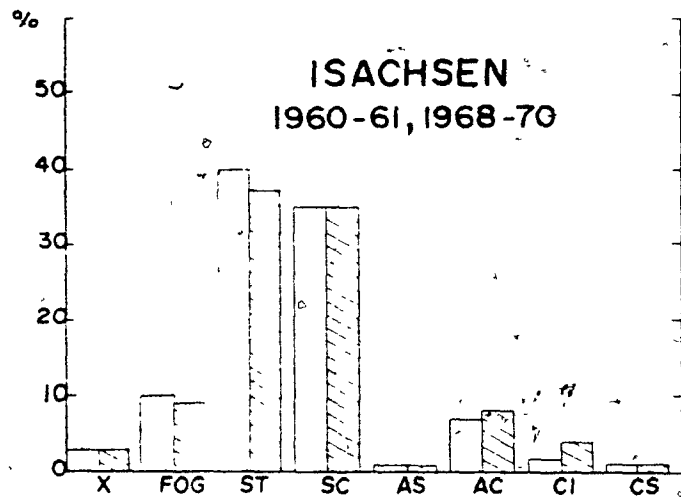
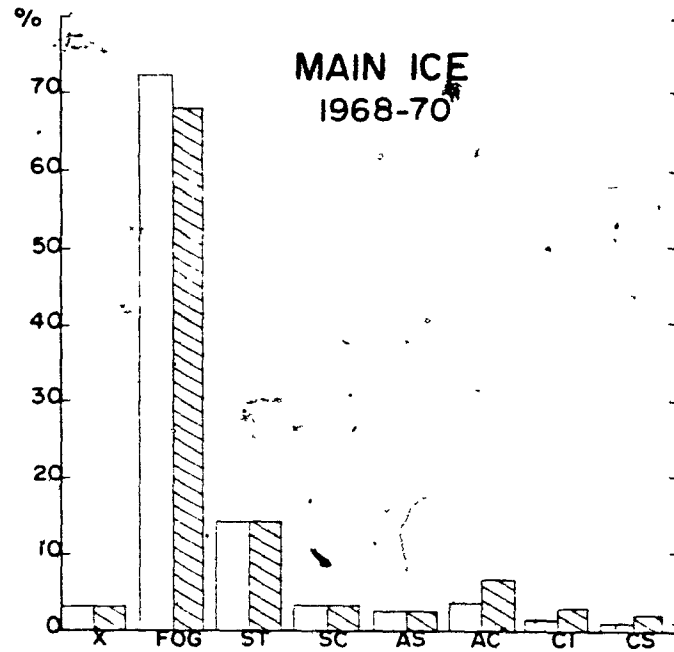
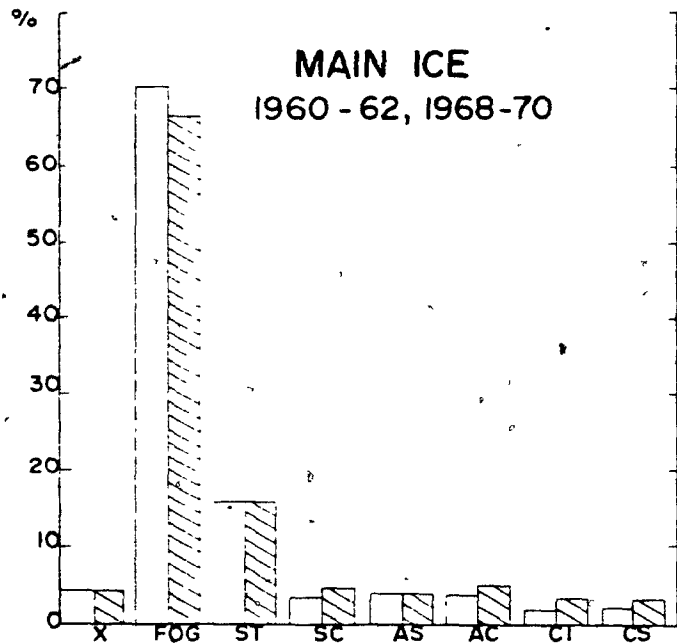
Turbulent fluxes are strongly positive with NE Island and Cyclonic flow and most negative, as in case of net long wave radiation, with NW'ly Polar Ocean flow.

The resulting melt roses show least melt with NW'ly Polar Ocean flow and the strongest melt with S'ly Island flow. When precipitation is taken into account, Polar Ocean SW'lies appear to result in the least net loss to the ice cap. All significantly frequent directions of cyclonic system circulation also show considerable compensation of melt by precipitation. SE'lies, in general, appear to produce the highest melt values and NW'lies the least.

Warm air advection is greatest with SE'ly flow, particularly in the case of Island circulation, and least with all types of NW'ly flow.

1: 4 Origin of Meighen Island Fog

The distribution of fog and cloud for Main Ice, North Land and Isachsen are reproduced from II 2 in Figure 1:4 a. The relative percent frequencies of low cloud and fog at the three stations suggest that much of the Meighen Island fog is stratus or stratocumulus cloud at Isachsen. It



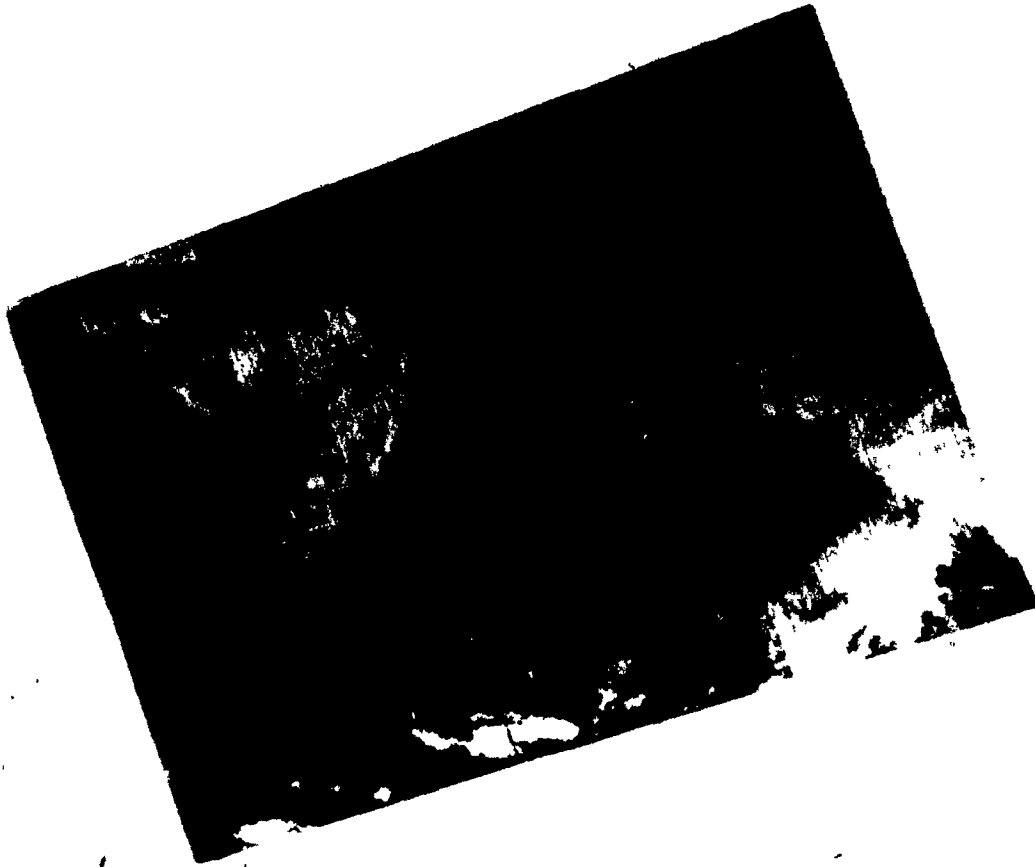
MEAN FREQUENCIES OF CLOUD TYPE

Figure 1: 4a

is the purpose of this section to show that a considerable portion of the fog experienced at Main Ice is actually low stratus and stratocumulus cloud, advected from the Polar Ocean by persistent strong winds, which runs into the 240 m amsl (800 ft) ice cap being observed as fog. This is the cold, often thin fog which shows up in the year and Type roses as being associated with W through N winds and Type I circulation. North Land, being 160 m (600 ft) lower than Main Ice experiences 20% less fog than Main Ice. Isachsen is not only 240 m (800 ft) lower than Main Ice and protected by 700 ft hills 3-5 miles N of the station, but is also 30 miles south of the N coast of the island and thus experiences 40% less fog than North Land.

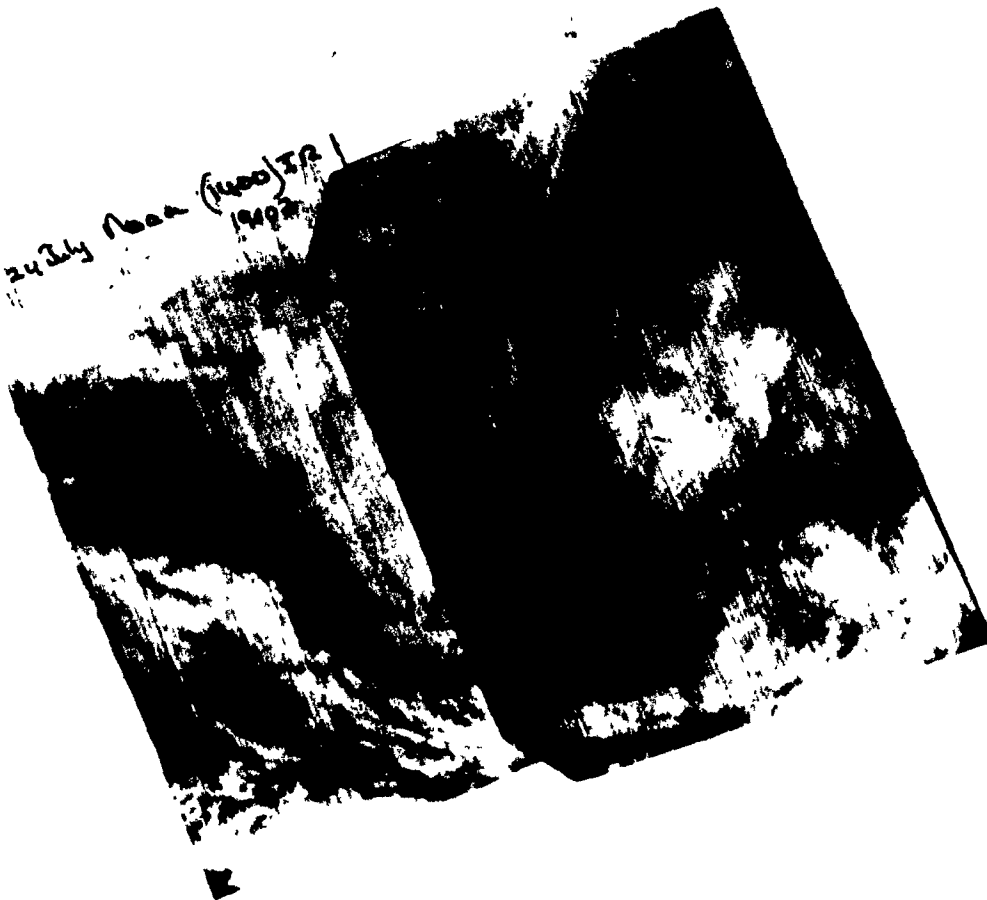
It has been suggested that this fog and low cloud are a result of the lead which sometimes opens between the Polar Pack and inter-island ice. This is doubtless the case on some occasions, but is not frequent enough to explain the almost constant fog at Main Ice. The frequency of occurrence of that particular lead in summer is in the opinion of the author sometimes overestimated, as flights in that area are normally made when the weather is good. This generally means with S'ly winds; S'ly winds usually open the lead. Similarly, the lead is only visible on satellite photographs when cloud cover is low, at which time the winds are likely to be from the S'ly sector. Once winds shift to N'ly, there is a period of perhaps a week when it is possible that the Meighen Island fog originates from the lead which is gradually closing. This however cannot account for the persistent fog in years such as 1968, where S'ly winds were almost absent.

It is often difficult to prove from satellite photographs that the Polar pack is covered with low cloud, due to lack of definition between



Visible |

Figure 1: 4b Satellite Photograph Illustrating Low Cloud Cover in Polar Ocean: compare Visible where cloud can be seen in Polar Ocean to Infrared where it can be seen that this cloud has a temperature close to freezing.



Infrared

Figure 1: 4b' cont'd

ice and cloud, but on several of the ESSA photographs for the years 1968, 1969 and 1970 texture or a change in cloud boundaries between pictures allowed identification of low cloud over the Polar pack. Infrared satellite photographs are also of use in distinguishing low cloud from ice, as shown in Figure 1:4b where there is definitely low cloud covering the Polar pack.

The Polar pack in summer is not solid and is often extensively puddled, providing an adequate moisture source to maintain a constant layer of stratocumulus. The meteorological records of the Trans

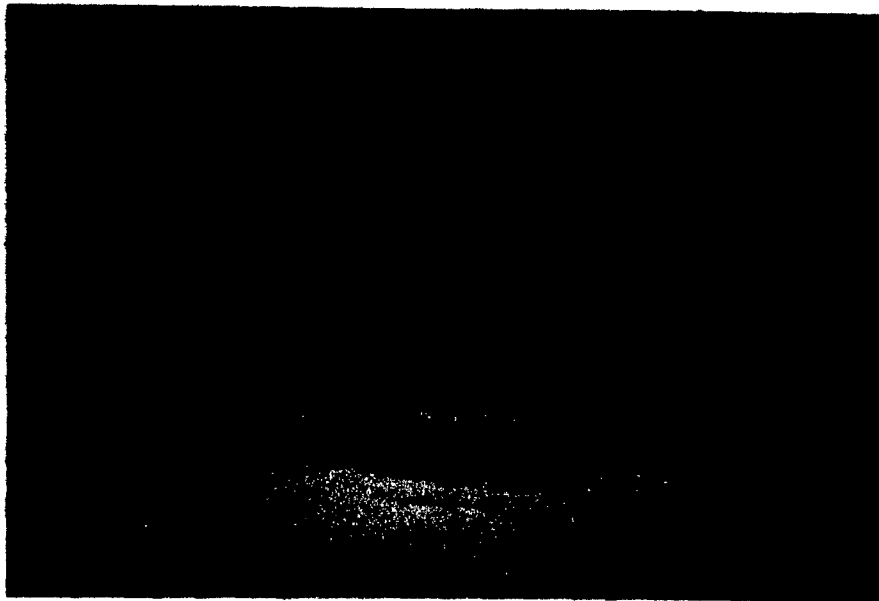


Figure 1: 4c N of Ellesmere Island Looking NE - Low
Sc to N and W.
(See Figure 1: 4e for location map)

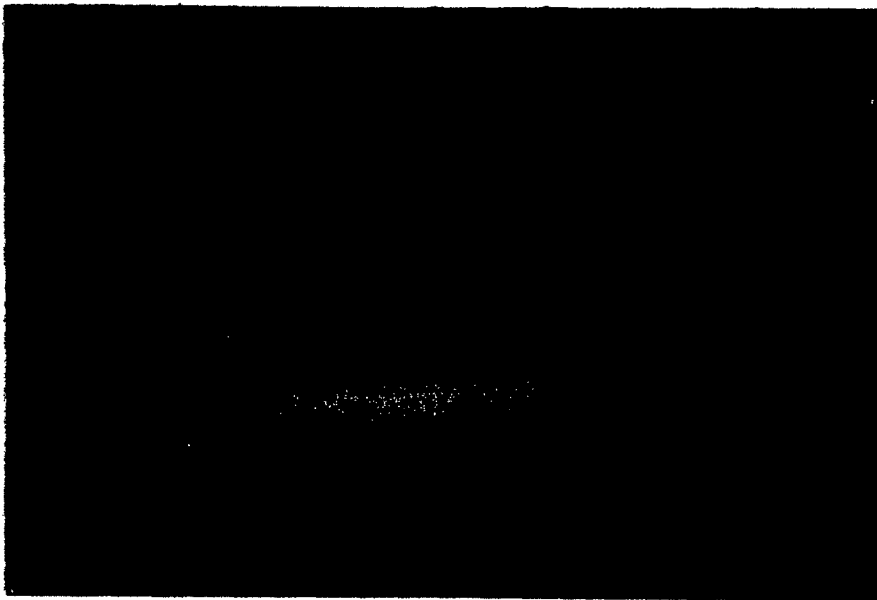


Figure 1: 4d Approaching Nansen Sound (see Figure
1: 4e for location map)

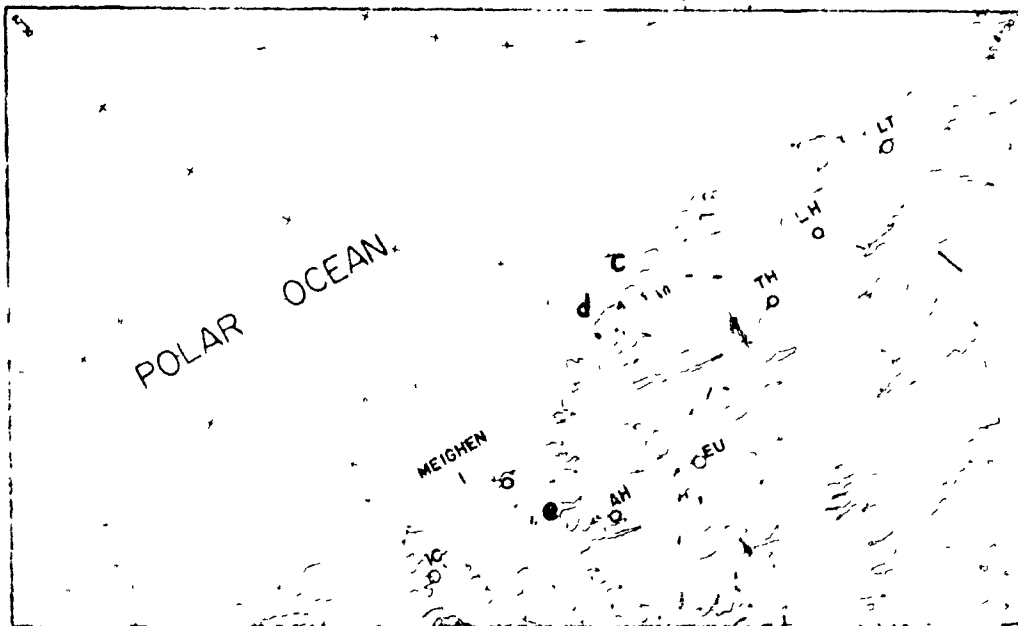
Polar Expedition which passed N of Meighen Island during the summer of 1968 (Koerner, 1970) show mean cloud cover of 8/10, 72 percent of which was low cloud. In addition they recorded visibility greater than 10 miles only 17 percent of the time during the summer season.

The constant strong winds resulting from the gradient between the Polar Ocean high and Baffin Bay low may be responsible for significant turbulence in the lowest levels below the frequent subsidence inversion experienced with these conditions (II 3:2). Figures 1:4c and d illustrate a cover of low stratocumulus which appears to stretch as far as the eye can see to the NW. The base of this layer ranged from 0 to 300 ft. These figures also illustrate another important point: along the steep coasts of Ellesmere Island and Axel Heiberg Island the cloud layer disappears or is blocked from continuing inland except perhaps where glaciers reach the sea. The cloud however dips into the N end of the straits and channels and as seen in Figure 1:4e fills the whole of the Sverdrup Channel - Peary Channel area in which Meighen Island is located.

Figure 1:4e also shows that land masses, even the size of the Fay Islands, tend to burn off this thin cloud layer. It has been noted by Stefansson (II 2: 5.1) and Savile (1961) that within 10 to 15 miles of the Polar Ocean, on the NW coasts of the W Queen Elizabeth Islands, the vegetation is particularly sparse. Initial analysis of data from the oil camp meteorological station at Cape Isachsen on the N tip of Ellef Ringnes Island in 1973 suggests that similar fog frequencies occur here as are experienced at North Land. In addition it appears from satellite photographs, from vegetation coverage and from contact with a party located on the SE corner of the Meighen Island (in 1970), that the low



Figure 1: 4e " E Sverdrup Channel looking W to holes burned in Low Sc by Meighen Island and the Fay Islands.



Location Map for Figures 1: 4c, d and e

cloud and fog often extends only a few miles south of the Ice Cap.

Finally it was seen in II 5: 2.1 that this "fog" is unstable in the lowest meter at Main Ice. Such conditions should tend to dissipate the fog by producing mixing, but the continual re-supply of low cloud from the Polar Ocean by the strong NW'lies counteracts this effect.

It would appear from these arguments that the persistent cold fog which accompanies strong NW'ly winds and Polar Ocean Type circulation is often actually low stratus or stratocumulus continuously blown onto the Island from the Polar pack. The 10 miles of land over which the low cloud travels before reaching the Ice Cap is not sufficient to dissipate the cover, and it is likely that any dissipation which occurs is largely compensated by the effect of orographic lifting. This orographic effect combined with the cool surface of the Ice Cap may result in the fog thickening somewhat as it reaches the top of the Ice Cap, or persisting longer than would otherwise be the case.

CHAPTER 2

THE SYNOPTIC ENERGY BALANCE DIAGRAM

The circulation Types give considerable insight into the synoptic reasons for the energy balance climate variations on Meighen Ice Cap. However, there are significant variations of climate and energy balance terms within the Types depending, for instance, on the time of the season when they occur, or on the state of the surface of the ice cap over which they occur, or on their degree of development and duration. Examination of the Type roses (1:3) and of the extensive discussions and Figures of the various parameters found in II 2, 3, 4 and 5 suggest the possibility of a further breakdown based on wind direction, temperature and fog and cloud amount. The most important indications of this are reviewed in the following section, but reference should be made to Volume II to fully appreciate the basis on which the Synoptic Energy Balance Diagram was conceived.

2:1 Basis for Further Breakdown

Temperature roses of the six years (II 3: 8), of the warm and cold years (1:2), and of the circulation Types (1:3) consistently show N'lies and NW'lies to be cold, NE'lies to be warmer and winds from the S'ly sector to have the highest temperatures, with some exceptions (e.g. S'lies in 1970 and SSW'lies in 1969 were cool).

Cloud cover shows a minimum for NE'lies, and in the warm years or with Type III flow less cloud is experienced with S'lies and SW'lies. Type I circulation and NW'lies produce fog occurrence maxima, while fog amounts are low for all wind directions in Type III circulation and

in warm years. The S'ly Type II circulations have high fog amounts while NE'lies appear to be considerably clearer.

Roses of the radiation components for 10/10 fog reflect the above temperature and sky condition variations (II 4:4). The solar incoming radiation expressed as percent of the clear sky value (II 4: 3.1) is high for the cool thin fogs accompanying N through W winds, and low for the warm thick SE'lies, while net long wave radiation shows maxima with NE'lies and SE'lies and a secondary maximum with SW'lies. The long wave radiation variations relate directly to the thickness roses (II 2:8) which show a warm lower atmosphere with NE'lies, SE'lies and WSW'lies.

Frequency distributions of percent incoming solar radiation in 10/10 fog for various wind directions suggest the significant temperature intervals to be $T < -2$; $-2 \leq T < 0$, $0 \leq T < 2$; $T \geq 2$ (in deg C). In cases with no fog, temperature is not as important but NE and NW sector winds exhibit significantly different radiation regimes, as do SE and SW sector winds.

Albedo is also dependent on temperature and was generally greater in fog. The drop in albedo with the loss of the snow pack produces the most striking effect in this term.

Wind roses of Richardson Number (II 5:2) show that with no fog and NE, SE or SW winds, or with "real" fog and S or NE winds, the lowest meter was stable; otherwise it was unstable. Sky condition was also seen to affect Richardson Number. These stability variations directly affect the sensible and latent heat fluxes, as seen in II 5:4.

In addition it should be noted that there is a tendency for Type II circulation to be accompanied by SE'ly sector winds and for warm and/or clear conditions to be associated with N'ly sector winds which tend

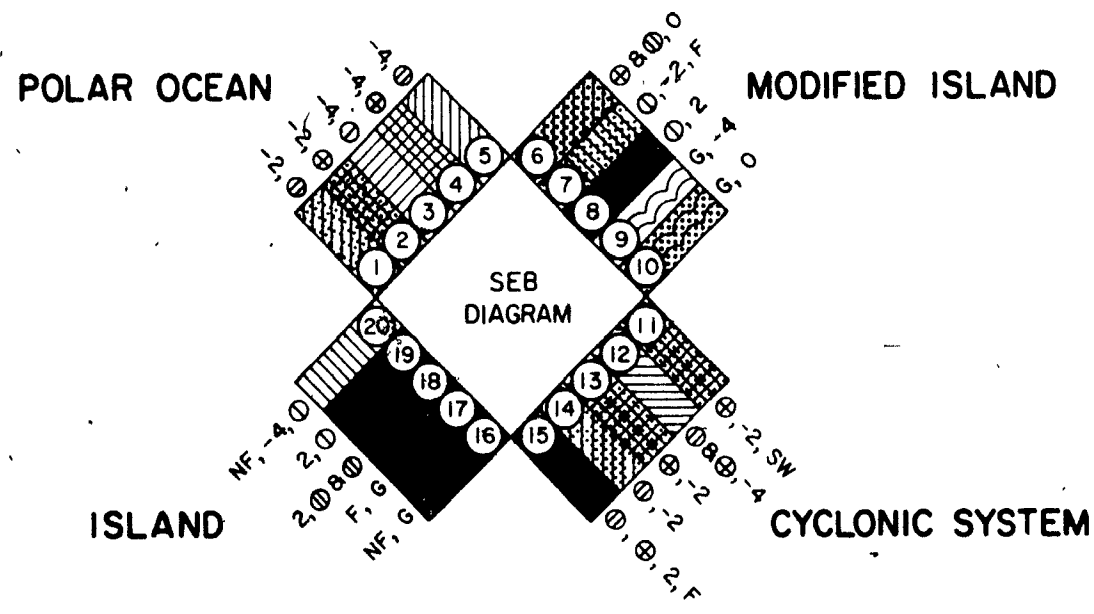
toward NE'lies. There appears to be significant variations in the energy balance climate with wind from the N through NW, NE, SSE and SW sectors; with temperatures in the suggested intervals; with sky cover; with occurrence of fog; and with circulation Type.

2:2 Creating the Synoptic Energy Balance Diagram

Bearing in mind the wind sector, temperature interval and cloud and fog cover divisions which result in variations in the energy balance components (2:1), an attempt was made to choose combinations of these climatic elements which would have a distinct surface energy balance. There appeared to be considerable advantage in using only the very basic climatic elements which are recorded at all stations and which can be interpolated with some success from the permanent station meteorological records. Precipitation amounts, though important to the mass balance, were not used in choosing the intervals as the Meighen-Isachsen precipitation relationship was not at all consistent. The final form of the intervals for the Synoptic Energy Balance Diagram (SEB Diagram) was determined by examination of calculated daily values of melt for each Type, in individual wind directions, for 4 intervals of temperature, and 3 intervals of sky cover, and considering the frequency of occurrence of fog. In addition, it was necessary to account for cases where the snow pack had melted exposing the glacier ice. As mentioned in 1:1.3, the emphasis in this study is on determining the reasons for lack of melt on Meighen Ice Cap as opposed to examining the mechanisms of melt. For this reason the glacier ice cases were separated only into warm and cold N'lies, and S'lies with or without fog, and the emphasis was placed on cases of Type I and II which tend to inhibit or counterbalance melt.

LEGEND

SYNOPTIC ENERGY BALANCE DIAGRAM



TEMPERATURE (°C)

$T < -2$ -4

$-2 \leq T < 0$ -2

$T \geq -2$ 0

$T \geq 0$ 2

CLOUD COVER (TENTHS)

$C < 6/10$ ⊕

$6/10 \leq C < 10/10$ ⊕

$C \geq 6/10$ ⊕ ⊗ ⊕

$C = 10/10$ ⊕

OVER GLACIER ICE

G

NO FOG

NF

FOG

F

SOUTH WEST WINDS

SW

WIND DIRECTION OCCURRENCE (%) IN CLASSES

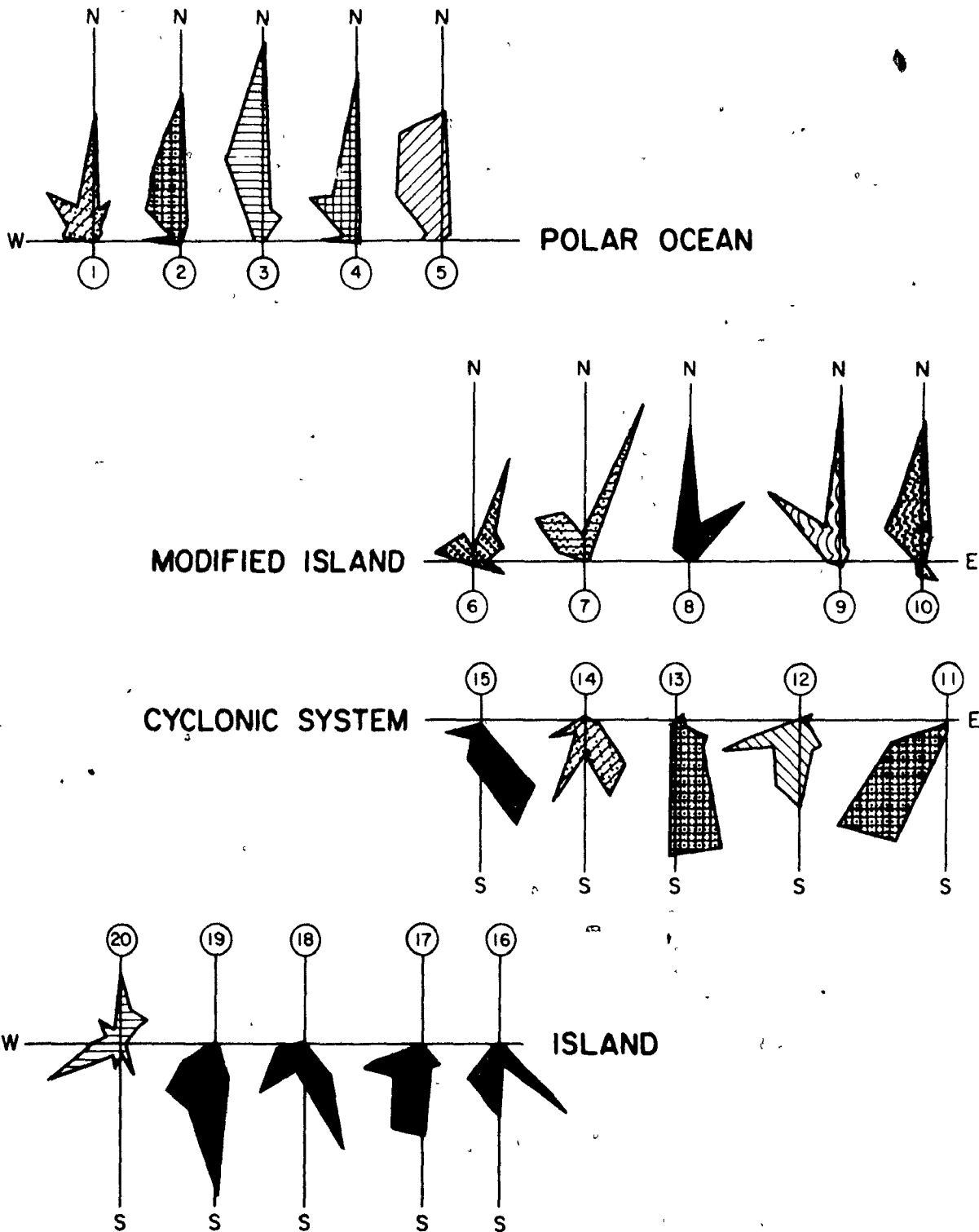


Figure 2: 2a

Figure 2: 2a shows the occurrence wind roses for each of the classes and indicates the temperature, sky cover and other conditions which determine the class boundaries. The classes have been grouped into four larger divisions on the basis of their synoptic Energy Balance regimes (i. e., a combination of Type, melt amount and precipitation amount).

These divisions represent:

Polar Ocean Conditions

Cyclonic System Conditions

Island and S'lies over glacier ice Conditions

Modified Island and N'lies over glacier ice Conditions

The classes are now plotted on a diagram where synoptic energy balance condition is schematically depicted by wind direction. The Polar Ocean classes are plotted as NW'ly, as winds from N through W dominate these conditions. The warm N'lies, NE'lies and glacier ice N'lies which make up the Modified Island Conditions have been plotted as NE'lies. The cyclonic system conditions have been plotted as SE'lies due to the tendency for SE'ly winds to dominate with Type II Cyclonic System circulations. The Island conditions and S'ly glacier ice conditions have been plotted as SW'lies as there was a tendency in the geostrophic roses for Island conditions to have a maximum in this direction.

The average daily melt for each class is plotted in this manner in Figure 2: 2b along with schematic maps illustrating the controlling feature of each of the four divisions. The line histogram represents the average melt in centimeters. The narrow solid bars represent measured precipitation and the shaded bars are the resultant net gain or loss to the glacier for that class. The net summer mass balance bars are shaded, depending on the temperature and sky cover conditions of the class as in Figure 2: 2a.

SYNOPTIC ENERGY BALANCE DIAGRAM

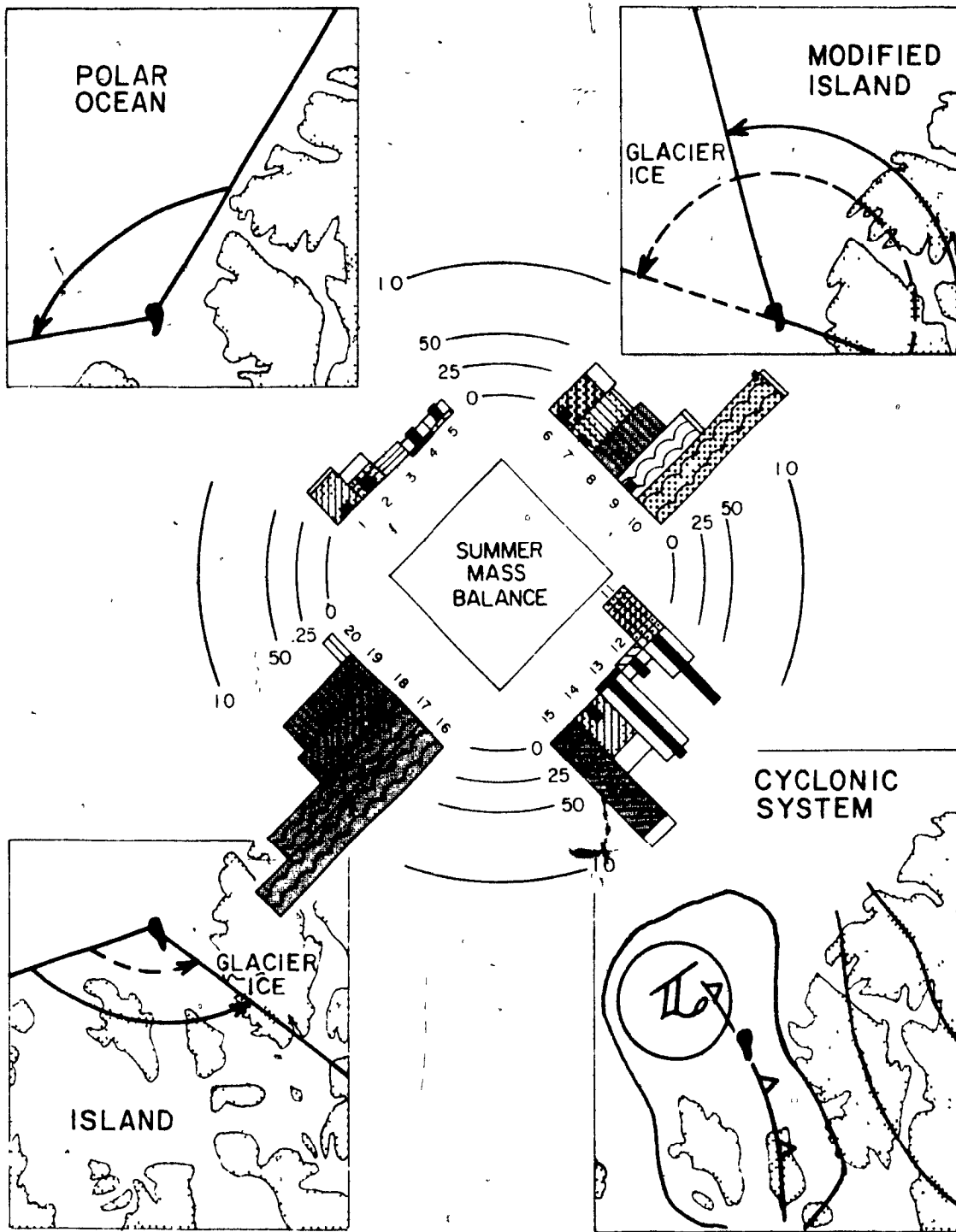


Figure 2: 2b See Figure 2: 2a for legend.

Five intervals of mass balance are ^{delimited} by the arcs joining the histograms. These relate to the net gain or loss to the Ice Cap at Main Ice, assuming that the class were to occur for the whole summer season (90 days) and assuming a mean winter accumulation of 17.5 cm. These intervals, which will be used in discussions in later chapters, are:

- 1) net summer accumulation - precipitation greater than summer ablation
- 2) net annual accumulation - net summer ablation is less than mean winter accumulation
- 3) negative mass balance of 0 to .25 cm/day - could be replenished by one accumulation year.
- 4) negative mass balance of .25 to .75 cm/day - would take several years of accumulation to replenish.
- 5) negative mass balance of greater than .75 cm/day - would take the best part of a decade of accumulation years to replenish.

The classes have been arranged so that the amount of melt decreases towards the north in each division. The mass balance results will be discussed in relation to climate, energy balance and class, in the sections that follow.

As a check on the significance of the classes in terms of energy balance regime, frequency distributions of mass balance, solar radiation absorbed at the ground and net long wave radiation have been plotted for each class (Figure 2: 2c).

The bimodal distributions of solar radiation absorbed at the ground are a result of albedo and would not show up in plots of insolation. With these exceptions, the distributions for Polar Ocean Conditions, Cyclonic

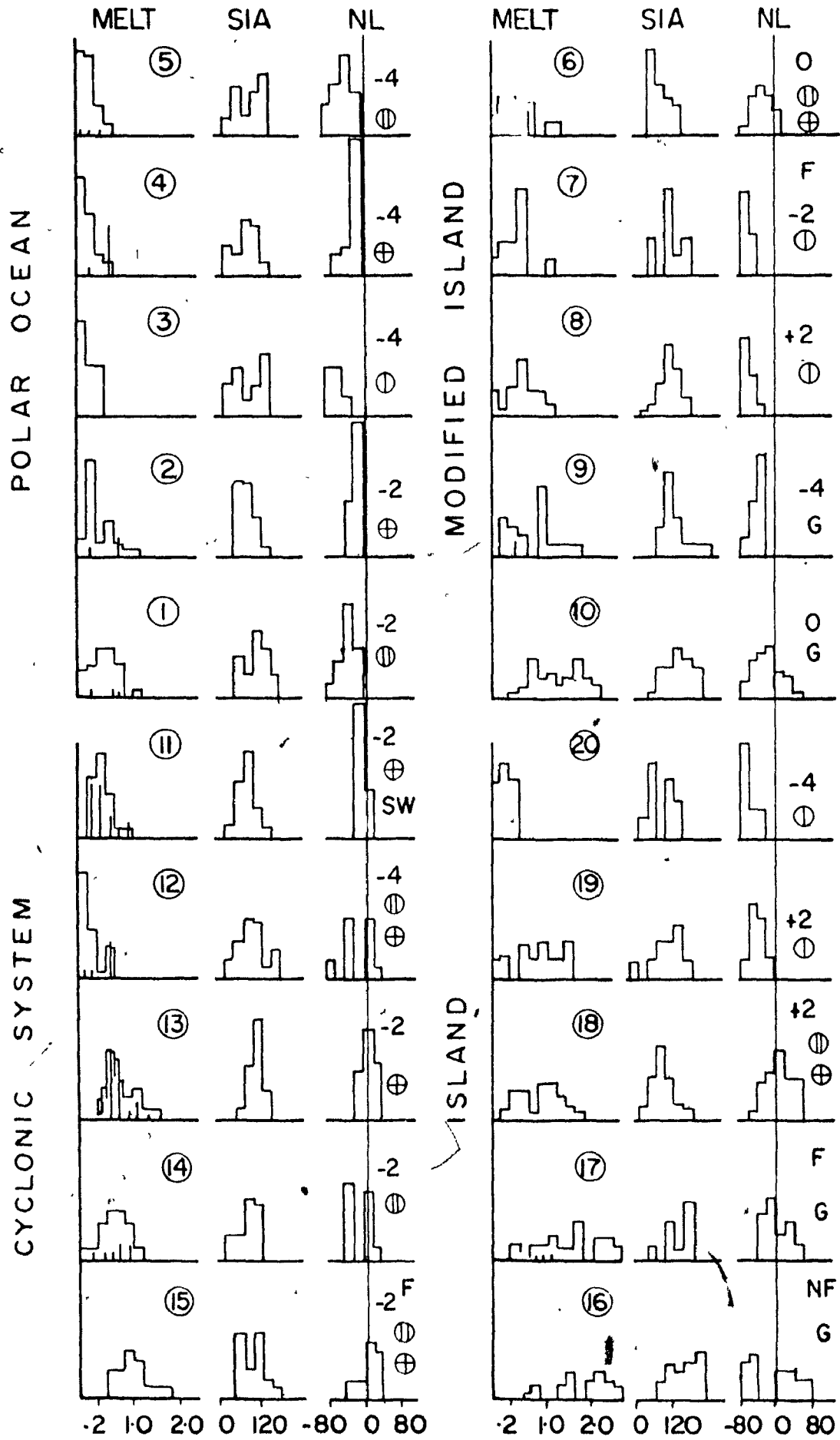


Figure 2: 2c Frequency Distribution in Classes - Melt, SIA (Solar Absorbed Radiation), NL (Net Long Wave Radiation)

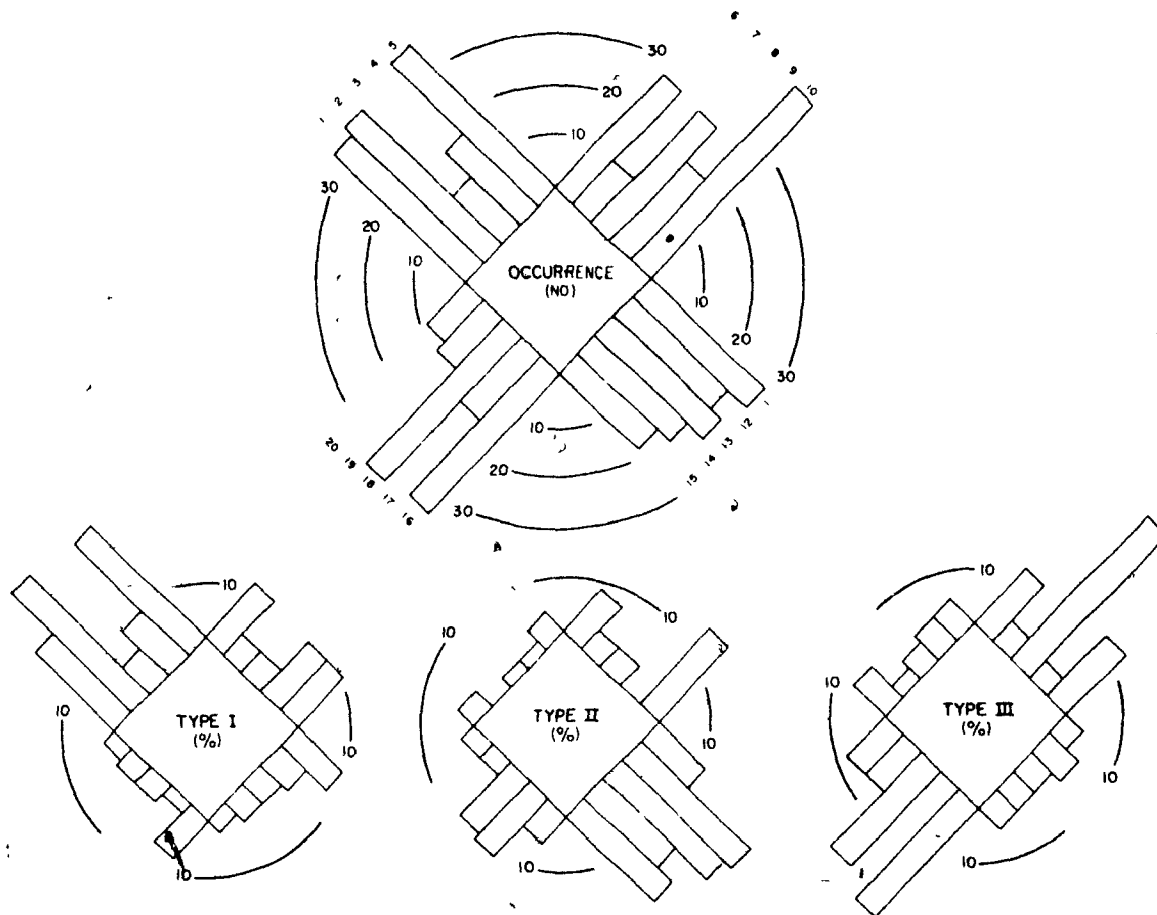


Figure 2: 2d Frequency of Occurrence of Classes and Percent Occurrence of Classes in Circulation Types

System Conditions, the snow pack Modified Island Conditions and the cold clear Island Condition class, show single modes and reasonably significant differences in Energy Balance regimes between classes. The N'ly glacier ice conditions tend to be bimodal, probably due to sky cover variations within these rather broad classes. The Island Conditions and S'ly glacier conditions show considerable variation within a class due, in the case of Island Conditions, to a difference in cloud height and, in the case of glacier conditions, to both sky cover and temperature differences. These variations were tolerated in view of the fact that the purpose of the present study is to examine the processes which inhibit or counteract ablation.

In Figure 2: 2d the number of occurrences of each class and the percent occurrence of classes in each circulation Type are plotted. All classes contain more than 10 values and, with the exception of the scattered sky cover classes, the six years of data is reasonably evenly distributed between classes.

Type I dominates the Polar Ocean conditions and there are a considerable number of Type I occurrences with N'ly glacier ice conditions. The warm scattered and overcast NW'lies (see Figure 2: 2a) of class 6 include a number of Type I circulations. The only other significant occurrence of Type I's is found with the cold, wet, SW'ly Cyclonic System Conditions which are likely a result of the encroachment of the Baffin Bay low into the Meighen Island region.

Type II circulation shows mainly as Cyclonic System Conditions, though several warm NE'lies and a considerable number of N'ly glacier ice occurrences result from passage of a system south rather than north of Meighen Island.

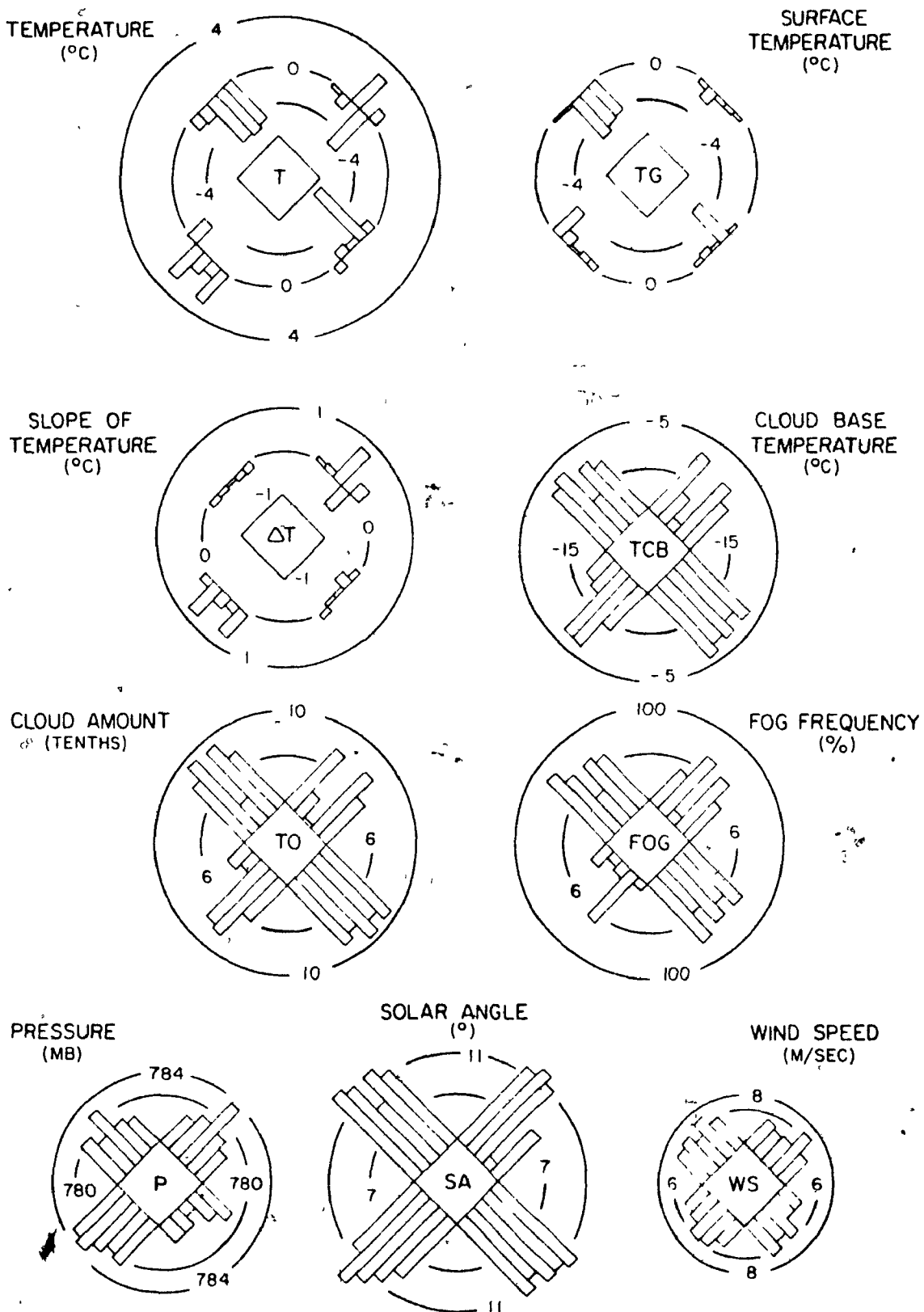


Figure 2: 3a See Foldout portion of Figure 2: 2a and Appendix I for Legends.

Type III dominates the Island, Modified Island and S'ly glacier ice (without fog) Conditions. Warm glacier ice N'lies also have a significant number of Type III occurrences.

In general the class and synoptic conditions relate in the expected manner to the circulation Types.

The synoptic energy balance diagram appears to be a reasonably good indicator of both the mass balance conditions and of the synoptic reasons behind the energy balance climate.

2:3 Energy Balance Regimes of the Classes

The energy balance regimes of the classes and thus of the Conditions and Types will now be examined, using plots of the components on the SEB Diagram. Reference should be made to Figures 2:2 a, b, c and d as well as to 2:3 a, b and c* in the discussions that follow.

2:3.1 Polar Ocean Climate

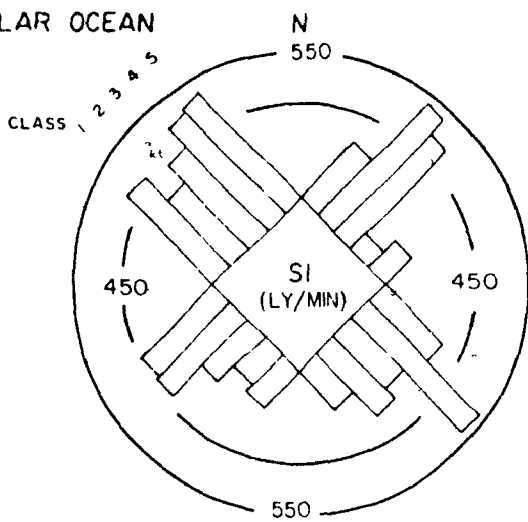
The early season cold Polar Ocean flow (class^d 3, 4, 5) with 75% occurrence of fog, results in mean ablation of less than 0.1 cm/day and modal ablation of 0 cm/day. The temperature lapse conditions in the lowest meter produce negative values of sensible and latent heat.

Under overcast or scattered sky cover, strong winds and low pressures are experienced. The cold thin fog allows high insolation but this is somewhat compensated for by high albedo values. Long wave incoming radiation is low from this cold fog and cloud.

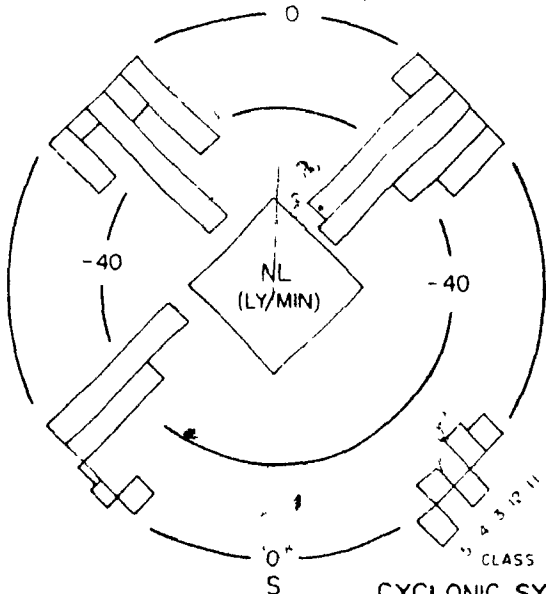
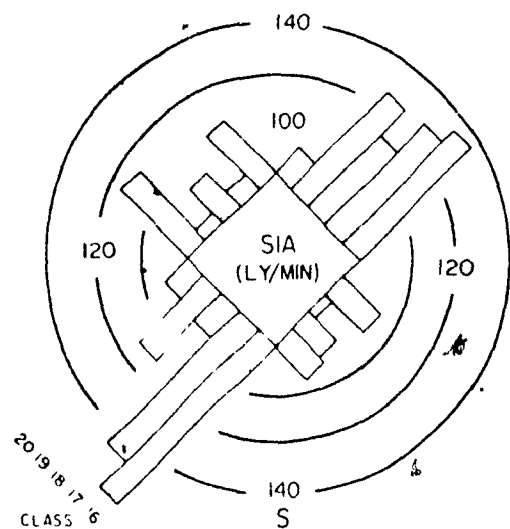
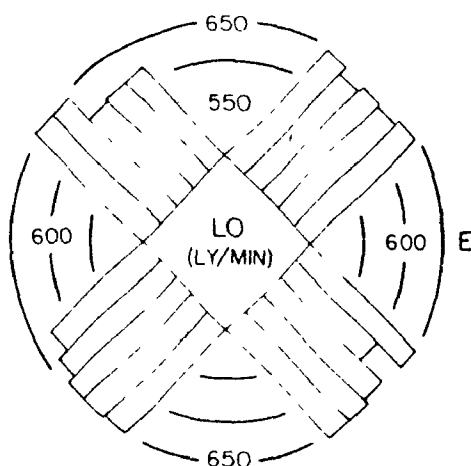
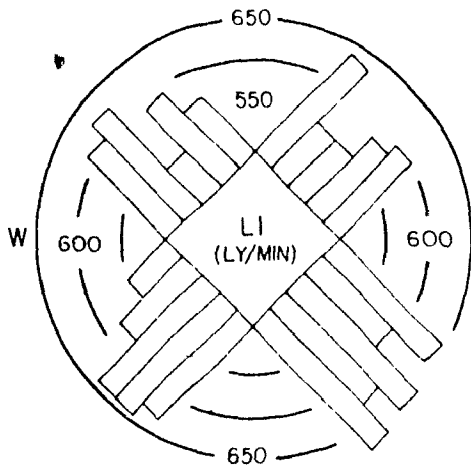
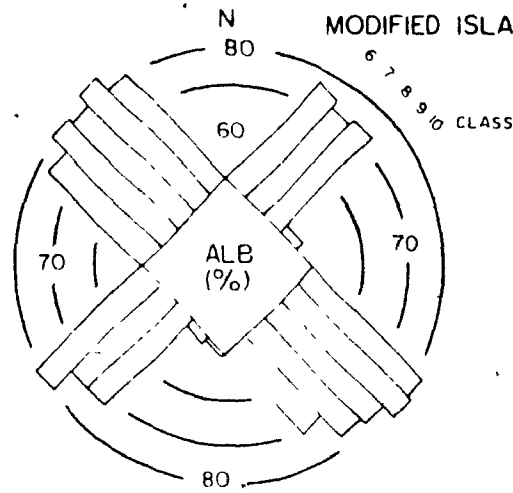
Broken conditions (class 5) produce the lowest mean values of melt, due to a 20 ly/day more negative net long wave balance than is exper-

* Figures 2:3a, b and c are also found on removable chart in pocket at back of text to aid in following the discussions.

POLAR OCEAN



MODIFIED ISLAND



ISLAND

CYCLONIC SYSTEM

Figure 2: 3b

SEB Diagrams of Radiation Components (SI = Solar Incoming Radiation, LI = Long Wave Incoming Radiation, SIA = Solar Absorbed Radiation, ALB = Albedo, LO = Long Wave Outgoing Radiation, NL = Net Long Wave Radiation)

enced with overcast conditions. Warm air advection reaches a minimum in this class. The average precipitation exceeds the melt for cold scattered conditions resulting in a positive summer mass balance.

Overcast cold Polar Ocean conditions (class 4) have lower insolation but the increased long wave incoming radiation more than compensates for this. Precipitation is still more than sufficient to counterbalance the ablation, producing a positive summer mass balance.

Scattered cold Polar Ocean fog (class 3) results in very low incoming long wave radiation. As these conditions tend to occur either early or late in the season, the solar angle is low and insolation is consequently low. The turbulent fluxes are less negative than for cloudy conditions but the resulting ablation is very similar to that of the other Polar Ocean classes.

For NW sector winds with temperatures greater than or equal to -2°C but less than 0°C , (classes 1 and 2) fog is even more frequent. Lapse conditions prevail and turbulent fluxes are negative. The thicker warmer cloud and fog transmit less solar incoming radiation and re-radiate more long wave radiation.

With overcast skies (class 2) insolation is low and albedo high. The greater values of long wave incoming radiation and less negative values of the turbulent fluxes result in average melt of .2 cm/day, with precipitation of .09 cm/day. This is still not sufficient to melt the winter accumulation.

For broken conditions (class 1), solar radiation absorbed at the ground is rather high, due to low albedo, and combined with the long wave incoming radiation of the cloud results in ablation greater than .3 cm/day which is not compensated by precipitation.

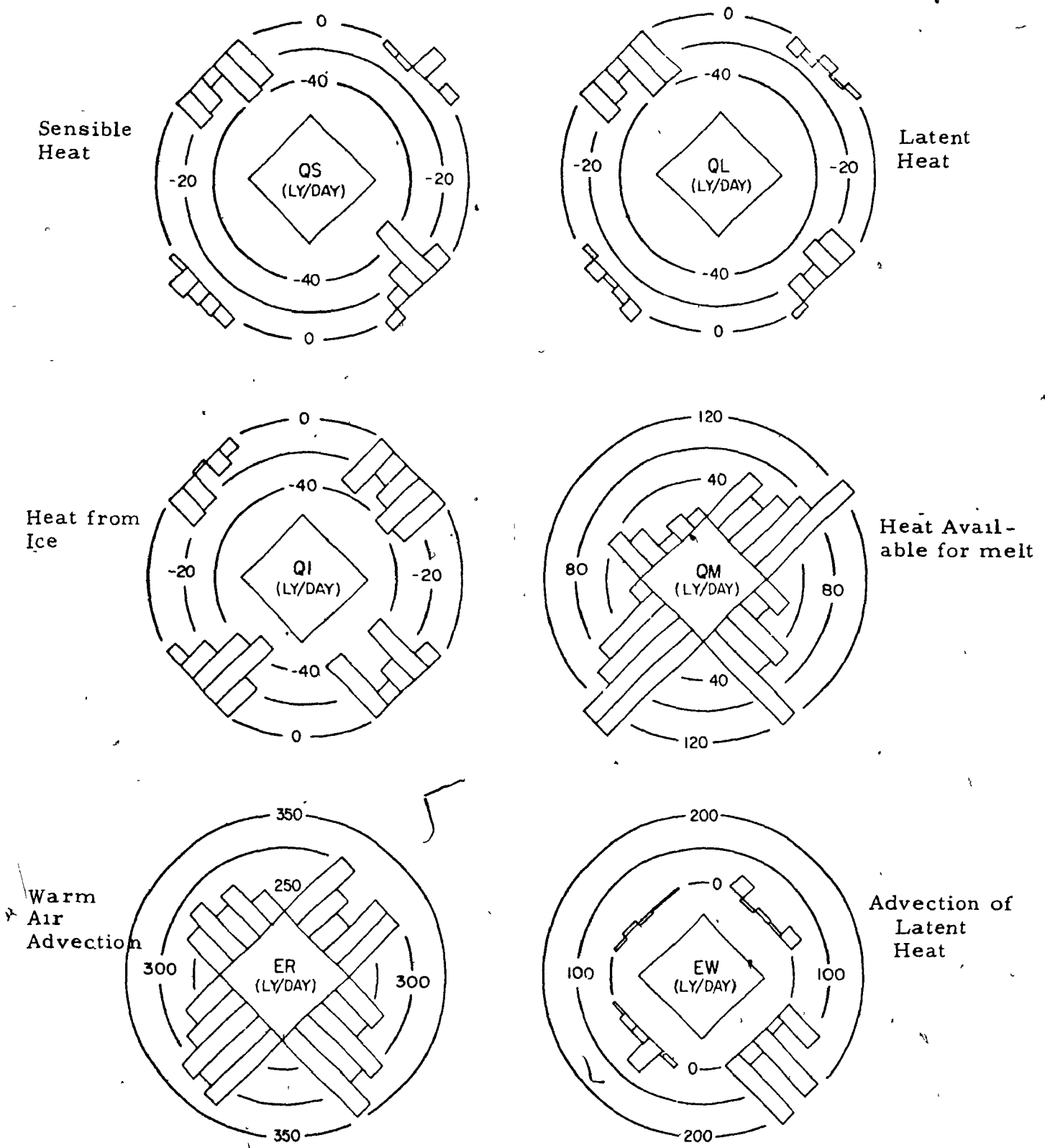


Figure 2: 3c SEB Diagrams for other Energy Balance Components

The NW'lies in class 7 (0 to -2°C , scattered, fog) are associated with Polar Ocean Circulation and account for the .2 cm/day values in the ablation histogram.

Type I circulation occurring over glacier ice late in the season is accompanied by cold temperatures, high fog and cloud amounts, strong winds and lapse conditions in the lowest meter (class 9). Insolation is low due to the low solar angle but the glacier ice albedo is responsible for relatively large values of solar radiation absorbed at the ground. The long wave incoming values resemble those of cold overcast NW'ly flow. The turbulent fluxes are just slightly negative. The bimodal distribution of melt, a reflection of varying sky cover conditions, shows a maximum at .2, .4 and .9 cm/day (the very high values resulting from a few cold clear occasions of Type III circulation). Some of the warm N'lies over glacier ice (class 10) are also a result of Polar Ocean Circulation and appear as the .6 cm/day mode in the ablation distribution.

2: 3.2 Modified Island Climate

Scattered cloud conditions with above freezing temperatures and NE sector winds emerge as the main class of Modified Island Conditions (class 8). Fog is infrequent, the pressure high and the winds light. The insolation values are reasonably high, but net long wave radiation is very negative due to the lack of cloud. Sensible heat values reach a maximum under these conditions, and latent heat values are positive. There is no precipitation, and ablation values average close to .5 cm/day.

Scattered conditions with below freezing temperatures, high fog

occurrence, and NE'ly flow (class 7) show a temperature inversion in the lowest meter suggesting "real fog" (II 5: 2. 1). The ablation in these situations is slightly less than that under the warmer fogless clear skies, due to the very small positive (and sometimes negative) values of the turbulent fluxes.

Type III circulation can also produce scattered or overcast skies with temperatures near or above freezing during the transition to clear skies (class 6). Under these conditions solar absorbed values are low, while net long wave radiation is only slightly negative and the resulting melt values are somewhat lower than for the scattered Modified Island class.

Modified Island conditions over glacier ice (class 10) show positive turbulent fluxes and high values of solar radiation absorbed at the ground (though insolation is low). The sky conditions tend to be scattered, with 50% occurrence of fog, thus long wave incoming values are not particularly low. Melt under these conditions appears from the bimodal histogram to lie in the 1.5 cm/day range.

2: 3.3 Cyclonic Activity Climate

All the Cyclonic System conditions have cloudy skies, high fog frequency, low pressures and relatively warm cloud base temperatures, suggesting low ceilings. There did not appear to be any significant difference between below freezing conditions with and without fog.

Before the passage of the front and/or trough, SE winds, temperatures around -1°C , low pressures and strong winds prevail (class 13 and 14). Lapse conditions in the lowest meter produce negative turbulent fluxes.

With overcast skies (class 13), insolation is low and albedo high resulting in very low values of solar radiation absorbed at the ground. Due to the positive long wave radiation balance, produced by the thick warm cloud, melt is considerable (ca. .7 cm/day). The precipitation accompanying these conditions is sufficient to counteract this melt and a slightly positive mass balance ensues. In the troposphere there is considerable warm air advection.

When the sky cover is broken (class 14), absorbed solar radiation increases but the net long wave balance is slightly negative, resulting in somewhat less melt than with overcast skies. The broken conditions are accompanied by considerably less precipitation, thus the mass balance remains negative.

If the warm sector reaches as far north as Meighen Island, temperatures rise above freezing as in class 15 and part of class 18. This strong SE sector flow is accompanied by low pressures and high fog and cloud amounts. Inversion conditions persist in the lowest meter and turbulent fluxes are positive. Though depletion of solar incoming radiation is great, due to the nature of the sky cover, low albedos partially compensate for this effect. The warm clouds produce a maximum of long wave incoming radiation and hence the greatest positive net long wave balance of any class. High melt values result (ca. 1. cm/day), and precipitation is insignificant by comparison. Warm air advection also reaches a maximum in this class.

If the low passes further north of Meighen Island, winds may never become SE'ly. Class 11 probably represents such occurrences as well as occasions where Type I circulation is in effect but the Baffin Bay low has moved N into the Polar Ocean and dominates the flow over the Meighen Island region. Overcast skies and below freezing temperatures

result in moderate values of solar radiation absorbed at the ground, in somewhat negative net long wave radiation and in negative turbulent fluxes. The melt is less than is experienced with SE'lies which advect island air into the sounding. Precipitation accompanying this SW'ly flow produces an average net summer accumulation of .4 cm/day, which is twice the average winter accumulation.

There are also occasions when the system passes south of the Island, producing conditions similar to the SE'ly cyclonic passage conditions but with NE'ly flow (see class 6).

When frontal activity occurs over glacier ice, the solar absorbed radiation increases considerably but, as this is not the dominant feature of the cyclonic system energy balance, melt values increase only to .8 cm/day. Precipitation in the form of snow is not very significant so considerable mass loss results from such occurrences.

2: 3.4 Island Climate

Island climate conditions in summer (classes 16, 18 and 19) are characterized by above freezing temperatures, high pressure, low wind speed and low frequency of fog. Similar average melt values are associated with cloudy Island flow and clear Island flow but for different reasons.

In the case of cloudy skies (class 18), long wave incoming radiation is high giving a net long wave balance close to zero. The bimodal distribution of melt likely results from differences in cloud height. Low cloud occurs in connection with the warm sector of Type III circulations while middle and high cloud dominate with Island conditions.

With scattered conditions (class 19), solar radiation absorbed at the

ground dominates, the net long wave balance being quite negative due to lack of cloud. The turbulent fluxes are significantly positive. These conditions result in melt values between .2 and 1.6 cm/day depending on the relative values of the radiation terms.

Southerly Island flow over glacier ice (class 16) is most frequently of the cloudy variety. The increase in solar radiation absorbed at the ground results in melt values of between 1.5 and 2.6 cm/day. With the increased importance of solar radiation at low albedos scattered conditions likely account for the highest mode (ca. 2.0 cm/day), while the infrequent Type I and Type III occurrences give melt values in the .6 - .8 cm/day range.

The final class (20) represents the cold clear fogless weather which occurs in April and May when anticyclonic activity dominates the Arctic Islands, and which can also be experienced in early June. Though surface temperatures average below freezing, inversion conditions prevail in the first meter. Sensible heat fluxes are slightly positive, but low humidities above the surface result in slightly negative latent heat flux values. Albedos are high, long wave incoming radiation is at a minimum and the solar angle is still relatively low. As a result, melt is frequently zero and does not exceed .4 cm. These conditions are most frequently accompanied by NE'lies or SW'lies and represent Island conditions occurring before the snow melt begins on the land.

Table 3: 1

Summer Season Means of Climatic and Energy Balance Components

	1960	1961	1962	1968	1969	1970
TG ($^{\circ}$ C)	-0.9	-1.4	-0.3	-1.0	-1.1	-2.0
SGI (ly/day)	348	386	421	446	436	461
ALB (%)	63	66	71	77	75	81
SGA (ly/day)	101	118	150	103	102	86
DFL "	627	620	618	606	622	613
RLU "	645	639	649	642	641	634
NL "	-19	-19	-31	-35	-27	-21
QS "	4	-5	-1	-16	-15	-16
QL "	0	-5	-3	-15	-13	-12
QI "	28	34	32	13	12	14
QM "	103	91	114	36	55	38
RO (cm we)	75	64	93	18	48	26
SN "	0	6(21)	10	10	26	17
Net "	-75	-58(-43)	-83	-8	-22	-9

TG = surface temperature, SGI = solar incoming radiation,
 ALB = albedo, SGA = solar absorbed radiation, DFL = long
 wave incoming, RLU = long wave outgoing, NL = net long
 wave, QS = sensible heat, QL = latent heat, QI = heat
 from ice, QM = heat available for melt, RO = melt,
 SN = snow, Net = Net summer mass balance.

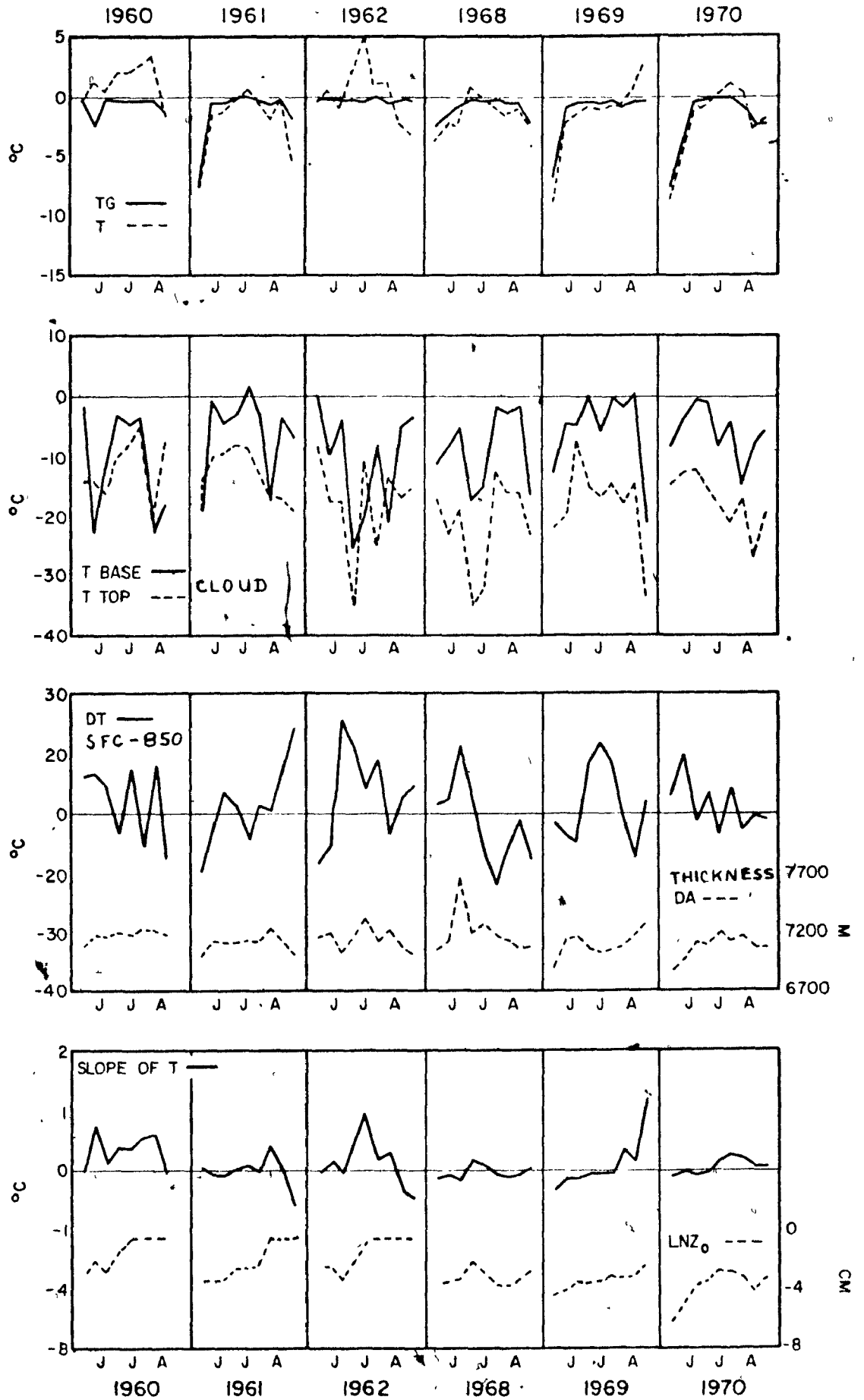


Figure 3: 1a

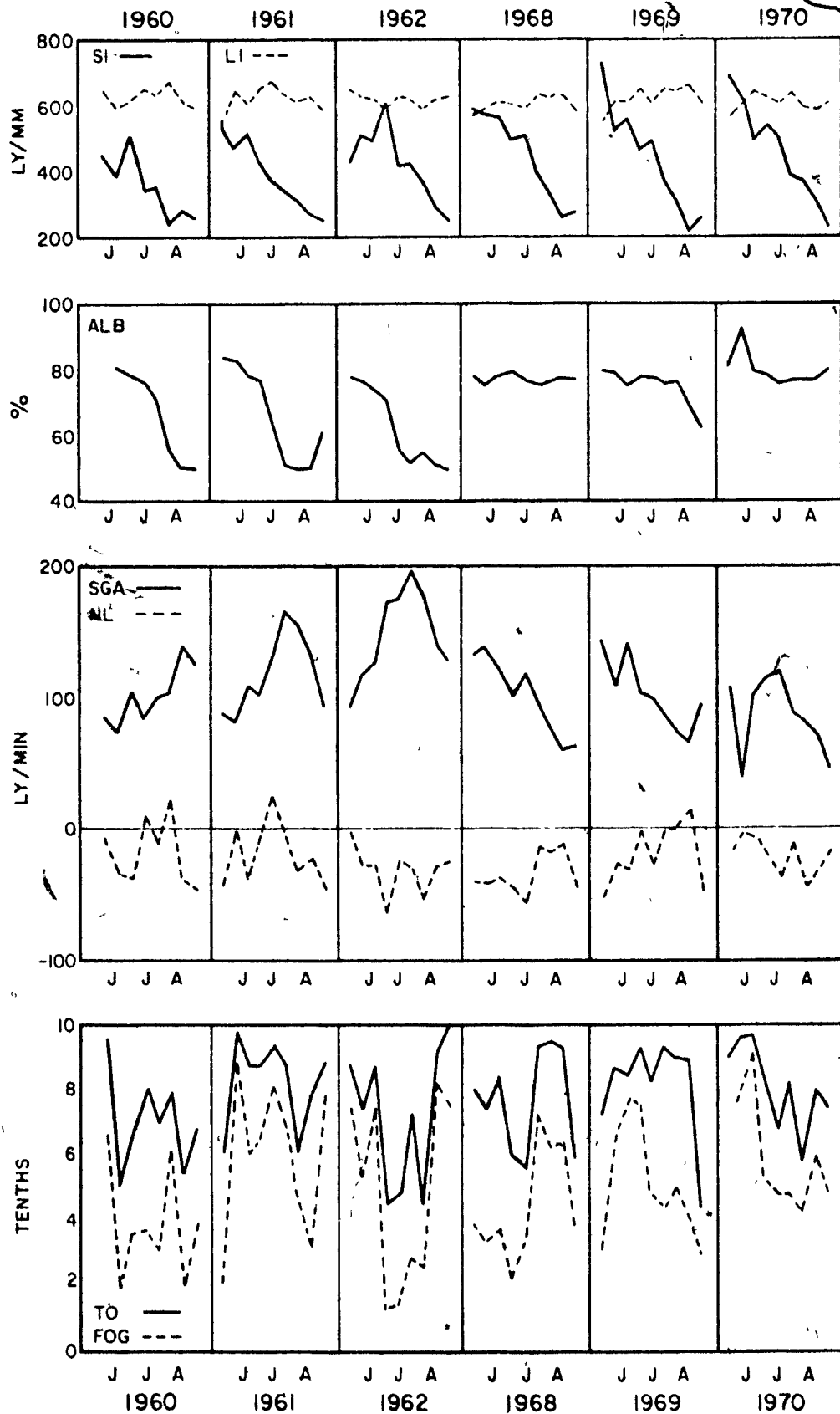


Figure 3: 1b

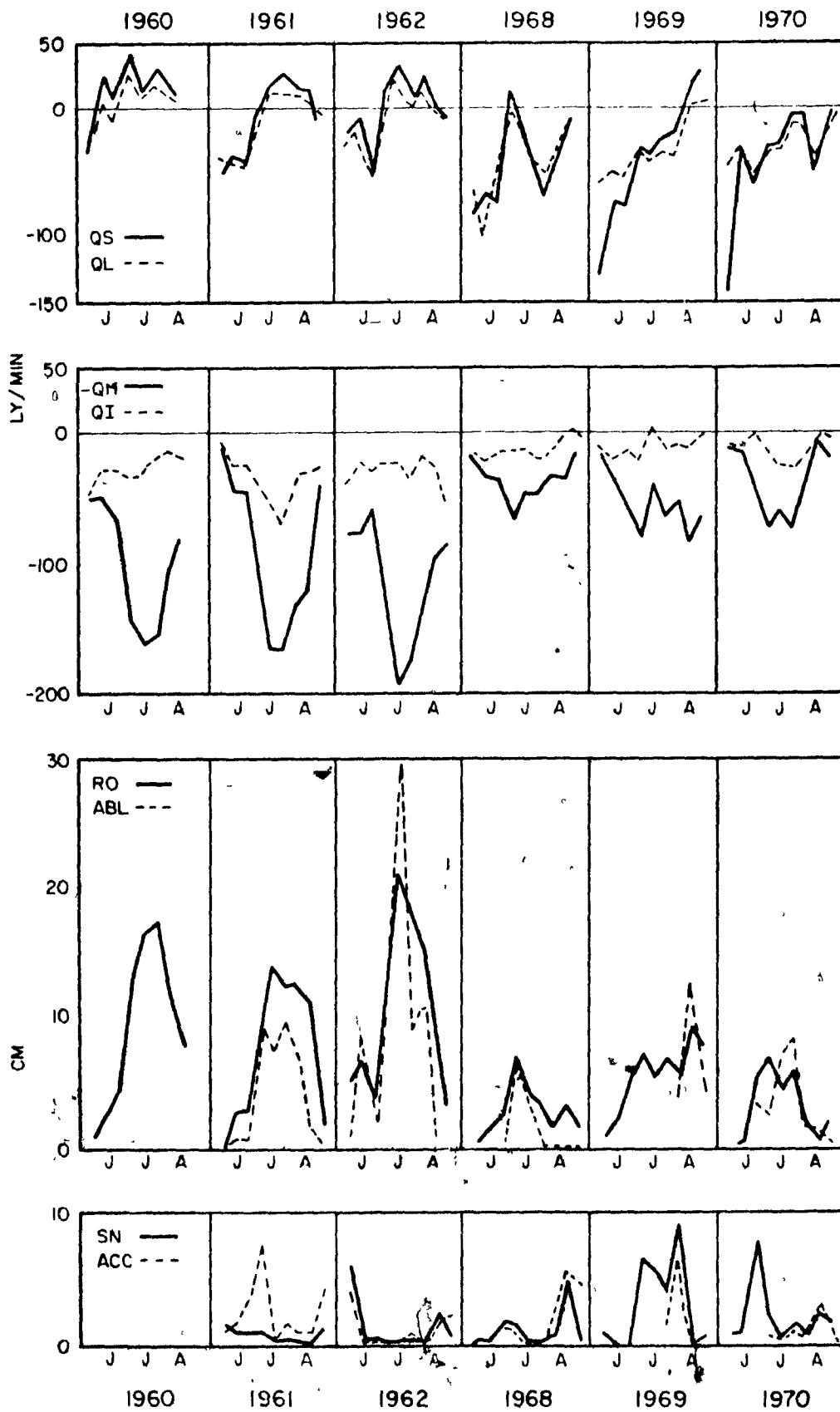
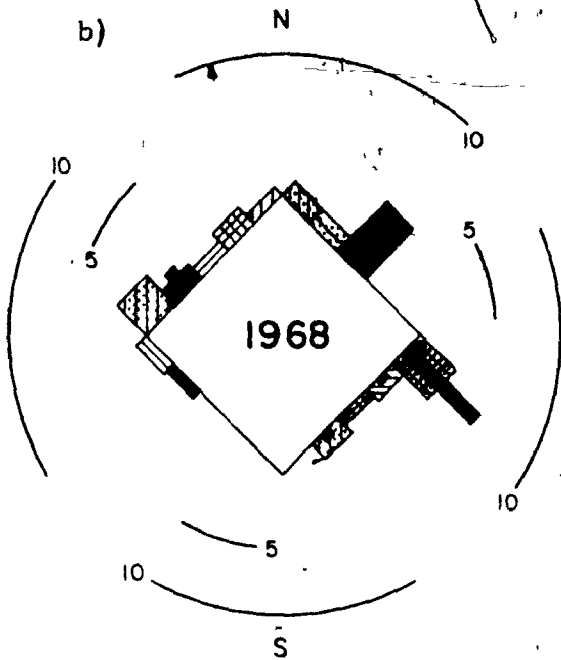
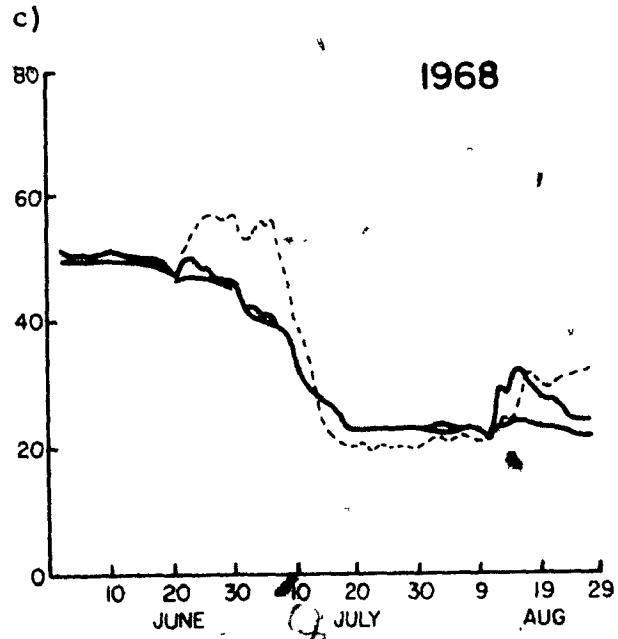
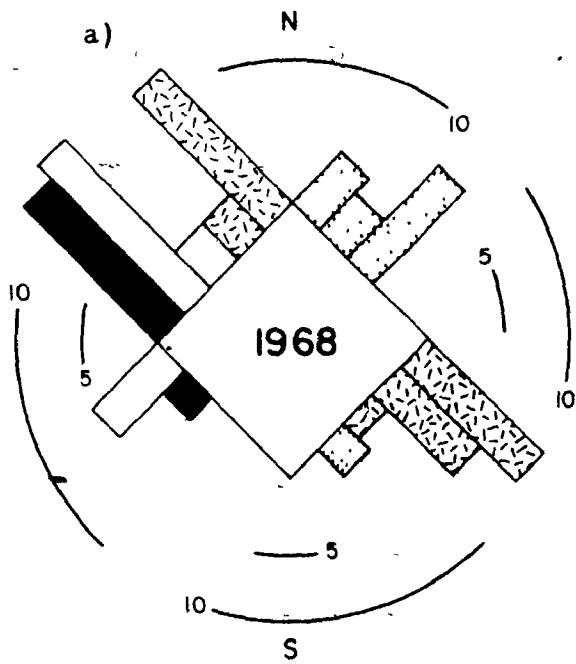


Figure 3: 1c



- a) SEB Diagram of % Occurrence of Classes - see Appendix I Foldout for Legend
- b) SEB Diagram of Total Summer Ablation and Accumulation (cm we) - see Figure 2: 2a Foldout for Legend
- c) Daily Plot of Surface Height (cm)

Figure 3: 2 Energy and Mass Balance of 1968

CHAPTER 3

CHARACTERISTICS OF THE SIX SUMMER SEASONS

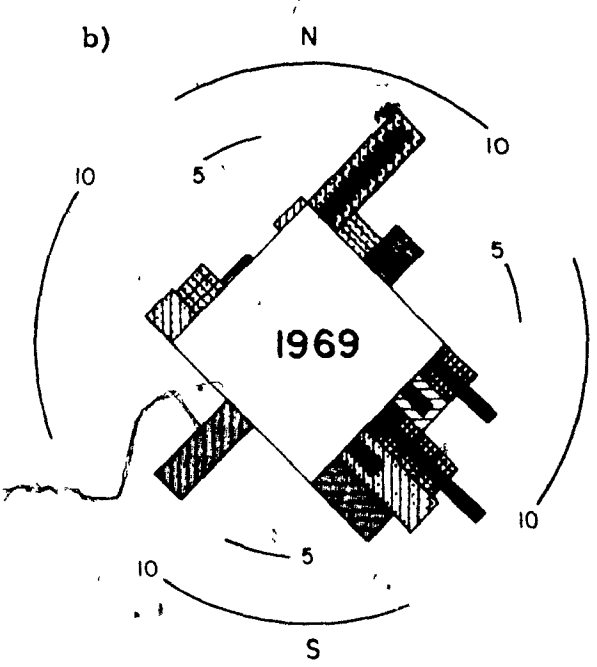
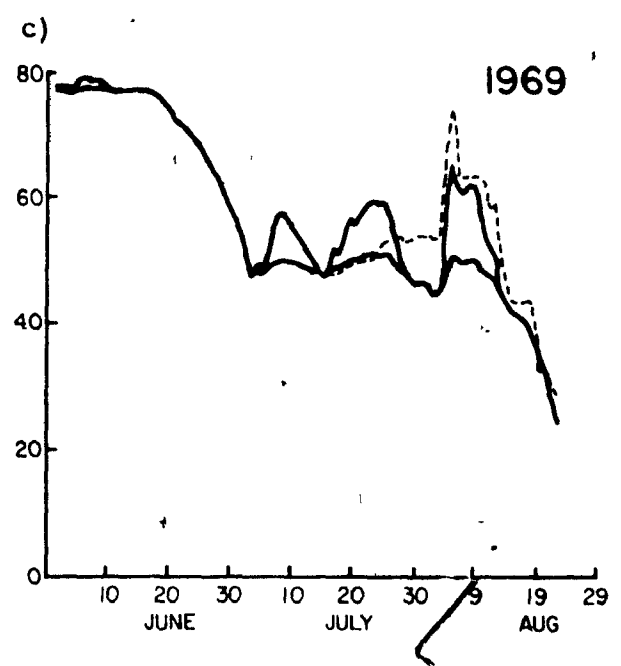
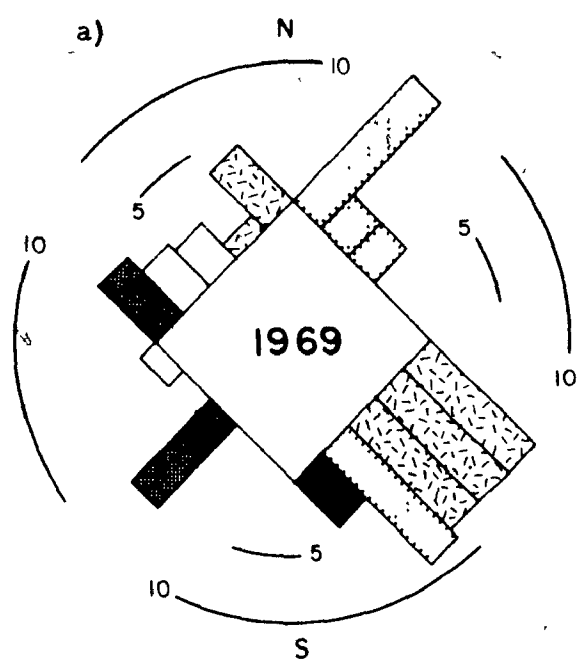
3: 1 Introduction

The climate and energy balance of each year is examined, using the SEB diagram in order to isolate the factors governing the summer mass balance of the individual years. Two SEB diagrams are presented for each year. The first gives the total melt and precipitation amounts for each SEB class, the bars being shaded according to the climatic limits of the class. The second shows the percent occurrence of each class, the bars shaded according to the mean net summer mass balance for that class (see Ch. 2 for discussion of the divisions). Additional information concerning the climate and energy and mass balance of the years is given in Table 3:1 (season means) and in Figures 3:1 a, b and c (ten-day means). Reference should also be made to the discussions and Figures of II 2 and 3.

The Polar Ocean years will be examined first, followed by the Island years.

3: 2 1968

N'ly Polar Ocean, Type I flow, was completely dominant in 1968. A brief period of cool Island flow in June initiated the melt. The temperatures in early June were higher than in other Polar Ocean years and fog amounts were relatively low, but the constant N'ly flow held the melt to less than .25 cm/day. At times during late June and early July the Baffin Bay low dominated in Type I flow, and the



- a) SEB Diagram of % Occurrence of Classes - see Appendix I Foldout for Legend
- b) SEB Diagram of Total Summer Ablation and Accumulation (cm we) - see Figure 2: 2a Foldout for Legend
- c) Daily Plot of Surface Height (cm)

Figure 3: 3 Energy and Mass Balance of 1969

cool SW'ly cyclonic Conditions (class 11) ensued. These occurrences were responsible for reasonably high melt values but also produced considerable precipitation, resulting in net accumulation.

A period of clear warm Modified Island flow (class 8), in early and mid-July, produced the only significant melt. Positive values of the turbulent fluxes, resulting from advection of warm air over the Ice Cap, were largely responsible for the relatively strong melting in these two periods.

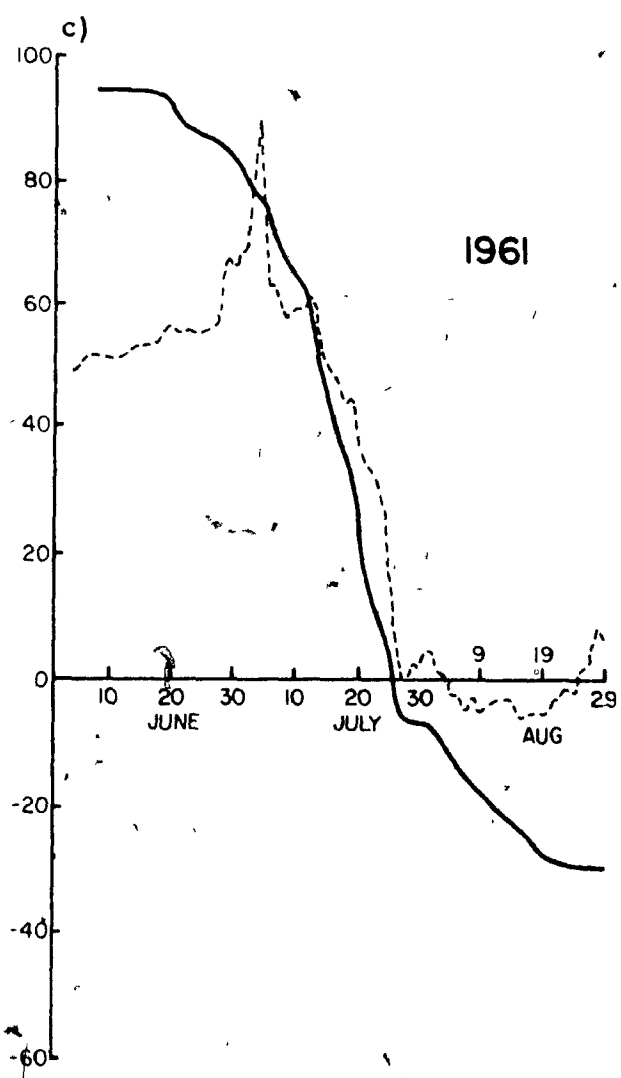
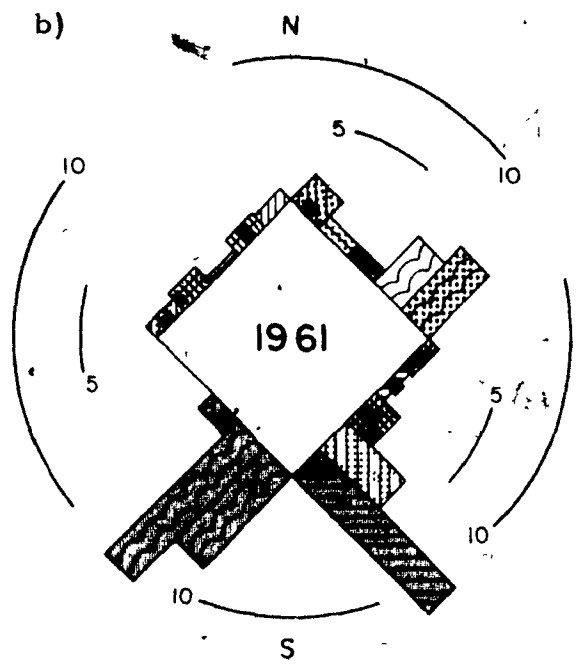
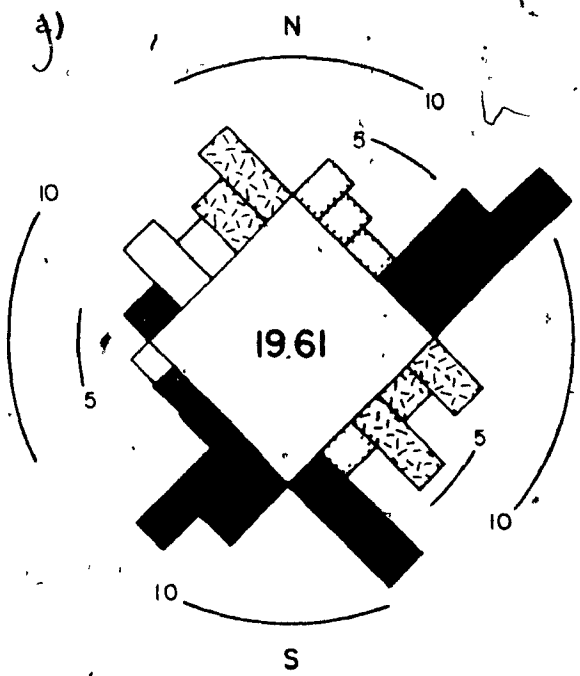
In late July and early August Polar Ocean flow took over once more. The constant rime and freezing drizzle deposited on the surface by the cool fogs accompanying this flow kept the albedo high and thus melt was negligible. Melting resumed late in the season, when Cyclonic System Conditions (mainly SE'lies) advected warm moist air over the Island, producing near positive values of the turbulent and net long wave fluxes and depositing considerable precipitation.

3:3 .1969

Cyclonic Activity Conditions dominated 1969. All classes of these conditions are well represented, including the NE'ly class (low passing S of the Island). Type I occurred in the beginning and at the end of the season, with the usual low melt values.

Low albedos (seen in both measured and calculated albedo curves) in late June were responsible for considerable melt at that time. The albedo values appear to be a result of rain accompanying NNE'ly flow, associated with a low tracking S of Meighen Island into Baffin Bay.

By July, Cyclonic System Conditions were established and the



- a) SEB Diagram of % Occurrence of Classes - see Appendix I Foldout for Legend
- b) SEB Diagram of Total Summer Ablation and Accumulation (cm we) - see Figure 2: 2a Foldout for Legend
- c) Daily Plot of Surface Height (cm)

Figure 3: 4 Energy and Mass Balance of 1961

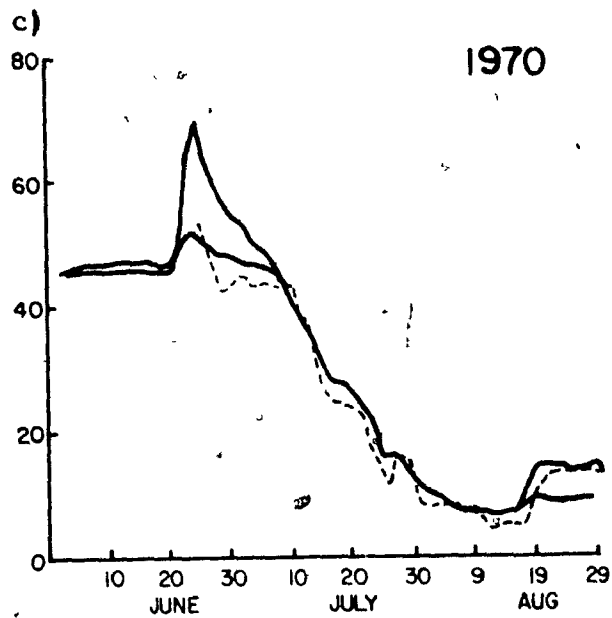
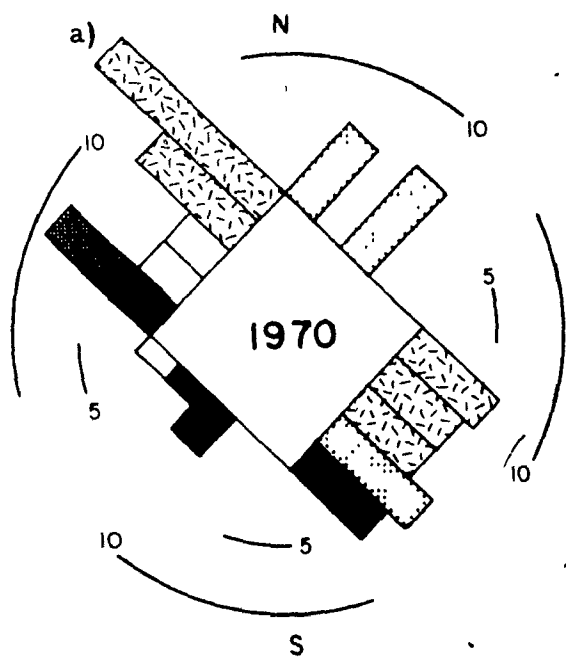
continuous passage of systems along the NW edge of the Islands produced high values of melt and precipitation while holding screen temperatures below freezing.

In mid-August the end of a cyclonic passage developed into cloudy Island flow (class 18), and high values of the turbulent and net long wave fluxes resulted in considerable melt at Main Ice and mean temperatures above freezing. Melt continued as clear Modified Island Conditions (Class 8) replaced the S'ly Island Conditions. The last few days of August saw the return of Polar Ocean Conditions and freezing temperatures.

3: 4 1961

As in 1969, Polar Ocean Conditions occurred at the beginning and end of the season, with the accompanying low melt values. Throughout June surface height measurements indicate steady accumulation. Heavy drifting and blowing snow, associated with strong pressure gradients between the Baffin Bay low and Polar Ocean High, are partially responsible for this accumulation. The surface height measurements show accumulation of close to 40 cm in late June and early July. This accumulation was not reflected in precipitation measurements due to the difficulties of measuring precipitation in strong winds. (In the calculations 40 cm was added to the initial depth of the snow pack to account for this accumulation.)

By mid-July cyclonic systems of the warm sector class (class 15) dominated. Melt proceeded rapidly and was not accompanied by solid precipitation, leading to complete loss of the snow pack. Once glacier ice was reached the calculated melt values increased considerably due



- a) SEB Diagram of % Occurrence of Classes - see Appendix I Foldout for Legend
- b) SEB Diagram of Total Summer Ablation and Accumulation (cm we) - see Figure 2: 2a Foldout for Legend
- c) Daily Plot of Surface Height (cm)

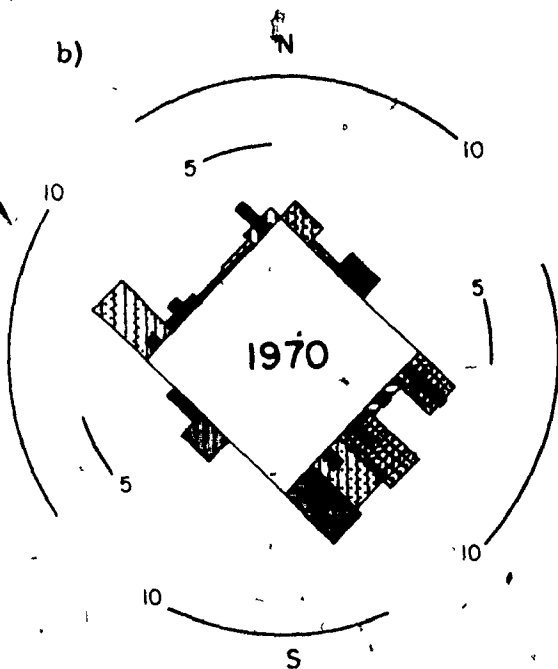


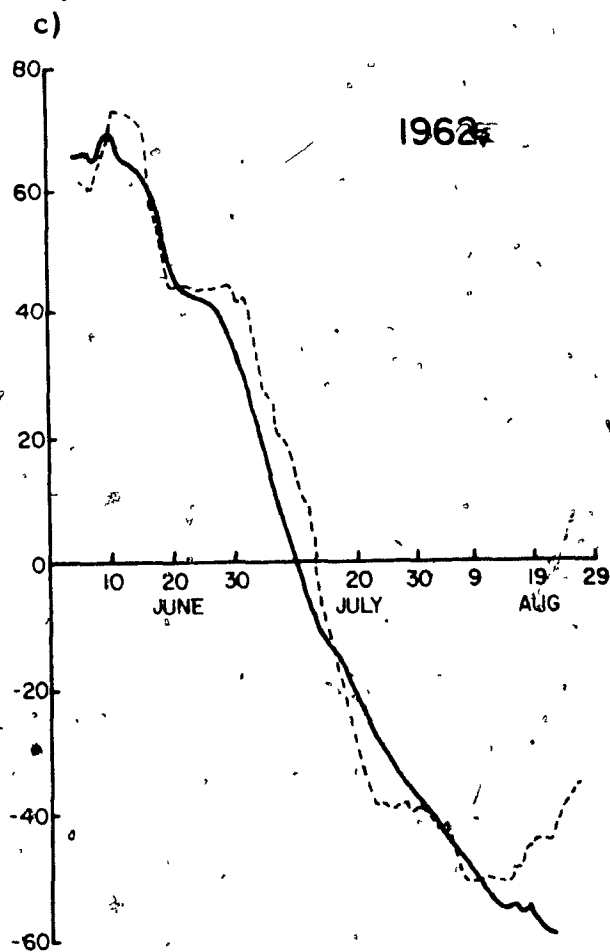
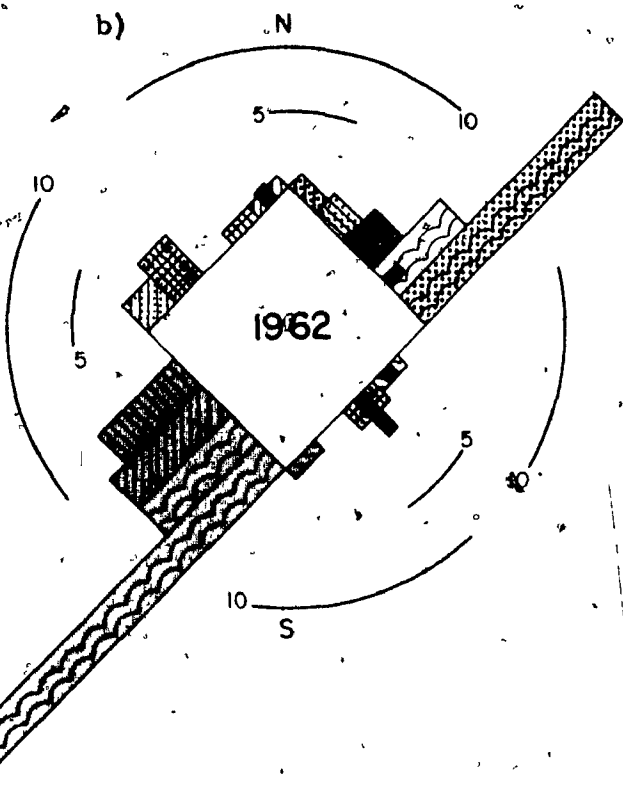
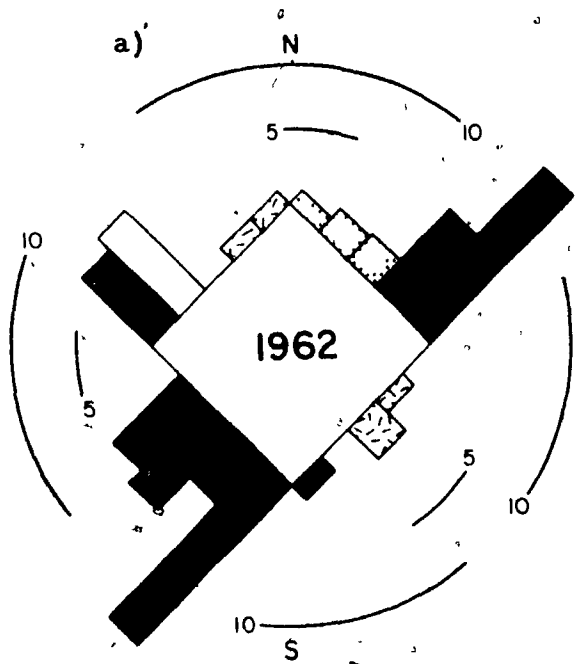
Figure 3: 5 Energy and Mass Balance of 1970

to the low albedo. The Cyclonic System Conditions occurring over glacier ice were not accompanied by solid precipitation and produced significant melt for the remainder of July and early August in the calculations. In August Polar Ocean and Island conditions alternated, but both caused melt until late August when persistent Polar Ocean conditions succeeded in depressing temperatures and melt.

Examination of the surface lowering measurements for the period after glacier ice is reached suggests continuous accumulation of snow during this period. Such conditions would drastically alter the energy budget for the period via albedo, in addition to compensating melt with accumulation. If the ice surface was repeatedly covered with snow, and the albedo held at 75% during this period, calculated melt would be decreased by 28 cm water equivalent or 31 cm surface height, and the calculated curve would agree with the measured surface height. The effect of this is further discussed in 4.

3: 5 1970

The season began with unusually cold Polar Ocean Conditions. There was no melt until late June when Type I flow was repeatedly replaced by the other two types, resulting in Type IV circulation. This rapidly changing circulation resembled Cyclonic System Conditions, which due to the periods of Polar Ocean and Island flow, yielded less precipitation than pure Type II Cyclonic System Conditions. Rain and relatively warm temperatures accompanying an early occurrence of this type decreased the albedo, resulting in a mid-season peak in absorbed solar radiation. In June and early July this was augmented by relatively high incoming long wave radiation from warm thick cloud.



- a) SEB Diagram of % Occurrence of Classes - see Appendix I Foldout for Legend
- b) SEB Diagram of Total Summer Ablation and Accumulation (cm we) - see Figure 2: 2a Foldout for Legend
- c) Daily Plot of Surface Height (cm)

Figure 3: 6 Energy and Mass Balance of 1962

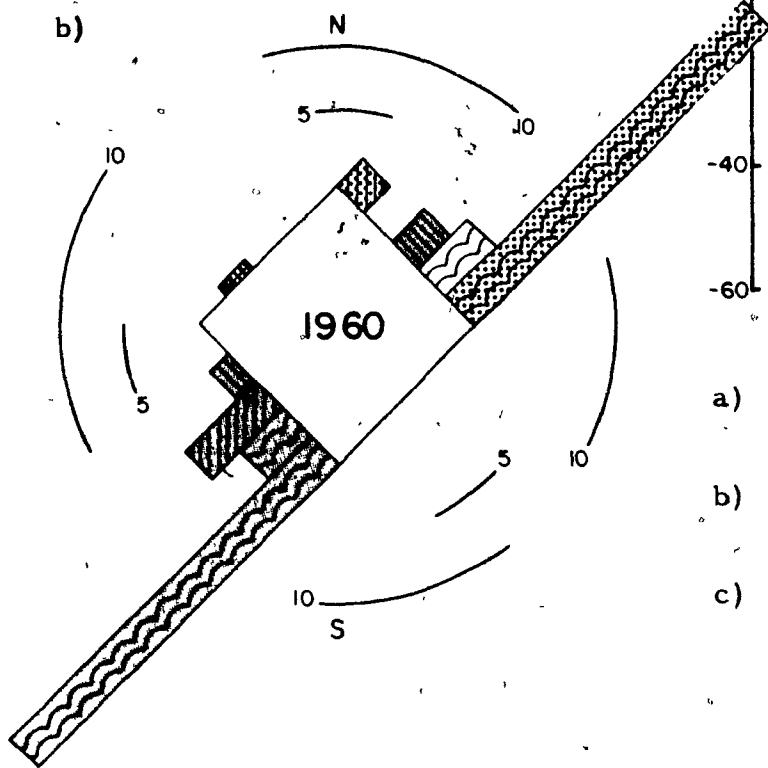
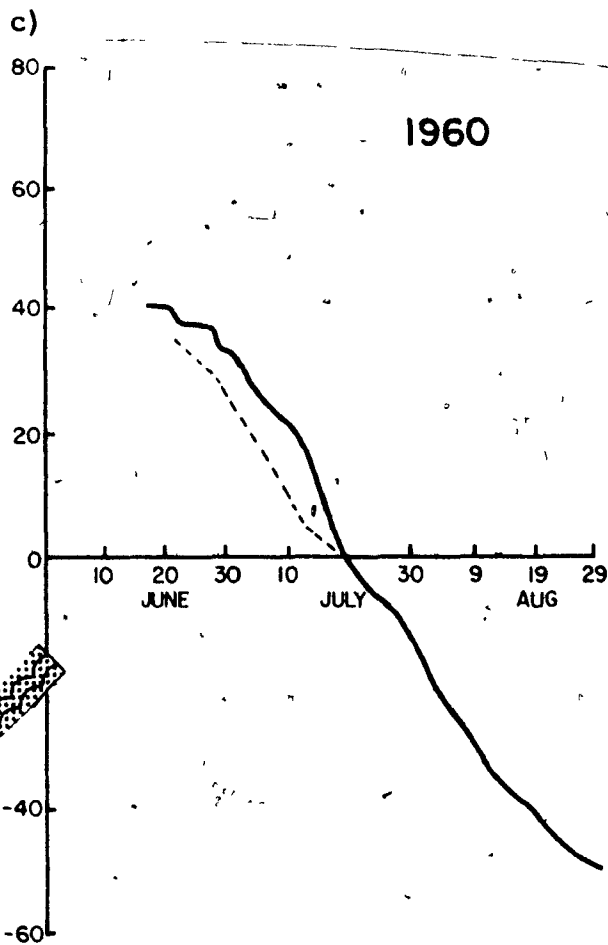
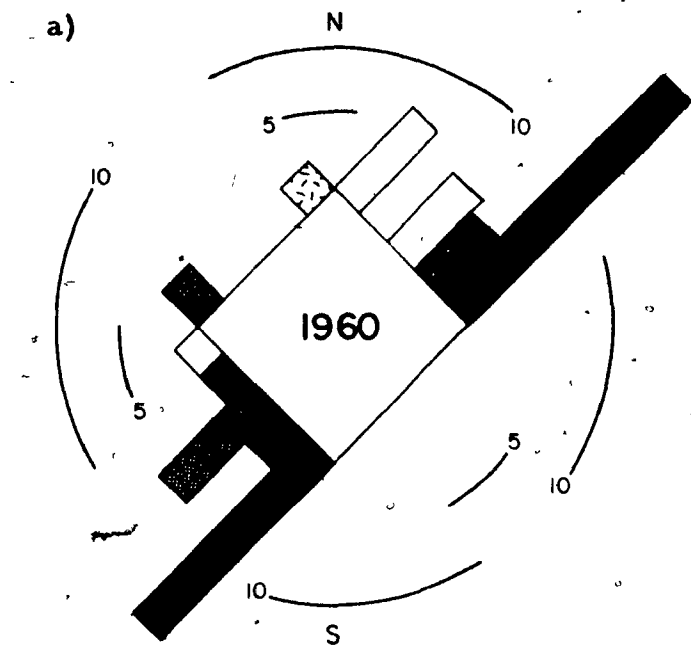
Two periods of Modified Island Conditions in mid-July and early August produced clear skies but are rather ineffectual for melting due to the high negative net long wave values. The Modified Island portions of the Type IV circulation (some of which showed up in class 1 as they were associated with N'ly winds which had recently passed over land) combined with the warm sector portions of the Type IV circulation to produce the most significant uncompensated melt in 1970.

A period of cool foggy Polar Ocean Conditions inhibited melt during mid-August. By late August fresh snow increased the albedo and solar incoming radiation was low due to solar angle. The moderate values of long wave incoming radiation were unable to balance these low values of absorbed solar radiation. Melt was insignificant while the cyclonic activity of Type IV deposited considerable snow.

3:6 1962

Island flow was established early in June, causing considerable melt and a decrease in surface albedo. These conditions were replaced briefly at the end of June by relatively warm Polar Ocean Flow. Fully developed clear Island conditions dominated July. The snow pack disappeared before mid-July and a strong mid-season peak in melt reflects the increased values of absorbed solar radiation and the accompanying positive values of the turbulent fluxes.

Though circulation began to alternate in late July, melt remained strong due to low albedo, and solid precipitation was not experienced until the last few days of the month, when a well-developed cyclonic system passed over Meighen Island.



- a) SEB Diagram of % Occurrence of Classes - see Appendix I Foldout for Legend
- b) SEB Diagram of Total Summer Ablation and Accumulation (cm we) - see Figure 2: 2a Foldout for Legend
- c) Daily Plot of Surface Height (cm)

Figure 3: 7 Energy and Mass Balance of 1960

When Polar Ocean Conditions were re-established in August, melt continued due to the low albedo of glacier ice: Surface lowering measurements suggest that the ice may have been snow covered in late August, resulting in cessation of melt at that time and in a decrease in total seasonal melt.

3:7 1960*

As in 1962 Island flow was established by early June while Polar Ocean circulation was only experienced during the transition between consecutive ridges. Island circulation alternated with the other types throughout the season, but there does not appear to have been any significant precipitation with the cyclonic systems.

The snow pack which was not deep initially had disappeared by mid-July. Melt peaked in late July due to the high albedo and remained high in early August due to positive values of net long wave radiation from the warm thick cloud and fog accompanying Island flow at this time.

The Island and Modified Island conditions of 1960 differ from those of 1962 in that they are dominantly cloudy Island conditions, where positive net long wave radiation rather than high solar incoming radiation is responsible for melt. This is perhaps a result of the frequently changing synoptic conditions of 1960, in contrast to the establishment in 1962 of a quasi-stationary high with S'ly flow and strong subsidence which tends to dissipate the fog and cloud.

Polar Ocean Conditions do not appear to take over until the last few days in August (from synoptic studies).

* The calculated values of energy balance in 1960 are least accurate due to the method of interpolating missing data and due to the lack of daily surface lowering records. However useful information can be obtained from examination of the results.

3: 8 Governing Factors

Polar Ocean Conditions completely dominate 1968, confining melt to a period of warm air advection under Modified Island conditions. The rime and fog accompanying the mid-season Polar Ocean flow was largely responsible, through albedo, for the lack of melt at that time.

1969 was controlled by Cyclonic System Conditions yielding near freezing temperatures, moderate melt values and high precipitation amounts and frequently experiencing positive mass balances. Significant uncompensated melt was experienced with cloudy Island Conditions and clear Modified Island Conditions occurring in late August; the former dominated by positive net long wave balances and the latter by high values of solar radiation absorbed at the ground.

The 1961 ablation regime was initially created by warm sector cyclonic circulation (high melt and little solid precipitation). Glacier ice conditions dominated from mid-July on, in the calculations. If the measured accumulation values had been used to augment the precipitation values in the calculations, melt would have been decreased by as much as 30 cm.

Following unusually low temperatures with Polar Ocean flow early in the season, 1970 experienced continual alternation of circulation types. This phenomenon produced conditions similar to Cyclonic System Conditions but with less precipitation, due to the intervening periods of Polar Ocean and Island flow.

Island conditions became established early in 1962 and dominated the season along with the resultant glacier ice conditions.

The 1960 season was controlled by Island conditions but brief appearances of Polar Ocean Conditions and Cyclonic Systems prevented the establishment of clear anticyclonic conditions as in 1962.

3: 9 Intervening Years

Climatic analysis of the intervening years suggests^o that 1964 resembled 1969 while 1967 was a slightly less developed case of Type II dominance. The season of 1966 appears to be similar to 1968 except that the mid-summer Type III occurrence lasted longer in 1966. In 1963 this mid-summer Type III period was almost long enough to make it an Island year. The very cold June of 1970 showed up in 1965 with a suggestion of Type II circulation in mid-season and Type III in August.

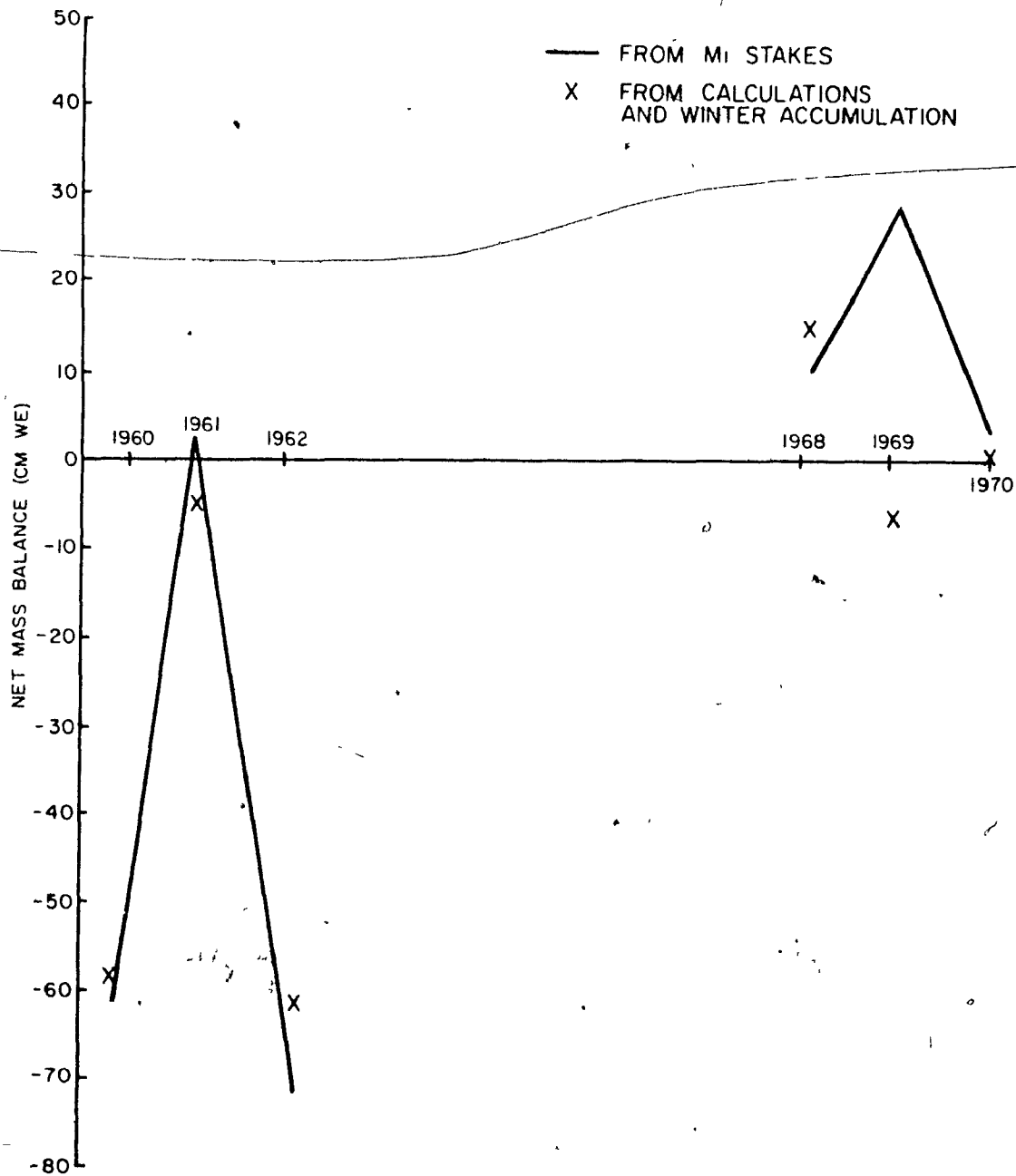


Figure 4: 1.1a Net Mass Balance from Stakes in Vicinity of Main Ice and from Calculated Summer Mass Balance Combined with Measured Winter Accumulation

CHAPTER 4

THE EXISTENCE OF MEIGHEN ICE CAP

4: 1 Mass Balance

4: 1.1 Net Mass Balance

Comparison of calculated net summer ablation with measured net mass balance is hazardous as the measurements were not made at the same time each year, and there is no satisfactory record of what occurred between the time of measurement and the beginning of the meteorological observations (and thus of the calculations). Assuming the calculated results are reasonable (with the exception of the problem of accumulation in August of 1961, see II 6:3 and 3:4) some information concerning the spring accumulation can be obtained from Figure 4: 1.1a. Here results of subtracting the calculated net summer ablation from the measured winter accumulation are compared with the mean net mass balance for the individual stakes in the vicinity of Main Ice. It should be noted that there is considerable variation in measured net mass balance between the four or five stakes used and that these variations do not appear to follow any specific pattern from year to year.

With these limitations in mind, some interesting trends emerge from Figure 4: 1.1a. In the summers where solid precipitation is less than 10 cm water equivalent (1960, 1962 and 1968) the value of measured net mass balance is slightly more negative than the calculated values. Two factors likely contribute to these differences in 1960 and 1962. It is quite possible that some ablation took place before the start of meteorological observations. As the surface height measurements were made near the camp, and drifting is always greater in the vicinity of buildings, it is quite possible that the snow pack was deeper at this site than at

the mass balance stakes. In this event the snow pack would disappear sooner at the mass balance stakes than at the camp, and the glacier ice melt rates would apply longer at the stakes than in the camp. These two effects are certainly sufficient to account for the small difference in measured and calculated values.

In 1968 winter accumulation was measured in late May and precipitation falling in late August would probably appear in the mass balance measurements as next winter's accumulation rather than as 1968 summer accumulation. If this was taken into consideration, the stake measurements and calculations would agree well. The winter accumulation values for 1967-68 are rather high, suggesting that the "spring" snow is included in this "winter" accumulation.

In 1970 the mass balance measurements were made on 30 April and the figure indicates snow in May of the order of 3 cm water equivalent, which is reasonable considering that very low temperatures persisted into early June that year.

Spring accumulation of 25 cm water equivalent is needed in May of 1969 to bring the calculated net mass balance up to the measured values. Snow and blowing snow were frequent during the latter part of May in this year, and though no records were kept it is quite possible that this much accumulation occurred in spring of 1969.

Before comparing the 1961 calculations with the measured values two adjustments must be considered in connection with accumulation which appears to have taken place in the latter part of the ablation season and which was not taken into account in the original calculations. Firstly, the amount of the accumulation must be added to the mass balance. Secondly, the effect of the lower albedo values on the energy balance must

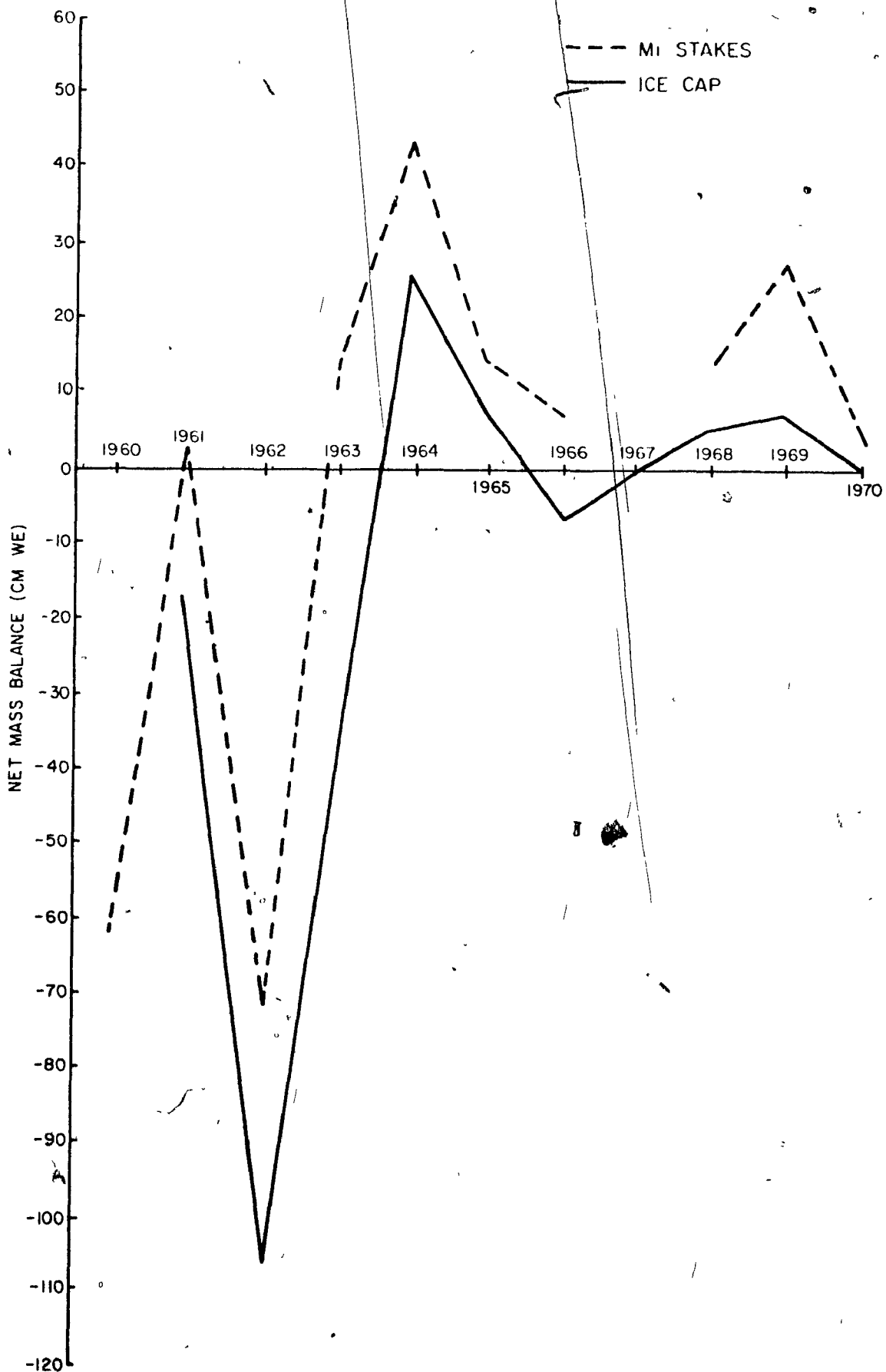


Figure 4: 1. 1b Net Mass Balance of Stakes in Vicinity of Main Ice and of Whole Ice Cap

be accounted for (as much as 26 cm, see 3:4). Applying these corrections gives a calculated net mass balance of -5 cm compared to +3 measured, suggesting 8 cm or more of spring precipitation, which is quite reasonable.

In Figure 4: 1.1b the net mass balance of the stakes near Main Ice is compared with that of the whole ice cap for the years 1961 to 1970.

The Island years (1962 and 1963) and the Cyclonic System years (1961, 1964, 1967 and 1969) show larger differences between the Main Ice and ice cap mass balance. The results suggest a steeper gradient of ablation with height in these years than in Polar Ocean years. The occurrence of Island conditions before mid-June, resulting in early loss of snow pack and consequent lowering of albedo at lower elevations and the better drainage are likely responsible for the gradients in the Island years. In cyclonic years it is probable that much of the precipitation falling as snow at the summit of the ice cap falls as rain at lower elevations where the influence of the warm land is felt. In Polar Ocean years, such as 1968, the albedo remains high over the whole glacier due to constant rime, etc., even after the snow pack disappears at lower elevations.

Paterson (1969) found ablation to be greater on east and south slopes of the ice cap and suggests this may be a combination of meteorological effects and improved drainage on the steeper slopes (See also 4: 3.2).

4: 1.2 Prediction of Mass Balance

Figure 4: 1.2a shows the results of using melting degree days from Meighen Ice Cap and Isachsen to estimate net mass balance. The general shape of both the Main Ice and Isachsen curve is good for the Island

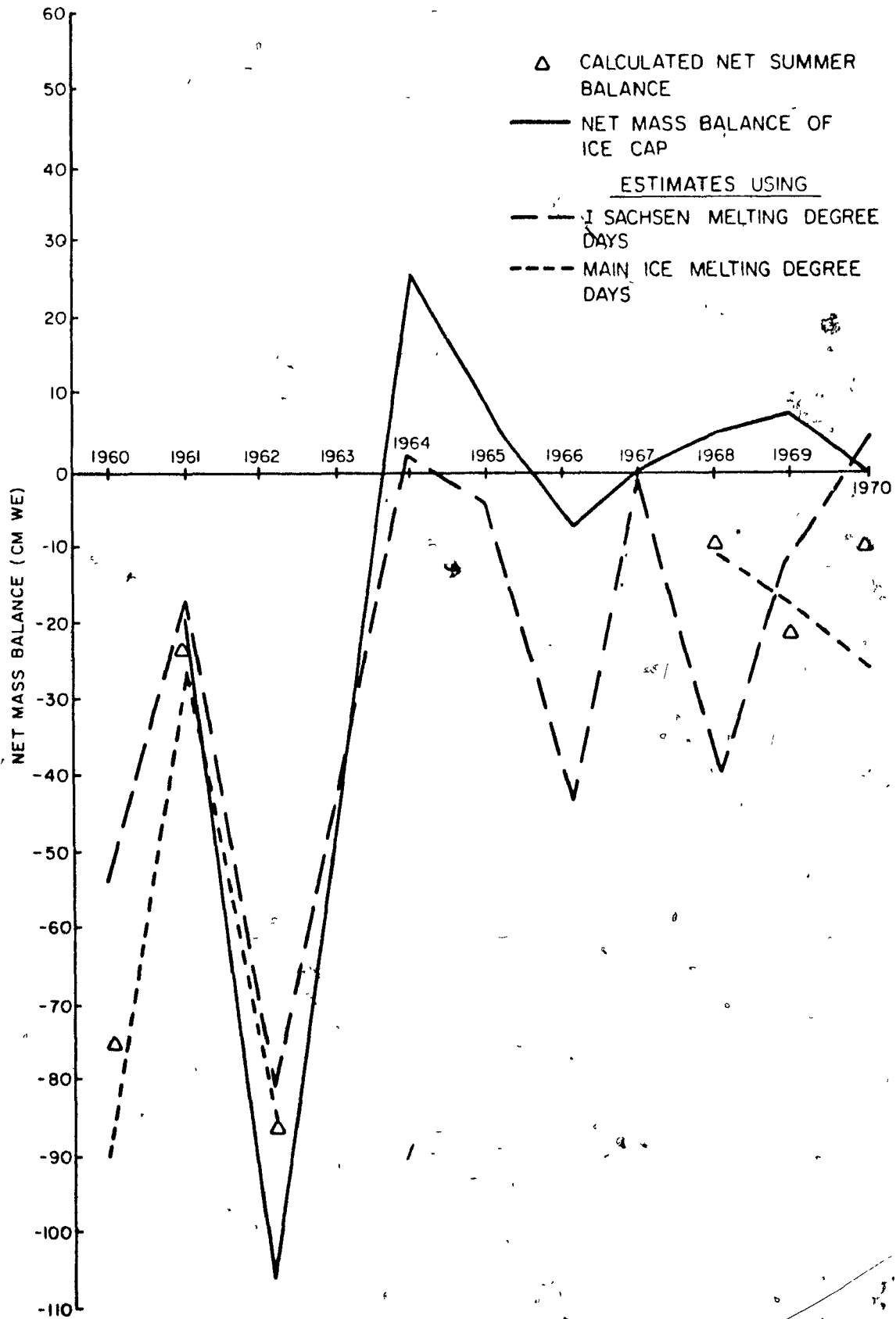


Figure 4: 1.2a IC and Mi Melting Degree Days used to Estimate Mass Balance

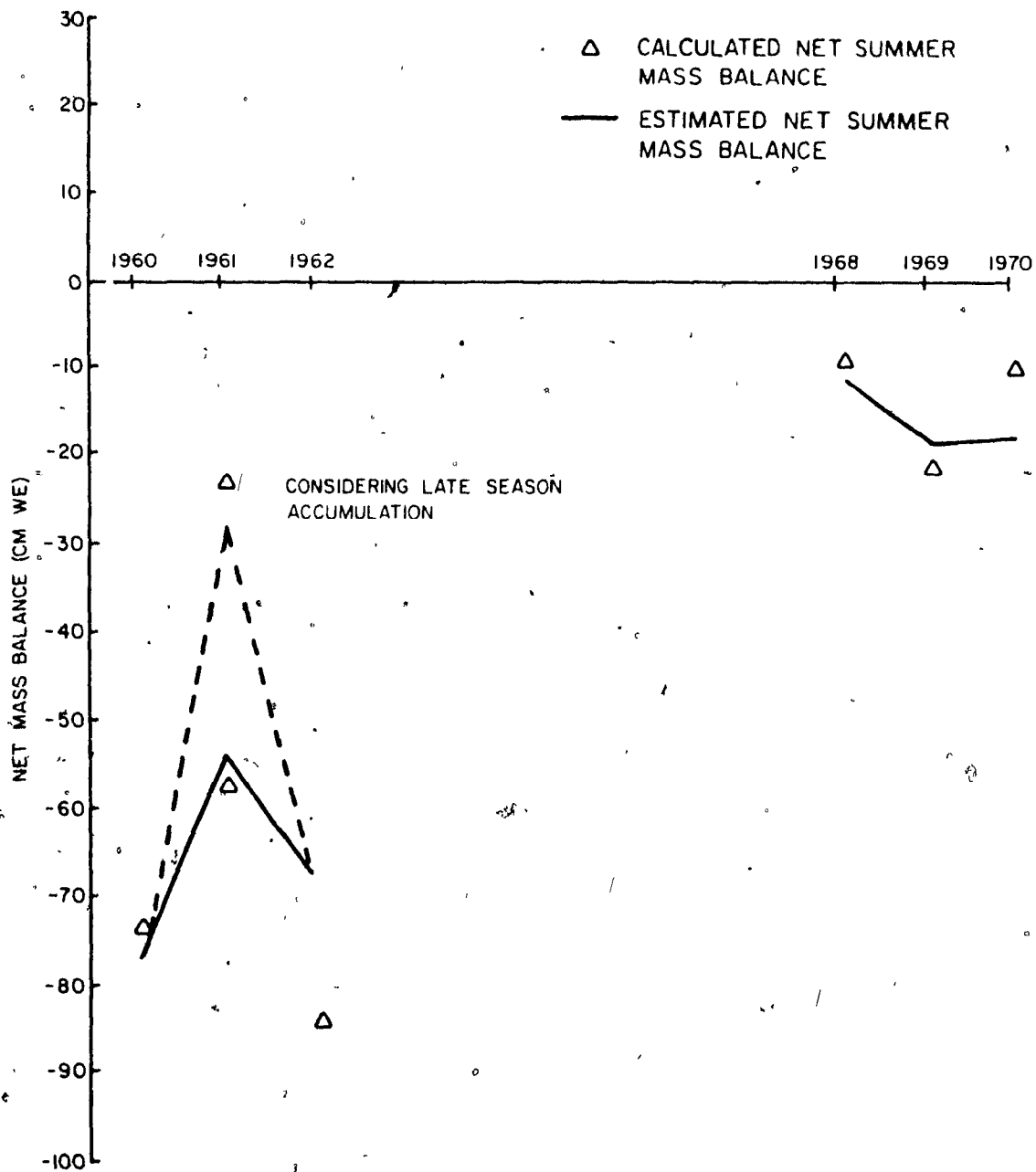


Figure 4: 1.2b SEB Diagram Frequencies used to Estimate Mass Balance

years when strong melt is experienced, and the Main Ice curve is quite good in the Polar Ocean years with the exception of 1970. Estimates, using Isachsen melting degree days for the strongly Polar Ocean years of 1966 and 1968, are particularly poor emphasizing the fact that Isachsen and Main Ice are in separate regimes under this Type of circulation.

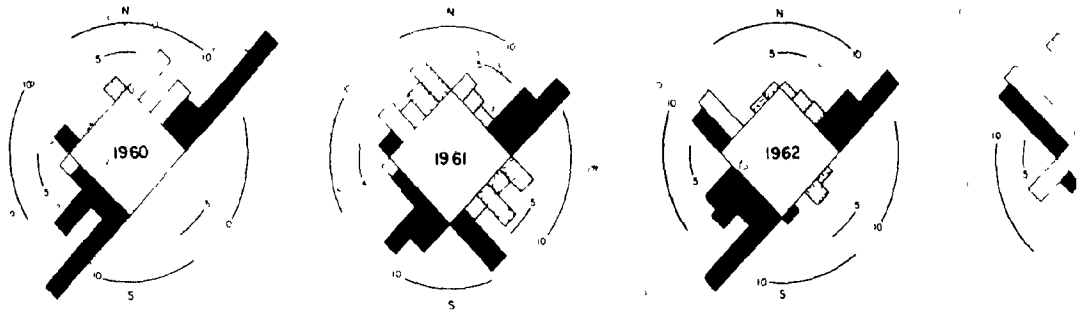
The estimates are improved by using the percent occurrence of classes in SEB diagram for each year, as shown in Figure 4: 1.2b. The general shape of the curve is good. Inclusion of a temperature class for temperatures $\gg 2^{\circ}\text{C}$ would improve the low estimate for 1962. The estimated value is 7 cm too high in 1970, due mainly to particularly large amounts of precipitation in that year with cool SW flow, and to the low melt values associated with clear modified Island conditions which occurred late in the season when solar angle was low and albedo high. In the other four years the estimated values of summer net mass balance are within 3 cm of the calculated values (calculated from three-hourly observations).

In addition, it was seen in 4: 1 and 2 that knowledge of the circulation Types prevailing during a year is useful in extrapolating from Main Ice summer net mass balance calculations to net mass balance of Main Ice area and of the whole ice cap.

4: 2 Factors Governing Mass Balance of Meighen Ice Cap

The Meighen Ice Cap mass balance regime is controlled by unusually low ablation and by spring and summer accumulation. Winter accumulation appears to be of little importance in mass balance of the Ice Cap. There follows a brief discussion of the factors governing the occurrence, on Meighen Ice Cap, of melt, of suppression of melt and of spring and

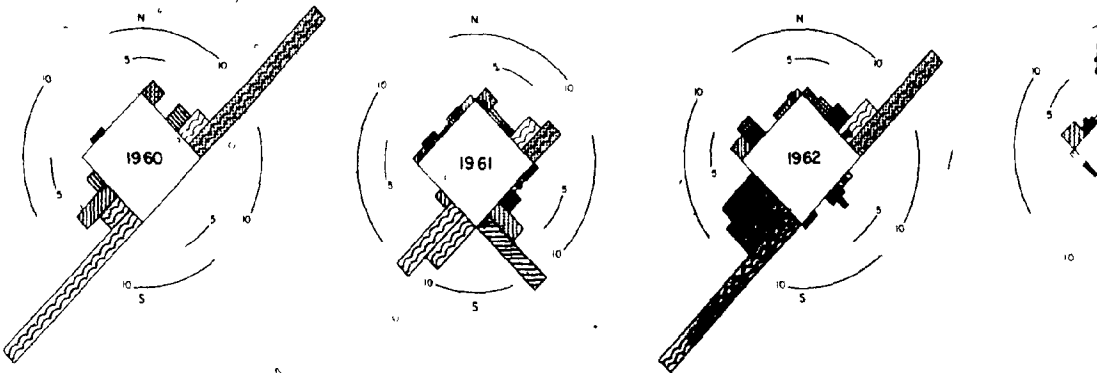
PERCENT OCCURRENCE OF SEB CLASSES



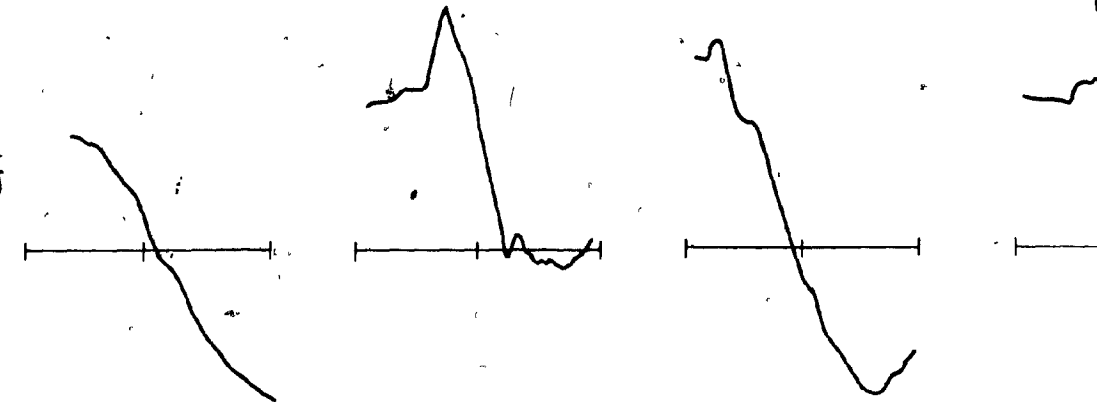
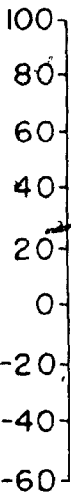
SUMMER ABLATION

&

SUMMER ACCUMULATION



SURFACE LOWERING (cm)



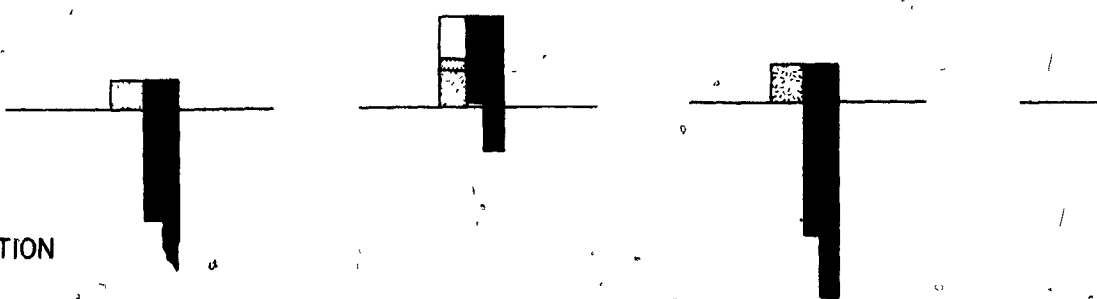
ACCUMULATION

SUMMER
SPRING
WINTER

MI

ICE CAPS

ABLATION



1960

1961

1962



Figure 4: 2.1 Summer Characterization (See...)

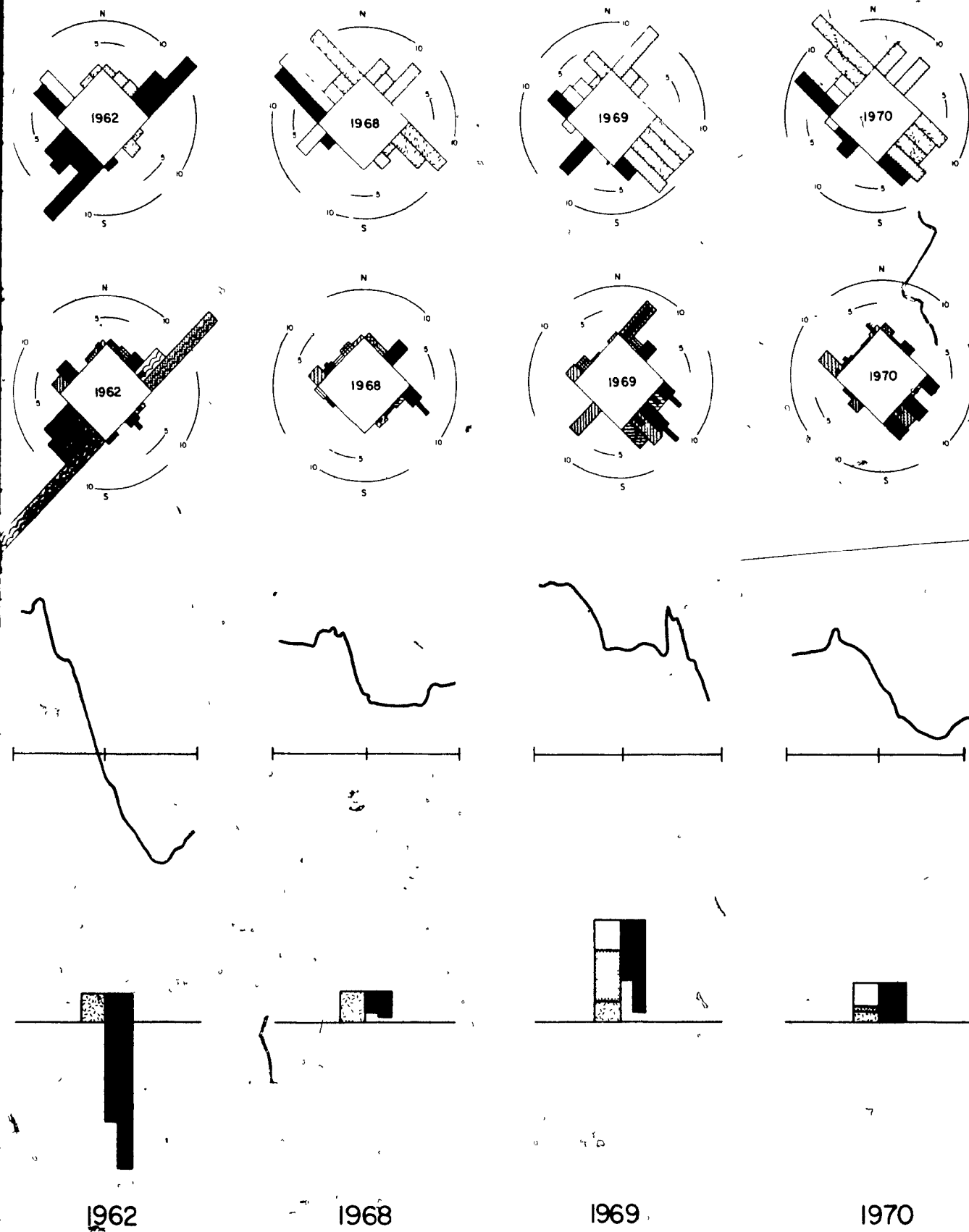


Figure 4: 2.1 Summary of Climate, Energy and Mass Balance Characteristics of Six Years of Main Ice Data. (See Figure 2: 2a and Appendix I for Legend.)

summer accumulation. Reference should be made to Figure 4: 2.1* which summarizes the climate, energy balance and mass balance characteristics of the six years of Meighen Island data.

4: 2.1 Melt

Over glacier ice on Meighen Ice Cap the strongest melting is experienced with the clear, warm, fogless conditions of light S'ly flow accompanying establishment of anticyclonic circulation and subsidence over the Arctic Islands. Turbulent fluxes are positive, due to advection of warm air over the ice cap, and absorbed solar radiation reaches a maximum due to clear skies and low albedo. Over snow pack the highest ablation occurs with warm cloudy conditions due to the decreased importance of solar radiation as a result of high albedo values. These conditions are most strongly developed on occasions when the warm sector of Cyclonic System circulation intrudes into the Meighen Island area.

The clear, warm conditions of NE'ly modified Island flow yields just slightly higher melt than below-freezing broken conditions accompanying SE'ly frontal activity emphasizing the importance of the long wave incoming radiation to the surface energy balance of a snow surface. Conditions producing melt on Meighen Ice Cap are not unlike those in neighboring Islands, the major difference being the frequency and duration of such conditions.

4: 2.2 Suppression of Melt

The SEB diagram illustrates that, even in Island years, Polar Ocean flow successfully suppresses melt, accounting for the comparatively low ablation values experienced on Meighen Ice Cap in relation to those found

* Figure 4: 2.1 is also available as a removable chart in the back pocket along with the SEB Diagrams of Energy Balance Components to complement discussions of this chapter.

in warm seasons on Axel Heiberg and Ellesmere Islands. The strong Polar Ocean flow advects cool, unstable fog and cloud from the ice pack onto the ice cap. Turbulent fluxes are negative due to lapse conditions of temperature and humidity in the lowest meter. The cool thin fog produces low values of long wave incoming radiation due to low temperatures and low emissivity. The high surface albedo produced by rime, freezing drizzle and light snow, which accompanies the cloud-fog, more than balances the high transmission of solar radiation through the thin fog. Strong winds continually replenish the fog and cause blowing and drifting snow. When temperatures remain below -2°C , melt is negligible and the frequent light snow associated with the cloud-fog results in slightly positive summer mass balance values with the colder Polar Ocean flow. Even when temperatures approach freezing, melt seldom exceeds .2 cm/day with flow off the cool Polar pack.

With the exception of the extreme NW coasts, Ellesmere and Axel Heiberg Islands are not affected by Polar Ocean flow due to the high mountains lining their coasts. Isachsen is also protected by hills to N and NW and is situated well inland from the Polar pack. The northern portion of Ellef Ringnes Island is adjacent to a considerable area of snow free land. The low albedo of the bare arctic tundra makes it an impressive heat source, effectively dissipating this low cloud and fog within some 20 miles of the coast. It should be noted, however, that the NW coasts of the Queen Elizabeth Islands show a lack of vegetation and that satellite photos show that snow is often very late leaving the northern hilly portion of Ellef Ringnes Island.

4: 2.3 Spring and Summer Accumulation

Passage of Cyclonic Systems S of the Meighen Island area contributes substantial amounts of snow to the ice cap. Though the thick warm clouds accompanying these conditions can produce considerable melt, temperatures remain below freezing unless the warm sector invades the Meighen region. Particularly with the colder instances of such conditions the precipitation more than compensates for the melt which takes place.

It should be noted that (see II 3), with passage of a system S of Meighen Island, Devon Ice Cap can be experiencing the highest melt of the season as a result of the thick warm cloud and strong winds of the warm sector, while Meighen Ice Cap experiences passage of the upper trough with below freezing temperatures and considerable solid precipitation.

The net mass balance measurements suggest that summers dominated by Cyclonic System flow and accumulation are normally preceded by considerable amounts of spring accumulation which can as much as double the depth of the snow pack before melt begins in earnest.

Accumulation is doubly important on Meighen Ice Cap as the loss of the snow pack results in a considerable increase in melt, or in some cases the initiation of melt, due to the lowering of albedo.

4: 3 The Existence of Meighen Ice Cap

4: 3.1 Origin and Maintenance

Examination of the storm tracks and 500 mb flow suggests that circulation could be discussed in terms of the position of the Arctic front in relating the general circulation to the mass balance on Meighen Ice

Cap. In Polar Ocean years the Arctic front would lie along the Mainland - Island border, while in Cyclonic System years it would stretch along the NW edge of the Islands and in Island years lie in the Polar Ocean.

It has been shown, II 3, that widespread warm clear skies are associated with the shift of the 500 mb cold low to the Siberian side of the Polar Ocean. It is conceivable that the Climatic Optimum (ca. 3000 years ago) was associated with such a circulation or ^{at} least with the positioning of the Arctic front well N of the Queen Elizabeth Island area. The disastrous effect of Island flow on the mass budget of the Ice Cap precludes its existence under these conditions. Koerner's ice core studies also suggest that Meighen Ice Cap did not survive the Climatic Optimum but has formed since (Koerner, 1968). It seems reasonable that, as the cold low gradually shifted towards North America at the close of the Optimum, the potentially highly baroclinic zone between the Polar pack and the Islands became, for an extended period of time, the predominant position of the Arctic front. If this were the case, there would be a period at the close of the Climatic Optimum when when Cyclonic System circulation and the resultant spring and summer accumulation would dominate the Meighen Island region. In this manner a permanent snow patch could slowly grow into the small ice cap which exists today. As the 500 mb vortex continued S across the Islands, the baroclinic zone would tend to shift to the N coast of the mainland; the resultant Polar Ocean circulation allowing the struggling ice cap to survive most summer seasons. Polar Ocean conditions appear to be the dominant pattern at the present time but the ice core shows a distinct ablation surface which Koerner (1968) estimates to be

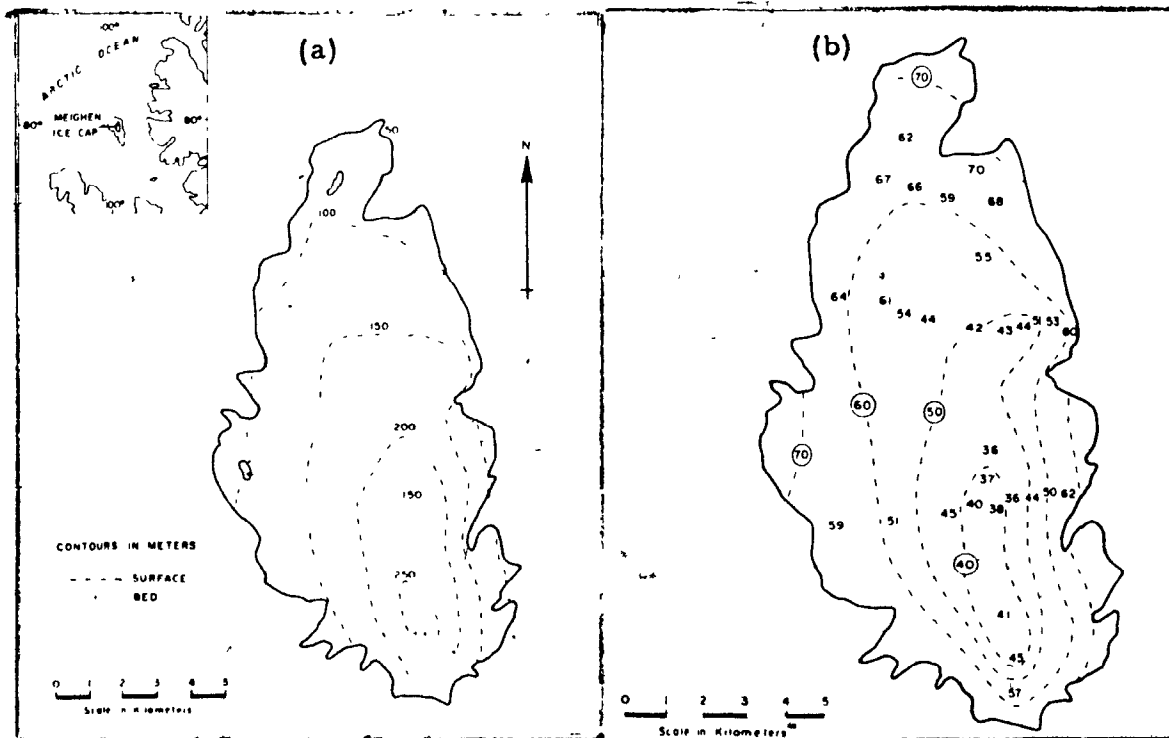
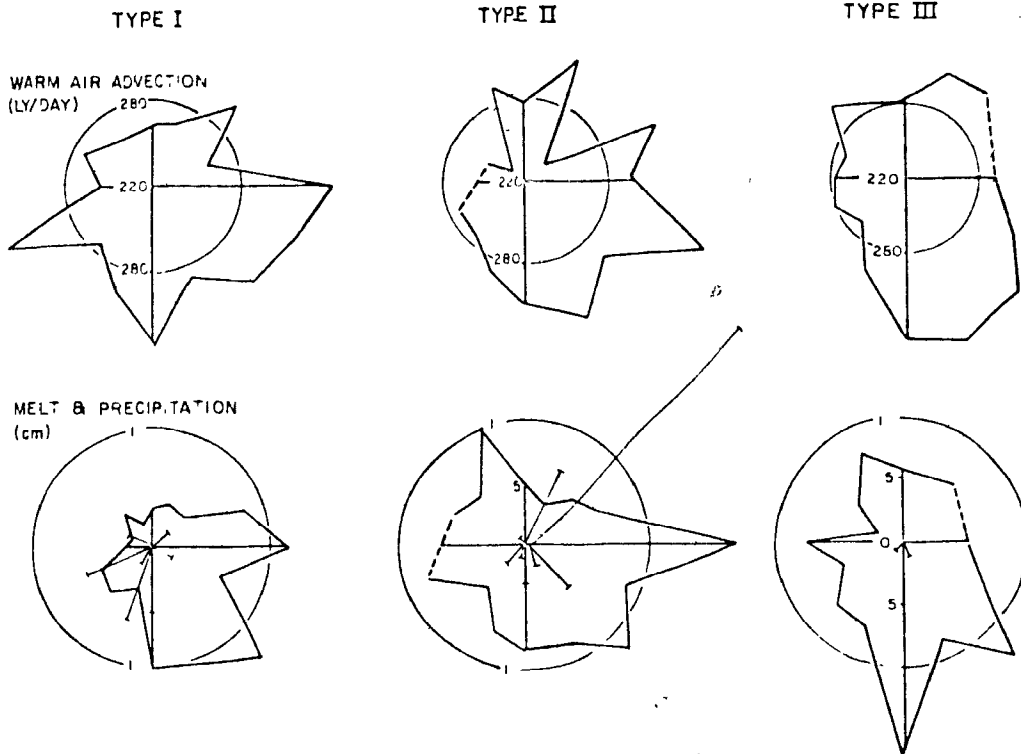


Figure 4: 3.2 Comparison of (a) Height Contours and (b) Equal Ablation Contours (after Paterson, 1969) with Type Roses of Warm Air Advection and Melt.

of the order of 500-600 years old, bearing witness to the power of Island circulation.

4: 3.2 The Shape

In Figure 4: 3.2 the height contour map of the ice cap and the map of calculated contours of equal ablation (after Paterson, 1969) are compared with the roses of melt and warm air advection. There is a striking correspondence between the direction of steep slopes (resulting from larger ablation gradients with height) and atmospheric flow producing high melt values (associated with strong warm air advection). In addition, considering that most Cyclonic System flow, and thus the major portion of spring and summer snow accumulation is associated with SE'lies, it is not unreasonable to picture the ice cap as a large snow drift facing into the SE winds, with the long leeward tail stretching N and NW'ly. The N tongue, once created, is additionally protected by the cool Polar Ocean flow.

4: 3.3 The Geographical Position

The circumpolar map (Figure 4: 3.3) shows Meighen Island to be a small Island in a large sea area, a situation not found elsewhere in the Canadian Arctic Archipelago. However, the map shows, in the Siberian Polar Ocean, numerous small islands in vast areas of ice choked sea, i.e., Henrietta, Schmidt and Ushakova. The temperature regime is similar to that on Meighen Island (Grosval'd and Krenke, unpublished) but the ice caps are generally larger (Chizhov and Bazeva, 1970) as the Soviet islands are more isolated from other land. Cyclonic systems also provide the accumulation for those Islands (Grosval'd and Krenke, unpublished).

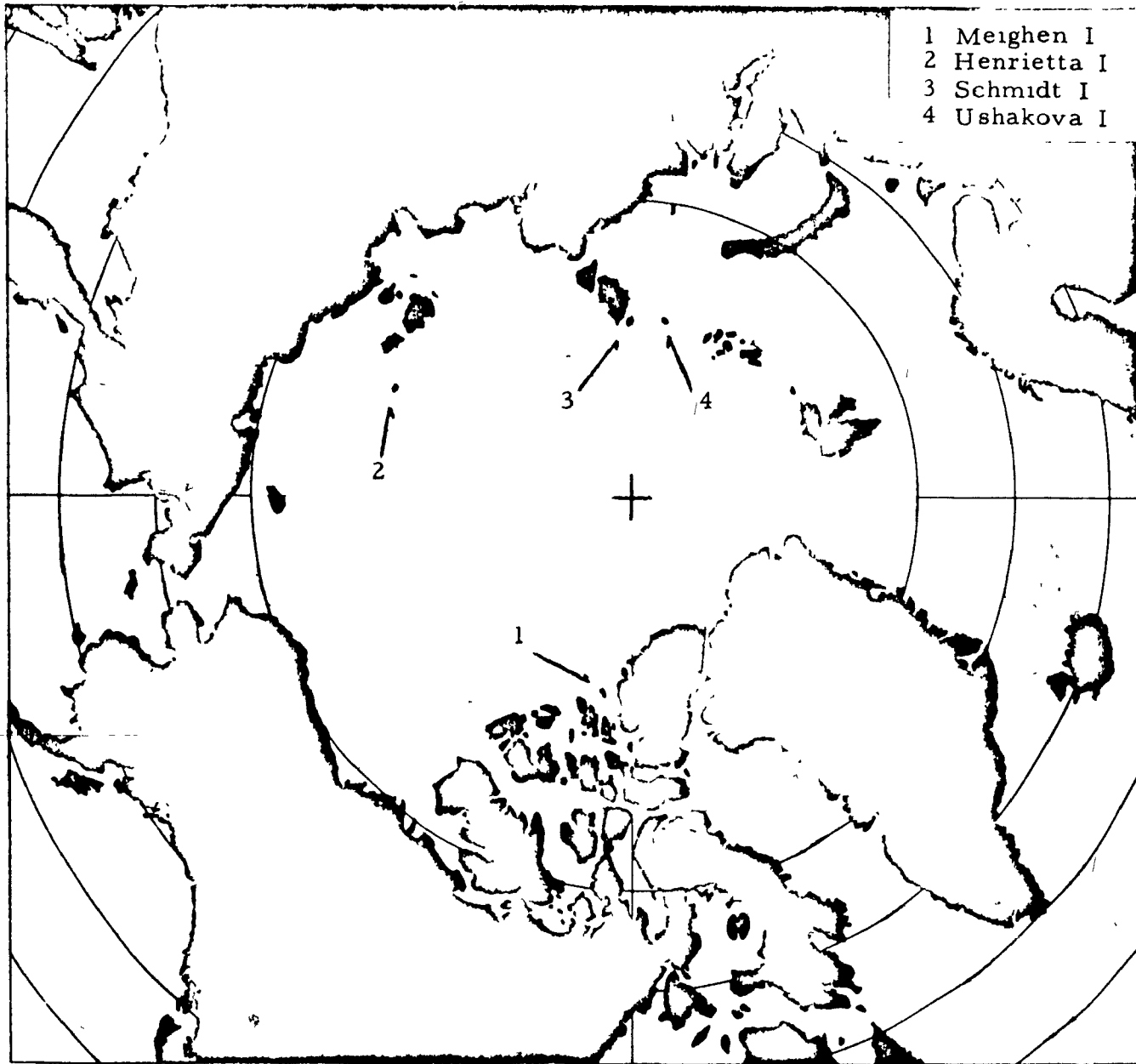


Figure 4: 3.3 Geographic Comparison of Meighen Island with other Queen Elizabeth Islands and with Islands of the Soviet Arctic

4: 3.4 Conclusions

Meighen Ice Cap exists:

because of Meighen Island's position on the edge of the Polar Ocean surrounded by expanses of ice covered sea (which effectively means that it lies in the Polar Ocean);

because it is sufficiently high to be in most of the cool thin Polar Ocean stratus and stratocumulus blown over the island by strong N'ly flow;

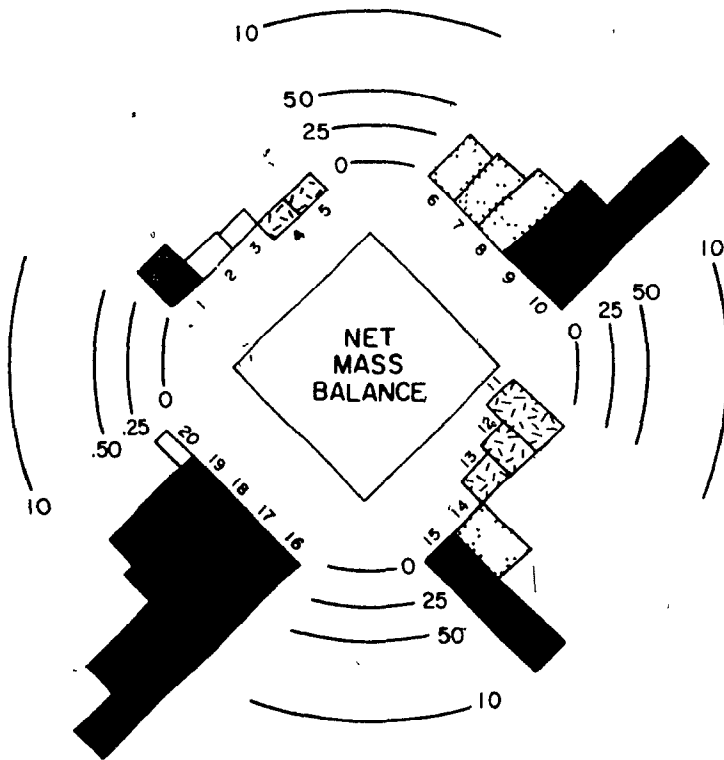
because it is not large enough to dissipate this cloud-fog;

and because, the ice cap, once formed, tends to increase or prolong cloud and precipitation through cooling and orographic effects.

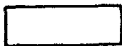
It is suggested that the ice cap originated after the Climatic Optimum during a period when steep horizontal temperature gradients were found along the NW edge of the Islands. Since then it has been maintained by Polar Ocean flow and is periodically given a new lease on life by the accumulation accompanying a Cyclonic System year, only to lose that and five or six Polar Ocean years' accumulation in one Island year.

LEGEND

SYNOPTIC ENERGY BALANCE DIAGRAM



NET SUMMER ACCUMULATION



NET ANNUAL ACCUMULATION



0 TO 25 CM NET ANNUAL ABLATION



25 TO 75 CM NET ANNUAL ABLATION



> 75 CM NET ANNUAL ABLATION

APPENDIX I

Foldout Legend for Synoptic Energy Balance
(SEB) Diagram Shaded According to Summer
Net Mass Balance.

REFERENCES

- Adams, W.P., 1966: Ablation and run-off on the White Glacier. Axel Heiberg Island, Canadian Arctic Archipelago. Axel Heiberg Island Research Reports, Glaciology, No. 1, McGill University.
- Ahlmam, H.W., 1935: The Fourteenth of July Glacier. Scientific results of the Norwegian-Swedish Spitsbergen Expedition, 1934. Pt 5. Geogr. Annlr. , Arg. 17, pp 167-218.
- Ahlmann, H.W., 1936: The firn structure on Isachsen's Plateau. Scientific results of the Norwegian-Swedish Spitsbergen Expedition, 1934. Pt 7, Arg. 18, pp 48-73.
- Ahlmann, H.W., 1948: Glaciological research on the North Atlantic Coasts. The Royal Geographical Society, Research Series, No. 1, 83 pp.
- Ahlmann, H.W., and S. Thorarinnsson, 1938: The ablation. Vatnajokull-scientific results of the Swedish-Icelandic investigations 1936-38, Chapter 5. Geogr. Annlr. Arg. 20, pp. 171-233.
- Ambach, W., 1963: Untersuchungen zum energieumsatz in der ablationszone des Grönlandischen Inlandseises. Meddeleser om Grönland, Bd. 174, Nr. 4.
- Andrews, R.H., 1964: Meteorology, No. 1. Meteorology and heat balance of the ablation area, White Glacier, Canadian Arctic Archipelago - summer 1960. Axel Heiberg Island Research Reports, McGill University, Montreal.
- Arnold, K.C. and D.K. MacKay, 1964: Different methods of calculating mean daily temperatures, their effects on degree-day totals in the high arctic and their significance to glaciology. Geogr. Bull., Ottawa, No. 21, pp. 123-129.
- Arnold, K.C., 1965: Aspects of the glaciology of Meighen Island, Northwest Territories, Canada. J. Glaciol., Vol. 5, No. 40.
- Arnold, K.C., 1966: The glaciological maps of Meighen Island N.W.T. Can. J. Earth Sci., Vol. 3, No. 6, Paper No. 19.
- Berlyand, M.E., 1956: Predskaznie i regulirovanie teplavogo rezhima prizemnogo sloya atmosfery (Prediction and Adjustment of the Heat Regime of the Surface Air Layer). - Leningrad, Gidrometeoizdat.
- Brooks, C.E.P. and N. Carruthers, 1953: Handbook of Statistical Methods in Meteorology. Her Majesty's Stationery Office, London. 412 pp.

- Budyko, M.I., 1966: Polar ice and climate, Proceedings of the Symposium on the Arctic Heat Budget and Atmospheric Circulation, The Rand Corporation, Santa Monica, California, RM-5533-NSF, p. 3-22.
- Can. Dept. Transp., Meteorol. Br., 1968: MANOBS, CIR-3450 DBS-30.
- Chizhov, O.P., and V.R. Bazeva, 1970: World Ocean. Problems of Geography, Sci. Publs Geogr. Soc. U.S.S.R., Volume 84, Moscow, pp. 243-253.
- Dalrymple, P.C., 1961: South Pole Micrometeorology program, 1 Data presentation. Tech. Rep. ES-2, Quartermaster Ras. Center, Natick, Mass.
- Dalrymple, P.C., Lettau, H. and Wollaston, S.H., 1966: South Pole micrometeorology program: Data analysis. Antarctic Research Series, Vol. 9., p. 22.
- Deacon, E.L., 1949: Vertical diffusion in the lowest layers of the atmosphere, Quart. J. Roy. Meteorol Soc., London Meteorological Office, No. 91.
- Doronin, Yu. P., 1969: Thermal interaction of the atmosphere and the hydrosphere in the Arctic. (Translated from Russian) Israel Program for Scientific Translation, Jerusalem (1970).
- Dunbar, Moira and Greenaway, K.R., 1956: Arctic Canada from the air. Ottawa, Canada. Defence Research Board.
- Fletcher, J.O., 1965: The heat budget of the Arctic Basin and its relation to climate, The Rand Corporation, Santa Monica, California, RM-5793-NSF.
- Goodall, D., 1971: Surface types of Meighen Ice Cap and surrounding land. Unpublished paper for Dept. of Engineering, McGill University.
- Grainger, M.E., and H. Lister, 1965: Wind speed, stability and eddy viscosity over melting ice surfaces. J. Glaciol. Vol. 6, No. 43, p. 101-127.
- Grosval'd and Krenke, A.N., unpublished: Glaciers of Franz Josef Land.
- Hare, F.K. and S. Orvig, 1958: The Arctic circulation, Arctic Meteorology Research Group, Pub. in Meteor. No. 12, McGill University, Montreal.
- Haurwitz, B., 1945: Insolation in relation to cloudiness and cloud density. J. Met., Vol. 2, No. 3, pp. 154-166.

- Havens, J.M., 1964: Meteorology and Heat Balance of the Accumulation Area, McGill Ice Cap. Canadian Arctic Archipelago - Summer 1960. Axel Heiberg Island Research Reports, Meteorology No 2, Montreal, 87 pp.
- Havens, J.M., F. Müller, G.C. Wilmot, 1965: Meteorology, No. 4. Comparative meteorological survey and a short-term heat balance study of the White Glacier, Canadian Arctic Archipelago - summer 1962. Axel Heiberg Island Research Reports, McGill University, Montreal.
- Holmgren, B., 1971: Climate and energy exchange on a sub-polar ice cap in summer: Part A: Physical climatology. Met. Instn. Upps Univ., Meddn. Nr 107, pp. 83.
- Holmgren, B., 1971: Climate and energy exchange on a sub-polar ice cap in summer; Part B: Wind- and temperature-field in the low layer on the top plateau of the Ice Cap. Met. Instn. Upps Univ., Meddn. Nr 108, pp. 43.
- Holmgren, B., 1971: Climate and energy exchange on a sub-polar ice cap in summer: Part C: On katabatic winds over the north-west slope of the ice cap. Variations of surface roughness. Met. Instn. Upps Univ., Meddn. Nr 109, Uppsala. 43 pp.
- Holmgren, B., 1971: Climate and energy exchange on a sub-polar ice cap in summer; Part D: On the vertical fluxes of water vapour at Ice Cap Station. Met Instn. Upps Univ, Meddn. Nr 110, pp. 29.
- Holmgren, B., 1971: Climate and energy exchange on a sub-polar ice cap in summer. Part E: Radiation climate. Met. Instn. Upps Univ, Meddn. Nr 111, 111 pp.
- Holmgren, B., 1971: Climate and energy exchange on a sub-polar ice cap in summer; Part F: On the energy exchange of the snow surface at ice cap station. Met. Instn. Upps. Univ, Meddn. Nr 112, Uppsala, 53 pp.
- Hornal, R., 1961: Detailed gravity surveys on Ellef Ringnes and Meighen Islands, Queen Elizabeth Islands, Northwest Territories, 1960. B.Sc. thesis, Queen's University, Kingston, Ontario.
- Hubley, R.C., 1954: The problem of short period measurements of snow ablation. Journal of Glaciology, Vol. 2, No. 16, p. 437-40.
- Hubley, R.C., 1957: An analysis of surface energy during the ablation season on Lemon Creek Glacier, Alaska. Trans. Am. Geophys. Un, Vol. 38, No. 1, p. 68-85.
- Jackson, C.I., 1969: The summer climate of Tanquary Fiord, N.W.T. Arctic Meteorology Research Group, Pub. in Meteor., No. 95, McGill University, Montreal, 65 pp.

- Keeler, C.M., 1964: Relationship between climate, ablation, and run-off on the Sverdrup Glacier, 1963 Devon Island, N.W.T. Research Paper No. 27, Arctic Institute of North America, Montreal.
- Koerner, R.M., 1968: Fabric Analysis of a core from the Meighen Ice Cap, Northwest Territories, Canada. *J. Glaciol.*, Vol. 7, No. 51.
- Koerner, R.M., 1970: Some observations on superimposition of ice on the Devon Island Ice Cap, N.W.T. Canada. *Geografiska Annaler* 52. A.1 p. 57-67.
- Koerner, R.M., 1970: Weather and ice observations of the British Trans-Arctic Expedition 1968-9. *Weather*, Vol. 25, No. 5, p. 218-228.
- LaChapelle, E., 1959: Errors in ablation measurements from settlement and sub-surface melting. *J. Glaciol.*, Vol. 3, No. 26, p. 458-67.
- Lister, H., 1962: Heat and mass balance at the surface of Ward Hunt Ice Shelf, 1960. Arctic Institute of North America, Research Paper No 19, 54 pp.
- Lister, H., and P.F. Taylor, 1961: Heat balance and ablation on an arctic glacier. *Meddelelser om Grønland*, Bd. 158, Nr. 7, 55 pp.
- Liljequist, G.H., 1956: Energy exchange of an Antarctic snow field, Part 1 A: Short-wave radiation. Norwegian-British-Swedish Antarctic Expedition, 1949-52. Scientific Results, Vol. II, Norsk Polarinstitut, Oslo.
- Liljequist, G.H., 1956: Energy exchange of an Antarctic snow field Part 1 B: Long-wave radiation and radiation balance. Norwegian-British-Swedish Antarctic Expedition, 1949-1952, Scientific Results. Vol. II, Norsk Polarinstitut, Oslo.
- Liljequist, G.H., 1957: Energy exchange of an Antarctic snow field Part 1 C: Wind structure in the low layer. Norwegian-British-Swedish Antarctic Expedition, 1949-1952. Scientific Results, Vol. II, Norsk Polarinstitut, Oslo.
- Liljequist, G.H., 1957: Energy exchange of an Antarctic snow field Part 1 D: Surface inversions and turbulent heat transfer. Norwegian-British-Swedish Antarctic Expedition, 1949-52. Scientific Results, Vol. II, Norsk Polarinstitut, Oslo.
- MacKay, D.K. and K.C. Arnold, 1965: Access to Meighen Island, N.W.T., Arctic, Vol. 18, No. 3.
- McKay, G.B Findlay and H. Thompson, 1969: A climatic perspective of tundra areas. International Union for Conservation of Nature and National Resources, pp. 10-33.

- Maykut, G.A. and N. Untersteiner, 1969: Numerical prediction of the thermodynamic response of Arctic sea ice to environmental changes. The Rand Corporation, Santa Monica, California, RM-6093-PR.
- McVehil, G.E., 1964: Wind and temperature profiles near the ground in stable stratification. *Quart. J. Roy. Meteorol. Soc.*, No. 90: pp. 136-46.
- Monin, A.S. and A.M. Obukhov, 1954: Dimensionless characteristics of turbulence in the surface layer, *Akad. Nauk. SSSR. Geofis. Inst. Turdy* 151, pp. 163-87.
- Müller, F. and N. Roskin-Sharlin, 1967: A high arctic climate study on Axel Heiberg Island, Canadian Arctic Archipelago - Summer 1961. Axel Heiberg Research Reports, Meteorology, No. 3, McGill University, Montreal, 81 pp.
- Müller, F. and C.M. Keeler, 1969: Errors in short-term ablation measurements on melting ice surfaces. *J. Glaciol*, Vol. 8, No. 52, p. 91-105.
- Ommanney, C.S.L., 1969: A study in glacier inventory, the ice masses of Axel Heiberg Island, Canadian Arctic Archipelago. Axel Heiberg Res. Rep. *Glaciol*, No. 3, McGill University, Montreal.
- Orvig, S., 1951: The climate of the ablation period on the Barnes ice cap in 1950. *Geogr. Annlr. Bd.* 33 (3-4).
- Orvig, S., 1954: Glacial meteorological observations on ice caps in Baffin Island. *Geogr. Annlr. Bd.* 36, pp. 197-311.
- Orvig, S., 1970: Climates of the Polar Regions, Elsevier Publishing Company, Amsterdam, 368 pp.
- Panofsky, H.A., 1963: Determination of stress from wind and temperature measurements. *Quart. J. Roy. Meteorol. Soc.* 89: 85-94.
- Paterson, W.S.B., 1967-1971: Polar Continental Shelf Project, Dept. of Energy, Mines and Resources - Mass Balance Studies. Ice.
- Paterson, W.S.B., 1968: A temperature profile through the Meighen Ice Cap, Arctic Canada. *Int. Ass. Sci. Hydrol.*, Publ. No. 79.
- Paterson, W.S.B., 1969: The Meighen Ice Cap, Arctic Canada: accumulation, ablation and flow. *J. Glaciol*, Vol. 8, No. 54, pp. 341-352.
- Petzold, D., 1971: Study of upper winds over Meighen Island. Unpublished term paper, McGill University, Montreal.
- Petzold, D., 1972: A Method of calculating albedo of snow surfaces. Unpublished paper for the Dept. of Geography, McGill University, Montreal.

- Rae, R.W., 1951: Climate of the Canadian Arctic Archipelago, Canada Department of the Environment, Toronto, 90 pp.
- Reed, R.J., and R.K. Surface, 1959: Arctic weather studies: summer season. Dept. of Meteorology and Climatology, University of Washington, Scientific Report, No. 5, 47 pp.
- Reed, R.J., and R.K. Surface, 1959: Arctic circulation studies, Dept. of Meteorology and Climatology, University of Washington, Final Report, 56 pp.
- Rusin, N.P., 1961. Meteorological and radiational regime of Antarctica. (Translated from Russian) Israel Program for Scientific Translations, Jerusalem.
- Savile, D.B.O., 1961: The botany of the northwestern Queen Elizabeth Islands. Can. J. Bot., Vol. 39, No. 4, p. 909-942.
- Savile, D.B.O., 1972: Microclimate and plant growth at Isachsen and Mould Bay. Arctic, Vol. 24, No. 4, pp. 306-307.
- Sellers, W.D., 1965: Physical Climatology. The University of Chicago Press, Chicago, pp. 272.
- Stebelsky, I., 1962: A microclimatological study in the Canadian Arctic. Unpublished B.A. thesis, University of Toronto.
- Stefansson, V., 1939: The problem of Meighen Island. Privately printed for Mr. Joseph Robinson, New York.
- Stefansson, V., 1942: Choosing sites for Arctic Stations. New York.
- Stefansson, V., 1944: The Friendly Arctic. New York.
- Sverdrup, H.U., 1935: The Ablation on Isachsen's Plateau and on Fourteenth of July Glacier in Relation to Radiation and Meteorological Conditions. Geogr Annlr., Arg. 17. pp. 145-66.
- Sverdrup, H. U., 1936: The eddy conductivity of the air over a smooth snow field. Geofys. Publ., Vol. 11, No. 7, pp. 5-49.
- Sverdrup, H.U., 1936: Results of the Meteorological Observations on Isachsen's Plateau. Geogr Annlr, Årg 18, pp. 34-47.
- Thorsteinsson, R., 1961: The history and geology of Meighen Island, Arctic archipelago. Geol. Surv. Can. Bull. 75.
- United States Navy, 1952: Study and Research-Arctic Weather, Task 3, Fourth Quarterly Progress Report.
- Untersteiner, N., 1961: On the mass and heat budget of arctic sea ice, Arch. Meteorol. Geophys. Bioklimatol., A, 12, 151-182, 1961.

- Untersteiner, N., 1966: Calculating the thermal regime and mass budget of sea ice, Proceedings of the Symposium on the Arctic Heat Budget and Atmospheric Circulation, The Rand Corporation, Santa Monica, California, RM-5233-NSF, p. 203-314.
- Vowinckel, E., and S. Orvig, 1962: Relation between solar radiation income and cloud type in the Arctic. J. Appl. Met. Vol. 1, No. 4, pp. 552-559.
- Vowinckel, E., and S. Orvig, 1966: The heat budget over the Arctic Ocean, Arch. Meteorol. Geophys. Biokl. Ser. B, 14, pp. 303-325.
- Vowinckel, E., and S. Orvig, 1967: Climate change over the Polar Ocean. I: The radiation budget. Arch. Met. Geoph. Biokl. Ser. B, 15, pp. 1-23.
- Vowinckel, E., and S. Orvig, 1969: Climate change over the Polar Ocean. II: A Method for Calculating Synoptic Energy Budgets. Arch. Met. Geoph. Biokl., Ser. B, 17, pp. 121-146.
- Vowinckel, E., and S. Orvig, 1969: The energy budget of an Atlantic cyclone. Arch. Meteor. Geophys. Biokl. Ser. B, 17, pp. 147-174.
- Vowinckel, E., and S. Orvig, 1971: Synoptic heat budgets at three polar stations. J. Appl. Met. Vol. 10, No. 3, p. 387-396.
- Vowinckel, E., and S. Orvig, 1972: EBBA- An Energy Budget Programme. Arctic Meteorology Research Group, Pub. in Meteor., No. 105, McGill University, Montreal, 50 pp.
- Wallén, C. C., 1948: Glacial-meteorological investigations on the Karsa glacier in Swedish Lappland 1942-1948. Geogr. Annlr. Arg. 30, Ht. 3-4, pp. 451-672.

8870000 m.

Andersen Point

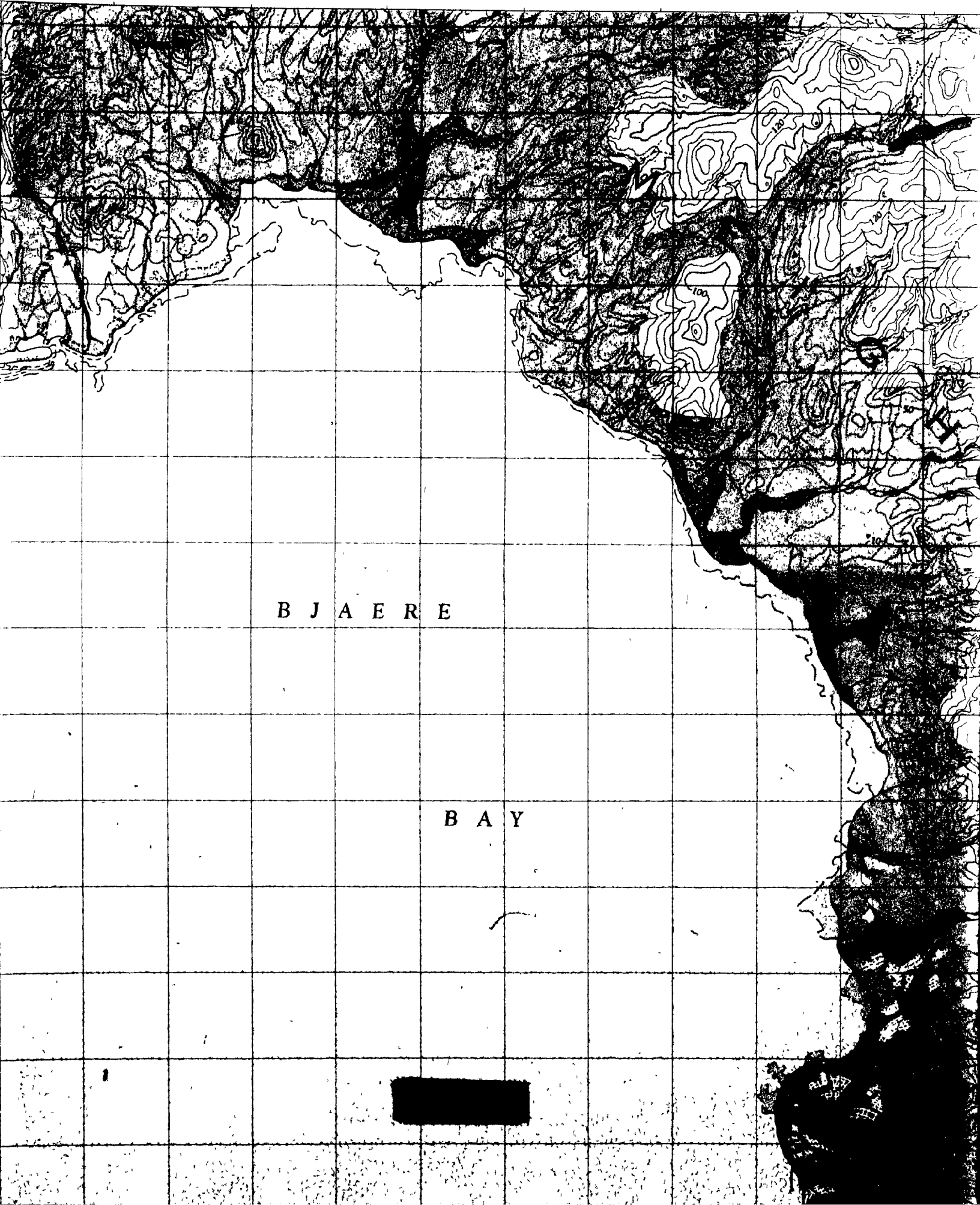


79°50'

1 of 3

800000 m.

P E A R Y



B J A E R E

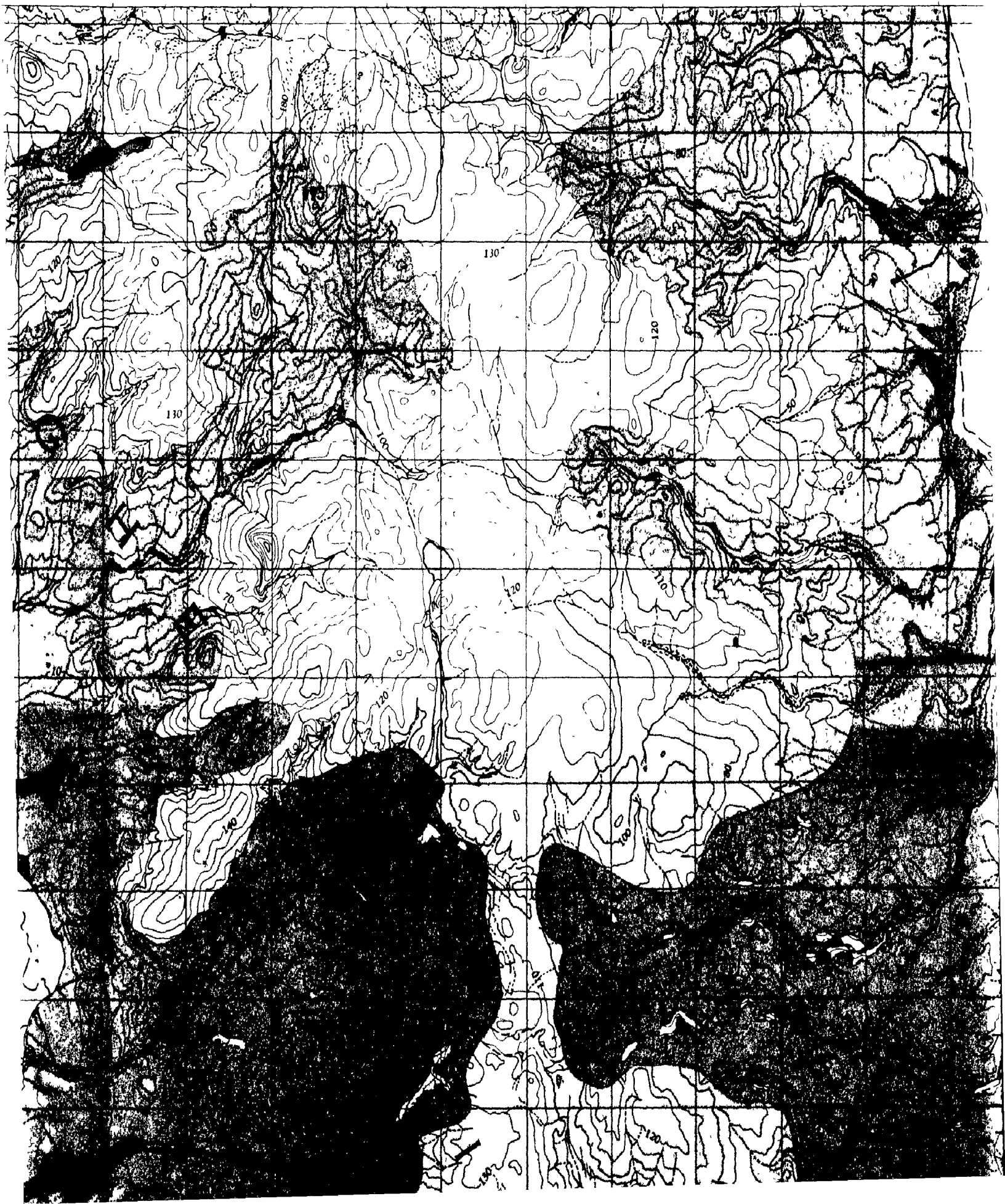
B A Y



99°15'

99°00'

98°45'



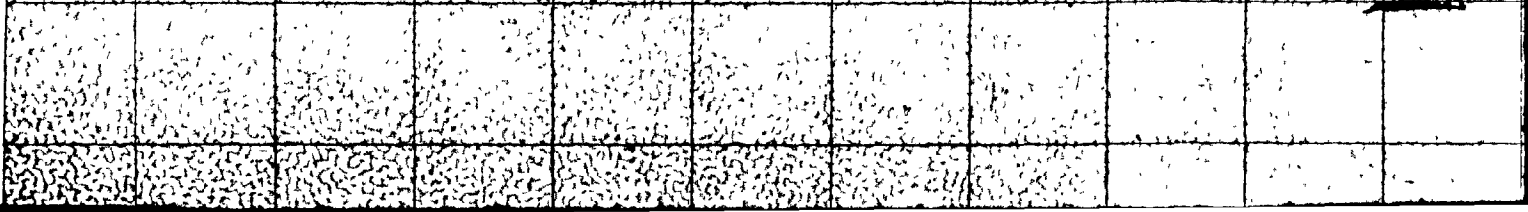
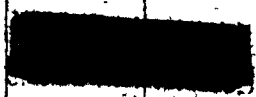
8 600 000 m

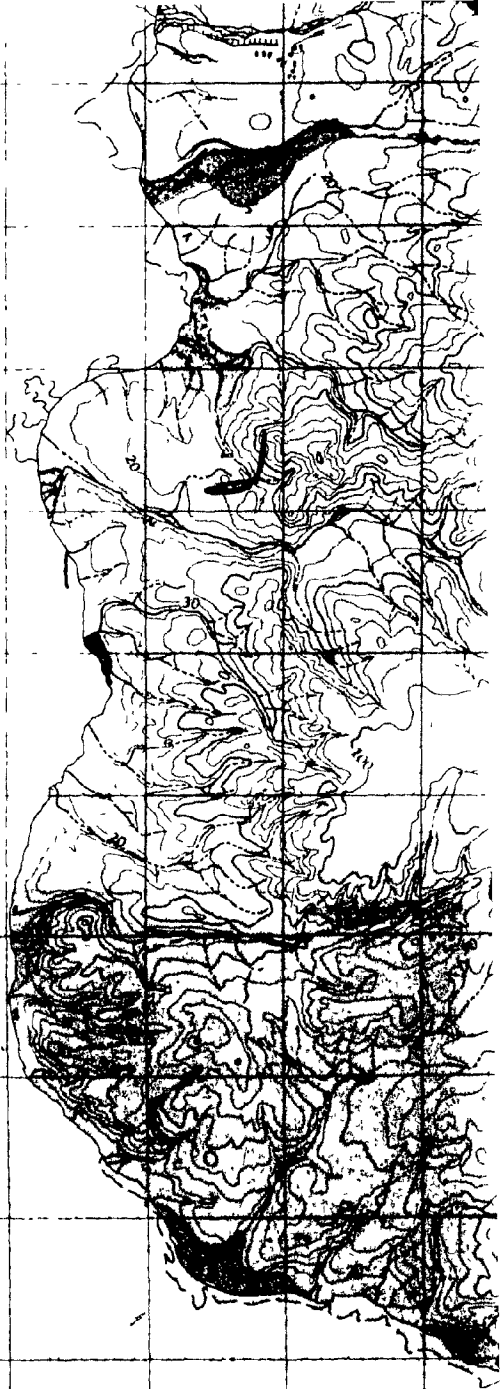
P E A R Y

79°45'

C H A N N

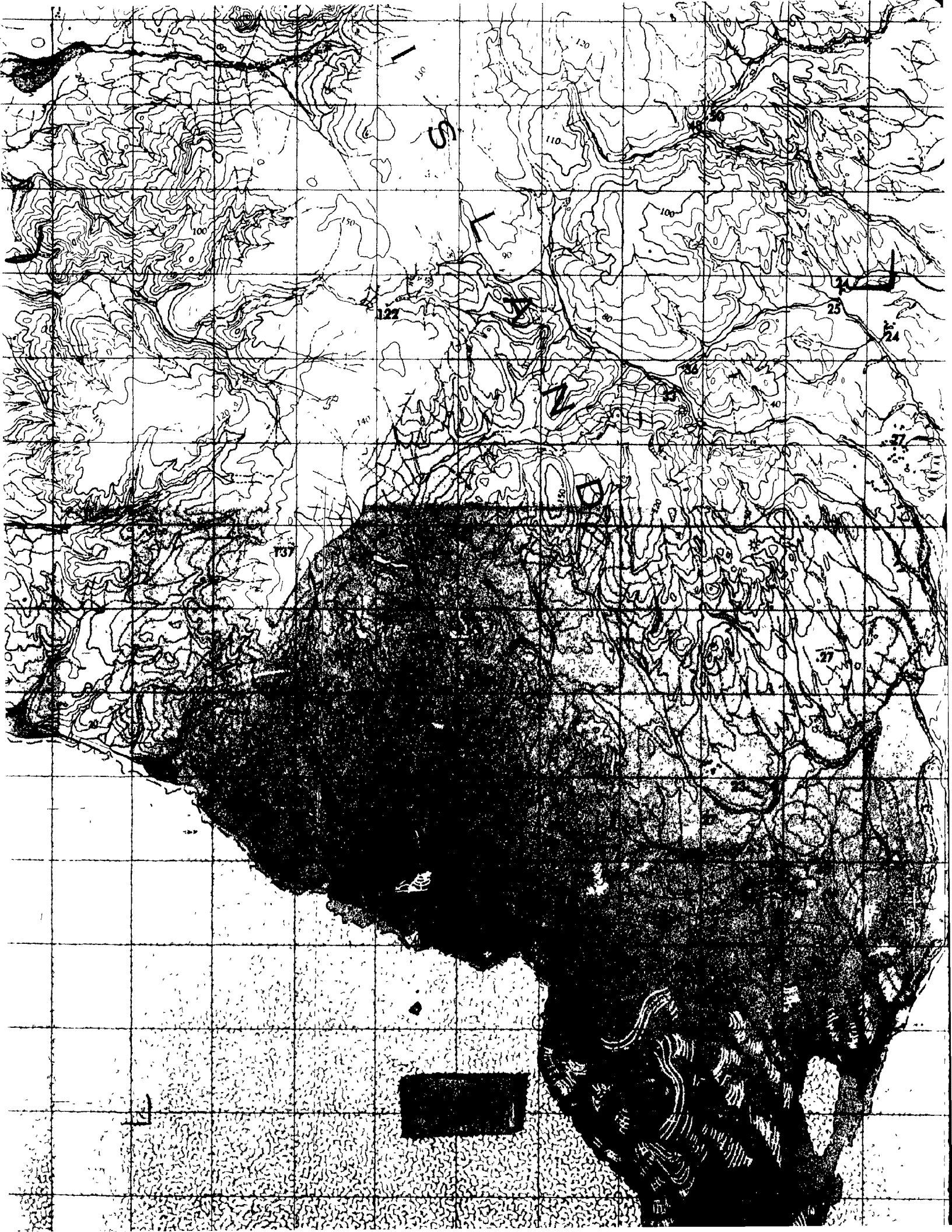
8 850 000 m.



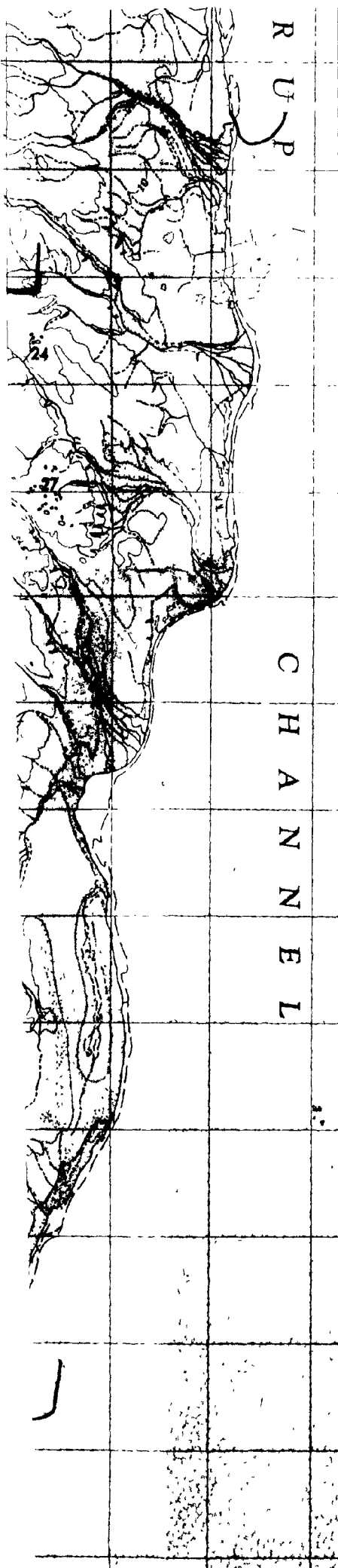


N E L

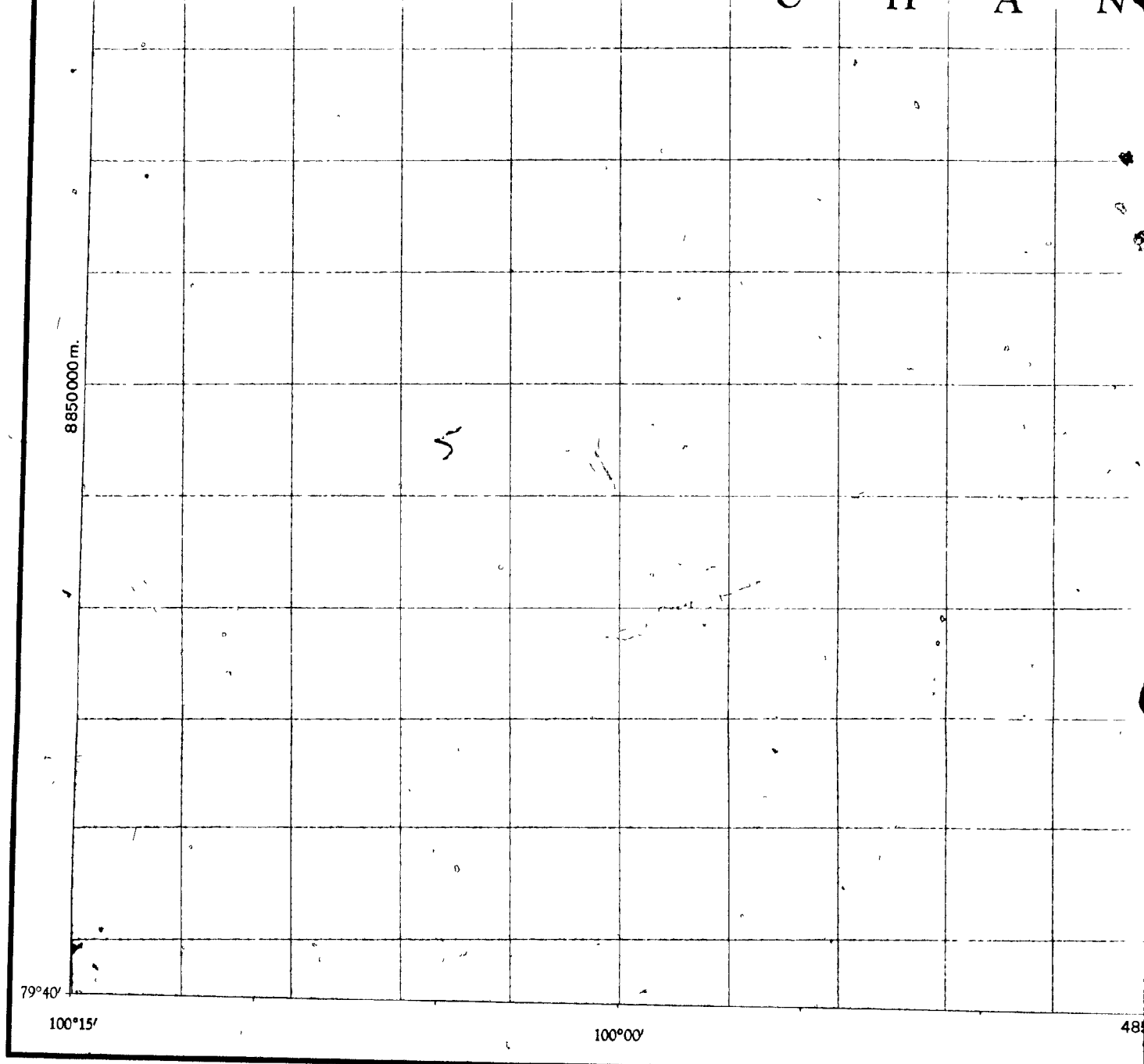




LEGEND



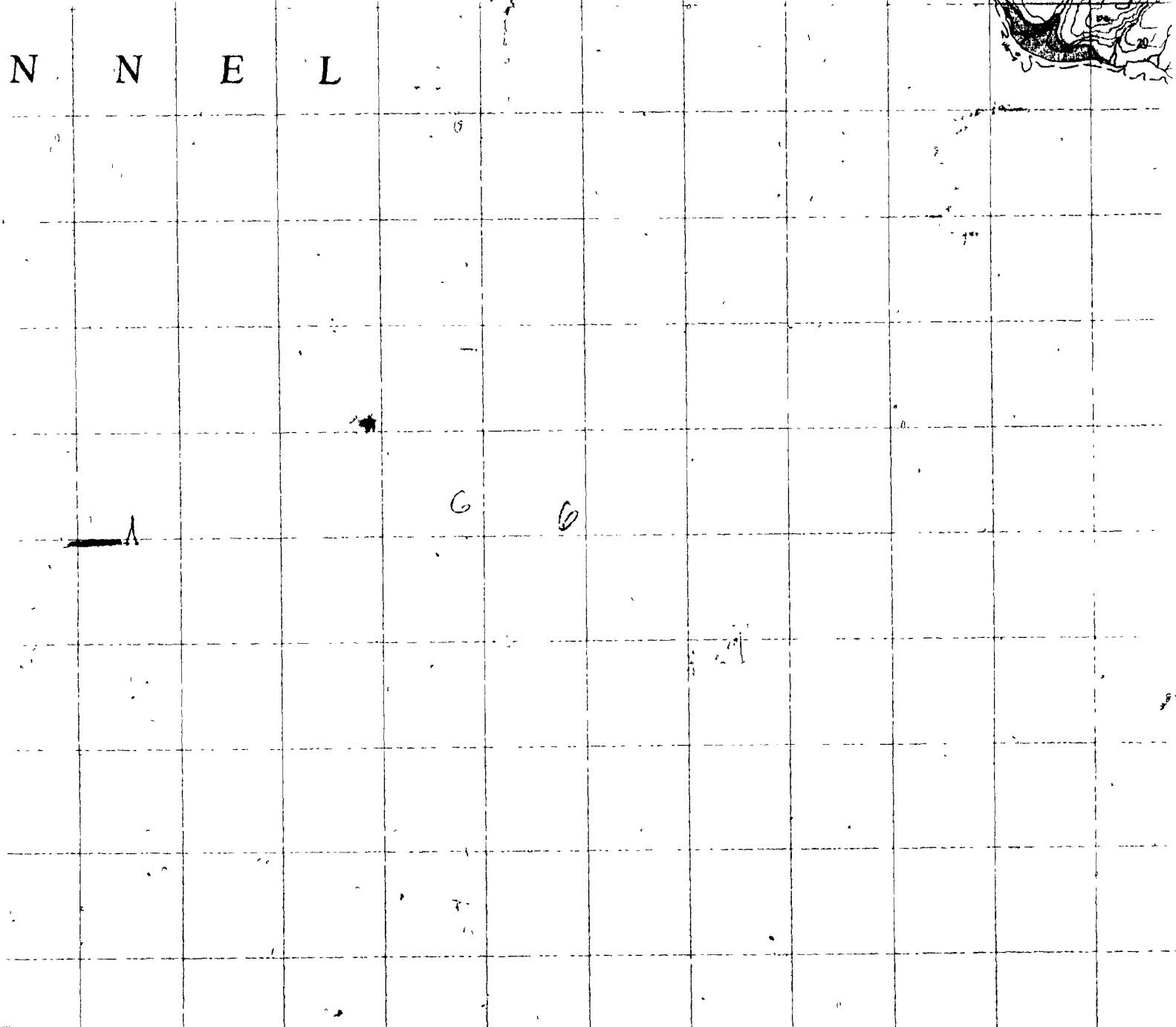
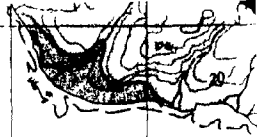
Historic site	⊕
Horizontal control points: on land	152 ^
on ice	241
Spot elevation (accuracy variable)	25
Lakes: perennial	
intermittent	
River	
Streams: perennial	
intermittent	
divided	
relic, marginal, superimposed	
River bed with channels	
Contours: land	
snow and ice	
beneath ice cap; calculated position	
beneath ice cap; assumed position	
Terraces: less than 1/2 the contour interval in height	
one half to one contour interval in height	
more than a contour interval in height	
Gullies: less than a contour interval in height	
more than a contour interval in height	
Steep sided hill (possibly ablation mound)	
Ice pushed ridges: less than 1/4 contour interval in height	
more than 1/4 contour interval in height	
Abandoned offshore bar	
Sand dunes	
Polas and winter sea ice, 10/10 cover, 5 August 1959	
Edge of sea ice	
Bottom fast ice	
Edge of bottom fast ice	
Ice ridge on bottom fast ice	
Dirt ridge on bottom fast ice	
Dirt on bottom fast ice	
Dirt on ice or snow	
Ice cap or snow bank limits	



Compiled, 1965, by the SURVEYS AND MAPPING BRANCH,
DEPARTMENT OF MINES AND TECHNICAL SURVEYS
from aerial photographs taken August 5, 1959 Printed 1965



N N E L



485 000 m
99° 45'

99° 30'

495 000 m
99° 15'

MEIGHEN ISLAND (S 1/2)

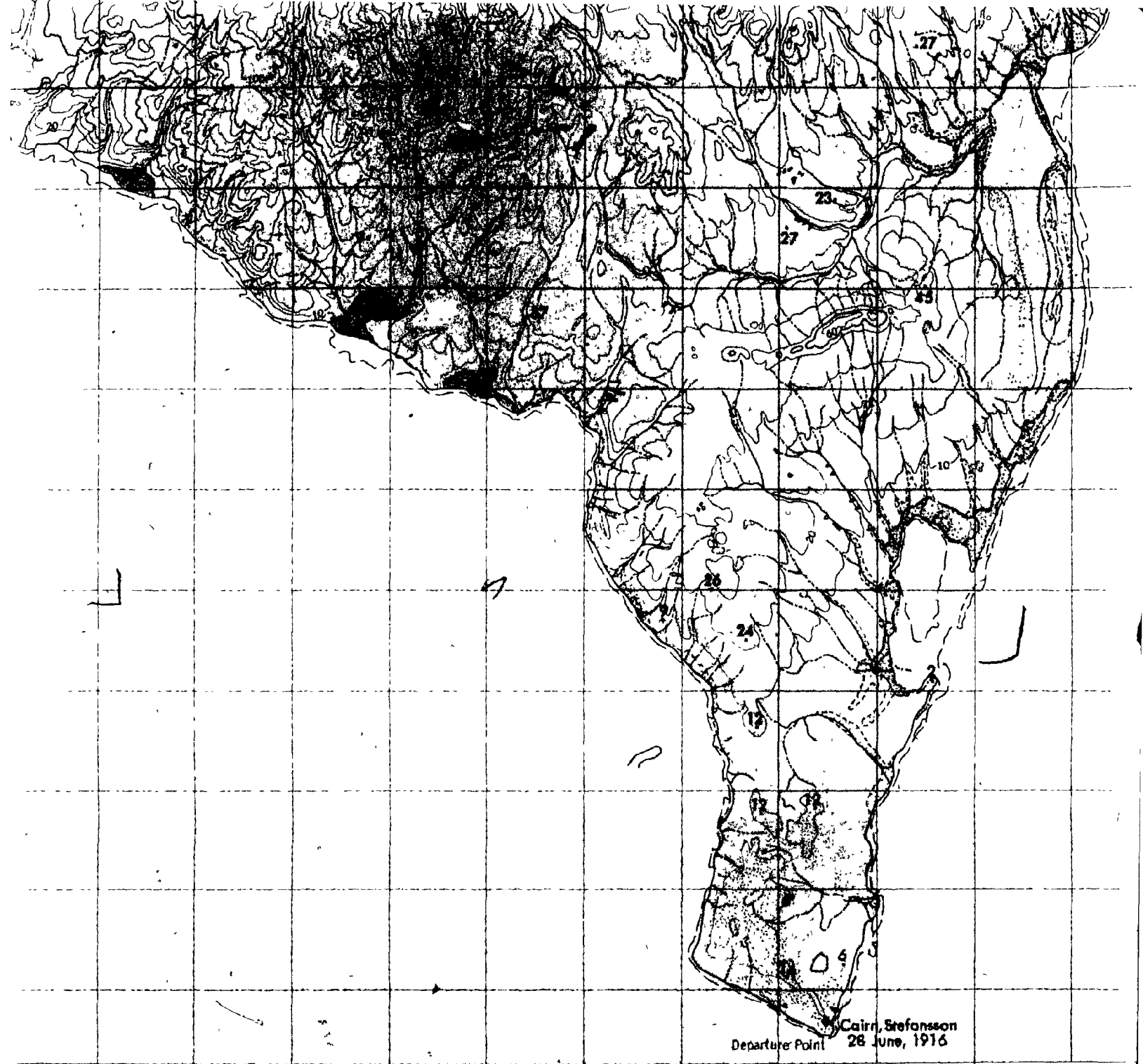
DISTRICT OF FRANKLIN
NORTHWEST TERRITORIES

SCALE 1:50,000



CONTOUR INTERVAL 10 METRES
North American Datum 1927

Some names on this map are not yet official
Corrections or additions are invited by the Surveys and Mapping Branch



00m
15'

99°00'

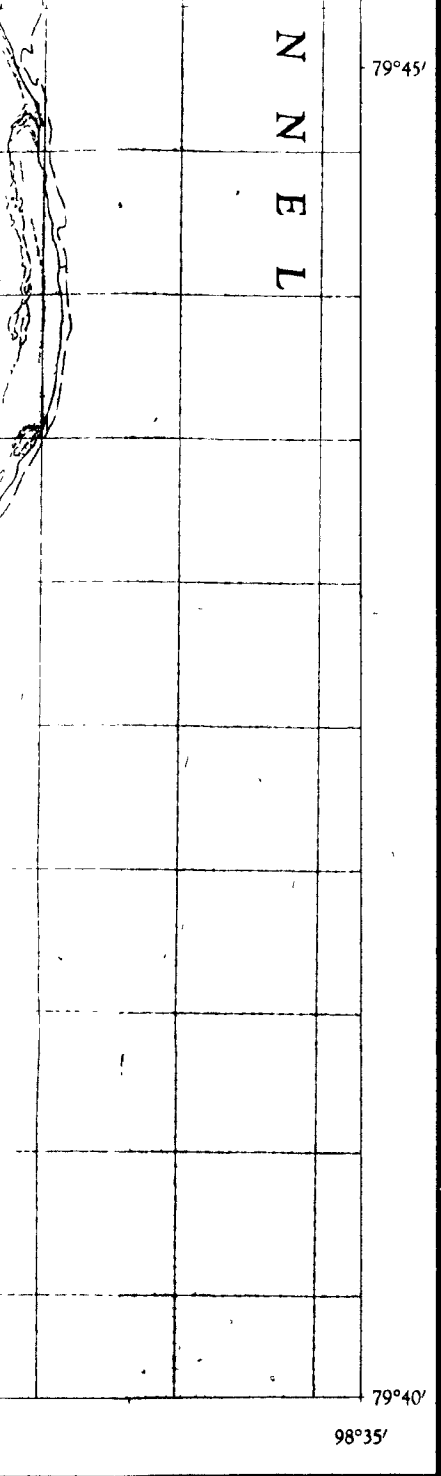
505000m.
98°45'

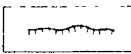
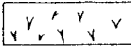
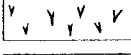
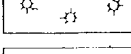
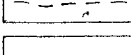
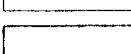
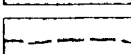
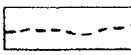
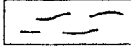
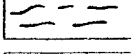
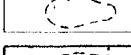
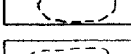
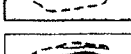
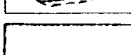
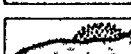
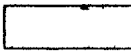
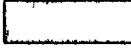
Cairn, Stefansson
Departure Point 28 June, 1916

Elevations in metres above mean sea level

The daily change of the
compass useless in the
centre of this map is.

1106



- one half to one contour interval in height 
- more than a contour interval in height 
- Gullies: less than a contour interval in height 
- more than a contour interval in height 
- Steep sided hill (possibly ablation mound) 
- Ice pushed ridges: less than 1/4 contour interval in height 
- more than 1/4 contour interval in height 
- Abandoned offshore bar 
- Sand dunes 
- Polar and winter sea ice, 10/10 cover, 5 August 1959 
- Edge of sea ice 
- Bottom fast ice 
- Edge of bottom fast ice 
- Ice ridge on bottom fast ice 
- Dirt ridge on bottom fast ice 
- Dirt on bottom fast ice 
- Dirt on ice or snow 
- Ice cap or snow bank limits 
- Nunatak 
- Polygons 
- Open water, foreshore flats 
- Snow and ice 
- Till areas 
- Sand, gravel, coarse pebbles 
- Mud and silt 

daily change of the north magnetic pole renders the magnetic compass useless in this area. The 1965 magnetic declination at the centre of this map is 151°30' west, annual change 15' decreasing



100°15'

100°00'

99°

80°15'

80°10'

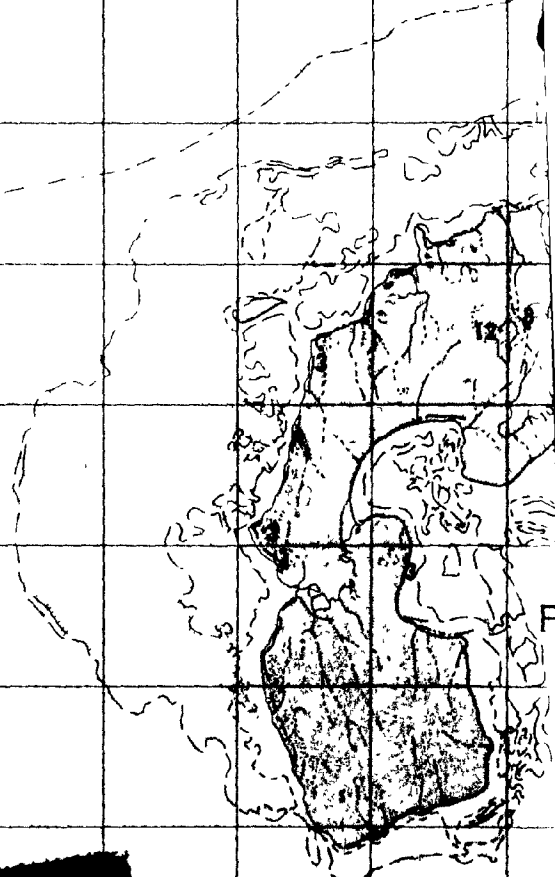
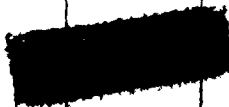
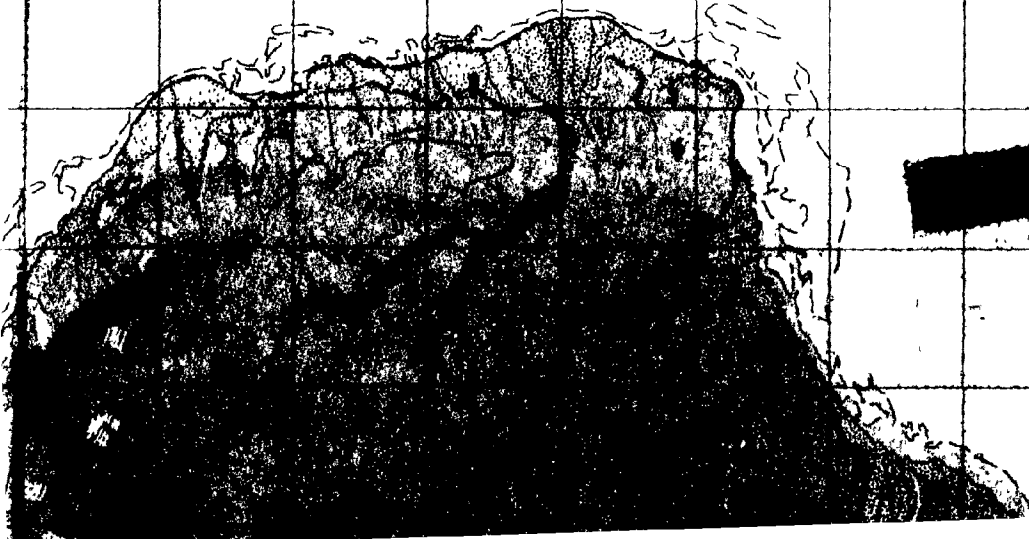
8900000m.

1 of



A R C T I C

O



99°15'

99°00'

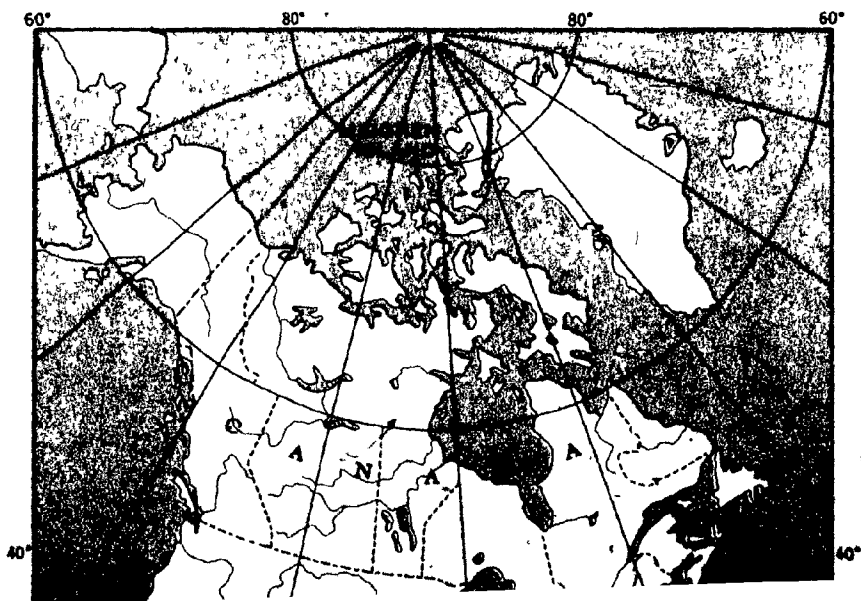
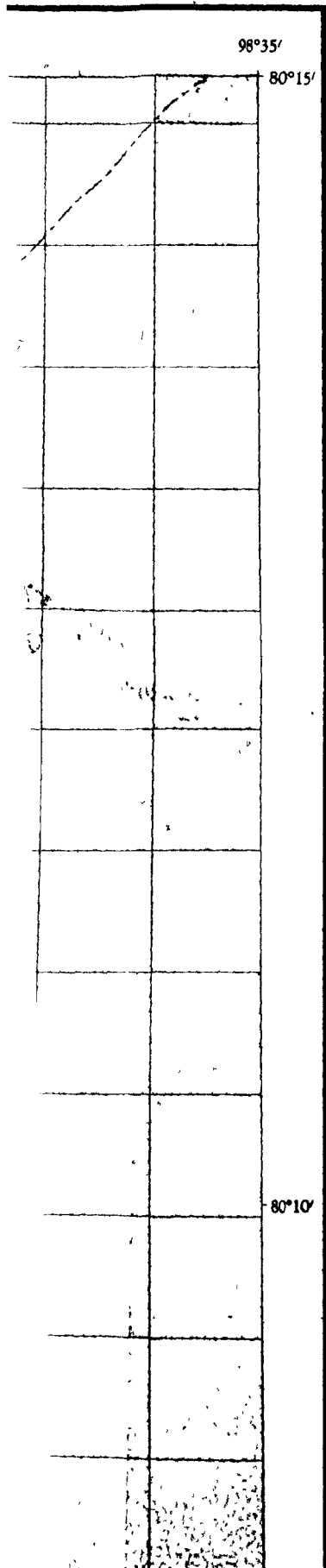
98°45'

O C E A N

PERLEY
ISLAND



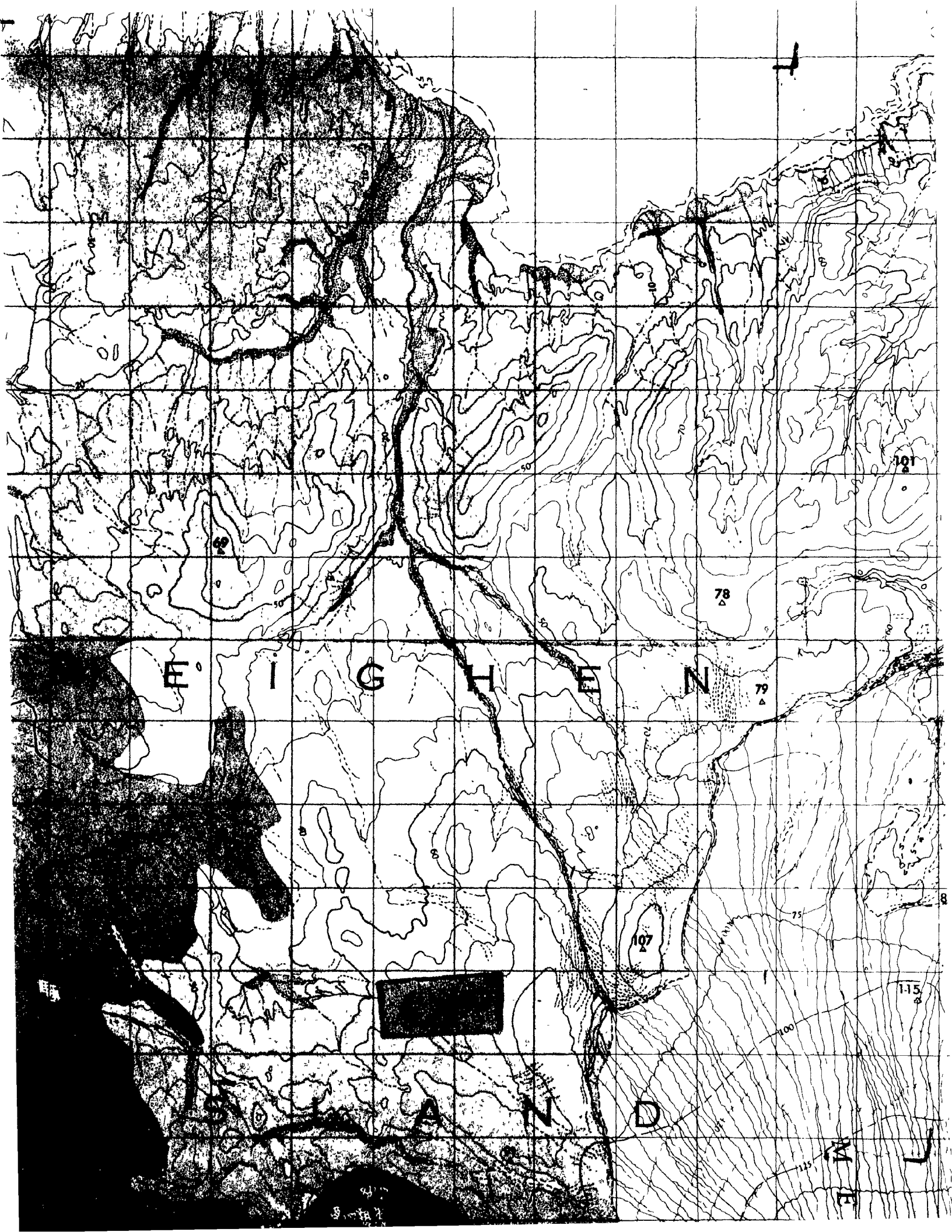
69 G - H (Parts)
560 B (Parts)



80°05'

8890 000 m.





E I G H E N

A N D

69

78

79

107

101

115

M E

S
V
E
R
D
R
U
P

C
H
A
N
N
E

Brocken Hill
Cairn, Stefansson
22 June 1916



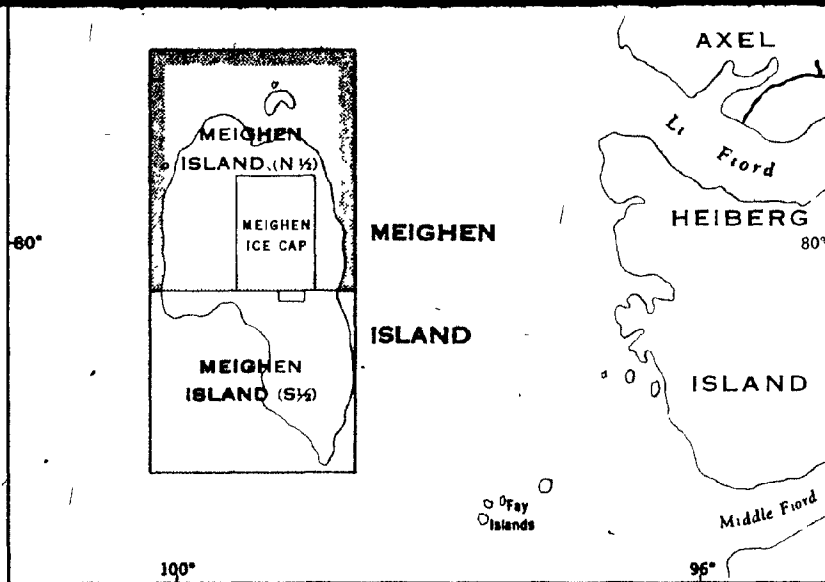
101

84

115

M
E
I
G

182



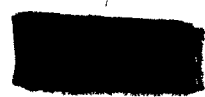
LEGEND

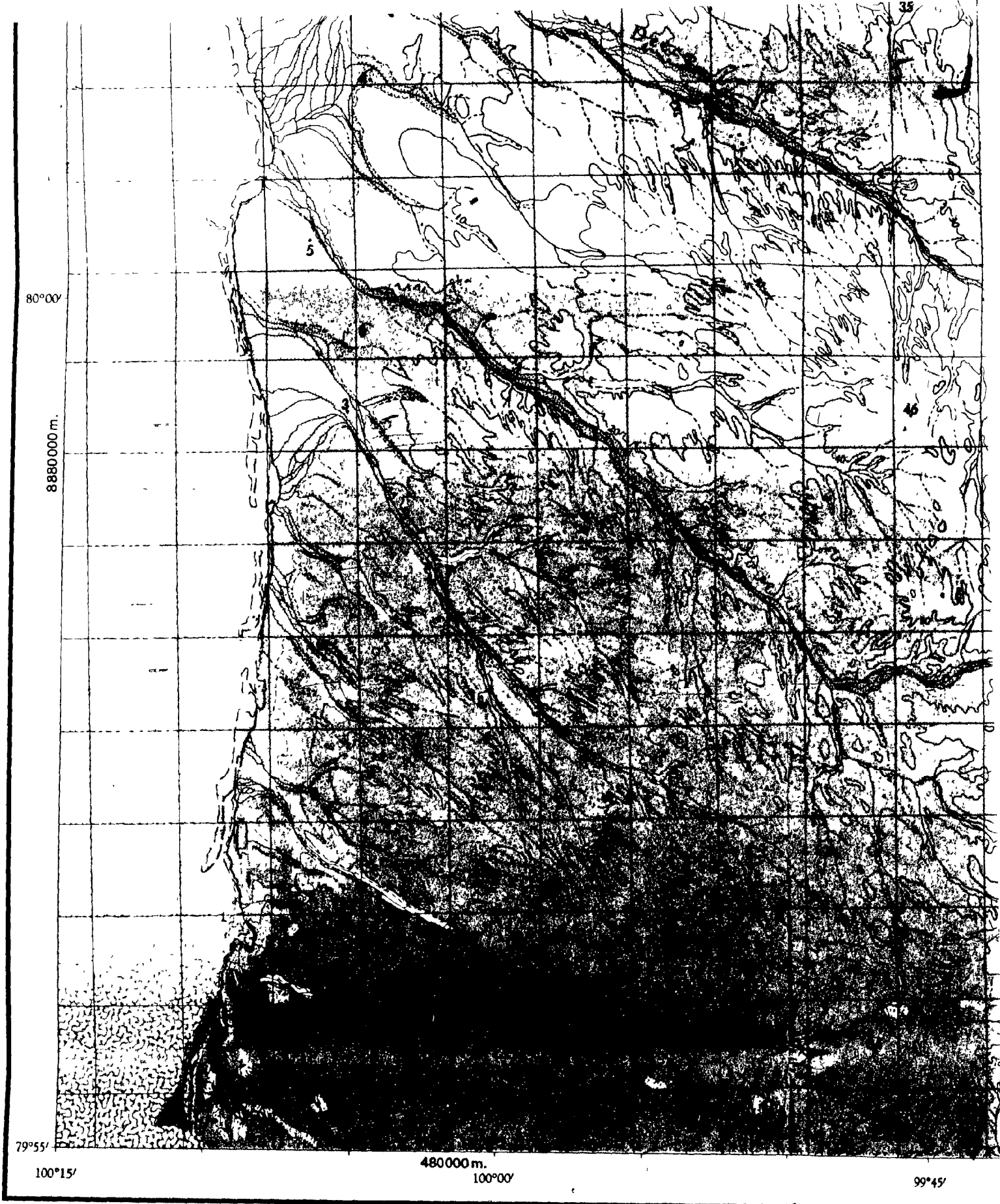
Historic site	⊕
Horizontal control points: on land	152 ▲
on ice	241 △
Spot elevation (accuracy variable)	25.
Lakes: perennial	
intermittent	
River	
Streams: perennial	
intermittent	
divided	
relic, marginal, superimposed	
River bed with channels	
Contours: land	
snow and ice	
beneath ice cap; calculated position	
beneath ice cap; assumed position	
Terraces: less than 1/2 the contour interval in height	
one half to one contour interval in height	
more than a contour interval in height	
Gullies: less than a contour interval in height	
more than a contour interval in height	
Steep sided hill (possibly ablation mound)	
Ice pushed ridges: less than 1/4 contour interval in height	

C
H
A
N
N
E

80°05'

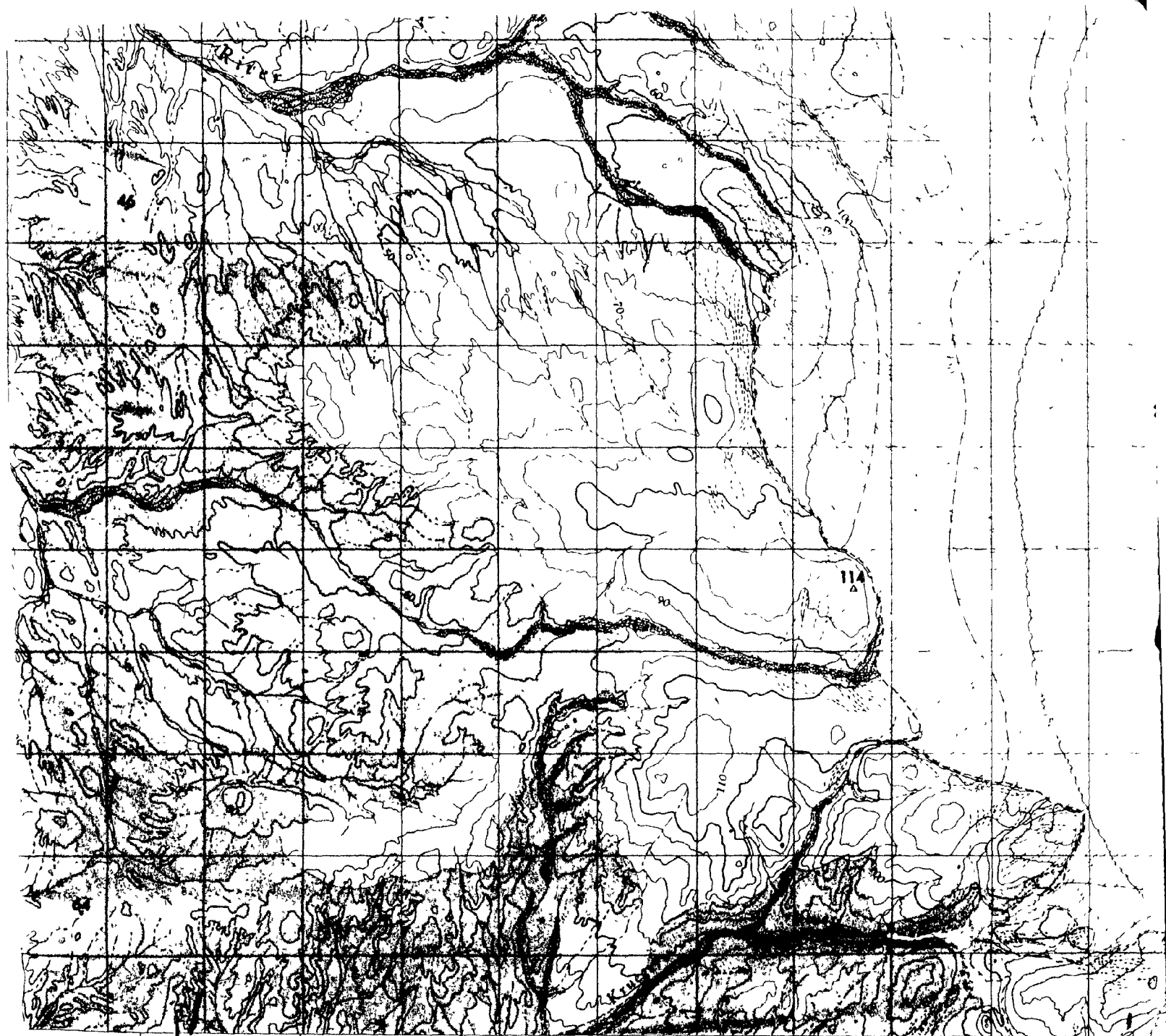
80°00'





Compiled, 1965, by the SURVEYS AND MAPPING BRANCH,
DEPARTMENT OF MINES AND TECHNICAL SURVEYS,
from aerial photographs taken August 5, 1959. Printed 1965





99°45'

490000m.

99°30'

99°15'



MEIGHEN ISLAND (N¹/₂)

DISTRICT OF FRANKLIN

NORTHWEST TERRITORIES

SCALE 1:50,000

Metres 1000 500 0 1000 2000 3000 4000 Metres

CONTOUR INTERVAL 10 METRES
North American Datum 1927

Some names on this map are not yet official
Corrections or additions are invited by the Sur-
veys and Mapping Branch

I
G
H
E
N

182

I
C
E

241

C
A
P

125

150

153

131

0182

99°15'

500000 m.
99°00'

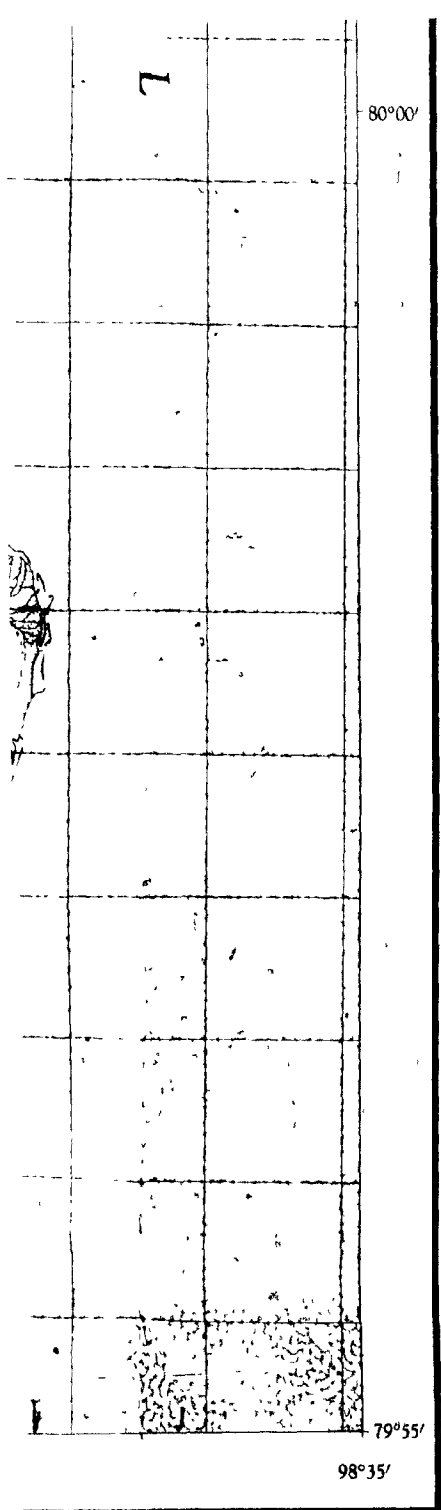
505000 m
98°45'

Elevations in metres above mean sea level

The daily change of the
compass useless in the
centre of this map is 1

1/2)

1106

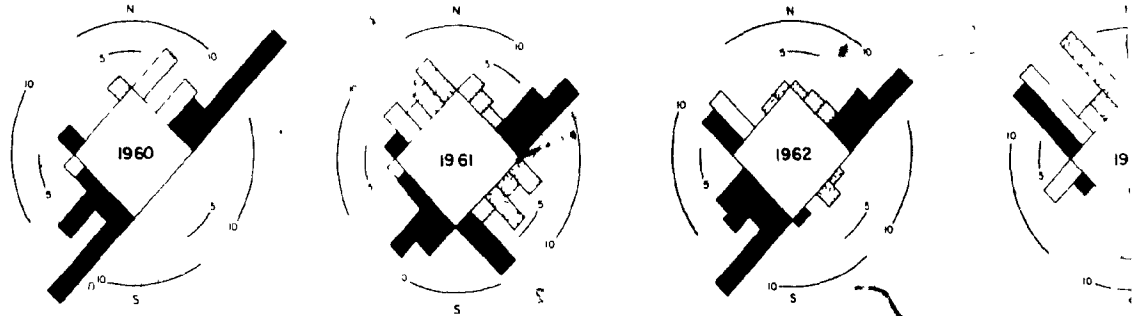


Gullies: less than a contour interval in height	
more than a contour interval in height	
Steep sided hill (possibly ablation mound)	
Ice pushed ridges: less than 1/4 contour interval in height	
more than 1/4 contour interval in height	
Abandoned offshore bar	
Sand dunes	
Pack ice of the open ocean, 9/10 to 10/10 cover	
Edge of circulating pack ice, 5 August 1959	
Polar and winter sea ice, 10/10 cover, 5 August 1959	
Edge of sea ice	
Bottom fast ice	
Edge of bottom fast ice	
Ice ridge on bottom fast ice	
Dirt ridge on bottom fast ice	
Dirt on bottom fast ice	
Dirt on ice or snow	
Ice cap or snow bank limits	
Nunatak	
Polygons	
Open water, foreshore flats	
Snow and ice	
Till areas	
Sand, gravel, coarse pebbles	
Mud and silt	

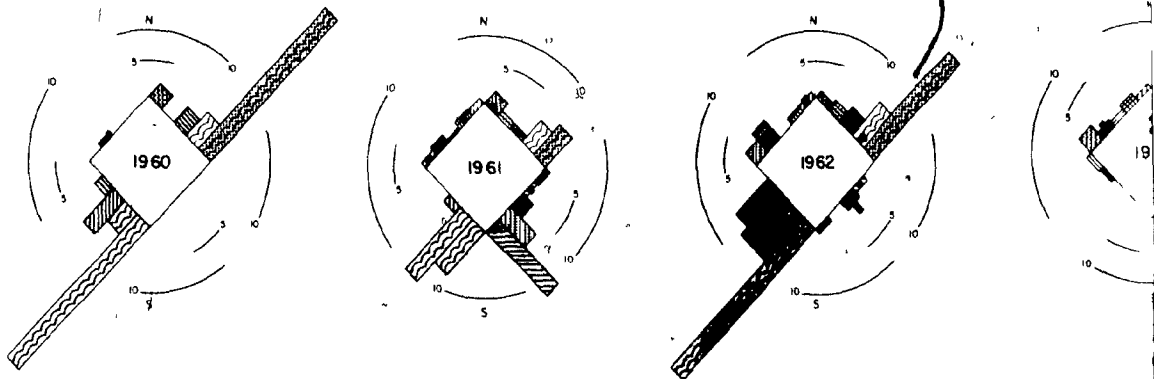
daily change of the north magnetic pole renders the magnetic compass useless in this area. The 1965 magnetic declination at the time of this map is 151° west, annual change 15' decreasing



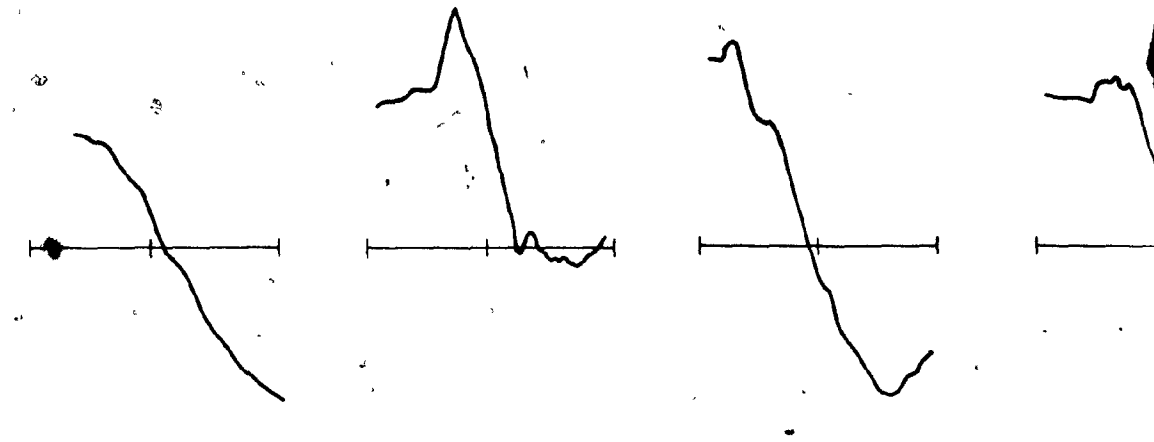
PERCENT OCCURRENCE OF SEB CLASSES



SUMMER ABLATION & SUMMER ACCUMULATION



SURFACE LOWERING (cm)



ACCUMULATION

SUMMER
SPRING
WINTER

ICE CAPS

ABLATION



1960

1961

1962

1963

1 of

Figure 4: 2.1 Summary Character (See Fi

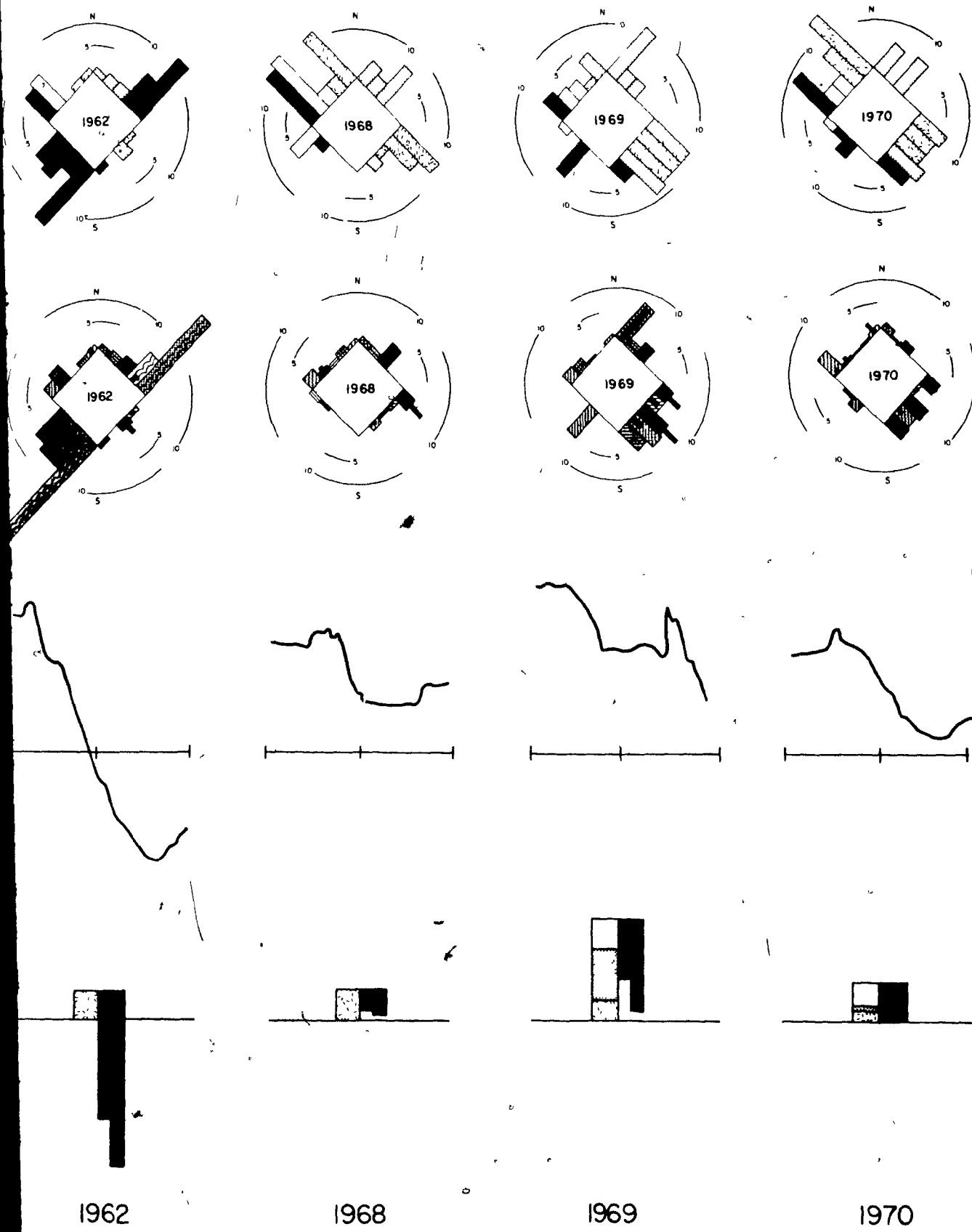


Figure 4: 2.1 Summary of Climate, Energy and Mass Balance Characteristics of Six Years of Main Ice Data. (See Figure 2: 2a and Appendix I for Legend.)



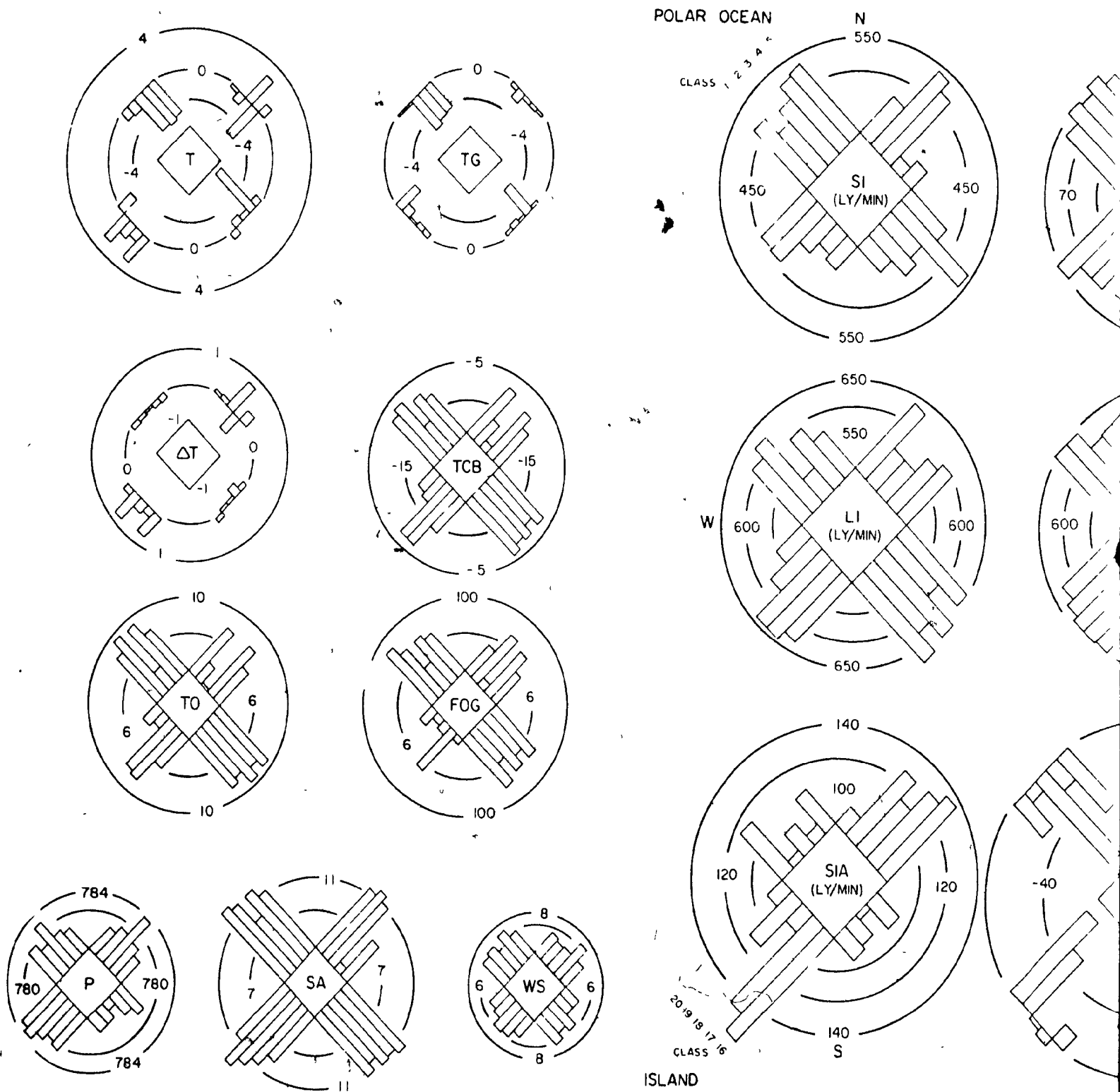
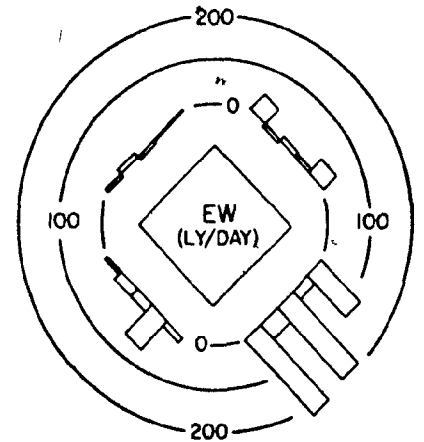
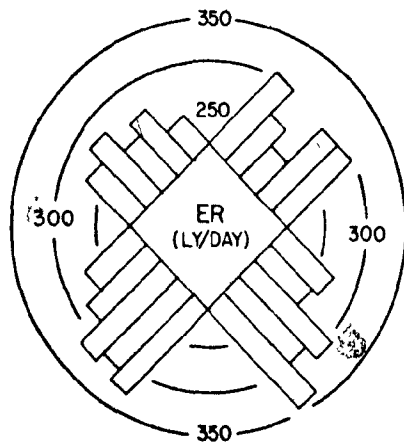
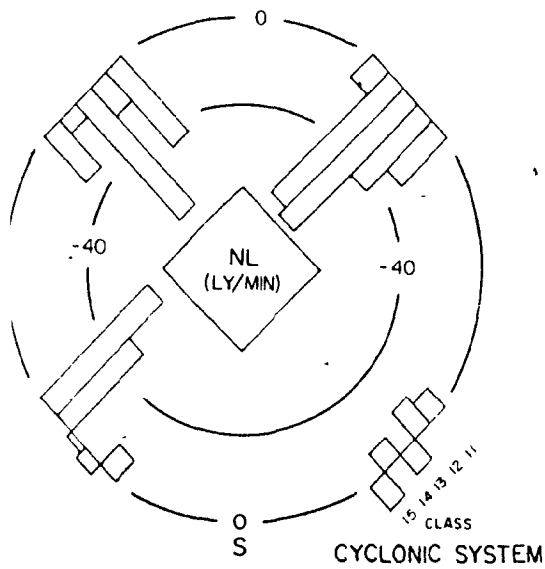
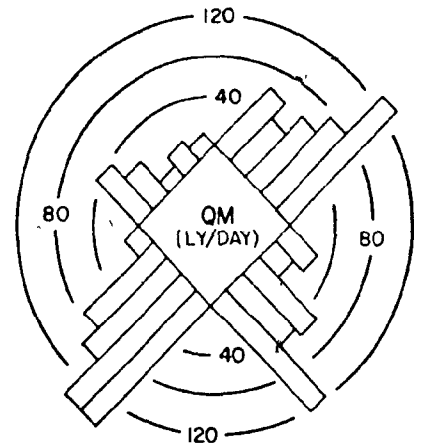
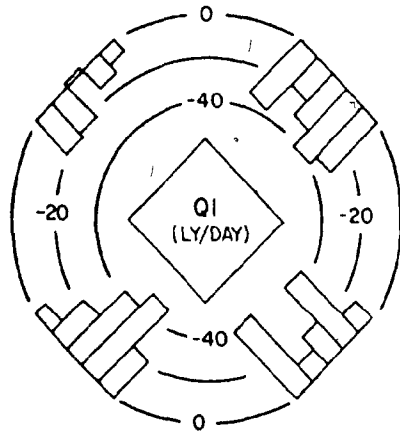
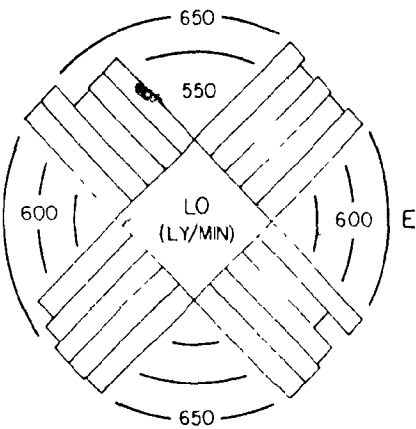
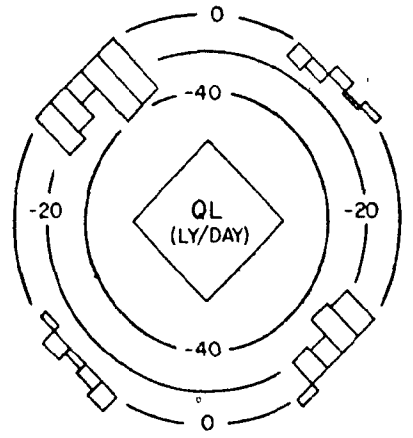
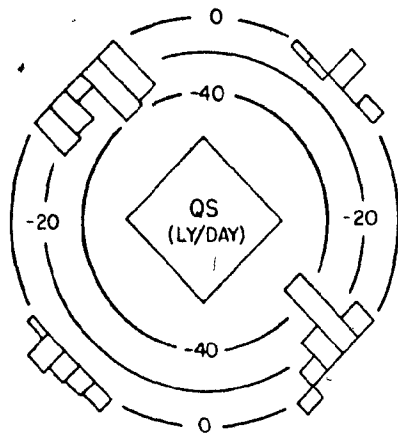
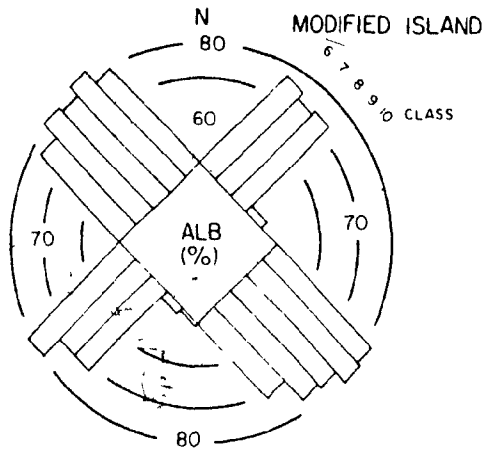


Figure 2: 3a, b and c SEB Diagrams of Climatic Components . (see Figure of abbreviations)

1 of



s of Climatic and Energy Balance
 . (see Figures in text for explan-
 viations)



THE ENERGY BALANCE CLIMATE
OF MEIGHEN ICE CAP, N. W. T.

by



BEA TAYLOR

A thesis submitted to the Faculty of Graduate Studies
and Research in partial fulfillment of the requirements
for the degree of Doctor of Philosophy.

Department of Meteorology
McGill University
Montreal, Canada

August 1974



VOLUME II

TABLE OF CONTENTS

VOLUME I

	Page
Abstract	iii
Résumé	iv
Preface	v
Acknowledgements	vi
Table of Contents	ix
List of Figures Volume I	xv
List of Tables Volume I	xviii
Chapter 1 INTRODUCTION	1
1: 1 Meighen Island	1
1: 1.1 The History	1
1: 1.2 The Mysteries	2
1: 1.3 The Approach	5
1: 2 Energy Balance Climate of Polar Ocean and Island Years	10
1: 2.1 Mean Summer Climate	10
1: 2.2 Wind Roses of Climatic Elements	11
1: 2.3 Summer Means of Energy Balance Components	12
1: 2.4 Wind Roses of Energy Balance Components	12
1: 3 Circulation Types and Energy Balance Climate	14
1: 3.1 Type I Polar Ocean Circulation	15
1: 3.2 Type II Cyclonic System Circulation	15
1: 3.3 Type III Island Circulation	15
1: 3.4 Type IV	16
1: 3.5 Circulation Types and the Mean Pressure Pattern	16
1: 3.6 Relationship of Wind Direction to Circula- tion Type	17
1: 3.7 Type and Energy Balance Climate	18
1: 4 Origin of Meighen Island Fog	
Chapter 2 THE SYNOPTIC ENERGY BALANCE DIAGRAM	25
2: 1 Basis for Further Breakdown	25
2: 2 Creating the Synoptic Energy Balance Diagram	27

	Page
2: 3 Energy Balance Regimes of the Classes	32
2: 3.1 Polar Ocean Climate	32
2: 3.2 Modified Island Climate	34
2: 3.3 Cyclonic Activity Climate	35
2: 3.4 Island Climate	37
 Chapter 3 CHARACTERISTICS OF THE SIX SUMMER SEASONS	 41
3: 1 Introduction	41
3: 2 1968	41
3: 3 1969	42
3: 4 1961	43
3: 5 1970	44
3: 6 1962	45
3: 7 1960	46
3: 8 Governing Factors	47
3: 9 Intervening Years	48
 Chapter 4 THE EXISTENCE OF MEIGHEN ICE CAP	 49
4: 1 Mass Balance	49
4: 1.1 Net Mass Balance	49
4: 1.2 Prediction of Mass Balance	51
4: 2 Factors Governing Mass Balance of Meighen Ice Cap	53
4: 2.1 Melt	54
4: 2.2 Suppression of Melt	54
4: 2.3 Spring and Summer Accumulation	56
4: 3 The Existence of Meighen Ice Cap	56
4: 3.1 Origin and Maintenance	56
4: 3.2 The Shape	58
4: 3.3 The Geographical Position	58
4: 3.4 Conclusions	59
 Appendix I LEGEND FOR SEB DIAGRAM	 60
 References	 61

VOLUME II

	Page
Table of Contents	iii
List of Figures Volume II	ix
List of Tables Volume II	xiv
Chapter 1 FIELD PROGRAM AND AVAILABLE DATA	1
1: 1 Introduction	1
1: 2 Meighen Island Stations	3
1: 2.1 Main Ice Station (Mi)	3
1: 2.2 Bore Hole Station (Bh)	3
1: 2.3 North Land Station (Nl)	3
1: 2.4 West Land Station (Wl)	3
1: 2.5 North Ocean Station (No)	3
1: 2.6 North Ice Station (Ni)	4
1: 2.7 South Ice	4
1: 3 Meteorological Data	4
1: 3.1 Screen Temperatures	4
1: 3.2 Humidity	5
1: 3.3 Atmospheric Pressure	6
1: 3.4 Wind	6
1: 3.5 Radiation	6
1: 3.6 Precipitation	8
1: 3.7 Cloud	8
1: 3.8 Other Observations	8
1: 4 Measurements in Snow, Ice and Ground During the Summer Season	8
1: 4.1 Surface Temperature and Condition	8
1: 4.2 Temperature at Depth	9
1: 4.3 Properties of Snow and Mud	7
1: 4.4 Surface Lowering	9
1: 4.5 Permanent Meteorological Station Data	9
1: 5 Glaciological Data	10
1: 5.1 Maps	10
1: 5.2 Mass Budget and Flow	10
1: 5.3 Bore Hole	10
Chapter 2 CLIMATIC ELEMENTS	11
2: 1 Surface Air Temperature	11
2: 1.1 Summer and Monthly Means	11
2: 1.2 Daily Temperature Range	14
2: 1.3 Melting Degree Days	15
2: 2 Humidity	15
2: 3 Pressure	16

	Page
2: 4 Wind Speed and Direction	17
2: 5 Cloud and Fog	20
2: 5.1 Mean Patterns	20
2: 5.2 Seasonal Variations	21
2: 5.3 Daily Variations	24
2: 6 Weather and Obstructions to Vision	25
2: 7 Precipitation	25
2: 8 Temperature in the Troposphere	28
Chapter 3 SYNOPTIC CLIMATOLOGY	31
3: 1 Introduction	31
3: 2 Type I	32
3: 2.1 Type I Case a	32
3: 2.2 Type I Case b	33
3: 2.3 General Characteristics of Type I	33
3: 3 Type II	36
3: 3.1 Type II Case a	36
3: 3.2 Type II Case b	36
3: 3.3 General Characteristics of Type II	37
3: 4 Type III	38
3: 4.1 Type III Case a	38
3: 4.2 Type III Case b	39
3: 4.3 Type III Case c	40
3: 4.4 General Characteristics of Type III	40
3: 5 Type IV	42
3: 6 Ten-Day Climate and Synoptic Situation	42
3: 6.1 1960	43
3: 6.2 1961	43
3: 6.3 1962	43
3: 6.4 1968	44
3: 6.5 1969	44
3: 6.6 1970	45
3: 7 Frequency of Circulation Types and Their Relationship to Climate	45
3: 8 Wind Direction and Synoptic Conditions	47
3: 8.1 1960	48
3: 8.2 1961	48
3: 8.3 1962	48
3: 8.4 1968	49
3: 8.5 1969	49
3: 8.6 1970	49
Chapter 4 MEASURED RADIATION COMPONENTS	50
4: 1 Diurnal Variations of the Radiation Components	50
4: 2 Daily Totals of Radiation Components	50

	Page
4: 3 The Influence of Weather on the Radiation Components	51
4: 3.1 Percent Solar and Long Wave Incoming	53
4: 3.2 Radiation Components and Sky Cover	53
4: 3.3 Radiation Components and Sky Conditions over Sun	57
4: 3.4 Solar Incoming Radiation and Sun's Visibility	57
4: 3.5 Radiation Components and Precipitation Type	58
4: 4 Radiation Component Wind Roses	58
4: 5 Surface Albedo	60
Chapter 5 SENSIBLE AND LATENT HEAT FLUXES	62
5: 1 Temperature, Humidity and Wind Speed Profiles-Theory	62
5: 2 Measured Profiles	65
5: 2.1 Calculations of R_i for 30-90 cm	67
5: 2.2 Profile Slopes	70
5: 2.3 Surface Roughness Z_0	74
5: 3 Sensible and Latent Heat - Theory	77
5: 4 Sensible and Latent Heat from Measured Profiles	77
5: 4.1 Relationship of Sensible to Latent Heat	79
5: 4.2 Diurnal Variation of Sensible and Latent Heat Flux	79
5: 4.3 Relationship to Temperature and Wind Direction	80
Chapter 6 CALCULATED ENERGY BALANCE COMPONENTS	81
6: 1 EBBA	81
6: 2 MIEBA	82
6: 3 Comparison of Measured and Calculated Radiation Components	84
6: 4 Errors in Ablation Measurements	85
6: 5 Modeling Run Off	86
6: 6 Comparison of Measured and Calculated Melt	87
6: 6.1 1970	88
6: 6.2 1969	88
6: 6.3 1968	89
6: 6.4 1962	89
6: 6.5 1961	90
6: 6.6 1960	90
6: 7 Calculated Surface Temperature	90

	Page
Appendix I	92
Appendix II	93
Appendix III	94
References	96

LIST OF FIGURES VOLUME II

Figure		Facing Page
1: 1	Map of the Queen Elizabeth Islands	1
1: 2a	Profile of Meighen Island and Ice Cap	2
1: 2b	Aerial Photograph of Meighen Island	3
1: 2c	Period of Operation of Meighen Island Stations	4
1: 2.1	Main Ice (M ₁)	3
1: 2.3	North Land (NL)	3
1: 2.6	North Ice (N ₁)	3
1: 3a	Periods of Temperature and Humidity Records	4
1: 3b	Periods of Pressure and Wind Records	6
1: 3c	Periods of Radiation Records	6
1: 3d	Meteorological Compound Main Ice	5
1: 3.1	Mini Screens and Mast	5
1: 3.5	Radiation Instruments	5
1: 5.2	Meighen Ice Cap Stake Network (after Paterson, 1969)	10
2: 1	Mean Air Temperature July and August	11
2: 1.1a	Meighen Island Mean Temperature compared to Island and Polar Ocean Mean Temperatures	12
2: 1.1b	Temperature: seasonal and ten-day means for various stations	13
2: 1.1c	Nine-day Running Means of Temperature	14
2: 1.2	Ten-day Means of Temperature Range	14*
2: 1.3	Melting Degree Days: seasonal and ten-day totals for various stations	15
2: 2	Relative Humidity: seasonal and ten-day means for various stations	16

* Figure is on the page indicated rather than facing it.

Figure		x Facing Page
2: 3a	Mean Pressure Patterns	16*
2: 3b	Station Pressure: seasonal and ten-day means for various stations	17
2: 4a	Wind Speed: seasonal and ten-day means for various stations	18
2: 4b	Monthly Wind Roses (Mi)	19*
2: 4c	Seasonal Wind Roses (Mi, NI, IC)	19
2: 5.1a	Mean Cloud Amount Contours	20*
2: 5.1b	Distribution of Low and Middle Cloud	20
2: 5.1c	Frequency Distribution of Cloud Type (Mi, NI, IC)	21
2: 5.2a	Cloud Amount: seasonal and ten-day means for various stations	22*
2: 5.2b	Seasonal Cloud Type Frequencies (Mi)	22
2: 5.2c	Seasonal Means of Fog Amount and Frequency	24
2: 5.3a	Daily Cloud Amounts (Mi)	25
2: 5.3b	Ten-day Means of Fog Amount	24*
2: 7a	Seasonal Precipitation Totals	26*
2: 7b	Total Accumulation Meighen Island	27*
2: 7c	Precipitation: seasonal and ten-day values for various stations	27
2: 8a	Isachsen Seasonal Mean Temperature Soundings	28*
2: 8b	Roses of Tropospheric Temperature	29
2: 8c	Isachsen Ten-day Mean Temperature Soundings	30*
3: 2.1a	Synoptic Charts: Type I Case a	32
3: 2.1b	Temperature Sounding: Type I Case a	32*
3: 2.2a	Synoptic Charts: Type I Case b	33
3: 2.2b	Temperature Sounding: Type I Case b	33*
3: 3.1a	Synoptic Charts: Type II Case a	36

Figure		Facing Page
3: 3.1b	Temperature Sounding: Type II Case a	36*
3: 3.2	Synoptic Charts: Type II Case b	37
3: 4.1	Synoptic Charts: Type III Case a	38
3: 4.2a	Synoptic Charts: Type III Case b	39
3: 4.2b	Temperature Sounding: Type III Case b	39*
3: 4.3	Synoptic Charts: Type III Case c	40
3: 7	Frequency Distribution of Types	45
3: 8a	Deviation of Actual Wind from Geostrophic	47
3: 8b	Roses of Geostrophic and Actual Wind	47
3: 8c	Seasonal Roses of Geostrophic Wind, Actual Wind and Temperature 1960-62	48
3: 8d	Seasonal Roses of Geostrophic Wind, Actual Wind and Temperature 1968-70	49
4: 1	Diurnal Summer Season Means of Surface Radiation Components (Mi)	50
4: 2	Daily Totals of Radiation Components: 1970	51
4: 3.1	Frequency Distribution of Solar and Long Wave Incoming Radiation and their relation to Temperature and Cloud Opacity	53
4: 4	Roses of the Radiation Components	59
4: 5a	Mean Albedo in Temperature Intervals	60*
4: 5b	Frequency Distribution of Albedo in Temperature Intervals	61
5: 1a	Profiles of Wind Speed: over a snow covered ice surface (after Doronin, 1969)	64
5: 1b	Profiles of Temperature: over a snow covered ice surface (after Doronin, 1969)	64
5: 1c	Change in Temperature Profile: over a snow covered ice surface on 25 August 1956, before and after frontal passage	64
5: 2	Frequency Distribution of Richardson Number (Ri) and Comparison of Mean Error of Temperature Profiles from Log Law and Power Law with Stability	67

Figure		Facing Page
5: 2.1a	Frequency Distribution of Richardson Number (Ri) for Fog and No Fog and Variation of Temperature and Wind Speed with Stability	68
5: 2.1b	Frequency Distribution of Richardson Number for Conditions of 1) No Fog at Mi or N1; 2) Fog at Mi and N1; and 3) No Fog at N1 but Fog at Mi.	69
5: 2.1c	Roses of Richardson Number (Ri) for Fog and No Fog	70
5: 2.2a	Frequency Distribution of the Slope of the Temperature Profile and Variation of Temperature with Temperature Profile Slope for Fog and No Fog	71
5: 2.2b	Frequency Distribution of Temperature Profile Slope and Variation of Temperature with Temperature Profile Slope for Various Stability Conditions	71
5: 2.2c	Ten-day Means of Temperature Profiles	71*
5: 2.2d	Roses of Temperature Profile Slope	72
5: 2.2e	Frequency Distribution of Vapour Pressure Profile Slope and Variation of Vapour Pressure with Vapour Pressure Slope, for Fog and No Fog	73*
5: 2.2f	Roses of Vapour Pressure Slope for Fog and No Fog	73*
5: 2.3	Frequency Distribution of Surface Roughness (Zo) and Variation of Temperature and Wind Speed with Surface Roughness for various Sky Cover and Stability Conditions	75
5: 4	Relationship of QS and QL Calculated Using 30 cm and 90 cm Observations with QS and QL Calculated Using 30 cm and 150 cm Observations	77
5: 4.1a	Relationship of QS to QL	78*
5: 4.1b	Frequency Distribution of QS and QL for Fog and No Fog	79
5: 4.2	Diurnal Variation of QS and QL	79*
5: 4.3a	Variation of QS and QL with Temperature for Fog and No Fog	80
5: 4.3b	Roses of QS and QL	81

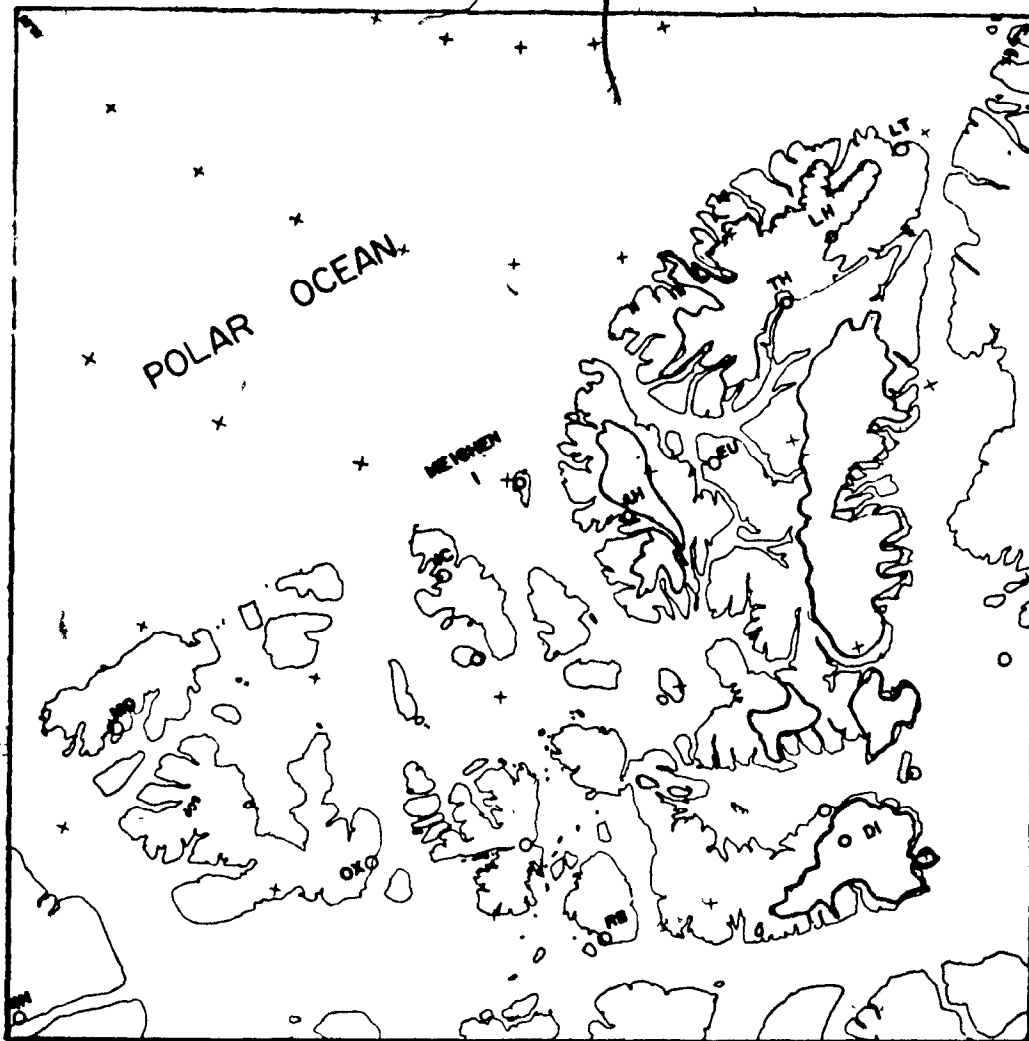
Figure		Facing Page
6: 3	Comparison of Measured and Calculated Radiation Components	84
6: 5	Initial Snow and Ice Profile	86*
6: 6	Measured and Calculated Melt: Six Years	88, 89
6: 7	Daily Mean Surface and Screen Temperatures for 1969 and 1970	90
A: 2	Measured (ZI) and Calculated (SGI) Incoming Solar Radiation for Observations with 10/10 Fog and 10/10 Cloud Only	92
A: 3a	Measured Temperatures in the Ice at Ten-day intervals in 1969 and 1970 (at Mi)	94
A: 3b	Measured and Calculated Temperatures in the Ice for 1970.	94*

LIST OF TABLES VOLUME II

Table		Facing Page
1: 3.5	Radiation Instrument Calibration Factors	7
2: 1.1	Mean Air Temperature Various Stations	11*
2: 5.2	Most Important Sky Cover in Ten-Day Periods	23
2: 6	Percent Frequency of Observations with Various Types of Weather	26
3: 6a	Ten-day Synoptic Conditions, Circulation Type and Main Ice Climatic Elements 1960-1962	43
3: 6b	Ten-day Synoptic Conditions, Circulation Type, and Main Ice Climatic Elements 1968-1970	44
3: 7a	Frequency of Circulation Types	46
3: 7b	Mean Ten-Day Totals for Circulation Types	46
4: 3.2a	Short Wave Radiation and Sky Cover	54
4: 3.2b	Long Wave Radiation and Sky Cover	55
4: 3.2c	Estimated Net Radiation and Sky Cover	56*
4: 3.3	Radiation Components and Sky Condition over the Sun	57
4: 3.4	Solar Incoming Radiation and Sun's Visibility	57
4: 3.5	Radiation Components and Weather	58
4: 5a	Albedo with Surface and Weather Conditions	60
4: 5b	Albedo with Surface Conditions (after Goodall, 1971)	60
5: 2a	Percent Frequency of Mean Deviation from Logarithmic Law	65
5: 2b	Mean Deviation from Logarithmic and Power Law	66
5: 2.1a	Richardson Number (Ri) and Sky Cover	68*

* Table is on the page indicated rather than facing it.

Table		Facing Page
5: 2.1b	Ten-day Means of Richardson Number	69*
5: 2.2a	Wind Speed Power Law Indices ($1/n$) for various Periods	69*
5: 2.2b	Ten-day Means of Profile Parameters	69*
5: 2.3a	Surface Roughness (Z_0) for Various Snow and Ice Surfaces	74
5: 2.3b	Ten-day Means of Surface Roughness (Z_0)	74
5: 2.3c	Surface Roughness and Surface Type	75*
5: 2.3d	Surface Roughness and Weather	76*
6: 2	Upper Air Sounding Set Up	82
A: 1	Clear Sky Short and Long Wave Incoming Radiation: Comparison of Measured and Calculated Values	92



LT = Alert; EU = Eureka; IC = Isachsen
MD = Mould Bay; RB = Resolute Bay;
OX = Rae Point; AH = Axel Heiberg Stations
TF = Tanquary Fiord; LH = Lake Hazen
DI = Devon Ice Cap

Figure 1: 1 The Queen Elizabeth Islands

CHAPTER 1
FIELD PROGRAM AND AVAILABLE DATA

1: 1 Introduction

Meighen Island is located on the NW edge of the Queen Elizabeth Islands bordering on the Polar Ocean (see Figure 1: 1). It extends 56 km in length with a maximum width of 40 km and is characterized by low relief in the form of rolling plains. The salient feature of this monotonous landscape is the ice cap which occupies the central portion of the island (see Figure 1; 2a). The ice cap covers approximately 80 km², has a maximum thickness of 120 meters and rises to only 268 m above sea level. This is remarkably low for a glacier even at 80°N.

The anomaly of Meighen Ice Cap has interested arctic researchers since 1956 when air photography confirmed its existence (Dunbar and Greenaway, 1956). The history and reasons for study of Meighen Ice Cap are discussed in detail in Volume I Chapter 1. R. Thorsteinsson (Geological Survey) carried out geological reconnaissance on the island and ice cap eleven years later, by dog sled. In 1959 Polar Continental Shelf Project began scientific investigations there which are still in progress. Vertical photographic coverage and accompanying survey ground control were undertaken in conjunction with National Research Council, Defence Research Board and Geographical Branch during the first two years. The necessary field work for this was carried out by K.C. Arnold (Geographical Branch) who also was responsible for the glaciological and meteorological work done during the years 1959-1962. Gravity measurements were made by R. Hornal (Dominion Observatory)



Figure 1: 2a Profile of Meighen Ice Cap from the East

and supported by seismic work in 1960. W.S.B. Paterson (Polar Continental Shelf Project) took over the glaciological program in 1963 and in 1965 directed the drilling of a bore hole through the thickest part of the ice cap. The resulting glaciological studies were undertaken by Paterson and R.M. Koerner (Institute of Polar Studies, Ohio State University and Polar Continental Shelf Project) and are continuing.

In 1968 with the financial and logistic support of Polar Continental Shelf Project the author initiated a surface energy balance study of Meighen Ice Cap with the objective of determining the reasons for the existence of Meighen Ice Cap by examining the components of the surface energy budget of the ice cap. The special requirements of the study are discussed in Volume I Section 1: 3. In response to these requirements two stations were maintained throughout the four field seasons and various other stations were established for shorter periods. The instrumentation was kept as basic as possible as discussed in Volume I Section 1: 3. In the present chapter the data obtained from this and previous field programs is outlined. Reference should be made to Volume I Chapter 1 for further discussion of the topographical setting of Meighen Island.

The remaining chapters in Volume II^{*} contain a detailed analysis of the observed climate, energy balance and synoptic regime of Meighen Island, the final chapter dealing with the computer model used to extend the two years of energy budget observations to the six years of climate data. In Volume I the results of these analyses and energy balance calculations are used to develop the Synoptic Energy Balance Diagram and discuss its implications regarding the synoptic-mass balance regime of Meighen Ice Cap.

* In this Volume references to sections of Volume I will be given as " I 1: 3" and to Volume II as " 1: 3".

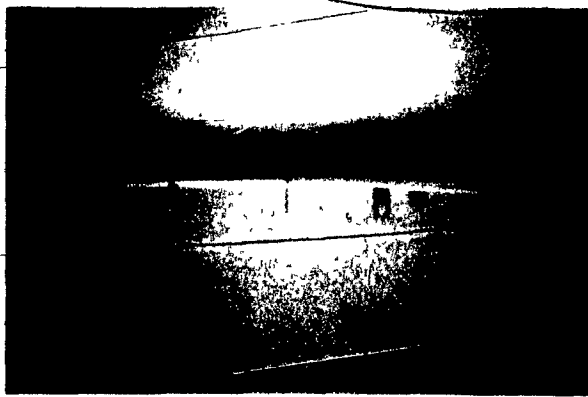


Figure 1: 2.1 Main Ice (M1) :
looking towards summit of ice cap
(Bh) from Mi meteorological area
(photo Petzold)

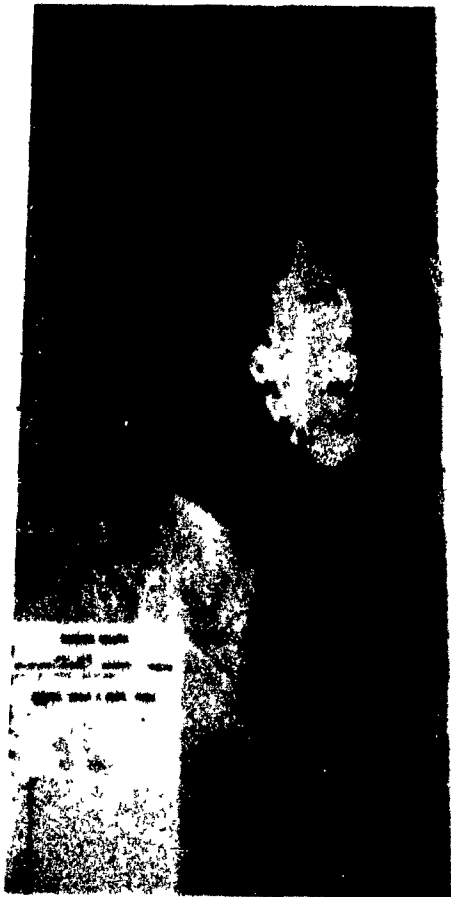


Figure 1: 2b Meighen Island
air photograph mosaic



Figure 1: 2.3 North Land (Nl) :
from NW before snow melt complete



Figure 1: 2.6 North Ice (Ni) :
looking NE across land to Polar
Ocean from Ni 'slush camp'

1: 2 Meighen Island Stations

The profile and map of Figures 1:2a and 1:2b show the location of the Meighen Island Stations.

1: 2.1 Main Ice Station (M1): situated at 241 meters on a secondary summit of the ice cap, 3 km north of the summit, it has served as the base camp for most of the glaciological and meteorological work since 1969 providing the most complete meteorological records. (See Figure 1: 2.1).

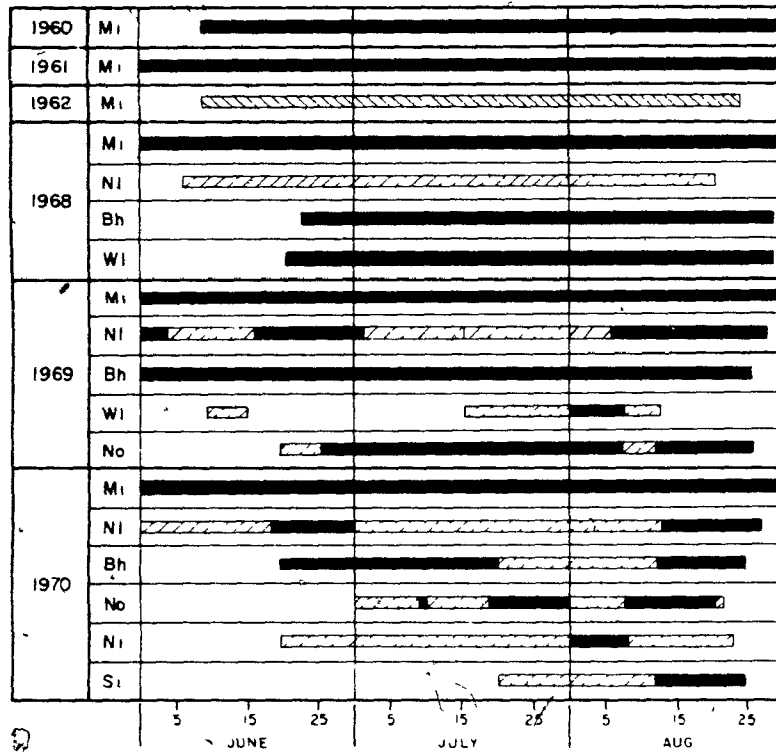
1: 2.2 Bore Hole Station (Bh): first occupied during the drilling of the bore hole, it is located on the summit of the ice cap and affords an unobstructed view of the island. (See Figure 1: 2.1).

1: 2.3 North Land Station (N1): located on land 1.5 km from the north end of the ice cap on top of a gentle hill (78 m. amsl), this station produced the second most complete meteorological records. It was first occupied in 1968. (See Figure 1: 2.3).

1: 2.4 West Land Station (W1): also established in 1968, it lies directly west of Main Ice, 3 km from the ice cap (110 m. amsl).

1: 2.5 North Ocean Station (No): situated 10 meters from the ocean on the sandy beach of the north coast, this station was used in 1969 and 1970.

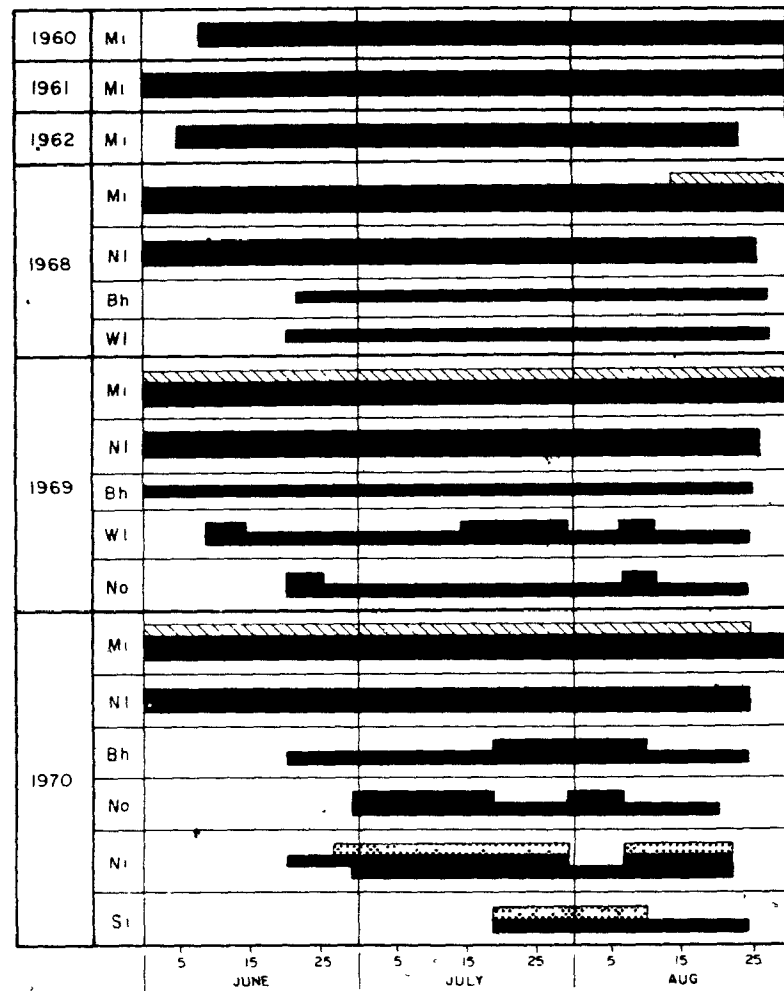
PERIOD OF OPERATION OF MEIGHEN ISLAND STATIONS



 UNMANNED
 3 HRLY OBS
 MANNED 3 HRLY OBS EXCEPT ONE OB
 6 HRLY OBS

Figure 1: 2c

PERIODS OF TEMPERATURE & HUMIDITY RECORDS



 TEMPERATURE AND HUMIDITY TRACE
 TEMPERATURE AND HUMIDITY OBSERVATIONS
 TEMPERATURE AT 30 90 & 150 CM
 TEMPERATURE AND HUMIDITY AT 30 90 & 150 CM

Figure 1: 3a

1: 2.6 North Ice Station (Ni): operated during 1970, it is situated half way between Main Ice and North Land, at 150 m. amsl, on the north slope of the ice cap. Weather permitting, Main Ice and North Land are visible from this station. (See figure 1: 2.6).

1: 2.7 South Ice: unmanned and serviced from Main Ice or Bore Hole Camps, this site is at 240 m. amsl on the steep southwest slope of the ice cap, approximately .5 km from the bore hole.

Figure 1:2c shows the periods during which the above camps were operated as meteorological stations. Distinction is made between periods when the stations were unmanned recording stations, and manned stations operating on continuous 3-hourly, 3-hourly except one observation, or 6-hourly basis.

1:3 Meteorological Data

In the following is an outline of the meteorological data secured to date on Meighen Island. Reference should be made to Figures 1:3a, b and c for the length of meteorological records obtained each year at the various stations for each of the parameters. The Main Ice meteorological compound is shown in Figure 1: 3d.

1: 3.1 Screen Temperatures

Thermohygrographs were maintained in Stevenson screens at all the meteorological stations for their total period of operation. The screens also held Canada Department of Transport, Meteorological Branch dry bulb, maximum and minimum thermometers. Haeni, aspirated



Figure 1: 3d M1 Meteorological Compound



Figure 1: 3.1 Mini Screens and Mast (M1)

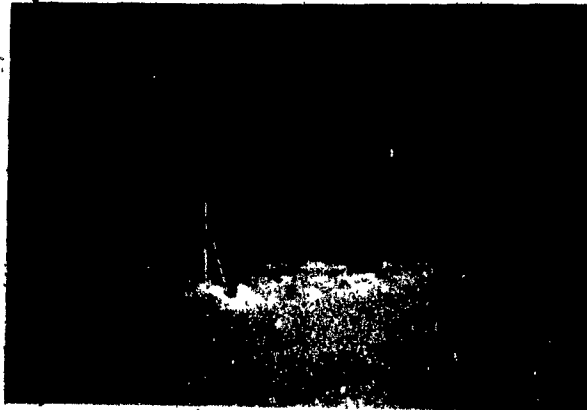


Figure 1: 3.5 Radiation Instruments

psychrometers were used at Main Ice, North Land, North Ocean and West Land, but considerable trouble was experienced with the fan mechanism. Complete records of un aspirated screen temperature were secured from all stations for their total period of operation.

Styrofoam screens, designed by the author, containing Haeni psychrometers or Meteorological Branch thermometers were used to obtain air temperatures at 30, 90 and 150 cm above the surface (see Figure 1: 3.1). These screens proved effective in protecting the thermometers from accumulations of rime, freezing drizzle or rain and blowing snow and, except on infrequent still clear days, from radiative heating. Profiles of temperature were obtained at 3-hourly intervals from Main Ice for 1968-70 and from North Ice and South Ice for 1970. The thermometers were calibrated by National Research Council after the 1969 and 1970 field seasons. The correction factors from these two calibrations were sufficiently consistent. Corrections were also made to account for the un aspirated readings.

In 1961 Stebelsky, using a sling psychrometer, measured air temperatures at 1 meter and near the surface, over the ice cap and land east of Main Ice under various weather conditions. The results have been discussed (Stebelsky, 1962).

1: 3.2 Humidity

Relative humidity traces were obtained for all stations, from the thermohygrographs. The regular 3-hourly or 6-hourly observations included wet bulb temperatures at Main Ice (30, 90 and 150 cm), North Land (150 cm), North Ice (90 and 150 cm), West Land (150 cm) and North Ocean (150 cm).

PERIODS OF PRESSURE AND WIND RECORDS

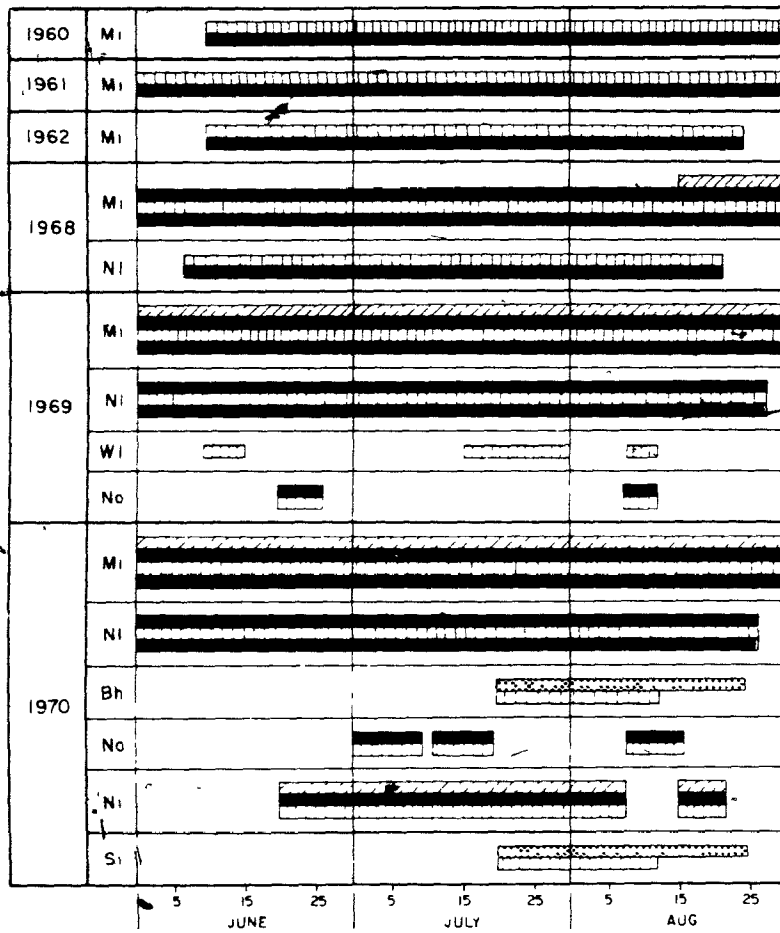


Figure 1: 3b

PERIODS OF RADIATION RECORDS

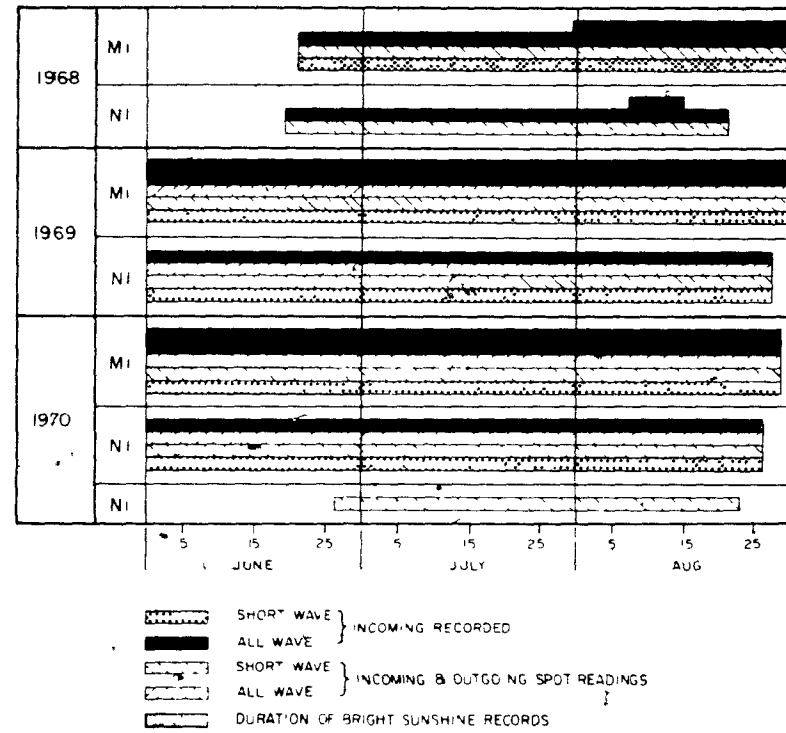


Figure 1: 3c

1: 3.3 Atmospheric Pressure

Station pressure and pressure tendency were recorded at Main Ice and North Land by a Fuess aneroid barometer and a three-day barograph, supplied by the Meteorological Branch. Sea level pressure was also obtained from Main Ice according to the Meteorological Branch reduction table for the station.

1: 3.4 Wind

Regular readings of wind speed and direction (ca. 150 cm) were secured for all stations. Meteorological Branch totalizing anemometers were used to obtain 3-hour run of wind records from Main Ice, North Land, North Ocean and North Ice. Small Fuess anemometers located at 30, 90, and 150 cm yielded 3-hourly profiles of wind for Main Ice (1968-70) and North Ice (1970).

With the intensification of the wind study in 1970, pibals were released twice a day from Main Ice and North Land, weather and personnel permitting. During the melt season of that year the 150 cm wind speed and direction were continuously recorded on a Science Associates All Purpose Wind Recording System at the Bore Hole and South Ice stations. In addition, 60 cm run of wind and instantaneous wind speed and direction were observed at these sites every three hours. Orange smoke generators, set off and photographed on the relatively steep south slope of the ice cap, produced information about the katabatic wind effect (Petzold, 1971).

1: 3.5 Radiation

Traces of short wave incoming insolation were obtained at Main Ice in 1968, from a Kipp and Zonnen solarimeter and drop bar millivolt re-

TABLE 1: 3.5

Radiation Instrument Calibration Factors				
Station	Instrument	1968	1969	1970
Main Ice ¹	Kipp and Zonens	570	570	570
	Davos short wave	265	276	250
	Davos long wave	266	279	248
North Land ² and North Ice	Kipp and Zonens	714	700 ³ /721 ⁴	686 ³ /728 ⁴
	Davos short wave	797	848	820
	Davos long wave	814	863	835

1 read on the drop bar milivolt records

2 read on a portable milivolt meter

3 up facing instrument

4 down facing instrument

corder, and in 1969-70 from a daily Belfort pyr heliograph. At North Land a weekly pyr heliograph was in operation. During the 1969-70 seasons the recording millivolt meter produced a continuous record of all wave incoming radiation, measured on a portable Davos pyr radiometer - pyranometer. Three-hourly spot readings of short wave incoming and reflected radiation (Main Ice, North Land and North Ice) and of all wave incoming and outgoing radiation (Main Ice and North Land) supplemented the continuous recordings. The portable pyr radiometer-pyranometer was used from time to time to measure short wave and all wave albedos over bare ground and over melting snow and ice surfaces. Duration of bright sunshine was obtained at Main Ice and North Land using regular Meteorological Branch Campbell-Stokes sunshine recorders. Figure 1: 3.5 shows the radiation instruments at Main Ice.

The radiation instruments were calibrated by the manufacturers before the 1968 field season. Subsequently the Kipp and Zonen solarimeters were calibrated by the Meteorological Branch Laboratory before the 1969 season and after the 1970 season. The Meteorological Branch laboratory also made an estimated calibration of the Davos pyranometer-pyrheliometer at these times and the Davos instruments were recalibrated in Davos in 1971. The Actinographs were calibrated at the end of the 1971 season. Table 1: 3.5 shows the calibration factors for the Kipp and Zonen and Davos instruments used in 1968, 1969 and 1970. The Main Ice Kipp and Zonen solarimeter, from which the major portion of the short wave radiation measurements used in the present study were obtained, showed no variation over the three years. The Davos long wave instrument calibration varied considerably, the 1968 to 1969 change probably resulting from deterioration of the polyethylene dome, and the 1969 to 1970 variation being a result of replacing the dome in 1970.

1: 3.6 Precipitation

Precipitation amounts were recorded 6-hourly at all manned stations, most of which were equipped with Meteorological Branch ordinary rain gauges. The precipitation records suffer from the inaccuracies common to all attempts to measure the accumulation of snow accompanied by high winds. However, duration and type of precipitation and, in particular, the type of snow crystals falling were noted.

1: 3.7 Cloud

Cloud opacity, amount, type and height were estimated and recorded according to MANOBS (1968) specifications at each observation. In 1969 and 1970 ceiling balloons assisted in the determination of the height of low cloud and the vertical visibility into obscuring phenomena.

1: 3.8 Other Observations

MANOBS specifications were also followed when observing weather, obstructions to vision and horizontal visibility. Records were kept of location and appearance of mirages and leads in sea ice.

1: 4 Measurements in Snow, Ice and Ground During the Summer Season

1: 4.1 Surface Temperature and Condition

An attempt was made to measure snow and ground surface temperatures in 1969 and 1970 at Main Ice and North Land using small styro-foam shielded thermisters. The nature, colour and relief of the various surfaces were recorded at all observations and estimates were made of the percentages of snow/slush/ice/bare ground when conditions changed.

1: 4.2 Temperatures at Depth

Paired thermistors attached to a cable were frozen in the ice near Main Ice to measure temperature at the following depths: 0.5, 1, 2, 4, 6 and 8 meters. These were read daily in 1969 and 1970.

At North Land during July 1969, 4 thermistors were sunk at approximately 5, 15, 25, and 30 cm in the active layer of the permafrost. These were read 3 times daily for the rest of the 1969 season and all of the 1970 season.

1: 4.3 Properties of Snow and Mud

During the 1969 and 1970 seasons, snow density and grain-size were measured in the vicinity of Main Ice when a change in the conditions occurred. Similarly, mud samples from near North Land were weighed, dried and reweighed to determine the water content of the mud.

1: 4.4 Surface Lowering

A square frame of slotted angle iron (1 meter by 1 meter), supported at the corners by stakes drilled in the ice, was used to determine surface lowering. Forty-eight readings were obtained from each square. Main Ice personnel carried out measurements on two squares twice daily and on two others daily in 1968, and on one square daily in 1969 and 1970. At North Ice a one-sided version of the square was read 6-hourly. Snow depth records were kept at North Land.

1: 4.5 Permanent Meteorological Station Data

The study also made use of the three-hourly meteorological observations from Isachsen and Eureka (see Figure 1: 1) and the upper air soundings from Isachsen.

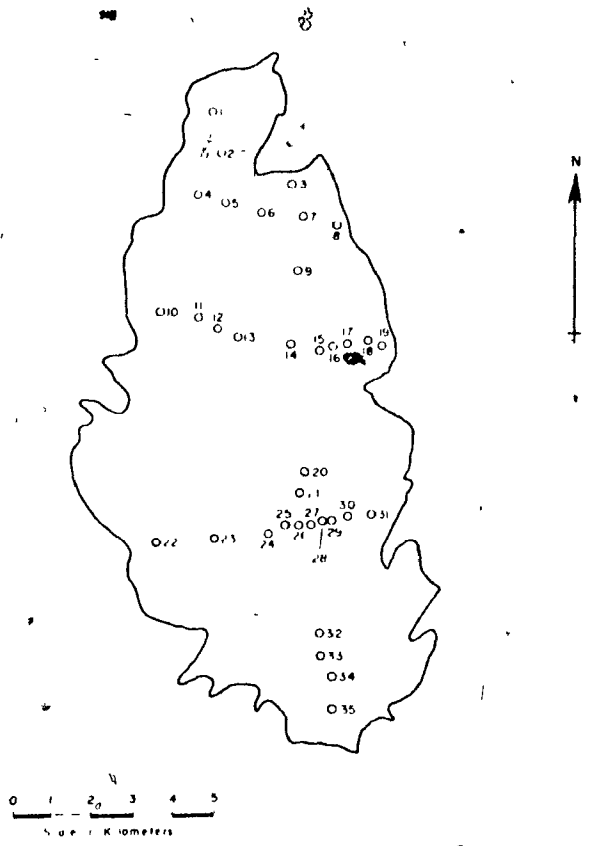


Figure 1: 5.2 Position and Number of Stakes on Meighen Ice Cap
 (after Paterson, 1969)

1: 5⁺ Glaciological Data

1: 5.1 Maps

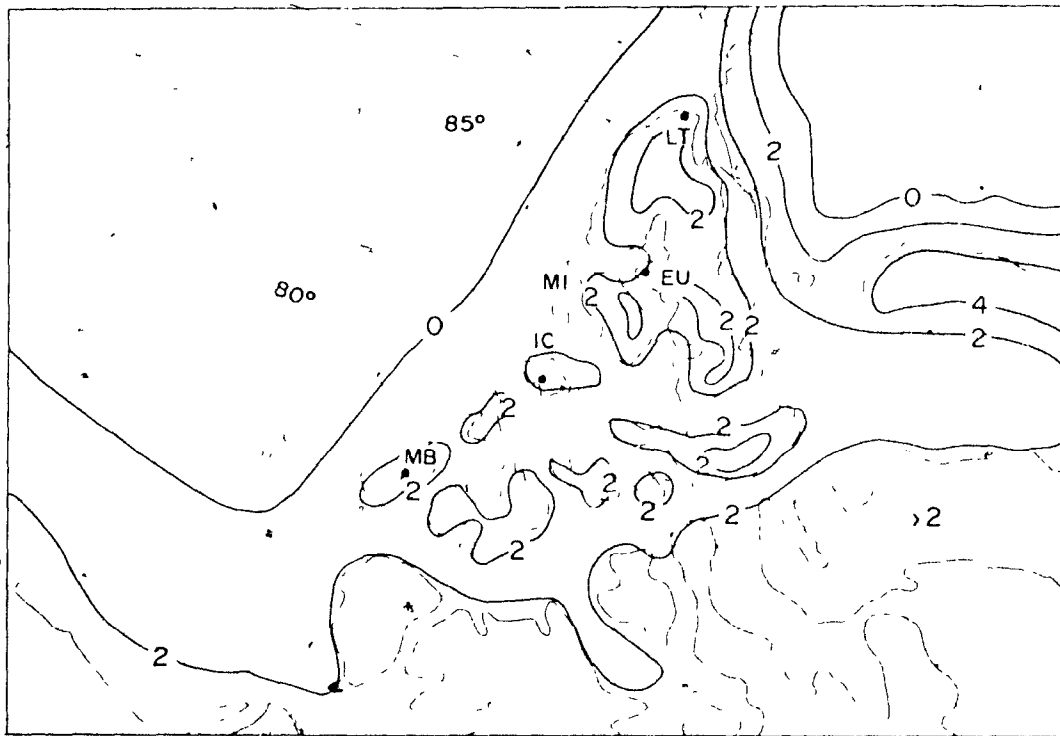
Glaciological maps of Meighen Island (1:50,000) and Meighen Ice Cap (1: 25,000) were produced from air photography and ground survey controls undertaken in 1959-60. Details of the production of these maps have been published by Arnold (1966).

1: 5.2 Mass Budget and Flow

A network of 35 stakes has been utilized for the 10 years of mass balance studies on the ice cap. Their approximate locations are shown on Figure 1: 5.2. Each spring since 1960 the winter accumulation has been measured carefully at each stake and snow densities evaluated. Ablation measurements were taken at these stakes approximately weekly during the summers of 1960-62 and a few times each season in 1968-70. The net balance for the previous year was determined each year in the spring survey. Tellurometer and theodolite traverses were made on the stakes in 1959, 1960, 1961 and 1964, to evaluate possible movements in the ice cap. The results of these glaciological data have been published by Arnold (1965) and Paterson (1968, 1969).

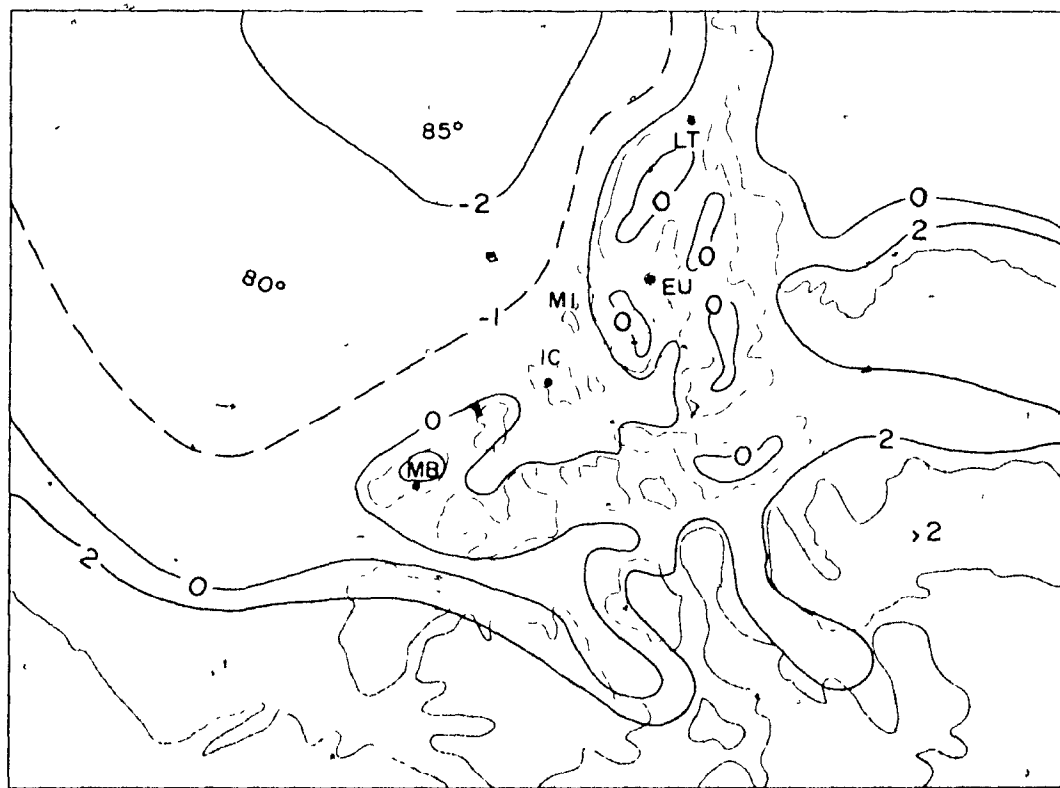
1: 5.3 Bore Hole

The 121 meter deep bore hole was drilled in 1965, using a CRREL thermal drill. The core recovered has been analysed by Koerner and the findings published (Koerner 1968). Temperatures were measured at 34 depths in the hole in spring of 1965, 1966, 1967, 1968 and 1969. The results of the 1965-67 data have been published (Paterson 1968). In addition, Paterson has evaluated the rate of closure of the bore hole.



MEAN AIR TEMPERATURE (°C), JULY

(Orvig 1970, after Prik)



MEAN AIR TEMPERATURE (°C), AUGUST

(Orvig 1970, after Prik)

Figure 2: 1

CHAPTER 2
CLIMATIC ELEMENTS

2: 1 Surface Air Temperature

Meighen Island's position on the edge of the Polar Ocean results in a duality of climatic regimes. This is particularly evident in the summer temperatures. Figure 2: 1 shows the July and August mean surface air temperature distribution over the area (Orvig 1970, after Prik). In July the snow free islands of the Archipelago are strongly heated while the archipelagic sea and continental shelf area of the Polar Ocean hover just above freezing. By August the zero degree isotherm has pushed south into the Beaufort Sea and the minus one degree isotherm approaches the continental shelf area.

Table 2: 1.1

	Mean Air Temperature, °C											
	3 YEAR				6 YEAR				20 YEAR			
	J	J	A	SS	J	J	A	SS	J	J	A	SS
Main Ice	-3.9	-0.2	-1.2	-1.8	-2.6	+0.6	-1.0	-1.0				
North Land	-3.0	+0.7	-0.0	-0.8								
Isachsen	-1.3	2.9	1.2	0.9	-1.1	4.0	1.4	1.4	-0.7	+3.3	+1.5	+1.3
Eureka	1.3	5.1	3.0	3.1	2.9	5.6	3.6	4.0	+1.9	+5.0	+3.4	+3.4
Alert									-0.7			

J = June, J = July, A = August, SS = Summer Season
3 year = 1968-70, 6 year = 1960-62 and 1968-70, 20 year 1951-70

2: 1.1 Summer and Monthly Means

Table 2: 1.1 suggests higher temperatures in the islands than indicated in Figure 2: 1 and shows the North Land temperatures to be consistent with those over the archipelagic sea and continental shelf area of the Polar Ocean. The summer temperature means indicate

that the Meighen Island temperature regime resembles that of the Polar Ocean floating ice stations rather than that of the other islands (see Isachsen, Alert, and Eureka). From Table 2: 1.1 it can be seen that the means are very similar for the ten years 1951-60 and the six years 1960-62 and 1968-70 at Isachsen and Eureka, the major difference being colder Junes in the six year period at Isachsen.

The six years of Meighen Island data appear to fall into two types, the warm years, 1960 and 1962, and the cold years 1961, 1968, 1969, 1970. At Isachsen the deviation from the sixteen year means for the cold years was -0.7 deg C while for the warm years it was almost twice as large ($+1.2$ deg C). This suggests that the cold years are more indicative of the recent climatic conditions of the region.

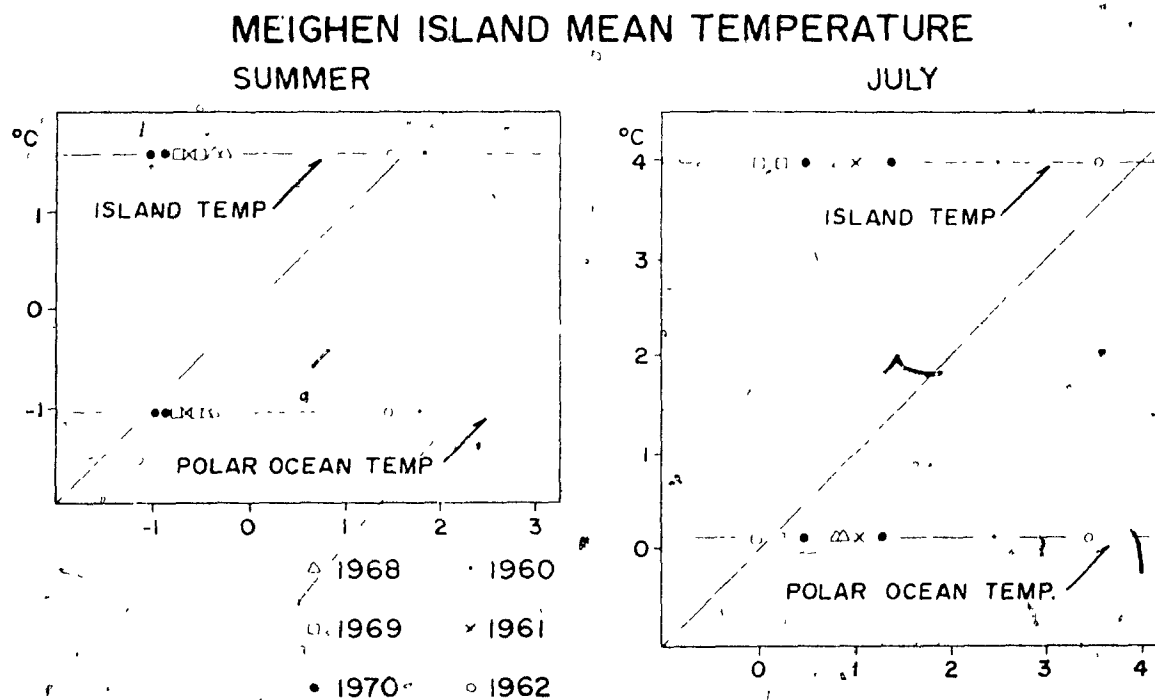


Figure 2: 1.1a

Summer season and July temperature means representative of two regions - the Polar Ocean and the islands bordering the Ocean - were

TEMPERATURE °C

Main Ice — North Land - - - Isachsen - - - Eureka — Axel Heiberg Base © Axel Heiberg Lower Ice - - -

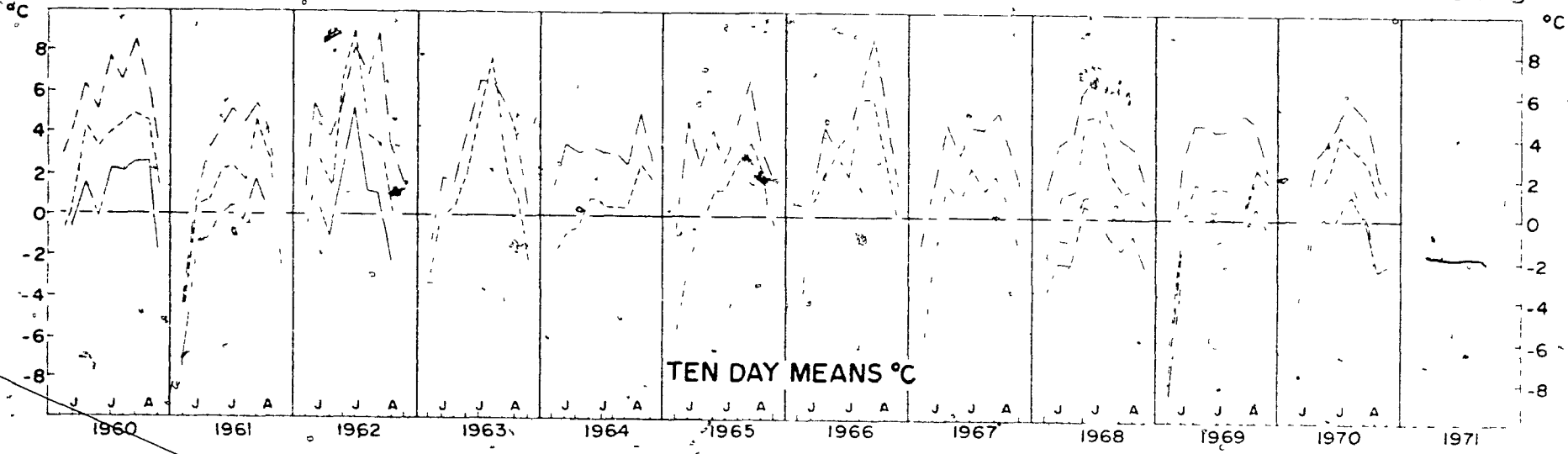
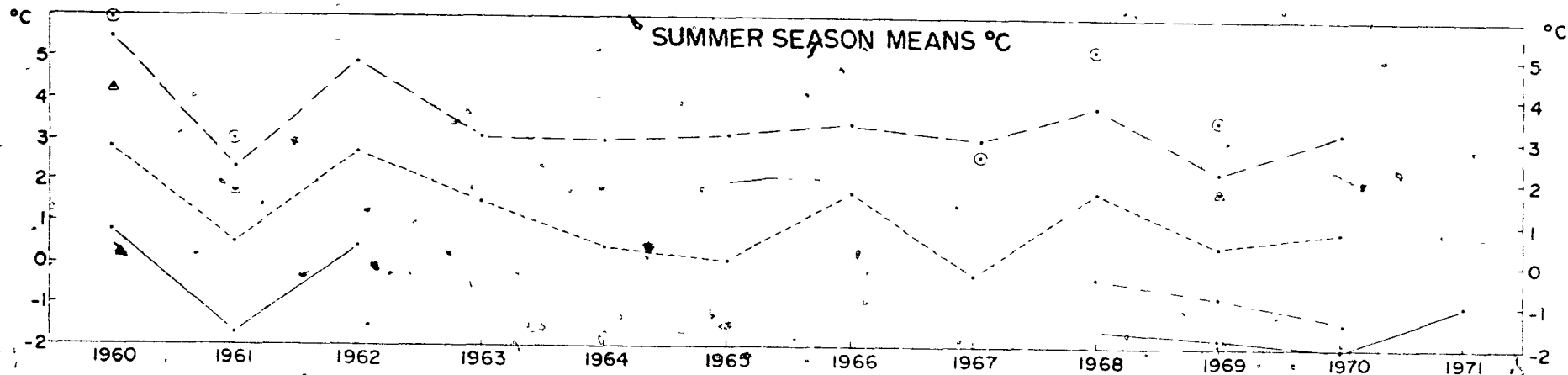


Figure 2: 1. 1b

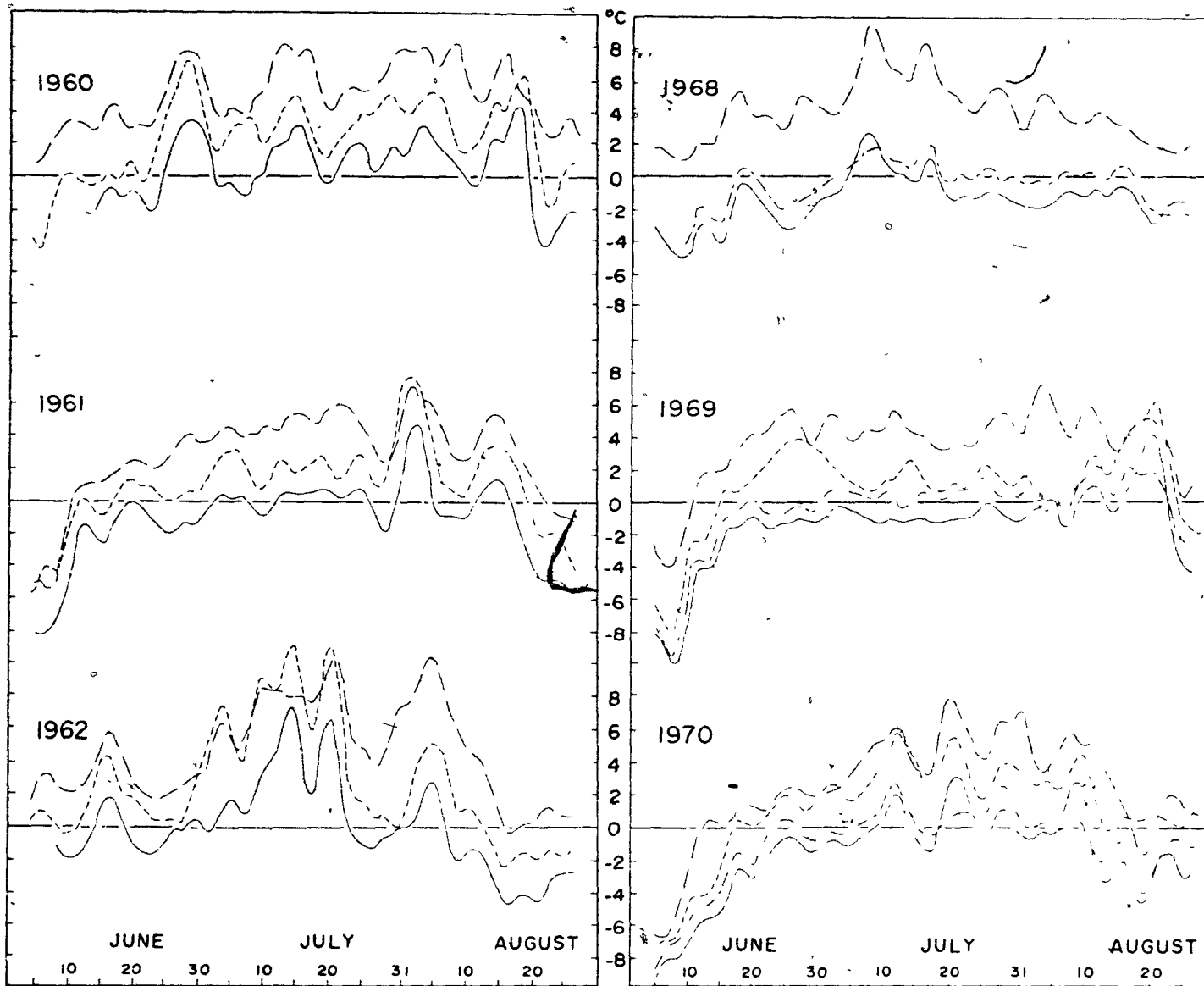
obtained using the Russian and American floating ice stations' data and the Isachsen and Alert records. The Main Ice means were increased one deg C to compensate for the elevation of the station.* The adjusted Main Ice means and the North Land means were then plotted against the Polar Ocean and Isachsen-Alert values. The results are shown in Figure 2: 1.1a. The cold years in all cases compare best with the Polar Ocean while the warm years resemble the Isachsen-Alert values. The years 1961, 1968, 1969 and 1970 could be termed "Polar Ocean years" and the years 1960 and 1962 the "Island years".

The summer season and ten-day means of temperature are shown in Figure 2: 1.1b. The summers of 1960 and 1962 stand out at all stations as being considerably warmer than any of the other years. At Isachsen, temperatures in 1963, 1966, and 1968 were slightly above the 12** year mean. The shapes of the Isachsen ten-day mean curves for these years are similar having a strong peak in mid-summer. On the basis of 1968, these short relatively warm summers at Isachsen represent "Polar Ocean years" on Meighen Island. Unusually low temperatures persisting into mid-June account for low seasonal means in 1965 and 1970. The absence of a mid-summer temperature maximum resulted in below average means in 1961, 1964, 1967 and 1969. With the exception of 1967, the coldest summer at Isachsen, these years experienced their summer maximum in mid-August. It appears that, of the twelve years studied, only 1960 and 1962 were "Island years".

Isachsen-Eureka temperature differences are greater in the colder years, as Eureka is less exposed to the Polar Ocean. Figure 2: 1.1c

* This correction was arrived at by comparing the North Land and Main Ice means and is only approximate.

** 1971 will be added to the figures at a future date (the means have been calculated but the year has not been studied in detail).



NINE DAY WEIGHTED RUNNING MEANS OF TEMPERATURE (%)

Figure 2: 1. 1c

of nine-day running means shows that, on occasion, Main Ice temperatures are higher than those at North Land. It will be shown in 3: 4.2 that this is the result of a strong temperature inversion formed by the combined effects of subsidence and the advection of warm air aloft. Situations such as this account for the decrease in the North Land to Main Ice temperature difference in 1970.

2: 1.2 Daily Temperature Range

Diurnal temperature variations on Meighen Island are small. The temperature maximum tends to occur around 14 MST and the minimum between 02 and 05 MST.

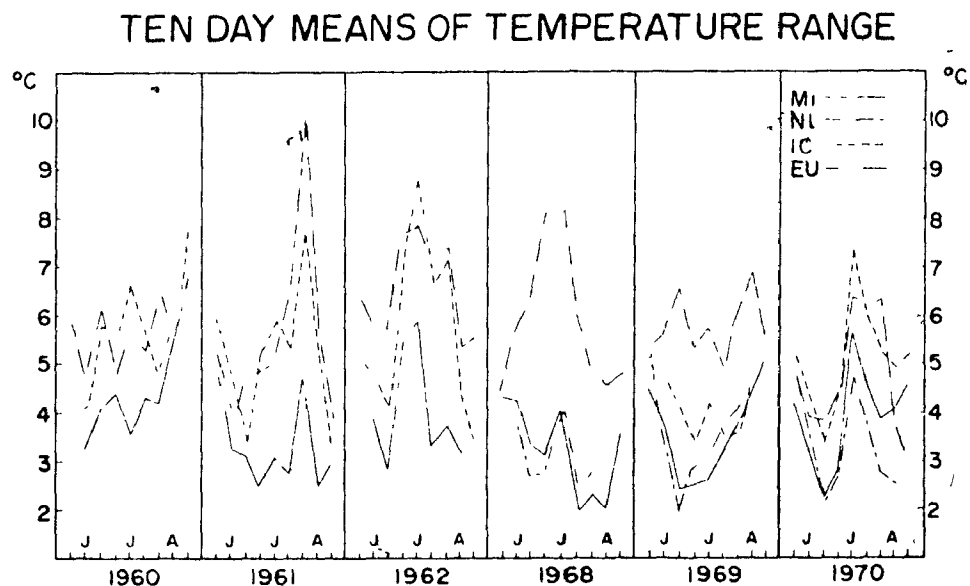


Figure 2: 1.2

Monthly means of daily temperature range at Main Ice and North Land are similar to those of the Polar Ocean stations. The ten-day means of daily range are found in Figure 2: 1.2. In the cold years the range is high in June. Once the temperature rises above freezing

MELTING DEGREE DAYS °C

Main Ice — North Land - - - Isachsen - - - Eureka - - -

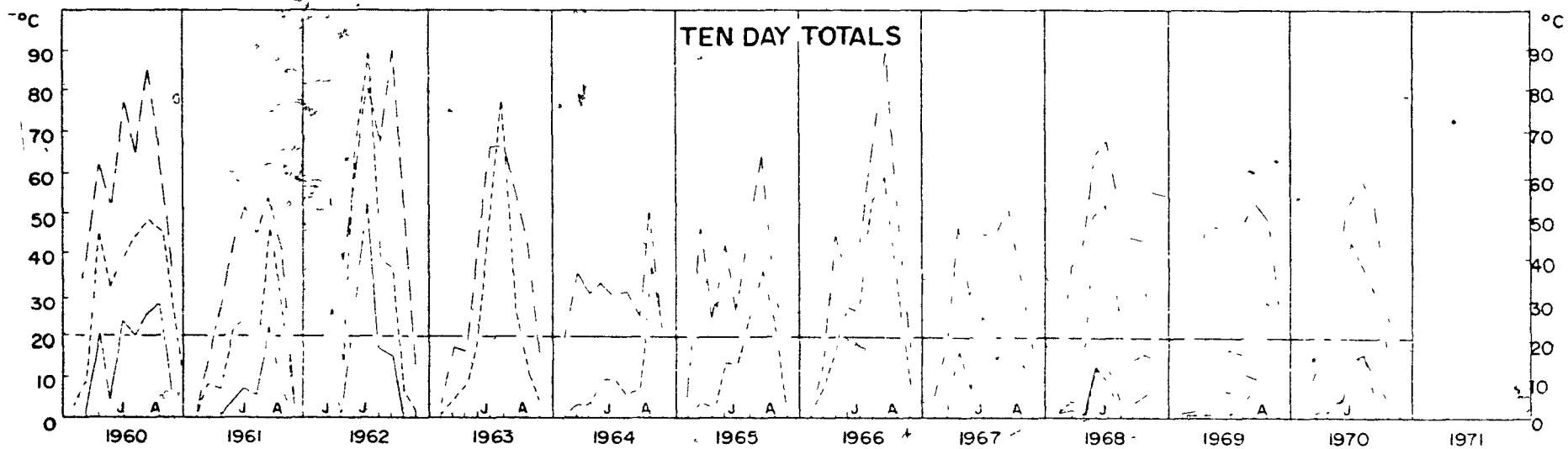
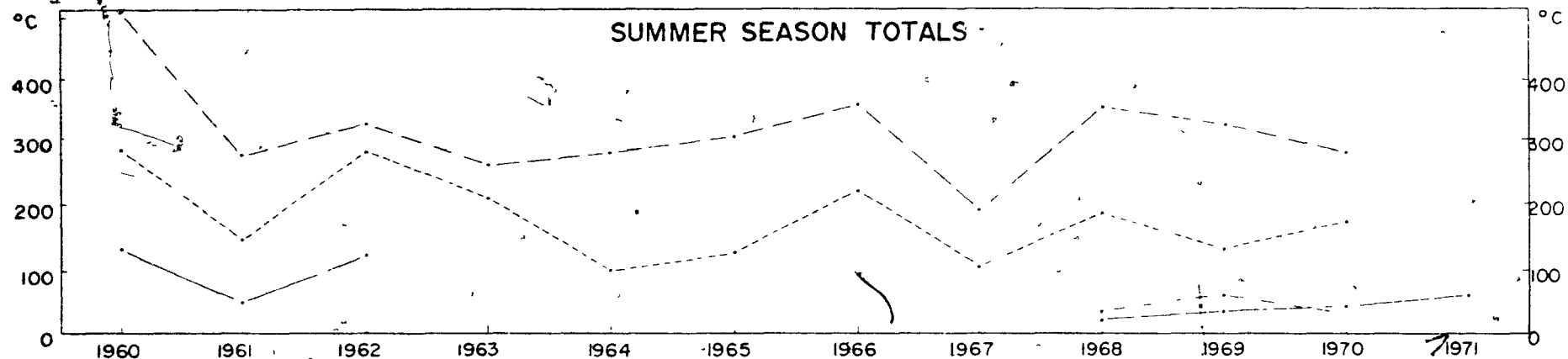


Figure 2: 1.3

on Meighen Island, the ranges tend to be low due to the effect of the ice cap and surrounding ice choked sea. The sea effect is seen to some extent at Isachsen and Eureka. During these periods, peaks in the range curves coincide with anomalies in the temperature curve, i. e., 10-20 July 1962 when Isachsen was warmer than Eureka and late July in 1970 when North Land was almost as cool as Main Ice (see Figure 2: 1.1b).

2: 1.3 Melting Degree Days

Melting degree days were calculated from the three-hourly observations, from the mean of these eight observations and from the mean of the maximum and minimum. As discussed by Arnold (1964), considerable error is introduced by the third method of calculation. The values presented in the following were obtained by the first method.

In Figure 2: 1.3 are plotted summer season and ten-day means of melting degree day totals for 11 years. Comparing melting degree days and temperature (Figure 2: 1.1b) shows that suppression of the mid-summer (July) temperature maximum (e. g., 1964 and 1969) is more effective in keeping ablation on Meighen Ice Cap at a minimum, than are low mid-June temperatures (e. g., 1965 and 1970). Small diurnal temperature ranges in late July and early August contribute to the relatively low melting degree day totals experienced at Main Ice in 1968.

2: 2 Humidity

Meighen Island relative humidities are equal to or higher than the floating ice island values and 10% and 15% higher than the Isachsen and Eureka values, respectively. The warm years have the lowest relative

RELATIVE HUMIDITY %

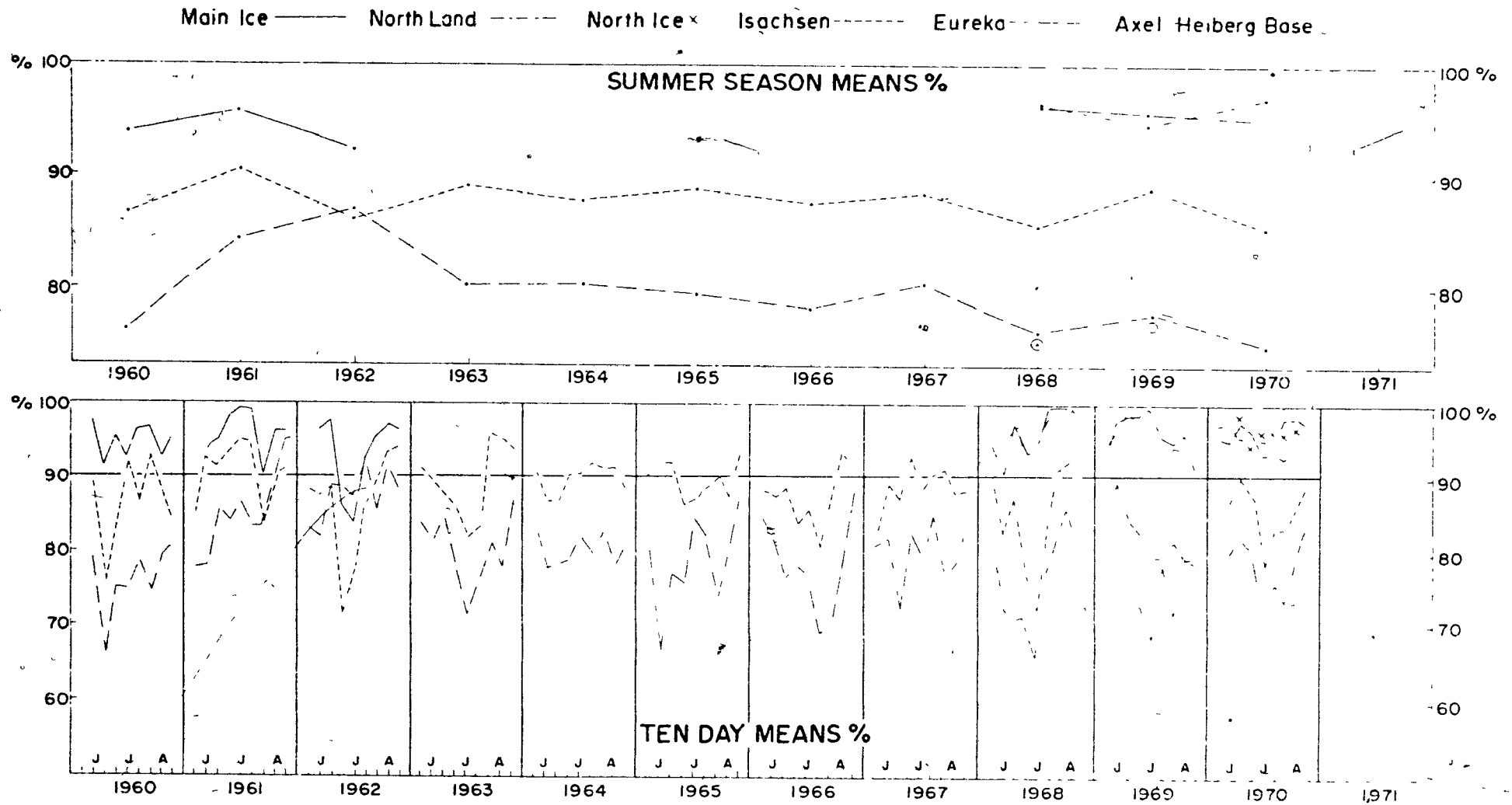
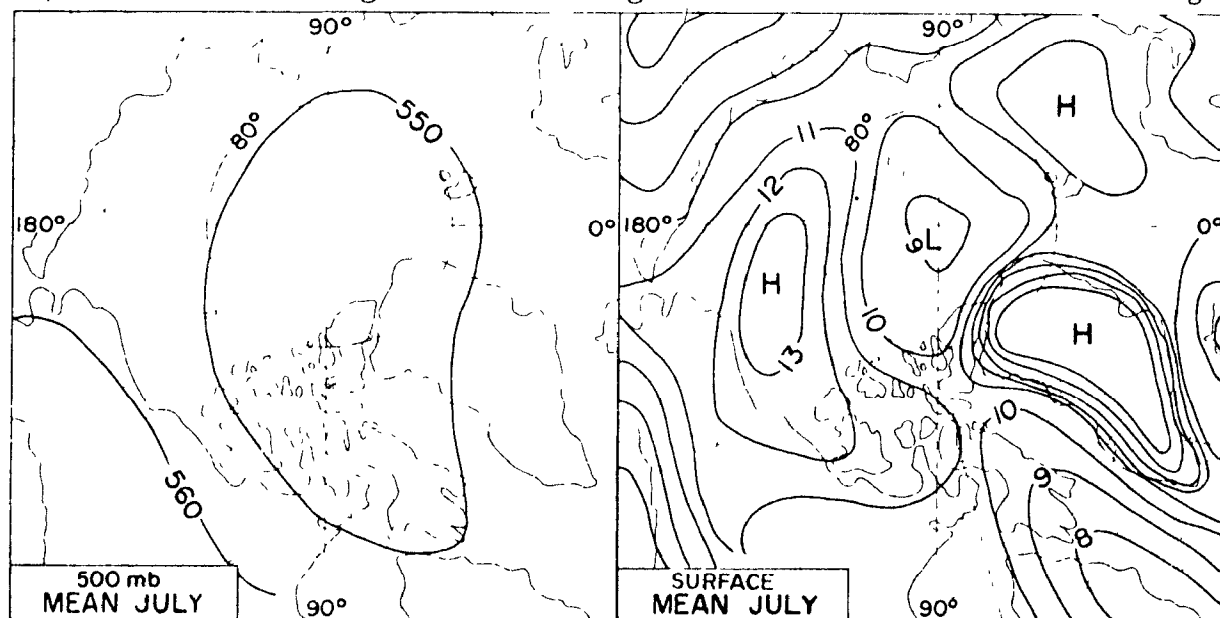


Figure 2: 2

humidities, though on Meighen Island they are still within the range of the Polar Ocean humidities. Yearly and ten day variations of summer relative humidity are plotted in Figure 2.2. Dew point temperature curves (not shown) are the same shape as the temperature plots though the station-to-station differences are greatly reduced. The shape of the Eureka relative humidity plot does not always coincide with that of Isachsen and Meighen Island, reflecting a combination of temperature and humidity differences. North Land dew point temperatures approach those of Isachsen while the Main Ice values are considerably lower. This suggests a loss of vapour content at the ice cap station through condensation due to lifting or other cooling processes.

2:3 Pressure

The mean July surface pressure configuration (Orvig 1970, after Prik) and the mean July contours of the 500 mb surface (after Hare and Orvig, 1958) can be seen in Figure 2:3a. Meighen Island lies in a surface trough



MEAN PRESSURE PATTERNS

Figure 2: 3a

STATION PRESSURE mb

Main Ice — North Land - - - Isachsen - - - Eureka - - - North Ice x

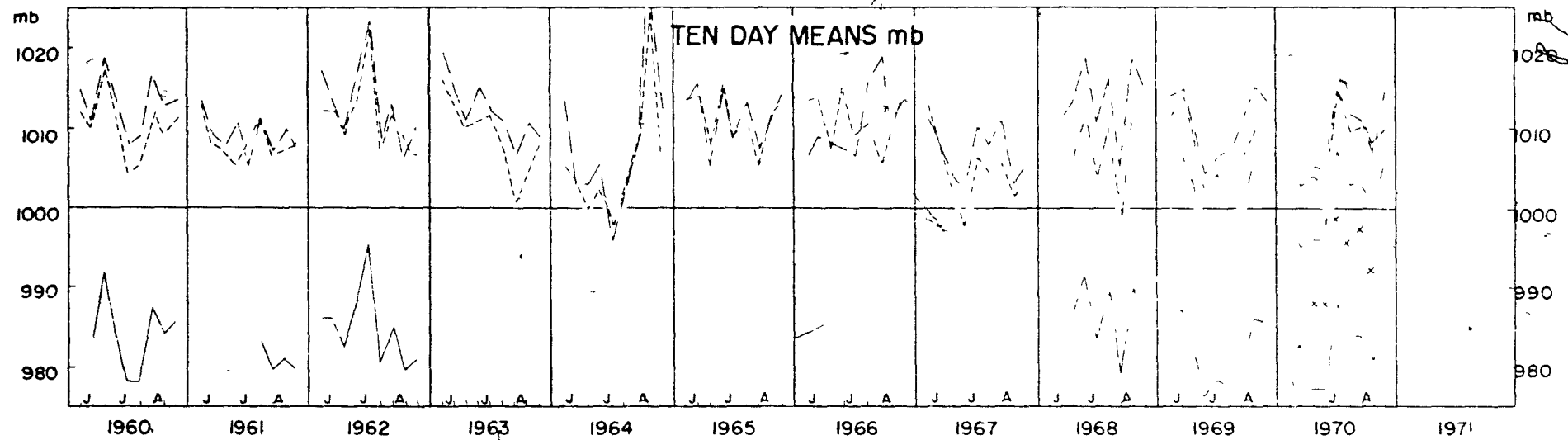
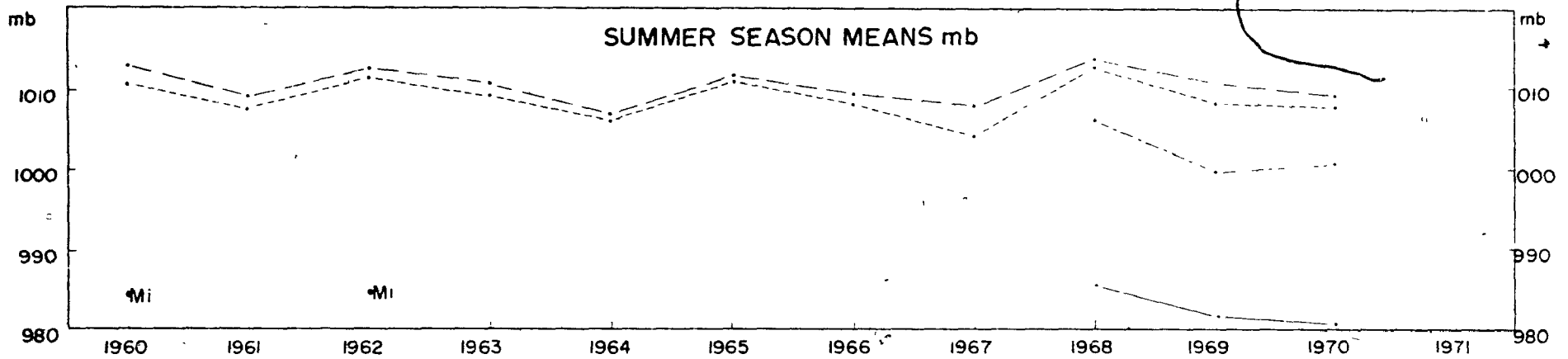


Figure 2: 3b

running from the region of the Pole to Baffin Bay. A large surface high covers the Beaufort Sea and adjoining Polar Ocean area. At 500 mb a low dominates the whole region. The mean pressure pattern and synoptic conditions are discussed in detail in II 3 and I 1:2.

Plots of seasonal and ten-day station pressure means" (Figure 2:3b) show similar variations at all stations. Pressures are high in the "Island years" and low in the years lacking mid-summer temperature peaks (1961, 1964, 1967 and 1969). With the exception of 1961, the low pressure years had strong low pressure periods in July. The highest seasonal pressure mean for the 11 years occurred in 1968.

2: 4 Wind Speed and Direction

Consideration should be given to the following station location descriptions (Atmospheric Environment Service, Department of the Environment, Canada).

Isachsen - "It is located on Deer Bay, a broad bay which cuts thirty miles inland from the west coast of the Island (Ellef Ringnes Island). The station proper is situated on the northeast side of a minor indentation at the east end of Deer Bay. A rocky ridge rises to six hundred feet about a mile south of the station where a long narrow finger of land juts into the bay. Inland the hills rise to heights of eight hundred feet three to five miles to the north and north west of the station and five hundred feet three miles to the north east."

Eureka - "Eureka lies close to the centre of the land mass of Ellesmere and Axel Heiberg Island, two large mountainous islands separated by the long and winding Eureka Sound. The station is situated on the north shore of Slidre Fiord . . . rolling hills under eight hundred feet in height surround the seventeen mile long fiord. Hills reach two to three thousand feet about six miles from the station in the north west, north east and south west quadrants. Five to six thousand foot mountains ring the station a distance of forty miles."

These conditions should be contrasted with the relatively exposed locations of the Meighen Island stations (see Figure 1:2a). The anemometer height on Meighen Island was usually under 2 meters, at Eureka it was 6 meters and at Isachsen 9 meters. As a result of the site and

WIND SPEED meters/sec.

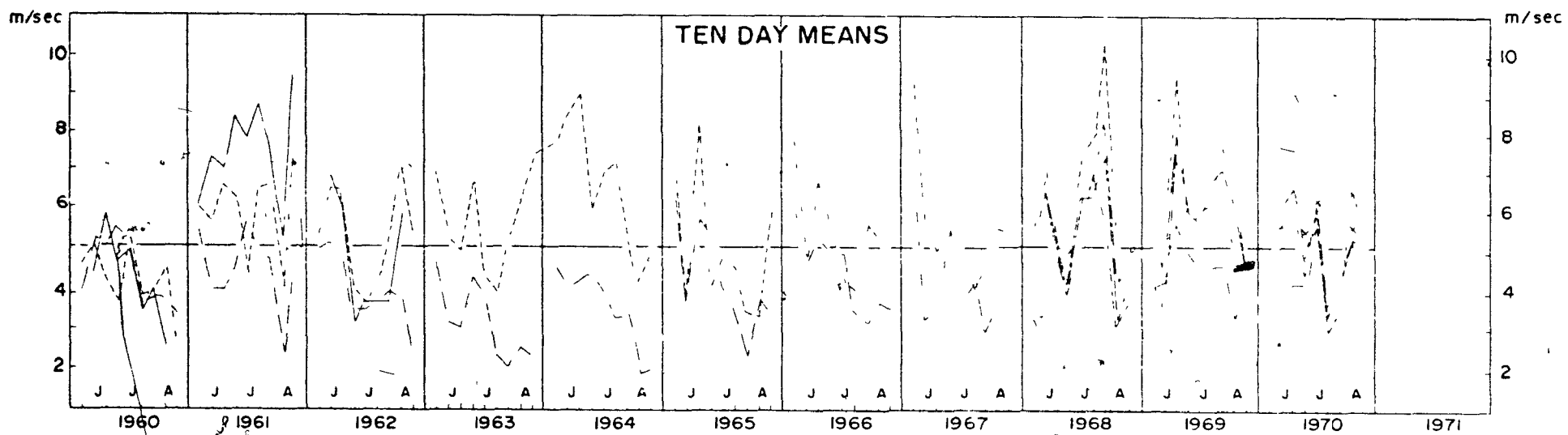
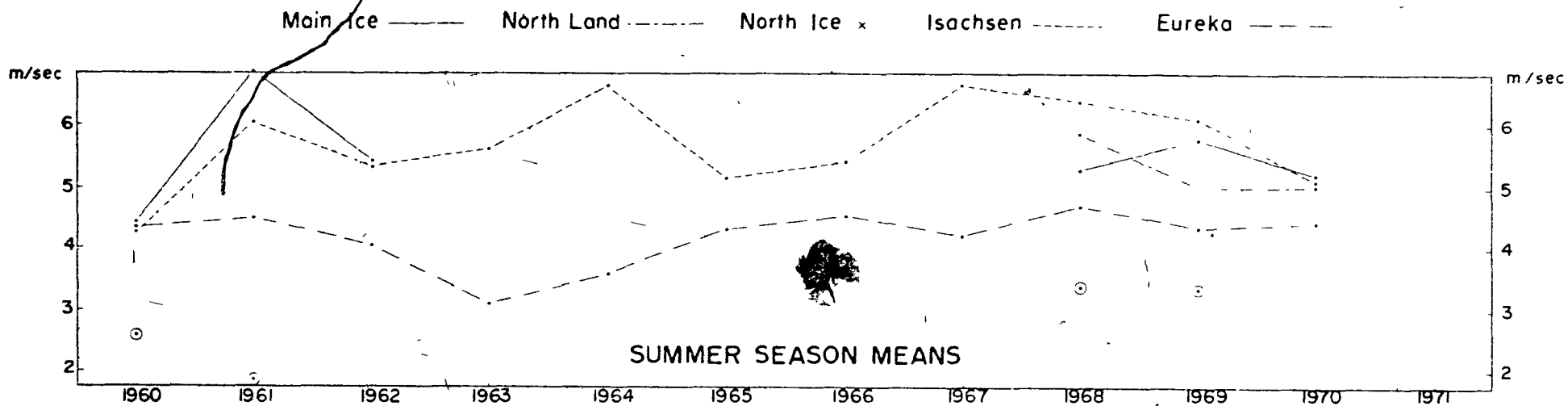


Figure 2: 4a

instrumentation differences, relationships between Meighen Island, Isachsen, and Eureka wind speed and direction are not consistent.

Figure 2:4a shows that, in general, wind speeds at Eureka and the Axel Heiberg Stations tend to be low. Isachsen, less sheltered than Eureka, less exposed than Meighen Island and with an anemometer height 7 meters higher than the Meighen Island Stations, has wind speed curves similar to Main Ice. On Meighen Island the strongest winds were recorded in 1961. There is a tendency towards high wind speeds in summers lacking a mid-summer temperature maximum (e. g., 1961, 1964, 1967 and 1969).

No striking pressure - wind relationship is evident in the ten-day means. The strong pressure maximum in July 1962 was associated with low winds and the most decided temperature peak of the six years: the prolonged cold spell of 1969 saw low pressure combine with low wind speeds and high pressure with high speeds. During the Main Ice melt season the wind speed curves for the four stations indicate the existence of similar wind speed regimes at all stations.

Figure 2:4b of monthly wind roses for Main Ice shows that N'lies predominate at the beginning and end of the season, while SSE, S and SW winds are most likely during the Meighen Island melt season.

Wind roses for Main Ice, North Land and Isachsen are shown in Figure 2:4c. The lack of E'lies on Meighen Island suggests a shadowing effect from the mountains of Axel Heiberg and Ellesmere Islands to the east. Local topography is responsible for the SSW and NE minimum usually present at Isachsen.

There is a strong predominance of northerly winds at all stations as suggested by the mean pressure pattern. These northerlies were

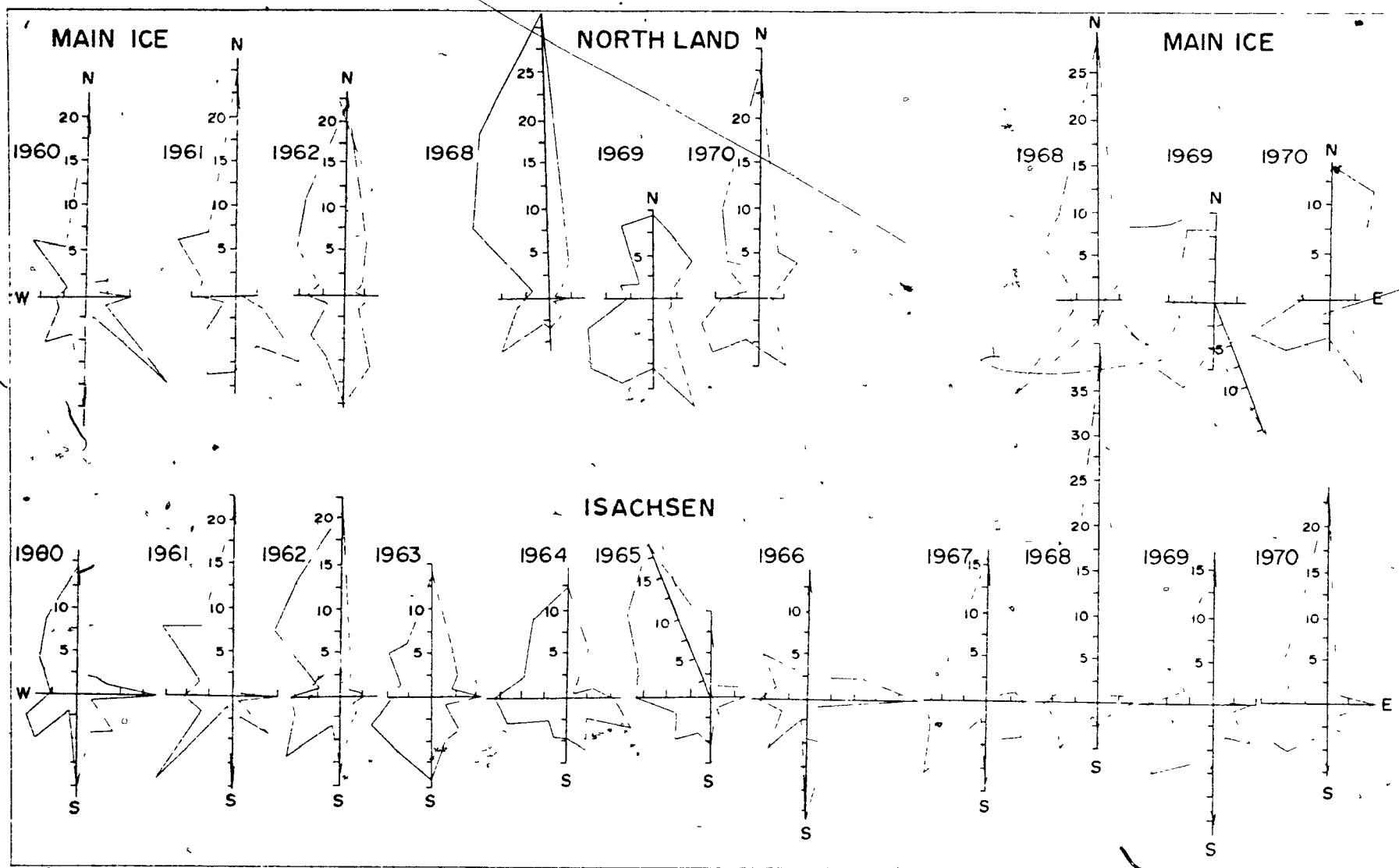


Figure 2: 4c

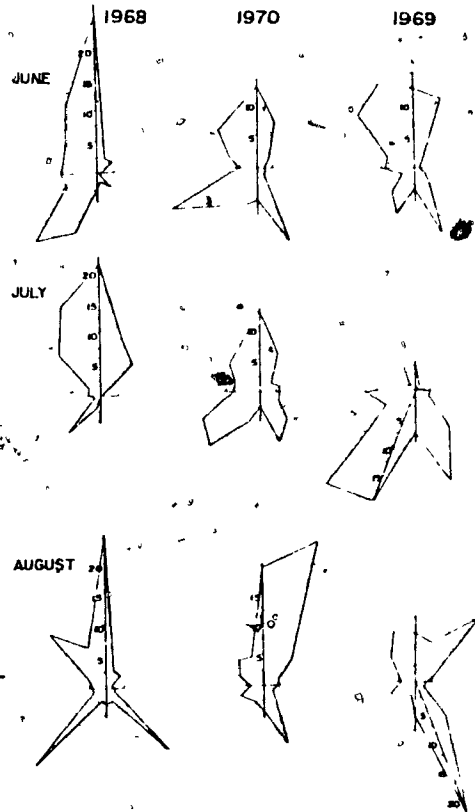
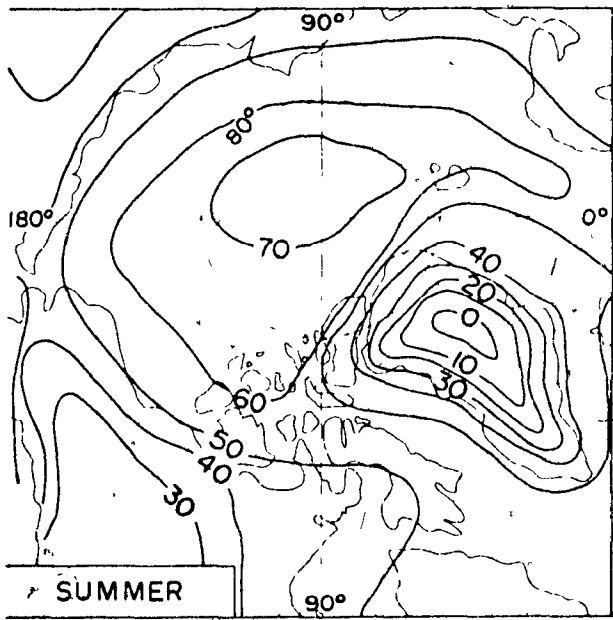
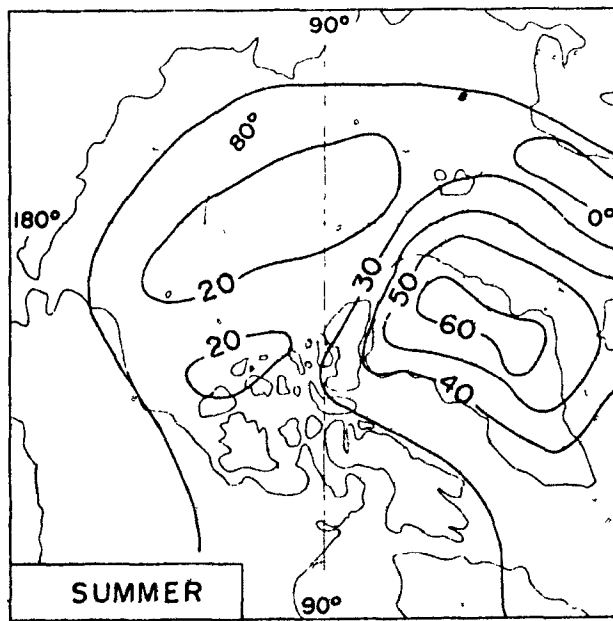


Figure 2: 4b

most strongly developed in 1968. Secondary maxima occur in the SW, S and SE quadrants. The synoptic reasons for these maxima will be discussed in detail for the six years of Meighen Island records in 3:8. The 11 years of Isachsen wind roses appear to fall into the following categories. In 1961, 1964, 1967 and 1969 winds out of all sectors from E through S to W were reasonably frequent in addition to the consistent N'lies. In 1965 and 1967 northerlies were more dominant, and there was a SE'ly minimum. West and SE minima occurred in 1960, 1966 and 1963, while in 1962 the E'ly maximum is also missing. In 1968 the N'lies dominated completely.



Frequency of St and Sc (%)



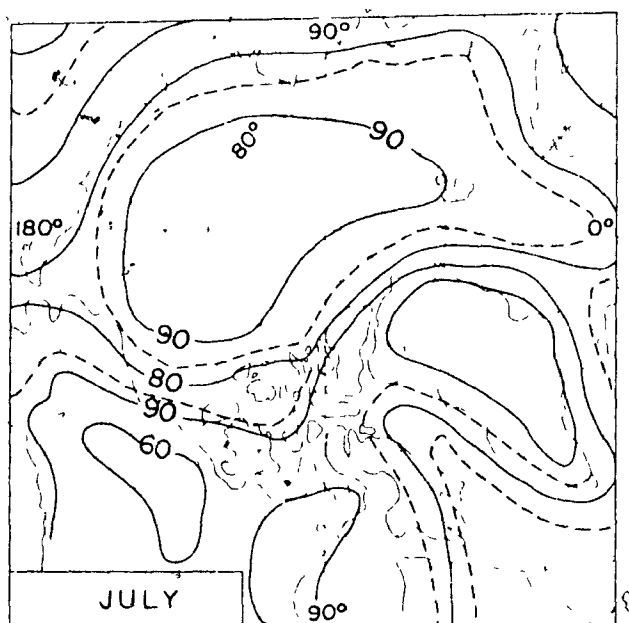
Frequency of As and Ac (%)

Figure 2: 5. 1b

2: 5 Cloud and Fog

2: 5.1 Mean Patterns

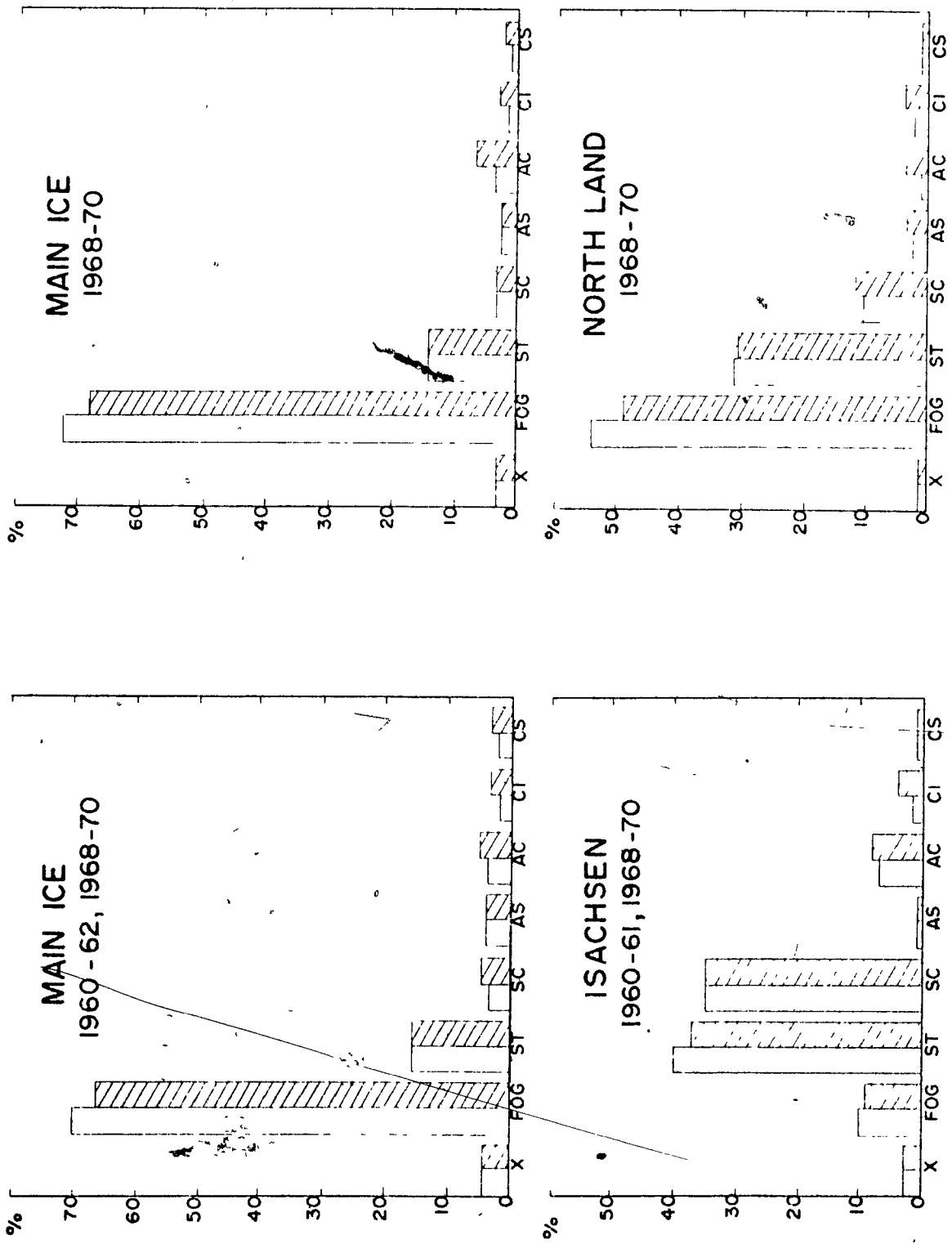
The configuration of mean cloud amount in July (after Orvig, 1970, with added details for the archipelago) is presented in Figure 2: 5.1a. Meighen Island and to a lesser extent, Isachsen can be seen to lie on the edge of the Central Polar Ocean cloud maximum, while Eureka experiences considerably lower cloud amounts.



MEAN CLOUD AMOUNT (%)

Figure 2: 5.1a

The distribution of low and middle cloud over the Arctic Basin in summer (after Orvig, 1970, with minor adjustments) appears in Figure 2: 5.1b. The extension of Polar Ocean stratus and stratocumulus into the western Queen Elizabeth Islands is reflected in these distributions. Middle cloud, on the other hand, shows slight maxima in the regions of the Baffin Bay low and on the North American side of the pole, where cyclone tracks converge (see I 1: 3.5).



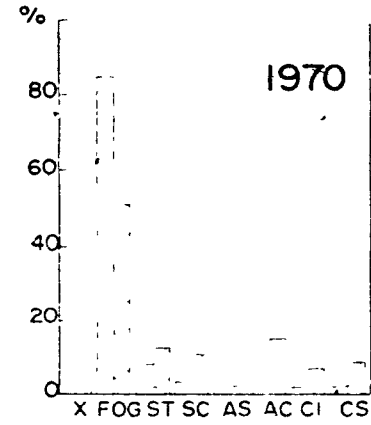
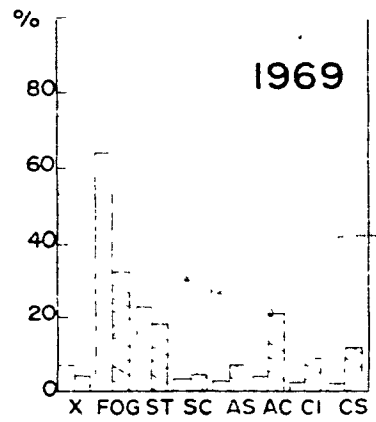
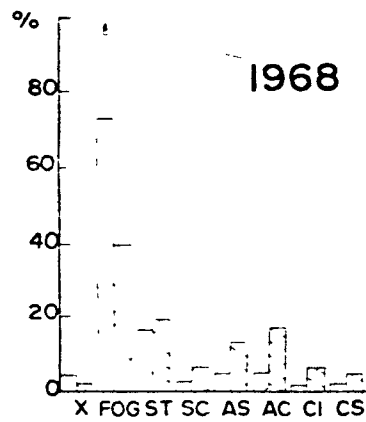
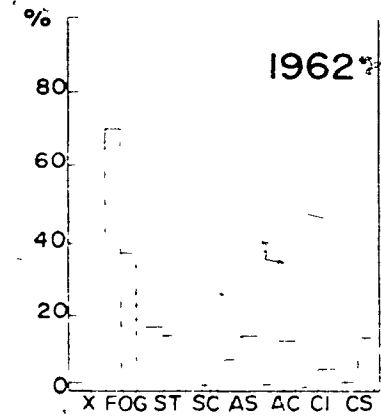
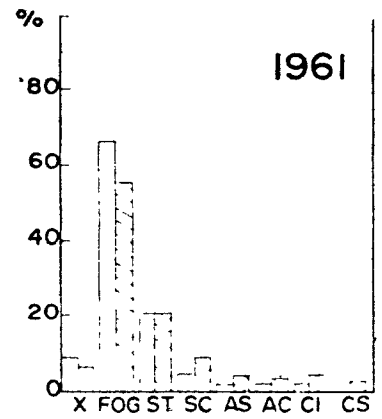
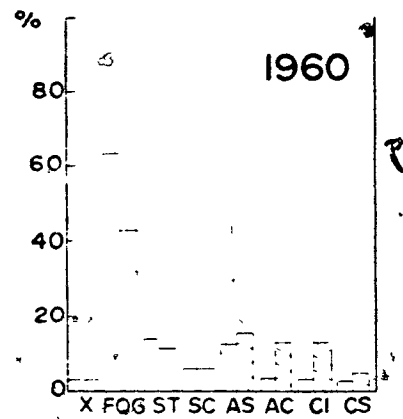
MEAN FREQUENCIES OF CLOUD TYPE

Figure 2: 5.1c (see Figure 2: 5.2b for legend)

Frequency distributions of cloud type for the summer season from Main Ice, North Land and Isachsen are found in Figure 2: 5.1c. At Main Ice fog is responsible for 70% of the sky cover in summer, stratus for 15% and altocumulus for only 5%. The observed frequency of middle and high cloud is an underestimate of the actual situation due to the ever present fog and low stratus. Twenty percent of the Main Ice fog is seen to be stratus or stratocumulus at North Land, and 60% of the Main Ice fog is either stratus or stratocumulus at Isachsen. The increase in fog from North Land to Main Ice is a result of the elevation of the ice cap station (ca. 800 ft). The remaining 40% difference between North Land and Isachsen results from the latter's location 40 miles from the north coast of Ellef Ringnes Island and 3 to 5 miles south of 700 ft hills. Stefansson comments that "both Prince Patrick Island and ours (Borden) are well supplied with vegetation inland and to the east while comparatively barren along the west coast (Polar Ocean coast)" and he suggests elsewhere that fog seldom extends more than 15 to 20 miles inland. (Stefansson, 1944 and 1942). A comprehensive discussion of the origin and characteristics of the Main Ice fog is found in I 1: 4.

2: 5.2 Seasonal Variations

Figure 2: 5.2a of seasonal and ten-day cloud cover shows similar variations at all stations. Cloud amounts are lowest in the "Island years" and tend to be highest in the years which lack mid-summer maxima. In the "Island years", ten-day cloud amounts were well below 7/10 for at least two periods. This was also the case in 1963 and 1968 which could be termed warm "Polar Ocean years". During



first layer:
frequency time
amount in %
of total cover in
first layer

all layers
frequency of
occurrence
of observations

SEASONAL CLOUD TYPE FREQUENCIES FOR MAIN ICE

Figure 2: 5.2b

CLOUD AMOUNT tenths

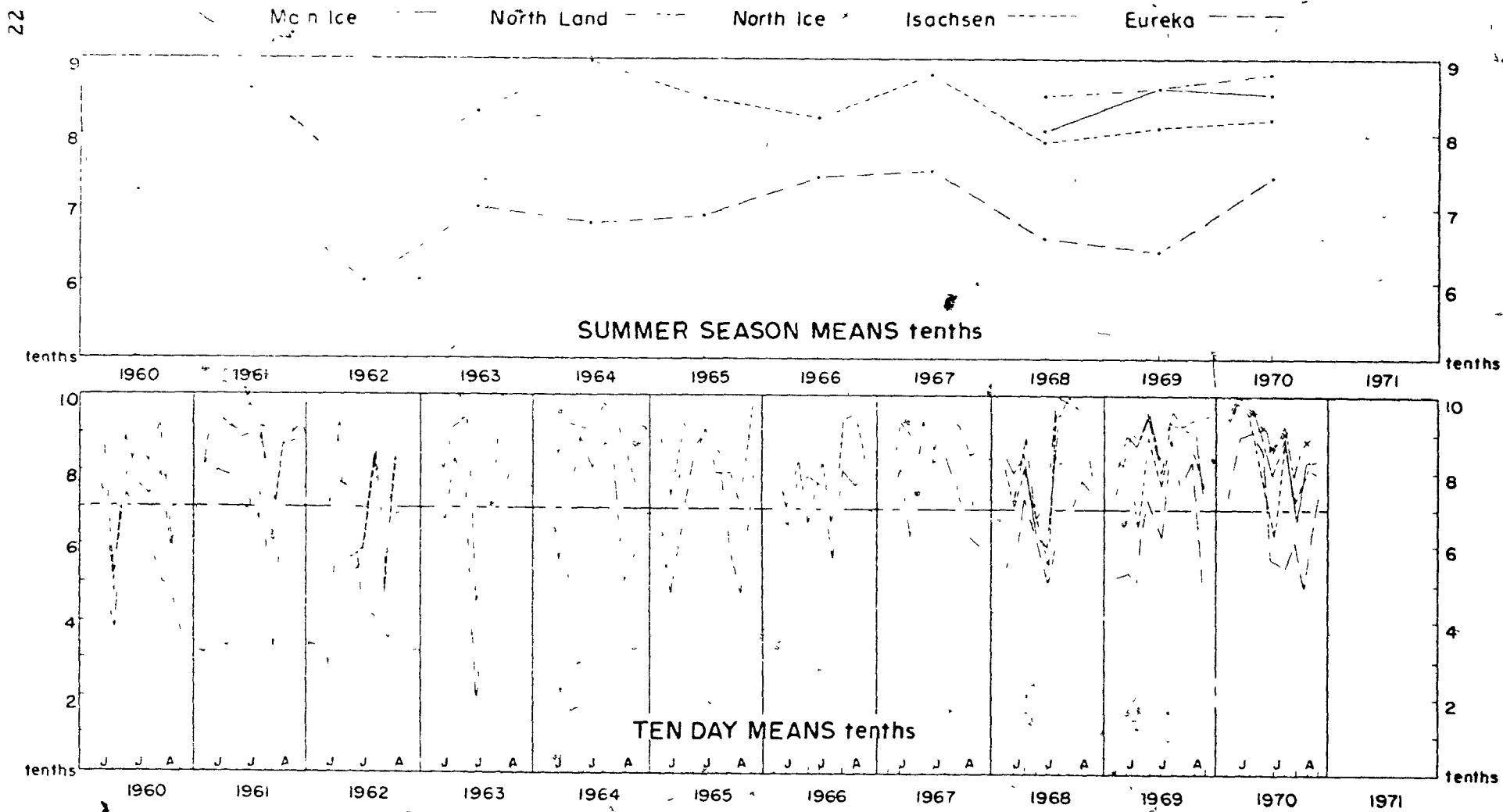


Figure 2: 5.2a

Table 2: 5. 2

Most Important Sky Cover Types in Ten Day Periods¹

Period ²	Main Ice	Period ²	Main Ice	North Land
1960 1	---	1968 1	ST, F	ST, SF
2	F, ST	2	F, SF	ST, SC
3	F, AS	3	F, SC	ST, SC
4	F, ST	4	F, ST	SF, F
5	F, ST	5	F, AC	F, ST
6	F, ST	6	F, SF	F, ST
7	F, AS	7	F, ST	SC, ST
8	F, AS	8	F, ST	ST, SC
9	F, AC	9	F, ST	ST, SC
1961 1	ST, X	1969 1	X, F	ST, X
2	F, X	2	F, ST	F, ST
3	F, ST	3	F, SF	F, SF
4	F, ST	4	F, SF	F, SF
5	F, ST	5	F, SF	SF, F
6	F, ST	6	F, ST	F, ST
7	F, SC	7	F, ST	F, ST
8	F, SC	8	F, AC	F, SF
9	F, ST	9	F, ST	F, SF
1962 1	---	1970 1	F, ST	F, ST
2	F, ST	2	F, ST	F, ST
3	F, ST	3	F, ST	F, ST
4	F, ST	4	F, X	F, ST
5	F, AS	5	F, AC	F, SF
6	F, AS	6	F, ST	F, SF
7	F, SF	7	F, CI	F, ST
8	F, AC	8	F, CS	F, ST
9	F, ST	9	F, ST	F, ST

1. Based on total amount of sky covered i.e., frequency of observation x mean amount.
2. Periods: 1) 1-10 June; 2) 11-20 June; 3) 21-30 June; 4) 1-10 July; 5) 11-20 July; 6) 21-30 July; 7) 31 July-9 August; 8) 10-19 August; 9) 20-29 August

cold "Polar Ocean years" amounts remain high throughout the season.

Frequency distributions of cloud type for the individual years (Figure 2: 5.2b) show that a decrease in low cloud amount accounted for the clearer skies in 1960 and 1962. Altostratus, which tended to be associated with warm air advection from the south (see 3:6), was more frequent in the warm years. The relatively high frequency of altocumulus in 1969 was a result of increased cyclonic activity in the Meighen Island area that year.

Table 2: 5.2 of most important cloud types in ten-day periods indicates that fog is consistently the dominant type of cloud cover at Main Ice. At North Land this was also the case in 1970 and most of 1969 but in 1968 fog was of primary importance only during mid- and late July. Stratus, stratus fractus and stratocumulus are, in general, the second most frequent cloud types. Altostratus shows up in several warm periods in 1960 and 1962. The high wind speeds of 1961 resulted in several periods of obscuration by blowing snow.

Evidence that Main Ice and Isachsen are in separate fog regimes appears in Figure 2: 5.2c (the fog amounts averaged for all occurrences of fog, shown in this figure, can be a result of the thickness and/or areal extent of the fog). From 1968 to 1970 there was a decrease of both fog frequency and mean cover at Isachsen, while on Meighen Island there was an increase of frequency and a slight decrease in amount. Cloud and fog conditions at Main Ice and North Land were very similar in 1969, though low cloud at North Land is sometimes fog at Main Ice. The lower total cloud amount at Main Ice than at North Land in 1968 and 1970 suggests that Main Ice was on occasion near or above the top of the fog.

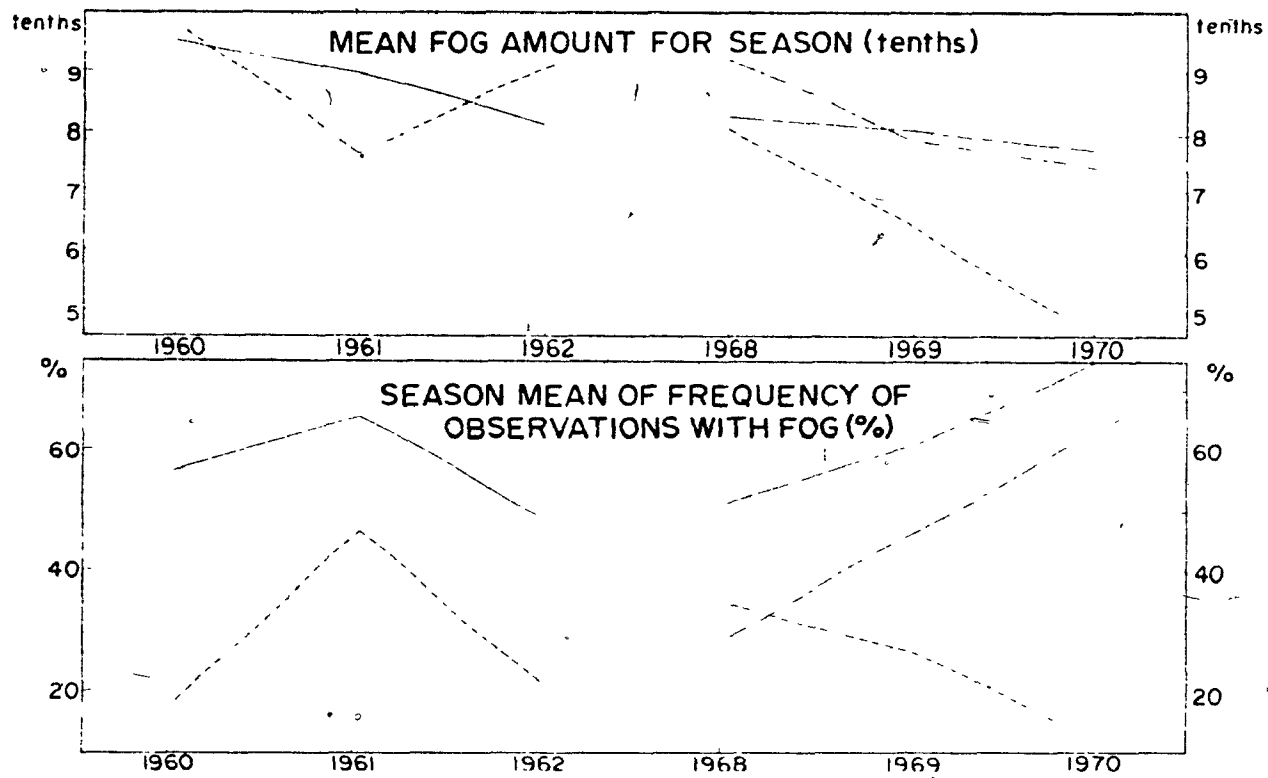


Figure 2: 5.2c Seasonal Means of Fog Amount and Frequency (see Figure 2: 5.2a for legend)

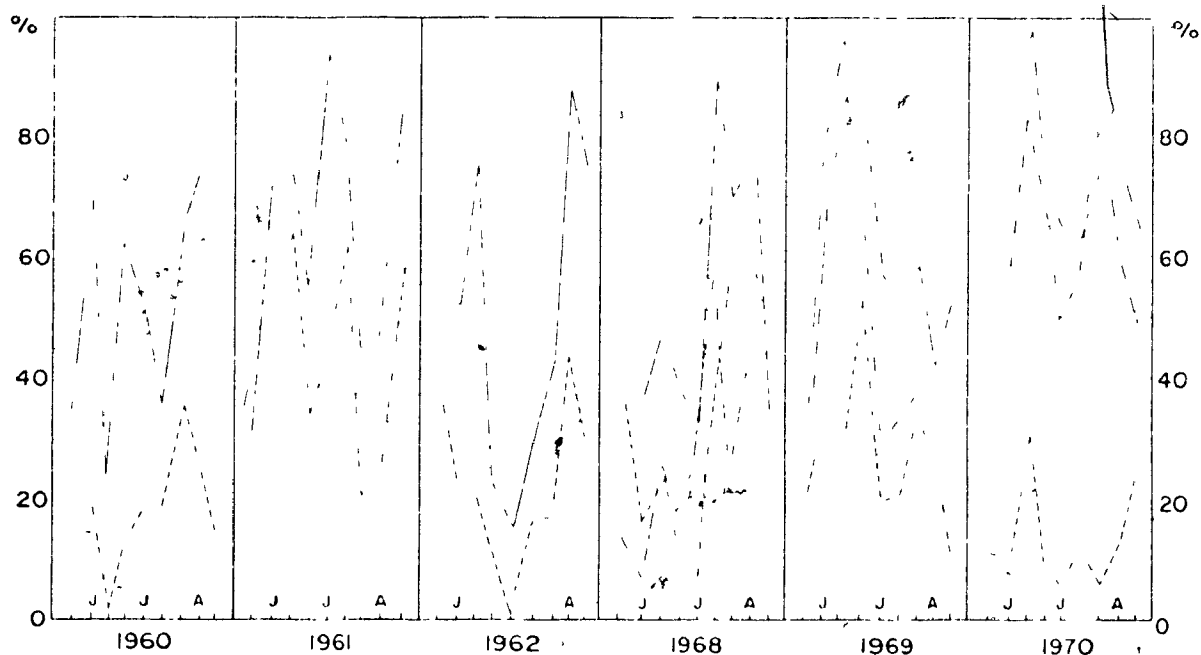


Figure 2: 5.3b Ten-day Means of Fog Amount (see Figure 2: 5.2a for legend)

2: 5.3 Daily Variations

Plots of ten-day cloud amount and fog frequency show no consistent seasonal trends. All cloud amount minima correspond to a minimum in the fog frequency curve, but during some periods total cloud cover is high despite low fog frequencies. All combined cloud and fog minima result in temperature maxima. Comparison of the daily mean cloud amounts (Figure 2: 5.3a) and the 9-day running means of temperature (Figure 2: 1.1c) further illustrates the temperature-cloud dependency on Meighen Island.

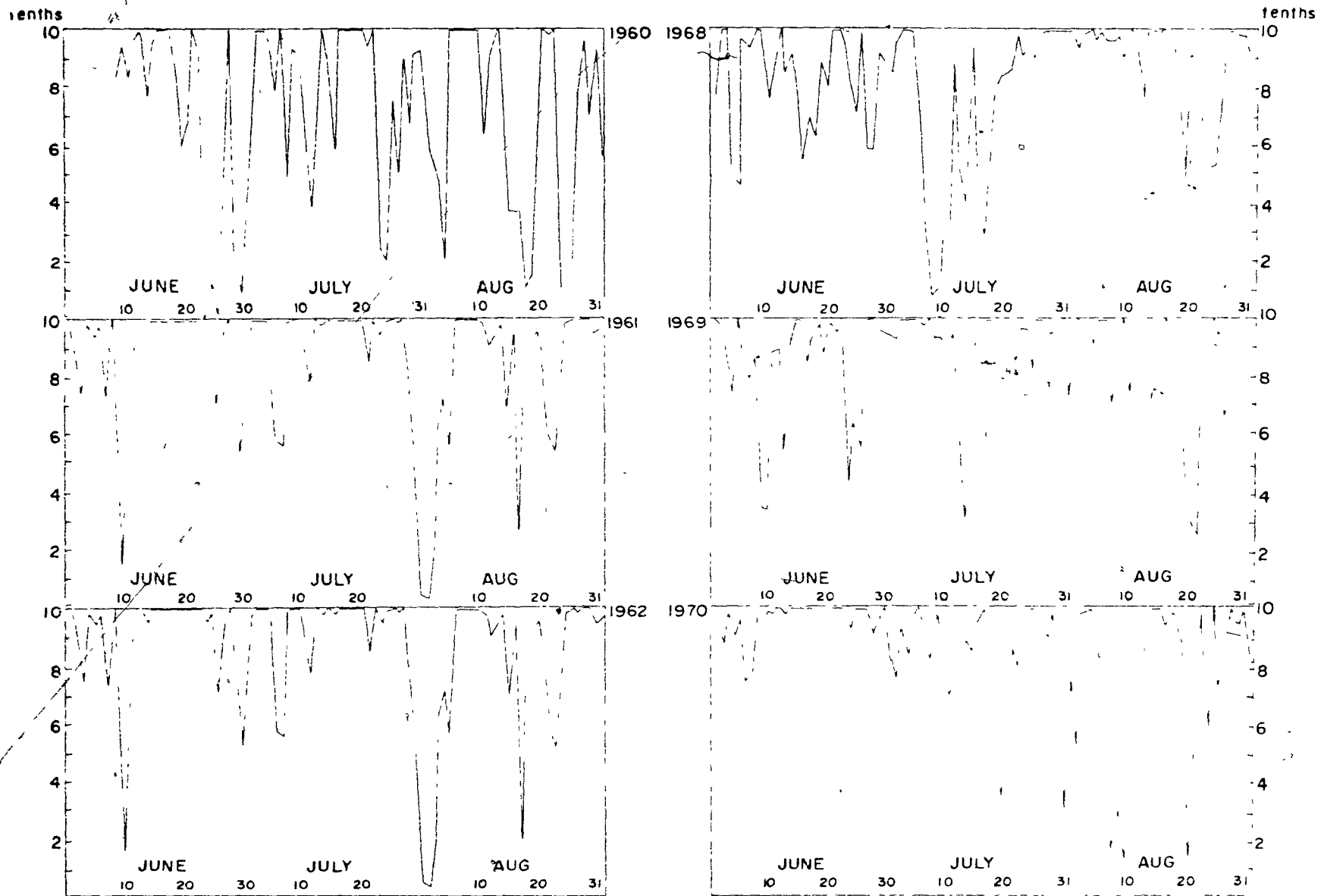


Figure 2: 5.3a Daily Cloud Amounts from Main Ice

2: 6 Weather and Obstructions to Vision

Table 2:6 gives the frequency of observations with various types of weather and obstructions to vision. Fog is by far the most frequent obstruction to vision on Meighen Island. The high winds of 1961 resulted in blowing snow at 19% of the observations in that season. Blowing snow is most likely in June and August when new snow is cold and dry. Both fog and blowing snow decrease in frequency from Main Ice to North Land to Isachsen.

The frequency of observations with various types of precipitation, show the expected relationships between Main Ice, North Land and Isachsen. (The values for 1960-62 are questionable as a result of observation methods.) Snow and freezing drizzle are the most common form of precipitation at Main Ice while at North Land rain and drizzle are also frequent. At Isachsen snow and rain predominate.

2: 7 Precipitation

The inaccuracies involved in precipitation measurements have been discussed by many authors (e.g., Holmgren, 1971; Muller, 1967; and Rae, 1951). Errors usually result in underestimates of precipitation amounts. In this study a trace of precipitation was taken to be 0.0025 inches in obtaining the daily and monthly total precipitation and in calculating the monthly totals of rain and snow. This may result in slight overestimates in some cases, and in discrepancies between the sum of the rain and snow amounts, and the amount of total precipitation.

Table 2.6

Percent Frequency of Observations with Various Type of Weather

	Year	Freezing		Snow		Fog	Blowing Snow		
		Rain	Drizzle	Rain	Drizzle			1*	2**
M1	1960	5	1	1	0	5	--	57	0
	1961	4	1	1	1	5	1	66	19
	1962	3	1	1	0	4	--	50	4
	1968	1	1	1	14	13	3	52	6
	1969	3	3	1	12	16	1	61	4
	1970	1	1	2	6	17	2	74	3
N1	1968	2	5	1	9	13	1	30	2
	1969	5	6	1	5	9	3	46	3
	1970	1	3	1	4	10	2	62	6
IC	1960	5	2	0	0	6	0	18	0
	1961	9	4	0	0	21	0	47	2
	1962	3	2	0	1	9	21	1	
	1968	4	9	0	1	17	3	35	0
	1969	5	3	0	1	18	0	27	0
	1970	5	5	0	1	17	1	13	2

* Snow and snow showers

** Snow grains, snow pellets, ice crystals and ice pellets

Total precipitation amounts are plotted in Figure 2:7a. Main Ice seasonal totals are similar to those of Isachsen, except in 1969 when the precipitation amounts at Main Ice were considerably greater.

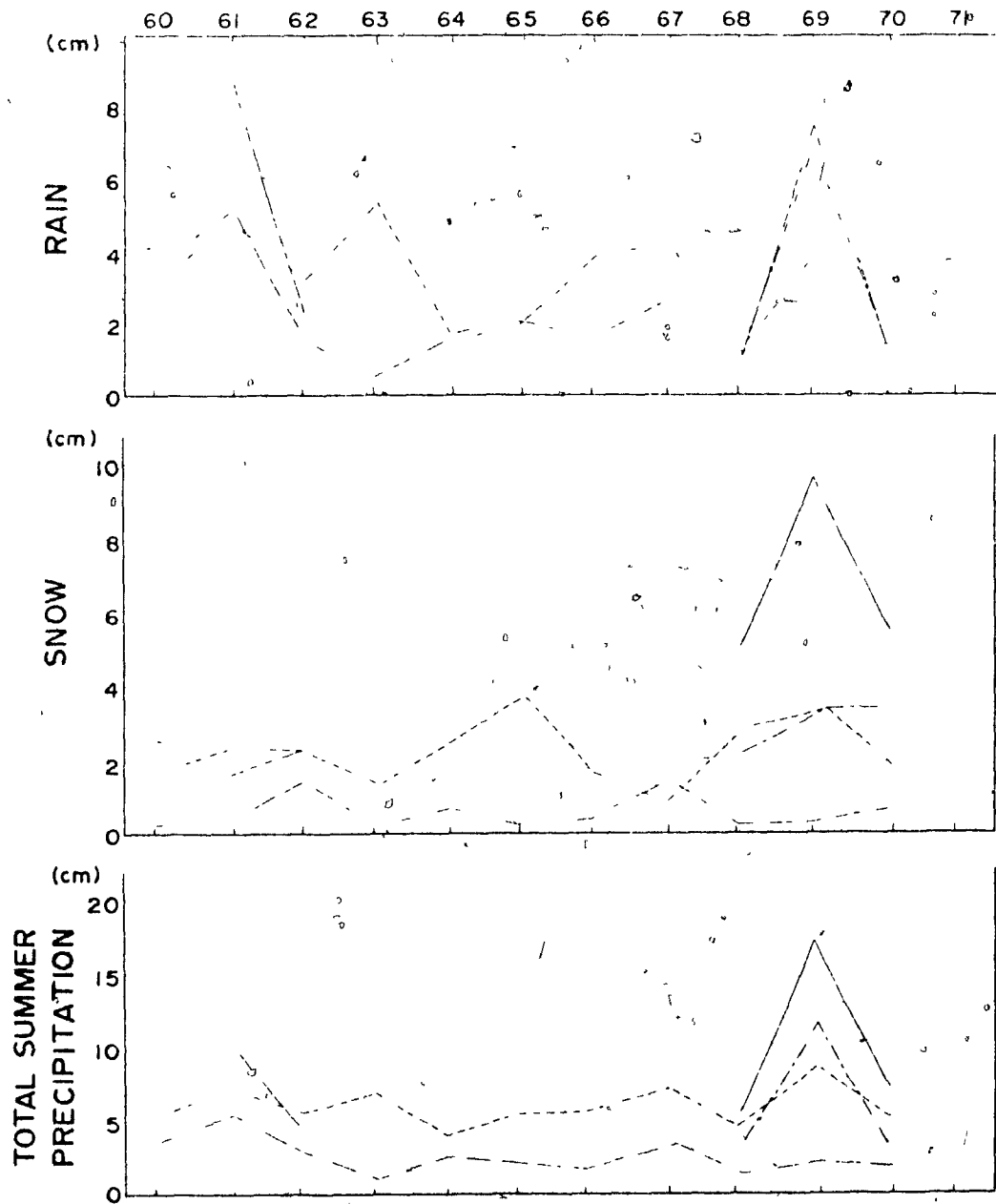


Figure 2: 7a Seasonal Precipitation Totals (see Figure 2: 7c for legend)

Seasonal totals of rain and snow tend to complement each other except in 1969 when both rain and snow amounts were high.

PRECIPITATION

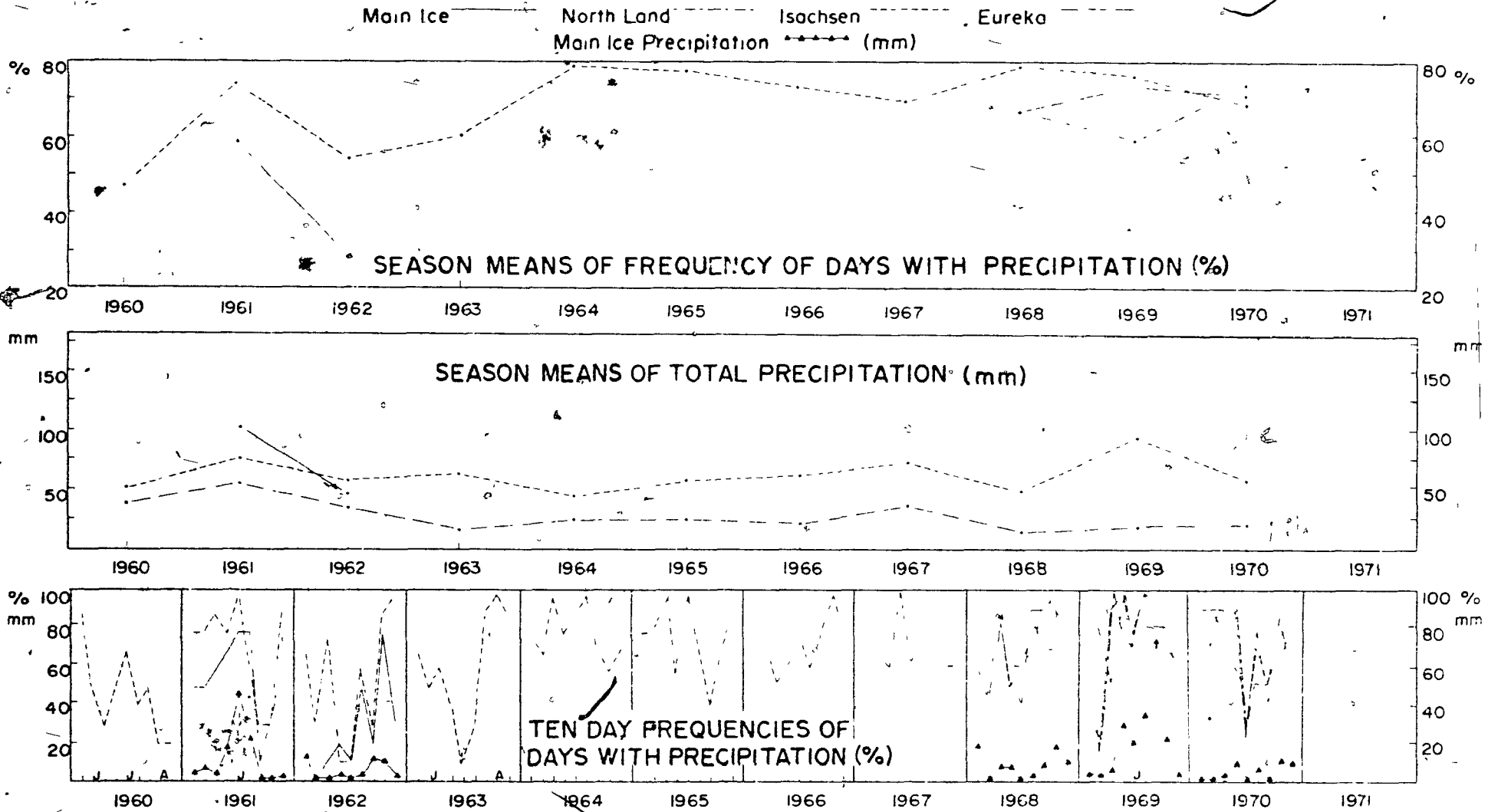


Figure 2:7c

Using the relationship between Main Ice and Isachsen precipitation for the five years 1961, 1962, 1968, 1969 and 1970 estimates were made of summer rain and snow amounts for Main Ice for 1963-67. These values together with the measured Main Ice values and the winter accumulation measurements (from Paterson 1969 and 1967-71) were used to obtain the total annual accumulation shown in Figure 2:7b. In years when the mass balance was strongly negative only summer precipitation in the form of snow was considered to contribute to the total accumulation.

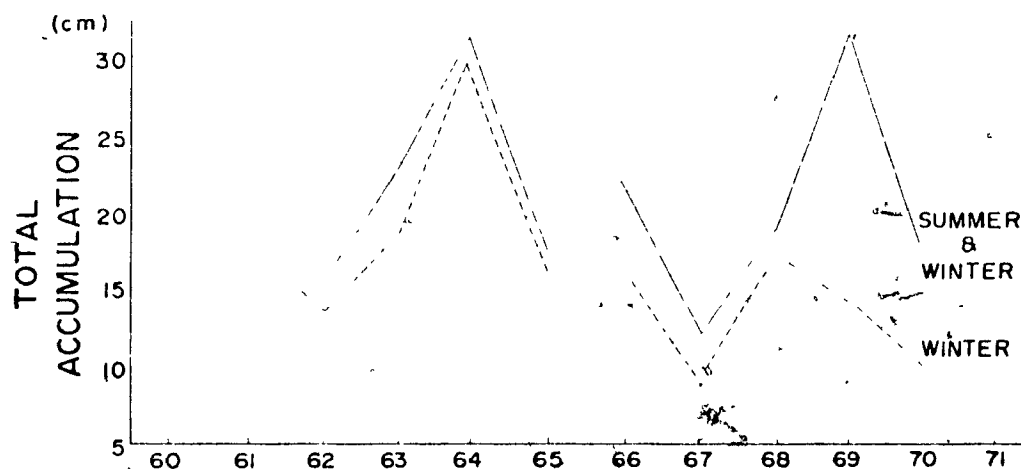


Figure 2:7b

The ten-day plots of days with precipitation show no significant seasonal trends (see Figure 2:7c). Plots of precipitation totals indicate amounts over 20 mm in ten-days only at the height of the summer season. In 1962, both frequency and amounts were low. Frequent light snow and drizzle in 1968 and 1970 resulted in low amounts and high frequencies in those years.

2: 8 Temperature in the Troposphere

The mean profile of temperature with height (50 mb intervals) from the Isachsen 12Z radiosondes of 1968, 1969 and 1970 is shown in Figure 2: 8a. The near isothermal layer below 850 mb is a reflection of the frequent inversions in the lower troposphere. Concerning the frequency of inversions over the Polar Ocean in summer Orvig (1970) says " The average importance of the inversion is best represented by the mean temperature difference between surface and the 850 mb level (1.5 km). In summer there is an indication of slight positive gradient only over the Beaufort Sea, i.e., warming with increasing height. All other areas of the Polar Ocean show slightly negative gradients. The gradients are much less than over the adjoining land

ISACHSEN SEASON MEAN TEMPERATURE SOUNDINGS (°C)

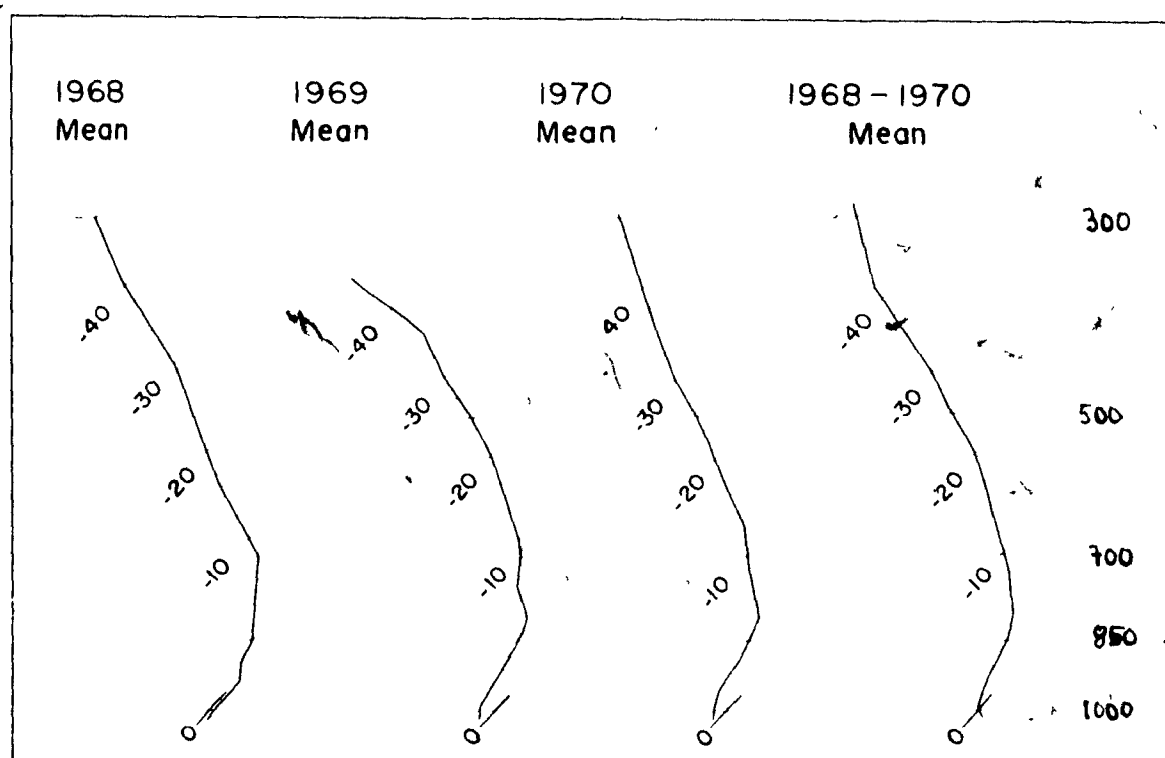
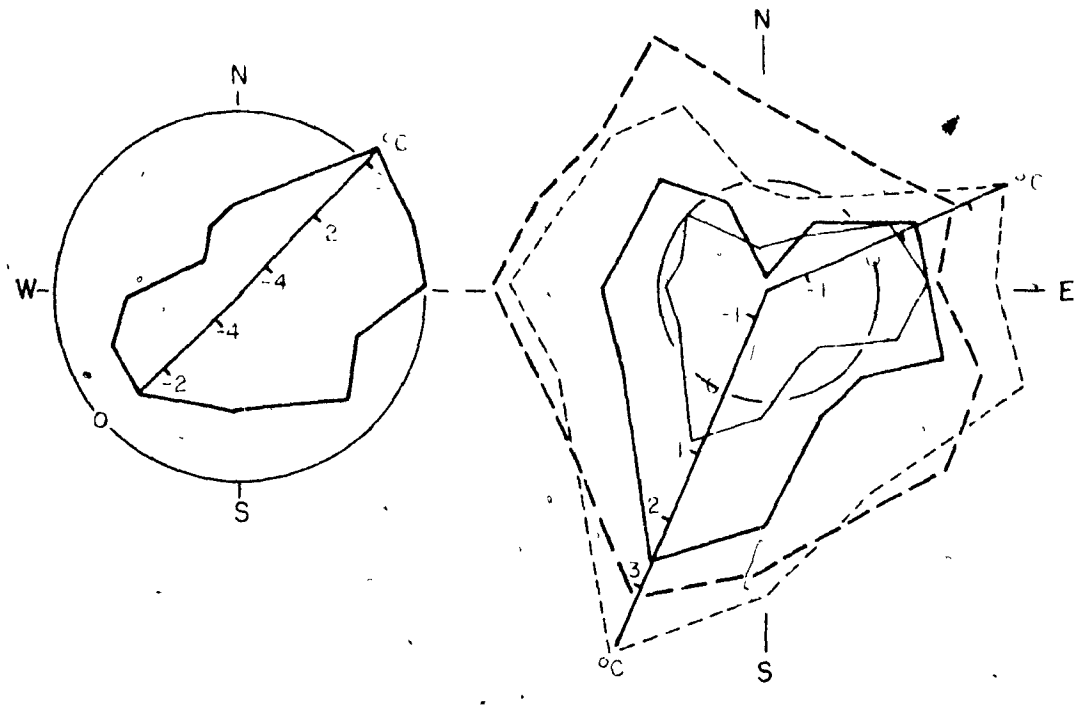


Figure 2: 8a

T = SURFACE TEMPERATURE °C
 ——— T-T 950
 - - - T-T 900
 ——— T-T 850
 - - - T950-T850
 +VE = LAPSE
 -VE = INVERSION



H850-H950

H500-H850

H300-H500

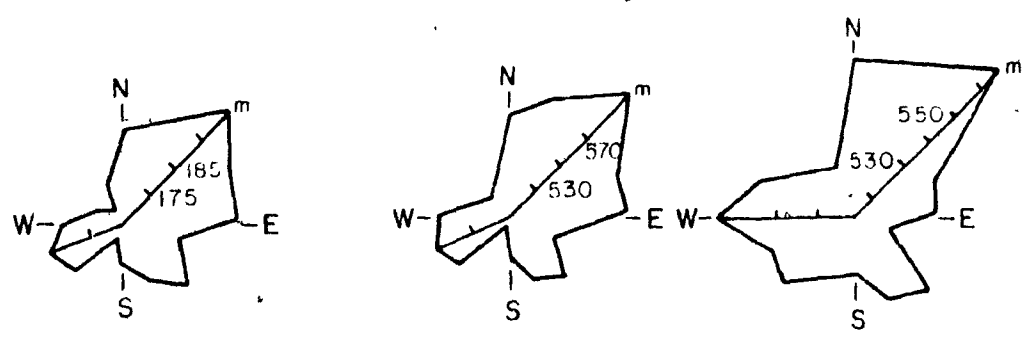


Figure 2: 3b Roses of Tropospheric Temperature

masses." Continental gradients can be as great as 8°C in summer. The mean value for Isachsen is 2.5°C . The inversion is most important in 1968 and least important in 1970.

Further information about the upper air conditions is given in Figure 2: 8b. The differences between Isachsen upper air temperatures and Meighen Island screen temperatures suggest the maximum temperature in the inversion lies near 900 mb except with N'ly winds when it appears to be higher. The variation with wind direction of the Isachsen 950 to 850 mb temperature differences is similar to that of the Main Ice - Isachsen sounding temperature differences suggesting no major inconsistency exists between the upper air conditions over Isachsen and Meighen Island.

Combining the temperature difference roses and thickness roses suggests the following: NW'lies are cold with lapse conditions to 850 mb. N'lies are warm with the strongest inversions experienced. NE'lies are warm with strong lapse conditions. SSW'lies are cold with strong lapse conditions. S'lies and SSE'lies are moderately warm and almost isothermal in the mean probably due to a combination of inversion and lapse conditions.

Figure 2.8c of ten day mean temperature profiles shows that in 1970 the entire tropopause remained cold until late June. In this year inversions were frequent only in late July and early August at which time Main Ice experienced anomalously high temperatures. There is evidence of an inversion in all periods in 1968 while in 1969 they appear in June and late August. Examination of individual soundings suggests that subsidence is the most important cause of summer inversions over Isachsen though advection is also frequently present.

ISACHSEN TEN DAY MEAN TEMPERATURE SOUNDINGS 1968 (°C)

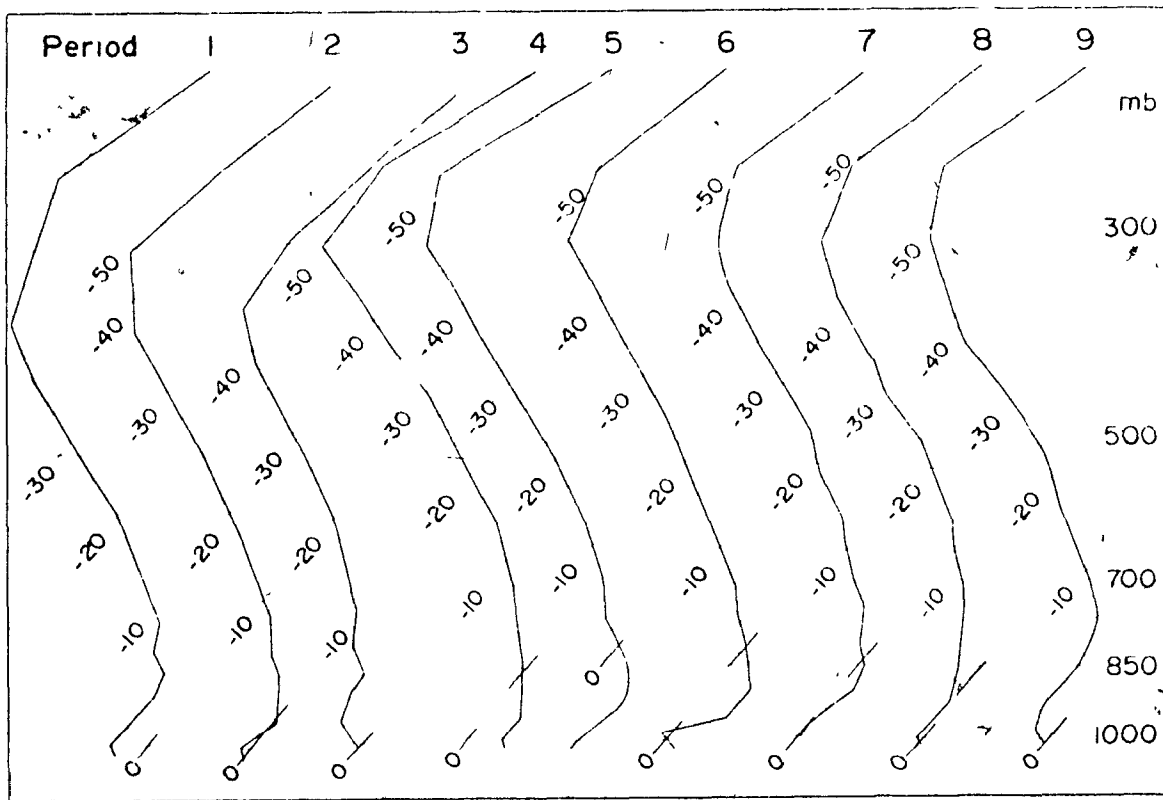


Figure 2: 8c

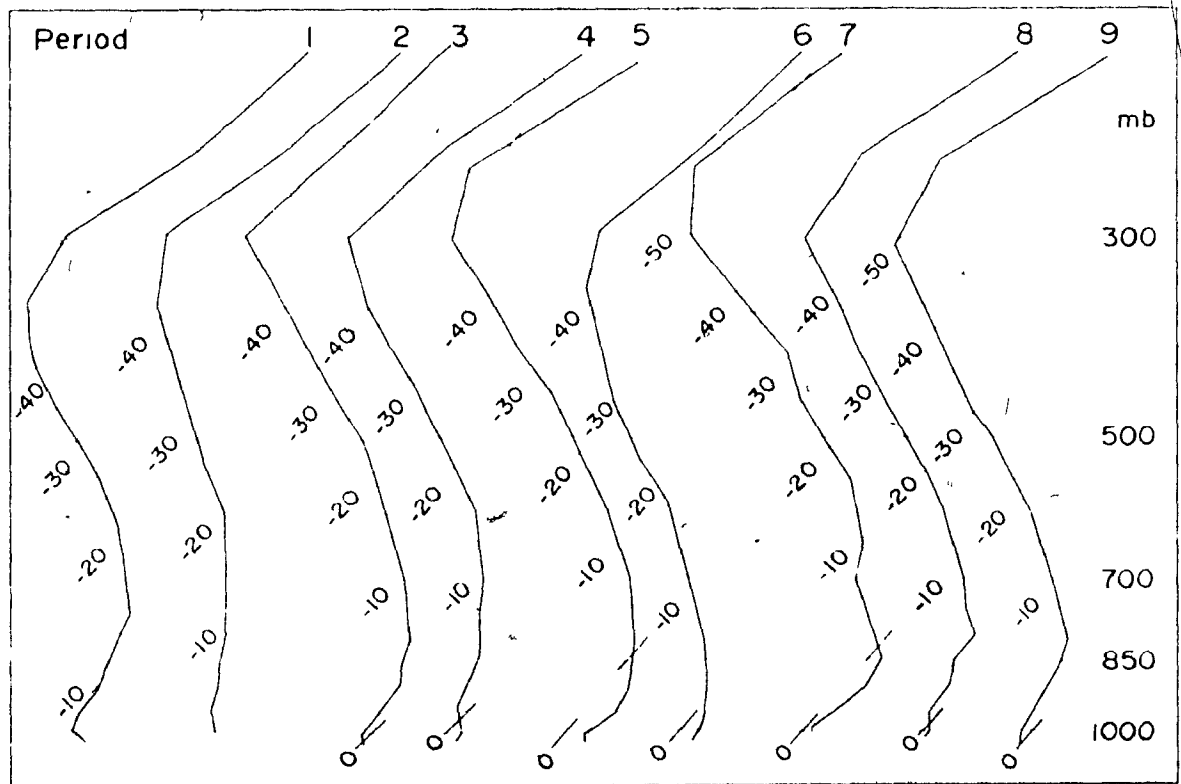
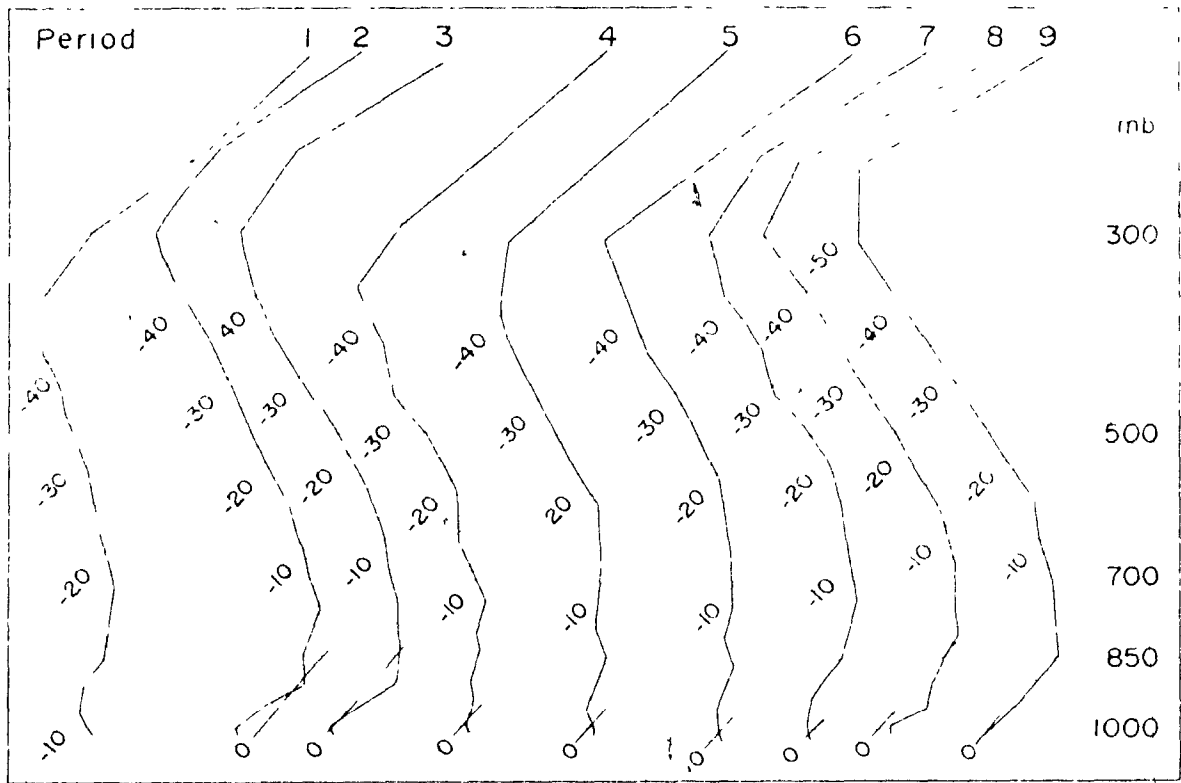


Figure 2: 8c cont'd

CHAPTER 3
SYNOPTIC CLIMATOLOGY

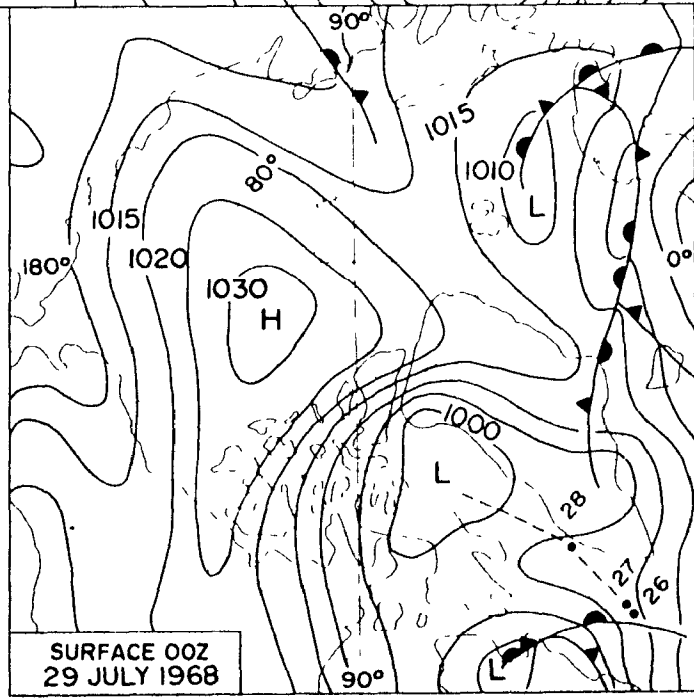
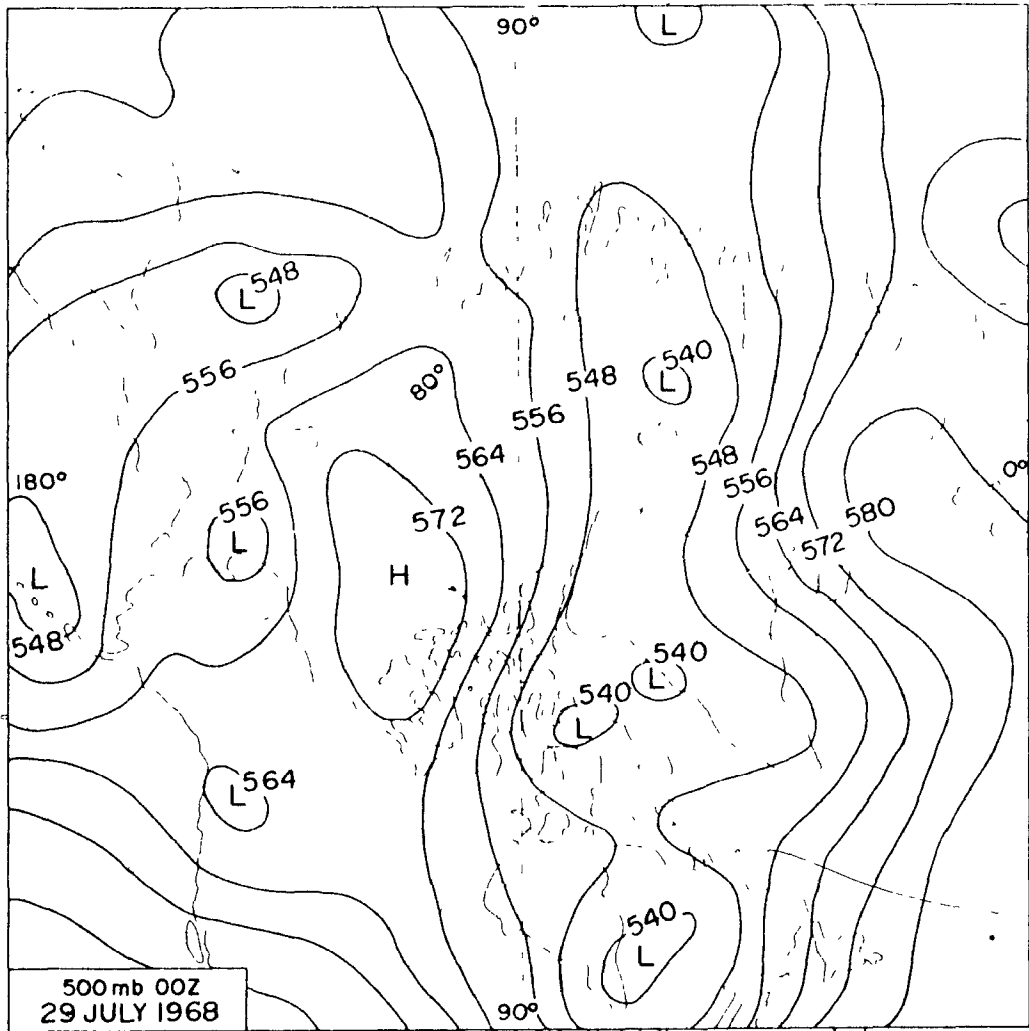
3:1 Introduction

In an effort to determine the relationship between synoptic scale phenomena and the summer climate of Meighen Island, an analysis of the daily synoptic situation was undertaken. Surface weather charts (1960-62*, 1968-70**) supplemented by satellite photographs (1968-70) were examined to determine the surface synoptic situation for each day of June, July and August in the years 1960-62 and 1968-70. The surface geostrophic wind for Meighen Island was extracted from these charts. In the analysis use was also made of 500 mb maps, Isachsen radiosonde data and Meighen Island meteorological observations including pilot ascents.

As a result of this study, four distinct circulation configurations were isolated such that variations in the relative importance of these circulation types, during a period, adequately accounted for the observed climatic characteristics of that period. Examples of the three primary circulation types are presented below, followed by a general discussion of the four types. Subsequently the climate of Meighen Island during the six summers is examined in terms of these circulation types.

* U.S. Department of Commerce, "Synoptic Weather Maps".

** Taglicher Wetterbericht. Amtsblatt des Deutschen Wetterdienstes.



TYPE I CASE A

Figure 3: 2.1a

3: 2 Type I

3: 2.1 Type I Case a - 00Z on 29 July 1968(17 MST on 28 July)

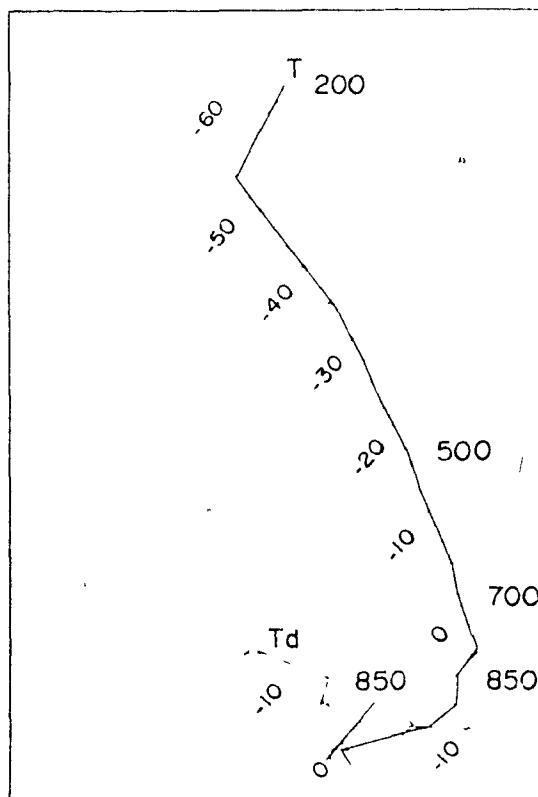


Figure 3: 2.1b

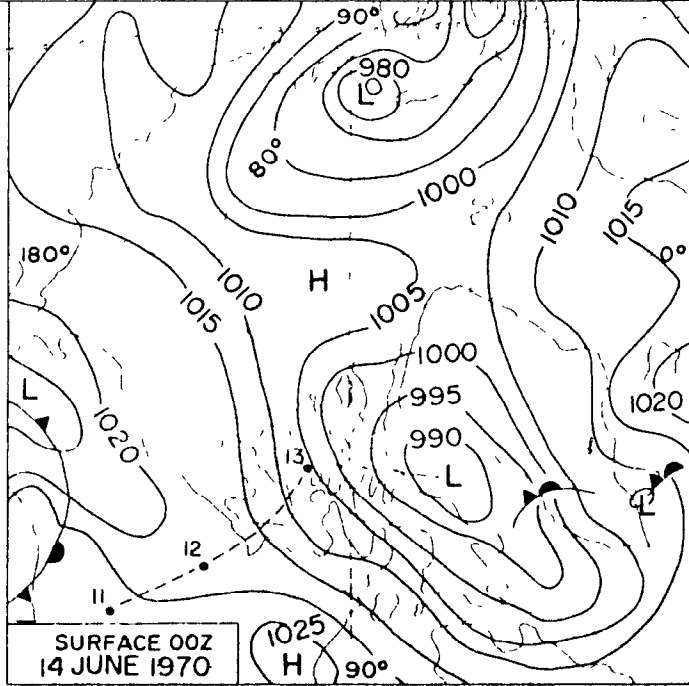
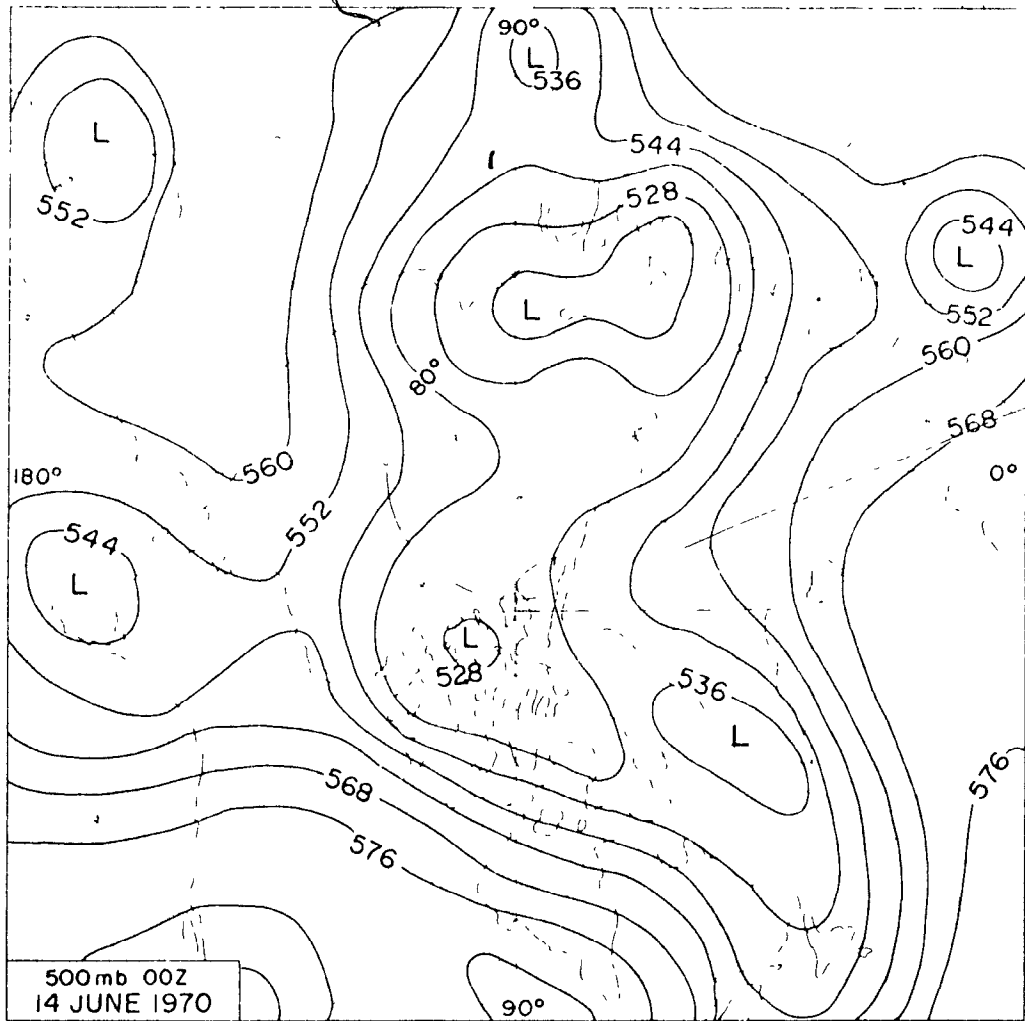
The surface situation showed a high pressure area in the Polar Ocean WNW of Meighen Island and a low pressure system in Baffin Bay with a strong gradient between them. The Baffin low tracked to Baffin Bay from the Labrador Sea. At 500 mb there was a multi-centered low stretching from Novaya Zemlya to southern Hudson Bay and a high in the Polar Ocean.

The satellite photograph showed cloud from the Polar Ocean stretching well into the north central Queen Eliza-

beth Islands obscuring Meighen Island and Ellef Ringnes Island but not appreciably affecting Axel Heiberg or Ellesmere islands.

At Main Ice the sky was totally obscured by fog, with visibility at one-eighth of a mile, winds N at 19 mph, temperature -1.05°C , relative humidity 100% and occasional light drizzle. Overcast stratus at zero feet above the station lowered to fog by 20 MST at North Land with a temperature of 0°C .

Conditions at Isachsen varied from 10/10 stratocumulus at 500 feet with fog and drizzle at 14 MST to 7/10 stratocumulus at 900 feet by 17 MST. The temperature was 2.8°C and the relative humidity 79%. N'ly winds were experienced at all levels in the troposphere. The tempera-



TYPE I CASE B

Figure 3: 2.2a

ture and moisture soundings showed a strong subsidence inversion with a maximum temperature of 7°C at 900 mb.

3: 2.2 Type I Case b - 00Z on 14 June 1970 (17 MST, 13 June)

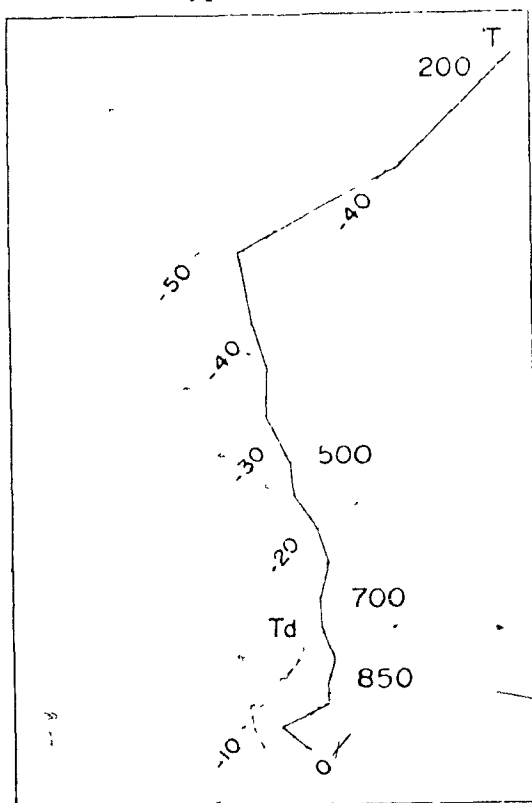


Figure 3: 2.2b

A strong Baffin Bay low extending NW into the Queen Elizabeth Islands at the surface was supported by a 500 mb low over the Parry Islands. The surface ridge west of the Islands was barely discernible at 500 mb.

At Main Ice the sky was obscured by fog and blowing snow, with winds N at 26 miles per hour, visibility 0 and temperature -5.4°C . Conditions at North Land worsened from 10/10 stratus at 800 feet at 17 MST to completely obscured in fog and blowing snow by 20 MST.

Isachsen reported 10/10 cover and blowing snow. The northerly surface winds veered with height becoming easterly by 500 mb. The temperature and moisture soundings showed strong mixing up to 950 mb, topped by an inversion with maximum temperature 900 mb. There was only slight evidence of subsidence at the 900 mb level.

3: 2.3 General Characteristics of Type I

This Type is characterized at the surface by a high pressure area west of Meighen Island in the Polar Ocean, and a low in Baffin Bay. The

dominant feature of the 500 mb map is a cold low in the Hudson Bay area. The position of the upper cold low in this circulation Type results in a predominance of storm tracks along the northern coast of mainland Canada and into Baffin Bay.

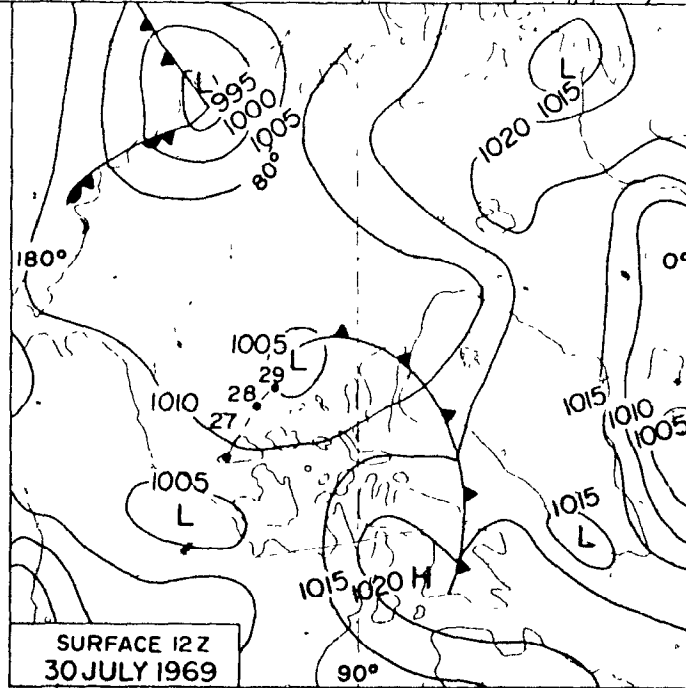
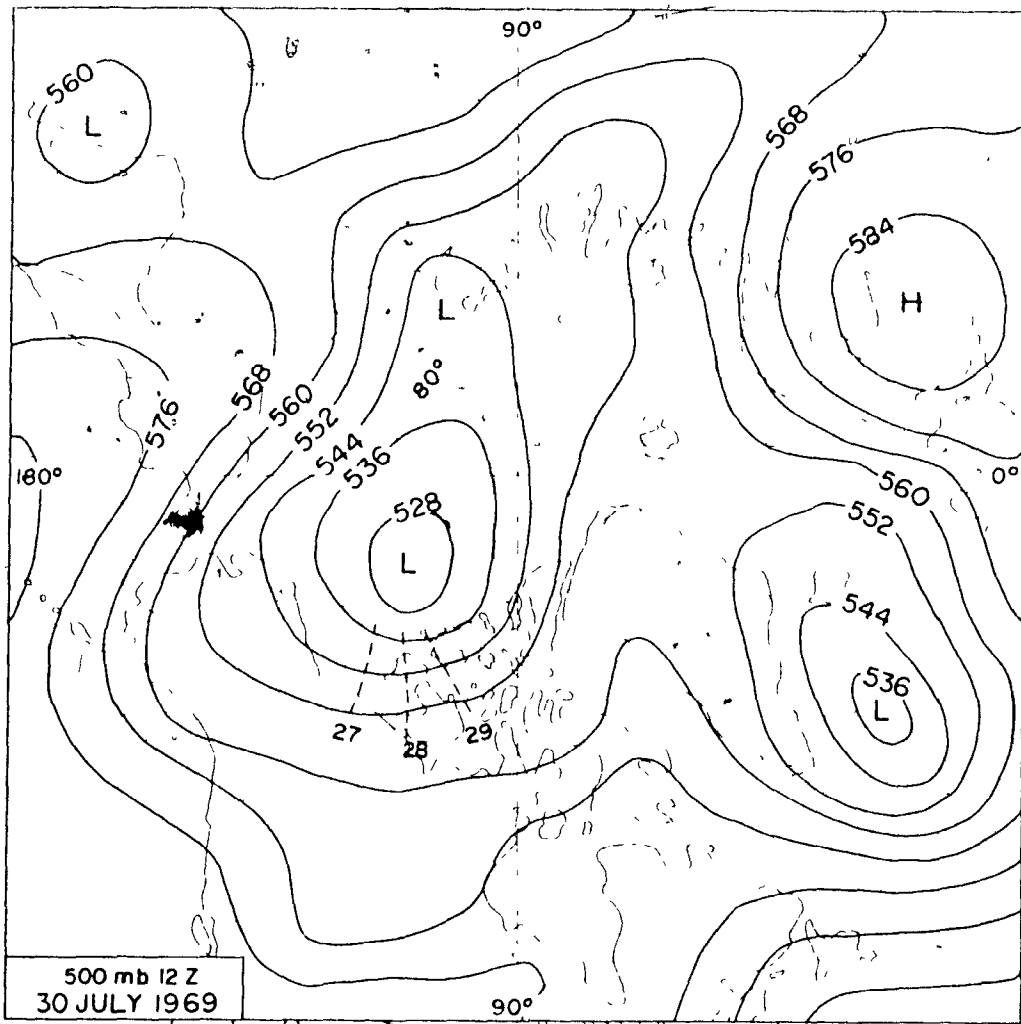
Northerly flow off the pack ice imports low stratus or fog from the Polar Ocean into the northern Queen Elizabeth Islands. The cool, frequently thin, Polar Ocean stratus or fog tended to dissipate once it has travelled 15 to 20 miles over warm land. Stefansson (1944) pointed out that on Prince Patrick and Borden Islands the coasts bordering the Polar Ocean are barren in comparison with the inland areas. Satellite photographs show that Axel Heiberg and Ellesmere islands often escape this Polar Ocean fog due to their height. As Meighen Island is relatively low and small, this type of circulation invariably results in fog or low stratus, at least as far south as the southern end of the ice cap. Isachsen is sheltered from the Polar Ocean and usually reports only low cloud under these circumstances.

The intensity and extent of the Baffin Bay low determines the strength of the wind in these situations; however it is frequently above 15 mph. Cloud associated with the Baffin Bay system is occasionally present above the fog, depending on the position of the system. If precipitation accompanies this circulation type it is usually in the form of drizzle or freezing drizzle, and the formation of rime is a frequent occurrence with temperatures a few degrees below freezing.

When the Polar Ocean high dominates the Meighen Island region, a strong subsidence inversion results. This subsidence inversion may be enhanced by an advection inversion caused by the intrusion of cold Polar Ocean air into the islands in the lowest levels. When the Baffin low

dominates, the surface layer is strongly mixed, though a trace of the subsidence inversion may be seen in upper levels.

Type I circulation generally results in cool, windy and foggy weather on Meighen Island. Axel Heiberg and Ellesmere islands, as seen in the satellite photographs, can experience relatively clear weather under these circumstances providing the Baffin cyclone remains in southern Baffin Bay. Havens et al (1967, p. 29) notes that clear weather prevailed at the Axel Heiberg stations from 16 to 18 June 1961. During this period on Meighen Island, high winds, cool temperatures and fog accompanied the Type I situation. At Tanquary Fiord (Jackson 1969, p. 32-37) the strong NE'ly flow set up by such a synoptic situation can produce fohn conditions. Holmgren (1971, p. 47) found that "Baffin Bay cyclones favour glacierization on Devon Island, no matter the season they appear". This is as would be expected due to advection from the cold water of Baffin Bay.



TYPE II CASE A

Figure 3: 3.1a

3: 3 Type II

3: 3.1 Type II Case a - 00Z on 30 July 1969 (17 MST, 29 July)

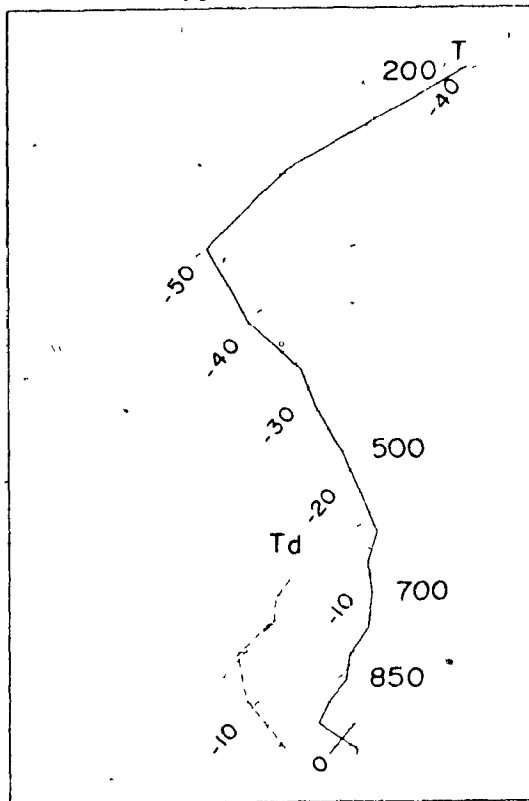


Figure 3: 3.1b

Land and West Land improved from obscured in fog at 17 MST to partially obscured with middle and high cloud by 20 MST. At Main Ice, 9.9 mm of rain and a trace of snow fell on 27 July, 1.7 mm of rain and a trace of snow fell on 29 July and .8 mm of rain fell on 30 July. Winds shifted from SSE at 05 MST on 29 July to S at 17 MST and to SSW by 23 MST.

The Isachsen radiosonde had a super-adiabatic lapse rate up to 950 mb, topped by an almost isothermal layer which, the moisture sounding suggested, could be due to subsidence.

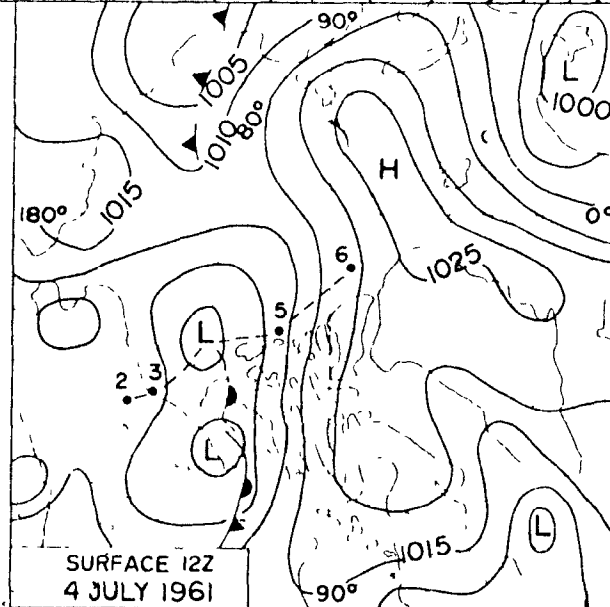
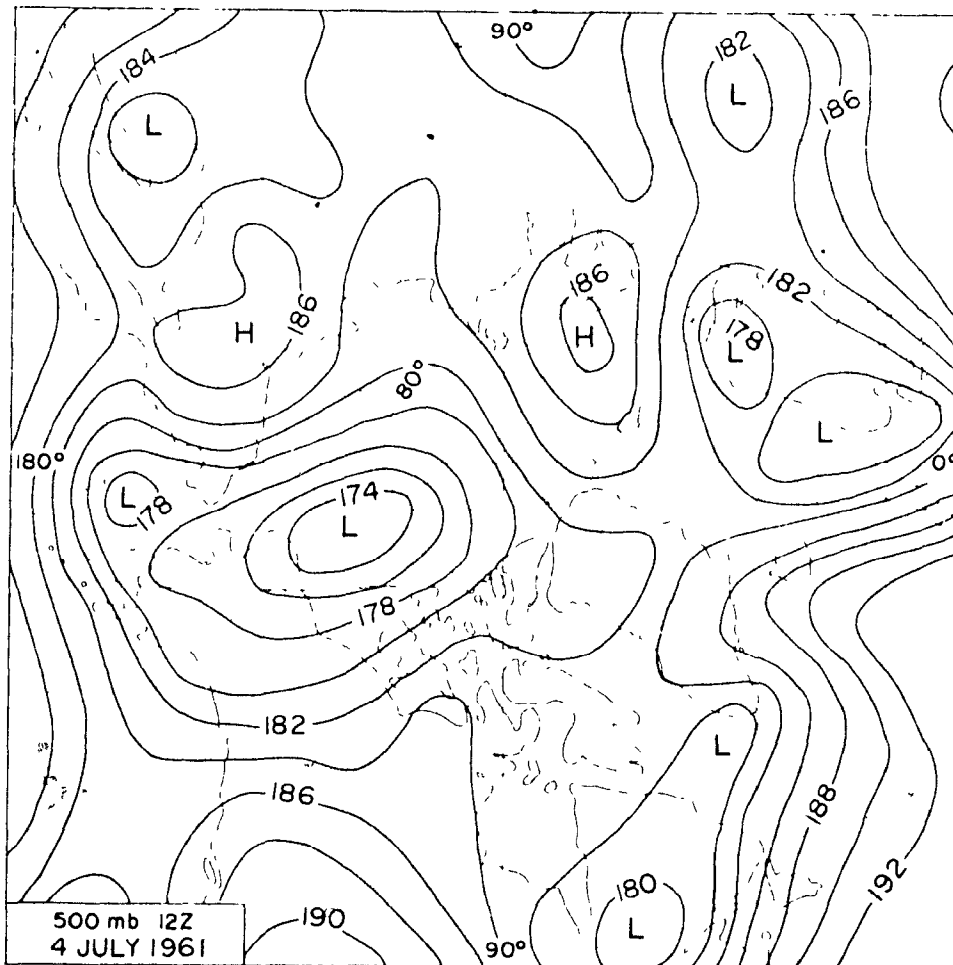
3: 3.2 Type II Case b - 12Z on 4 July 1961 (05 MST, 4 July)

A surface low and front tracked NE along the edge of the Archipelago around a 500 mb cold low located north of Alaska.

At 500 mb a short wave trough moved around a cold low centered in the Polar Ocean west of Meighen Island. Associated with this trough a surface low and cold front tracked northeast along the edge of the Archipelago to a position west of Meighen Island by 30 July. The satellite photographs showed a wide band of thick cloud associated with the front passing Meighen Island by 29 July.

The conditions at Main Ice, North

Land and West Land improved from



TYPE II CASE B

Figure 3: 3.2

Winds of 35 mph from the SE preceded passage of this system at Main Ice. The sky was obscured by fog and blowing snow with a temperature of 0°C and a trace of snow reported.

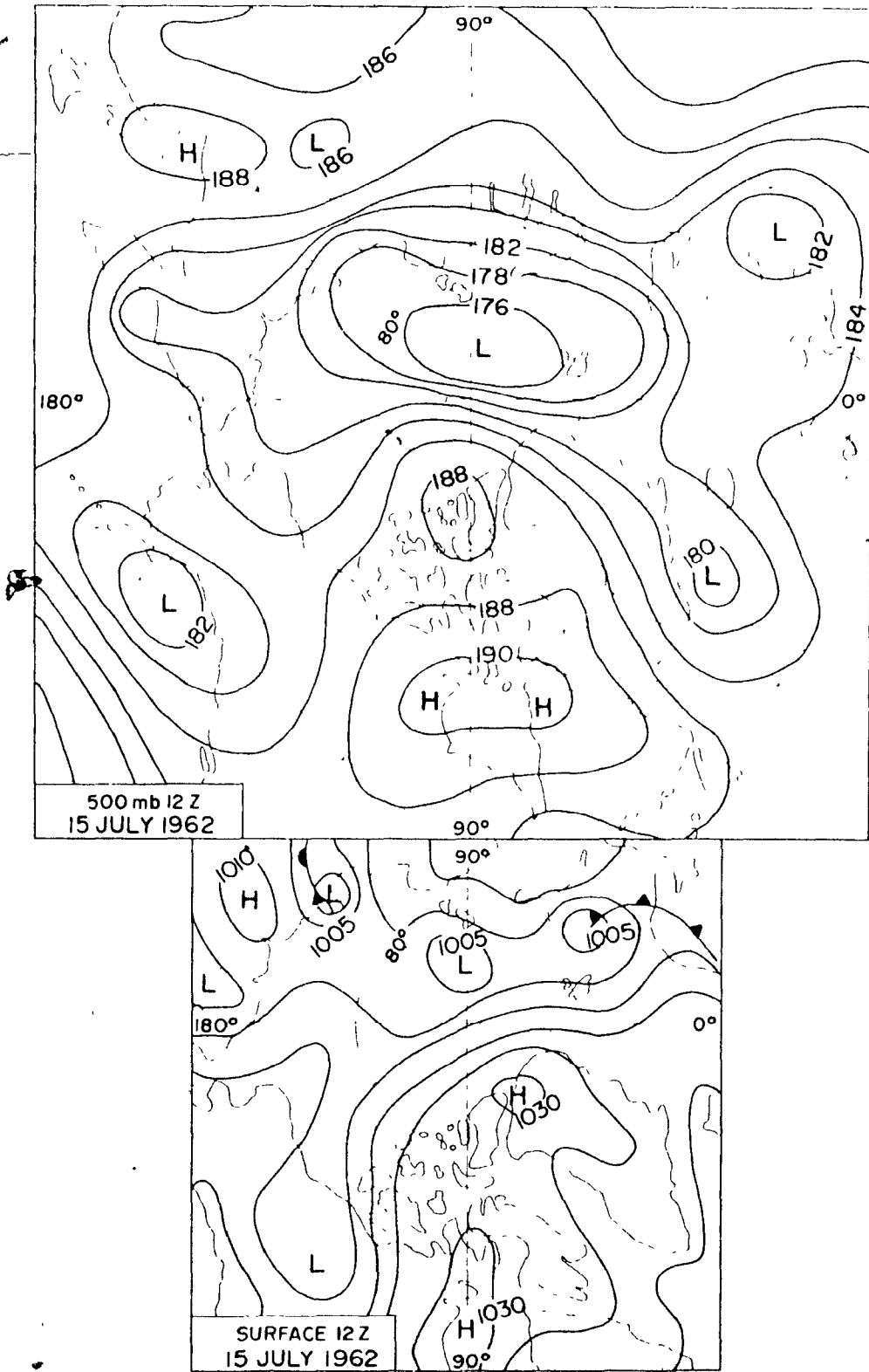
Muller (1967, p. 23) discussed the 5 July situation as one of anomalous precipitation amounts. On Meighen Island 2.5 mm water equivalent of snow fell on 3 July, and 9.4 mm of rain on 4 July. On 5 July at Axel Heiberg Base Camp 11.5 mm of rain was recorded.

3: 3.3 General Characteristics of Type II

Circulation of Type II features a 500 mb cold low in the Polar Ocean north of Alaska. Lows, developing in the strongly baroclinic zone between the radiationally heated land of Siberia and Alaska and the cold Polar Ocean, pick up moisture over the ice-free areas of the peripheral seas. They travel around the upper cold low in a short wave trough. This results in tracking of surface lows and well developed baroclinic zones northeast along the northwest edge of the Archipelago.

Reed (1959) in a detailed study of the cloud structure of arctic cyclones found that in the layer between 0 and 5,000 feet the cloud cover averaged nearly 100% and exhibited only slight relationship to the synoptic pattern. This is presumably due to the ever-present Polar Ocean stratus and fog. Above 5,000 ft., however, the disturbance closely resembled mid-latitude cyclones. Cloudiness was related to temperature advection (warm advection - cloud amount maximum; cold advection - cloud amount minimum).

Conditions on Meighen Island during passage of the cold frontal system coincide with these findings. Prior to passage the winds are SSE, fog obscures the sky and rain indicates the presence of nimbo-



TYPE III CASE A

Figure 3: 4.1

stratus above the fog. With passage of the cold front, winds shift to SW and eventually the fog breaks to reveal decreasing amounts of middle and high cloud. Temperatures remain cool. The clear period is short lived. Once the low is past the Island, cold and foggy N'lies prevail until the next system approaches.

The temperature sounding shows the sharp tropopause discussed by Reed (1959) in connection with the arctic jet. The lowest layers are unstable, but there is a slight suggestion of subsidence around 850 mb.

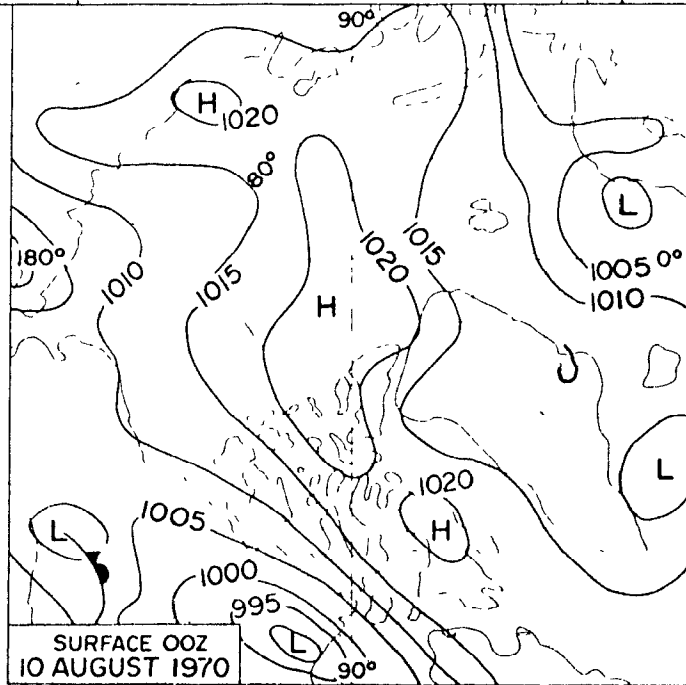
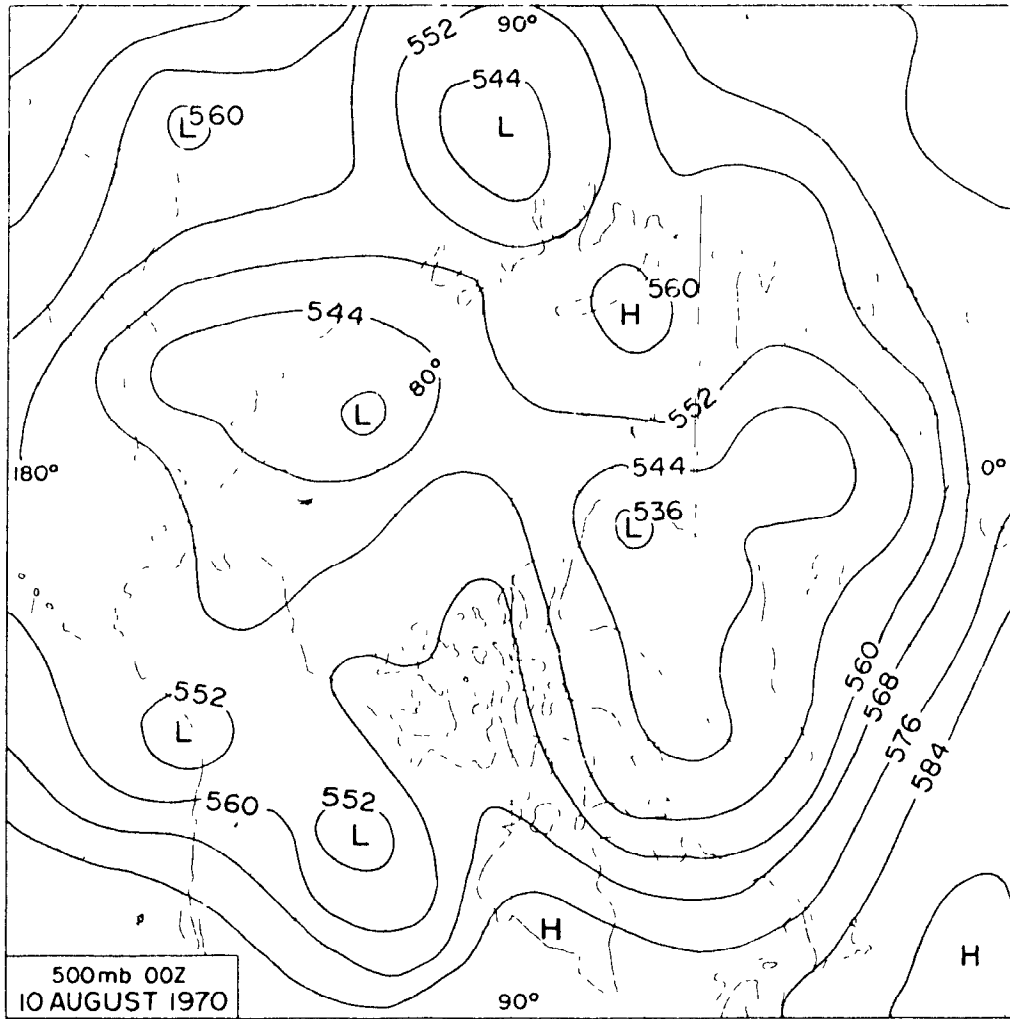
Type II circulation results in temperatures near freezing and the largest precipitation amounts recorded on Meighen Island. Strong winds are common in these systems. This type of circulation is also responsible for precipitation maxima on Axel Heiberg Island as in Case b above. On Devon Island, strong warm S'ly winds result. In fact the periods of strongest melt experienced on Devon Island in 1961 and 1962, discussed by Holmgren (1971, p. 41-46), correspond to temperatures near freezing, SW winds, fog, middle cloud and considerable precipitation on Meighen Island.

3: 4 Type III

3: 4.1 Type III^o Case a - 12Z on 15 July 1962 (05 MST, 15 July)

In this fully developed case of Type III, the 500 mb cold low was displaced to the Soviet side of the Polar Ocean and an extensive high covered the whole of the Archipelago south to Hudson Bay. At the surface a ridge extended from Hudson Bay to northern Greenland.

Small amounts of altostratus, altocumulus and cirrostratus were



TYPE III CASE B

Figure 3: 4.2a

the only clouds accompanying these conditions. The temperature reached its seasonal maximum of 10.1°C .

The sky at Isachsen was clear, the wind was S at 2 mph and the temperature reached 13°C .

The example used by Holmgren (1971, p. 49) to illustrate anti-cyclonic development in 1962 (18 July) is the latter part of the Type III case. By this time a cyclonic system is approaching the northern Queen Elizabeth Islands, having travelled around the Polar Ocean from the Soviet side.

3: 4.2 Type III Case b - 00Z on 10 Aug 1970 (17 MST, 9 Aug)

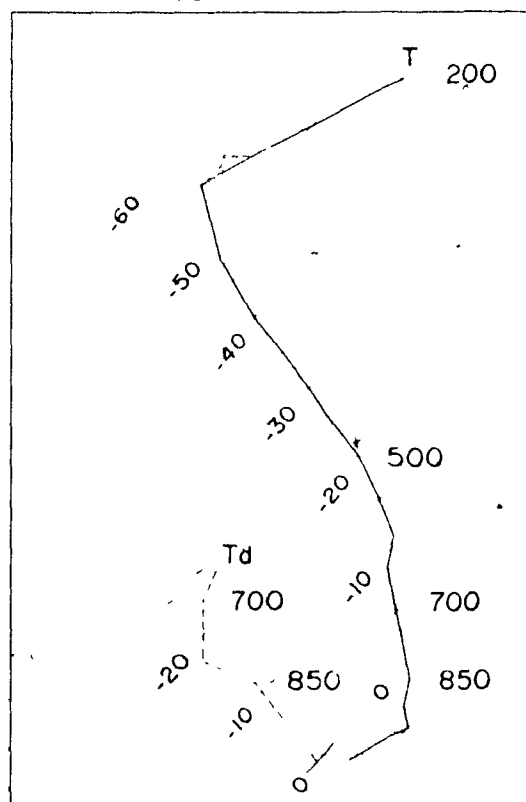
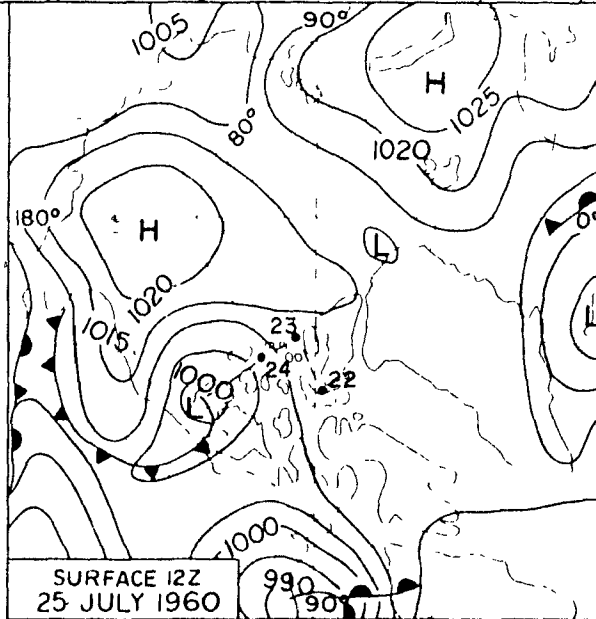
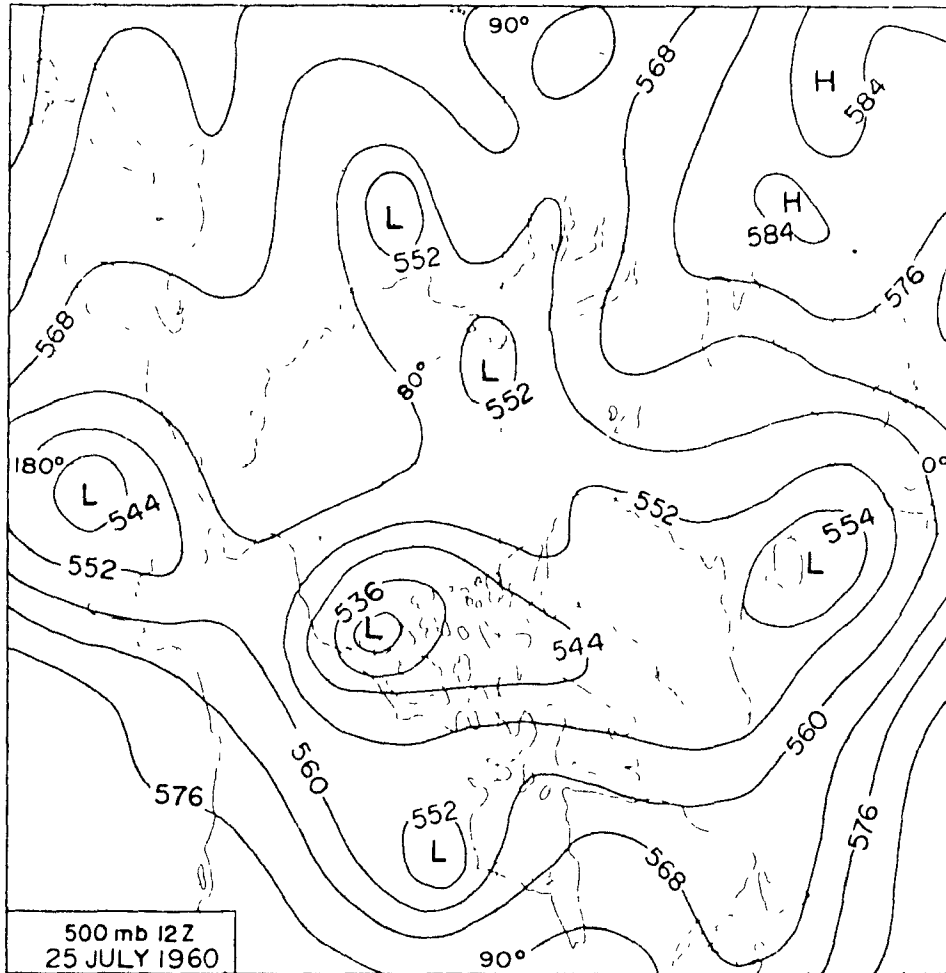


Figure 3: 4.2b

The period 8-11 August has been analysed in detail by Petzold (1971) in connection with a study of upper winds over Meighen Island. Though the ridge line of the surface ridge lies west of Meighen and surface winds are N'ly, southerly flow spreads upwards from the 900 mb level reaching 500 mb by 10 August.

The satellite photographs suggest that the extreme northern edges of the islands were experiencing some cloud.

Fog or low stratus was noted by observers at several Meighen Island stations to lie to the north in the Polar Ocean and advanced to cover the island at the close of the clear period. Mirages of Axel Heiberg and the Fay Islands were well developed during the period and estimated to be 2,000 feet deep.



TYPE III CASE C

Figure 3: 4.3

Thin cirrus cloud was reported at all stations. The relationship of temperatures at the various Meighen Island stations and Isachsen were unusual: Main Ice 4.1°C , North Ice 3.3°C , North Land 2.6°C and Isachsen 3.9°C . Winds were NE'ly on Meighen and WSW at Isachsen.

The temperature sounding for Isachsen showed two strong subsidence inversions, the first from the surface to 950 mb, or approximately 1,800 feet, and the second around the 650 mb level.

3: 4.3 Type III Case c - 12Z on 25 July 1960 (05 MST, 25 July)

Another variation of Type III developed when a surface low tracked into the islands from the south and then turned westward towards Banks Island, allowing a small ridge to develop through the lower troposphere over northern Ellesmere Island.

At Main Ice skies were clear and the wind was ENE at 4 mph with a temperature of 2.8°C . Isachsen being closer to the low pressure system, was warm (5.6°C) but had 8/10 stratocumulus and easterly winds of 16 mph.

3: 4.4 General Characteristics of Type III

A complete development of Type III such as that shown in Case a involves positioning of a cold low on the Siberian side of the Polar Ocean and a ridge over the eastern Canadian Arctic and Greenland. Surface lows track around the central Polar Ocean occasionally penetrating the Queen Elizabeth Islands from the west but more often being deflected along the edge of the Islands to die near the Pole.

With this type of circulation the warm ridge in eastern North America can dominate the flow for periods of more than a week. On these

occasions, the whole of the western Arctic experiences high temperatures, light winds and clear skies. In fact Isachsen temperatures often exceed those of Eureka during these periods. Temperatures on Meighen Island soar as the warm southerly flow pushes the Polar Ocean fog well off the coast.

Though complete cases of Type III are infrequent, partial development of this type of circulation is connected with all significantly warm periods on Meighen Island. The essential feature of this development is the intrusion of a ridge over the eastern Islands or Greenland at some level in the lower troposphere, resulting in southerly flow at that level over Meighen Island. This southerly flow combined with subsidence blocks the advance of Polar Ocean stratus into the Meighen Island region. It is evident from satellite photographs and Meighen observers' notes that the fog or low stratus remains in the Polar Ocean some distance north of Meighen Island.

Type III is characterized by anomalously warm, clear weather on Meighen Island. This circulation normally extends far enough east to produce similar conditions on Axel Heiberg and Devon Islands. The period of anticyclonic blocking and foehn winds at the Axel Heiberg stations, discussed by Muller (1967, p. 55), corresponded to Type III conditions on Meighen Island. Similarly, the 1962 situation chosen by Holmgren (1971, pp. 47-51) to illustrate domination of extensive warm-cored anticyclones, coincides with the end of the Type III period discussed in Case a. Eureka and Tanquary Fjord (Jackson 1969) do not normally fall under the influence of this type.

3: 5 Type IV

A fourth classification is needed to account for occasions when the 500 mb cold low tends to be centered over the Pole. Under these circumstances there is a rapid alteration between the other three types producing a variety of surface weather conditions. Type IV was significantly frequent only in 1970 and has not been illustrated.

3: 6 Ten-Day Climate and Synoptic Situation

The degree to which the summer synoptic conditions over Meighen Island can be represented by these four types is illustrated in Tables 3: 6a and 3: 6b. Here a brief description of the ten-day synoptic situation is tabulated against the circulation type chosen for the period with the help of daily surface and 500 mb maps. In some cases two Types occurred in succession during the period. Included in the tables are ten-day means or totals of various meteorological elements from Main Ice. Plots of ten-day means, discussed in sections 2: 1 through 2: 7, give further details on the climatic situation during each period. Reference should also be made to the plots of nine-day running mean temperatures and daily mean cloud amounts found in Figures 2: 1.1c and 2: 5.3a. In general, the four circulation Types adequately depict the actual synoptic situation during all six years and account for all significant deviations from the mean of temperature, cloud amount, fog frequency and precipitation totals.

There follows a brief discussion of the synoptic climatology of each of the six years as seen from Tables 3: 6a and 3: 6b and the Figures of sections 2: 1 - 2: 8.

Table 3: 6a

TEN DAY SYNOPTIC CONDITIONS, CIRCULATION TYPE AND MAIN ICE CLIMATIC ELEMENTS

Year	Period	Summary of Synoptic Situation ²	Circ. Type	Melting	Precip. total	Fog frequency	Cloud type ³	Cloud cover (/10)	Wind	
				degree days (°C)					(mm)	(%)
1960	2	R over QEI gives way to PO H and BB L	III, I	1.7	--	70	F, ST	9.1	NW/NNW	4.4
	3	R moves over QEI lying W of MI by 26th	III	20.8	--	25	F, AS	4.7	N	6.0
	4	R followed by L, then R followed by PO L	I or IV	3.8	--	61	F, ST	2.9	N	4.7
	5	H over GL then R W of MI pushed E to MI	III	23.1	--	52	F, ST	7.6	SE/WSW	5.0
	6	L in QEI trades W and small R over GL	III	18.0	--	35	F, ST	7.3	SE/E	3.5
	7	H moves across QEI followed by L	III	24.9	--	65	F, AS	7.9	SE	4.1
	8	H in PO with ridge to GL	III	28.1	--	76	F, AS	5.9	N/NW	2.5
	9	H in PO with Ts pushing into QEI from S	I	5.3	--	74	F, AC	7.1	N	3.9
	1961	1	H moves from PO over QEI to GL	I, III	0.0	3.4	30	ST, X	8.0	N/W
2		H in PO and L in BB	I	0.3	6.5	73	F, X	9.9	N/SSW	7.4
3		H in PO battles with L in BB	I	0.3	3.0	74	F, ST	9.1	N	7.1
4		Ts from E SIB move NE along edge QEI	II	3.4	17.5	54	F, ST	9.0	SE	8.5
5		Ts from E SIB move NE along edge QEI	II	7.0	46.6	94	F, ST	9.7	SE/SSE	7.9
6		Ls move around PO then H pushes into PO	III, I	5.0	22.6	80	F, ST	9.1	SW/NNW	8.8
7		R to GL from SIB H, SIB H moves into PO	III, I	22.2	0.1	45	F, SC	6.1	N	7.7
8		R in PO moves to BB, SIB H moves to PO	I, III, I	7.5	0.4	46	F, SC	8.7	NW/SE	5.2
9		H in PO, Ls track S of ARC	I	0.0	3.8	88	F, ST	9.0	N	9.6
1962	2	H in W ARC with R to GL, Ls track through QEI	III	9.5	0.0	52	F, ST	8.0	N	7.1
	3	H over PO weak Ls S of ARC	I	0.6	0.5	75	F, ST	9.2	N/NNW	6.2
	4	H moves E followed by L, then H moves into BB	III	23.8	3.1	22	F, ST	5.5	NNE/S	3.1
	5	H over QEI interrupted by small L's	III	52.9	0.3	15	F, AS	5.8	S	3.7
	6	H over QEI followed by T's along edge QEI	III, II	16.8	3.4	33	F, AS	8.3	SW/W	3.7
	7	H moves N of QEI to GL followed by L	II, II	15.3	12.0	43	F, SF	4.6	N	3.7
	8	H in S PO, L in BB	I	0.6	10.7	88	F, AC	9.2	N	5.9
	9	H in SIB PO and Ls track S of QEI	I	0.0	1.3	75	F, ST	8.6	N	6.3

1 Ten-day periods. 1) 1-10 June, 2) 11-20 June, 3) 21-30 June, 4) 1-10 July, 5) 11-20 July, 6) 21-30 July, 7) 31-9 August, 8) 10-19 August, 9) 20-29 August.

2 Abbreviations: PO = Western Polar Ocean; BB = Baffin Bay, L = Low, H = High, QEI = Queen Elizabeth Islands, ARC = Archipelago, MI = Meighen Island, R = ridge, T = trough, GL = Greenland, S/B = Siberian, RUS = Russian, HB = Hudson Bay.

3 First and second most important cloud type.

4 Most frequent wind direction and second most frequent direction if important.

3: 6.1 1960

The occurrence of Type III circulation in early June accounts for the unusually warm June of 1960. With the exception of the first period in July, Type III predominated from the onset of summer in late June to its demise in late August. During this time numerous warm spells occurred resulting in ten-day melting degree day totals of over 20°C. Though fog was not less frequent than normal, the total cloud amount was below the six year mean in all Type III periods. When Type I took over in early July the cloud amounts, fog frequencies and melting degree day totals reverted to early spring values.

3: 6.2 1961

Polar Ocean conditions existed in June, due to the dominance of Type I circulation. The cyclonic systems of Type II brought considerable precipitation to the Island during most of July. For the remainder of the season Types I and III alternated, resulting in several marked warm and cold spells, the highest temperatures and clearest skies occurring during a Type III situation in early August. Examination of individual wind maxima shows that the anomalously high wind speeds in 1961 resulted from unusually strong pressure gradients. These were found between the Polar Ocean high and Baffin Bay low, or in connection with the cyclonic systems of Type II circulation.

3: 6.3 1962

The early dominance of Type III circulation resulted in significant melting degree day totals by mid-June. Polar Ocean conditions intruded in late June but gave way to strongly developed Type III circulation in

Table 3, 6b

TEN DAY SYNOPTIC CONDITIONS, CIRCULATION TYPE AND MAIN ICE CLIMATIC ELEMENTS

Year	Period	Summary of Synoptic Situation ²	Circ. Type	Melting degree days (°C)	Precip. total (mm)	Fig frequency (%)	Cloud type ³	cover (/10)	Wind direction ⁴ (16 pts.)	speed (m/sec)
1968	1	H moves across S ARC followed by L then H in PO	III, I	0.2	1.8	40	ST, F	8.5	SW	5.1
	2	H in PO and L in BB which moves W to S of QEI	I, III	1.6	0.4	37	F, SF	7.9	N	6.6
	3	H in PO and L in BB	I	0.1	6.1	47	F, SC	8.4	N	4.9
	4	H builds from PO across QEI to GL	I, III	11.3	5.4	37	F, ST	6.3	N	4.0
	5	Strong L in BB dominates	I	7.7	0.4	33	F, AC	5.9	N	6.3
	6	H in PO and L in HB	I	0.0	1.7	90	F, SF	9.5	N	6.3
	7	H in PO dominates	I	0.1	7.4	70	F, ST	9.9	N	7.5
	8	L in QEI pushed out by H moving to W QEI	II, I	0.2	17.4	77	F, ST	9.6	WSW	3.0
	9	H over QEI with L's tracking in from SW	II	0.2	7.4	30	F, ST	7.8	SE	4.3
1969	1	H with R to GL followed by L then PO-H, BB-L	III, I,	0.0	2.6	29	X, F	7.8	SSE	4.7
	2	H in SW ARC	I	0.1	0.2	78	F, ST	8.9	NW	3.8
	3	H in PO, L moves over QEI and up BB	I	0.1	25.5	96	F, SF	8.6	NNE/N	8.0
	4	L NW of QEI in PO	II	0.7	28.1	83	F, SF	9.6	SW	6.0
	5	L moves to NW of QEI	II	0.1	18.5	56	F, SF	8.2	SW/SSW	5.7
	6	Ls track along N edge of QEI	II	2.4	33.0	53	F, ST	9.6	SSW	6.7
	7	Ls track around L in PO	II	5.3	74.5	59	F, ST	9.1	SSE	7.1
	8	H in PO with R to GL, Ts across QEI from PO	III	10.6	19.2	43	F, AC	9.3	SSE	6.0
	9	H GL to SIB rotates to H in PO	III, I	15.3	0.8	54	F, ST	6.9	NE	4.2
1970	1	R in PO, strong Ls track across S QEI to BB	I	0.0	1.7	86	F, ST	9.4	NW	5.4
	2	R in PO, strong Ls track across S QEI to BB	I	0.0	2.1	89	F, ST	9.9	N	6.1
	3	rapid motion around L in PO	IV	0.4	3.5	98	F, ST	9.8	WSW	6.6
	4	L in PO moves to BB, new L in PO	IV	1.7	9.1	69	F, X	8.9	SW	5.0
	5	H moves N into QEI pushed W into PO by BB-L	III, I	12.4	0.2	64	F, AC	7.8	N/WSW	5.5
	6	H over GL gives way to PO-H	III, I	14.8	4.7	63	F, ST	8.9	SE/WSW	3.1
	7	H from PO moves down Ellesmere Is L	III	8.3	0.7	78	F, CI	6.5	NNE	4.6
	8	Ellesmere H moves S, H in PO and L in BB	I	3.2	9.6	74	F, CS	8.2	N	5.3
	9	R builds into QEI with L in PO	III	0.3	8.8	64	F, ST	8.2	SSE	5.0

1, 2, 3, 4 see footnotes Table 3. 6a

July and early August. During this unusually warm period Main Ice and Isachsen temperatures often exceeded those at Eureka. Clear skies, light winds and insignificant amounts of precipitation were experienced, except during a short spell of Type II circulation late in the period. By mid-August Polar Ocean conditions took over once more.

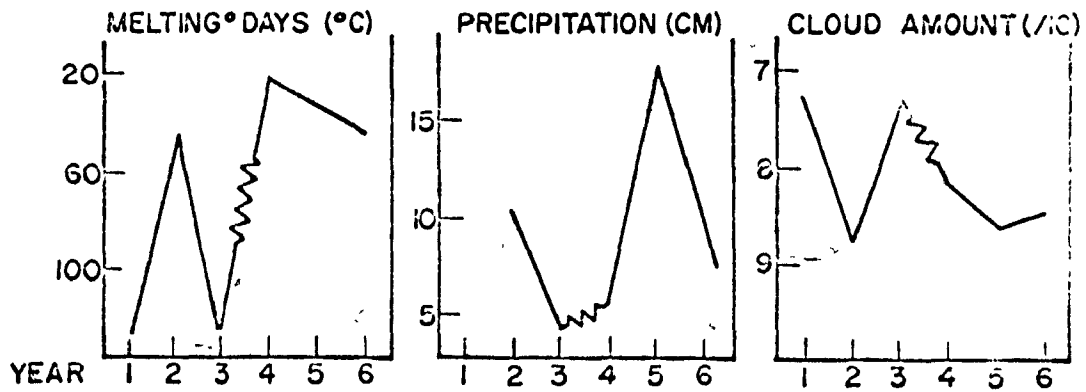
3: 6.4 1968

Polar Ocean conditions dominated in 1968. Type I was replaced briefly in June by Type III circulation, causing an amelioration of June temperatures. By July, above-freezing temperatures existed in the lower troposphere up to 850 mb, and a significant number of melting degree days resulted from a Type III occurrence around 8 July. In mid-July satellite photographs showed that, despite prevailing northerly surface winds, southerly flow at upper levels held the Polar Ocean fog off the north coast of the Islands. Significant precipitation amounts were recorded during three periods when the inversion was replaced in lower levels by lapse conditions. In late August Type II circulation brought strong cyclonic activity to the Meighen Island area.

3: 6.5 1969

June 1969 was dominated by Polar Ocean conditions and the accompanying subsidence inversions, but a brief intrusion of Type III occurred early in the month. The Type II circulation, which persisted during July and early August, resulted in anomalously large amounts of rain and snow and consistent below-freezing temperatures. Lapse conditions were maintained in the lower troposphere throughout the Type II circulation. Not until mid-August did mean temperatures rise above freezing.

SUMMER SEASON MEANS (JUNE JULY AUGUST)



FREQUENCY OF CIRCULATION TYPES

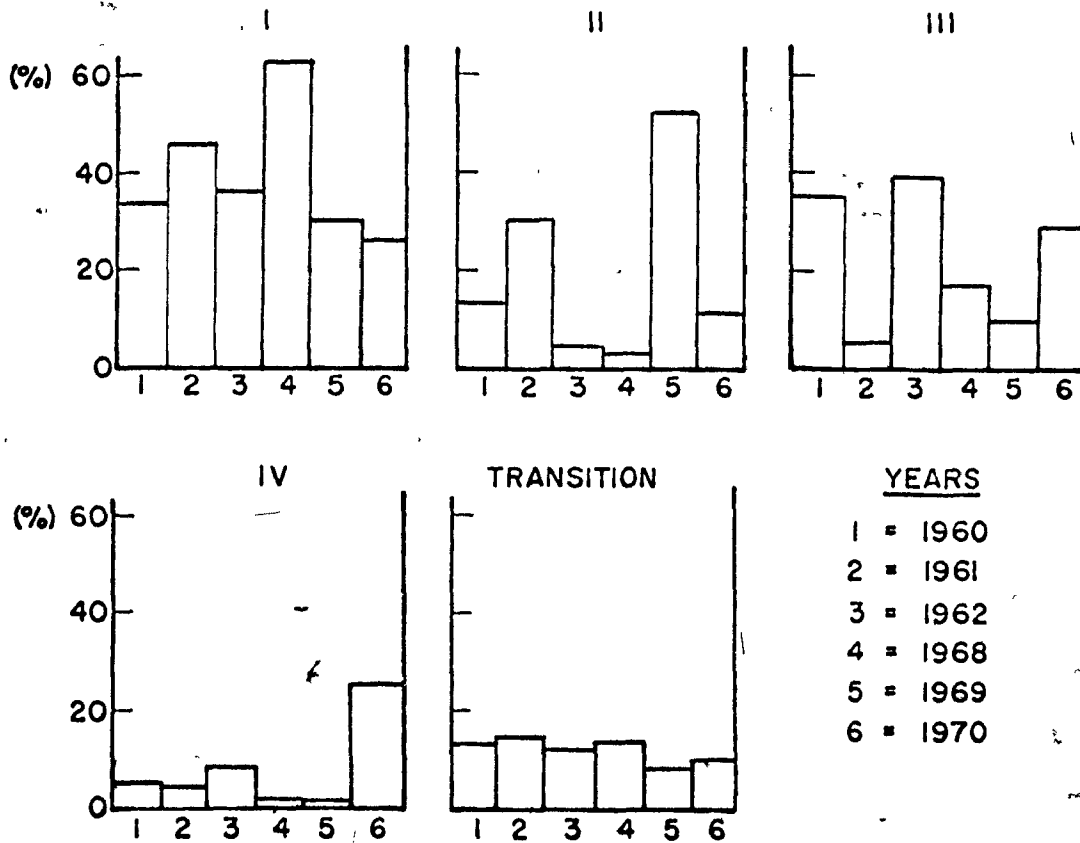


Figure 3:7

At this time a strong Type III situation produced high temperatures and clear skies at Main Ice and Isachsen. Eureka, on the other hand, experienced below-freezing temperatures and North Land was considerably colder than Main Ice or Isachsen. Temperatures dropped rapidly at the end of August as Polar Ocean flow was re-established.

3: 6.6 1970

The season began with Polar Ocean conditions throughout the troposphere, as shown in the temperature sounding. By the end of June the Type I circulation was constantly being replaced by the other two types producing the Type IV transition situation. Considerable warming took place in the lower troposphere. As July advanced, clear instances of Types III and I emerged, resulting in several definite warm and cold spells. The two main temperature maxima at Main Ice corresponded with maxima at Isachsen and Eureka but were not evident in the North Land curve. The upper flow structure, illustrated in Case b of Type III and discussed in detail by Petzold (1971) was responsible for these temperature relationships. Mid-August saw the re-establishment of flow from the Polar Ocean, but this was interrupted again in late August by a weak Type-III situation. Lapse conditions and temperatures near freezing in the lower troposphere appeared to prevail in periods experiencing the highest precipitation amounts of the season.

3: 7 Frequency of Circulation Types and Their Relationship to Climate

Figure 3:7 illustrates the relative importance of the circulation types during the six years studied. Polar Ocean conditions dominated in 1961 and 1968, cyclonic systems, in 1969 and Greenland ridge situa-

Table 3: 7b

Mean Ten Day Totals for Circulation Types*

Type	I	II	III	IV
Melting Degree Days ($^{\circ}\text{C}$)	1.1	3.2	20.1	1.1
Precipitation (mm)	3.8	32.2	6.5	6.3

* from ten day periods when only one type dominated

Table 3: 7a

Frequency of Circulation Types (%)

Type	I	II	III	IV
Island Years	38	9	37	7
Polar Ocean Years	42	24	15	18
Six Years	39	19	22	8

tions in 1960 and 1962. In 1970 Polar Ocean and Greenland ridge conditions alternated, at times so rapidly that Type IV resulted. The transition frequencies represent days when the situation was changing between types. This accounted for around 10% of days in all years. The dominance of Polar Ocean conditions in the cold years (1961 and 1968-70) and of advection from the Islands under the influence of Type III in the warm years (1960 and 1962) is evident from Table 3:7a.

Referring to the seasonal means and circulation frequencies in Figure 3:7 the characteristics of the circulation types are further illustrated. Frequencies of Type I, the Polar Ocean circulation, appear to explain the lack of melting degree days and thus suppression of ablation on the ice cap. Seasonal precipitation amounts correspond to the frequency of Type II, the frontal passage type. Type III frequencies reflect the mean cloud cover.

Ten-day precipitation amounts and melting degree day totals were averaged for the three types of circulation using ten-day periods when only one type dominated (see Table 3.7b). Type I averages 0.1 of a melting degree day and a trace of precipitation per day. Less than half a melting degree day results from Type II, but precipitation totals for a ten-day period average over 30 mm. This should be compared with the mean winter accumulation of 170 mm. Type III accounts for 20 melting degree days in a ten day period, which amounts to more than half the total seasonal melting degree days accumulated in a Polar Ocean year. On occasion, significant amounts of precipitation are produced by lows associated with a general Type III circulation.

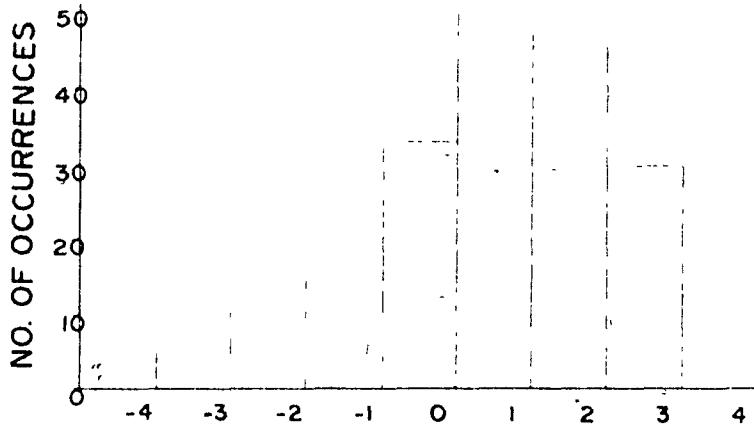


Figure 3: 8a
 Deviation of actual
 wind from geostrophic
 16 points (+ ve =
 counterclockwise)

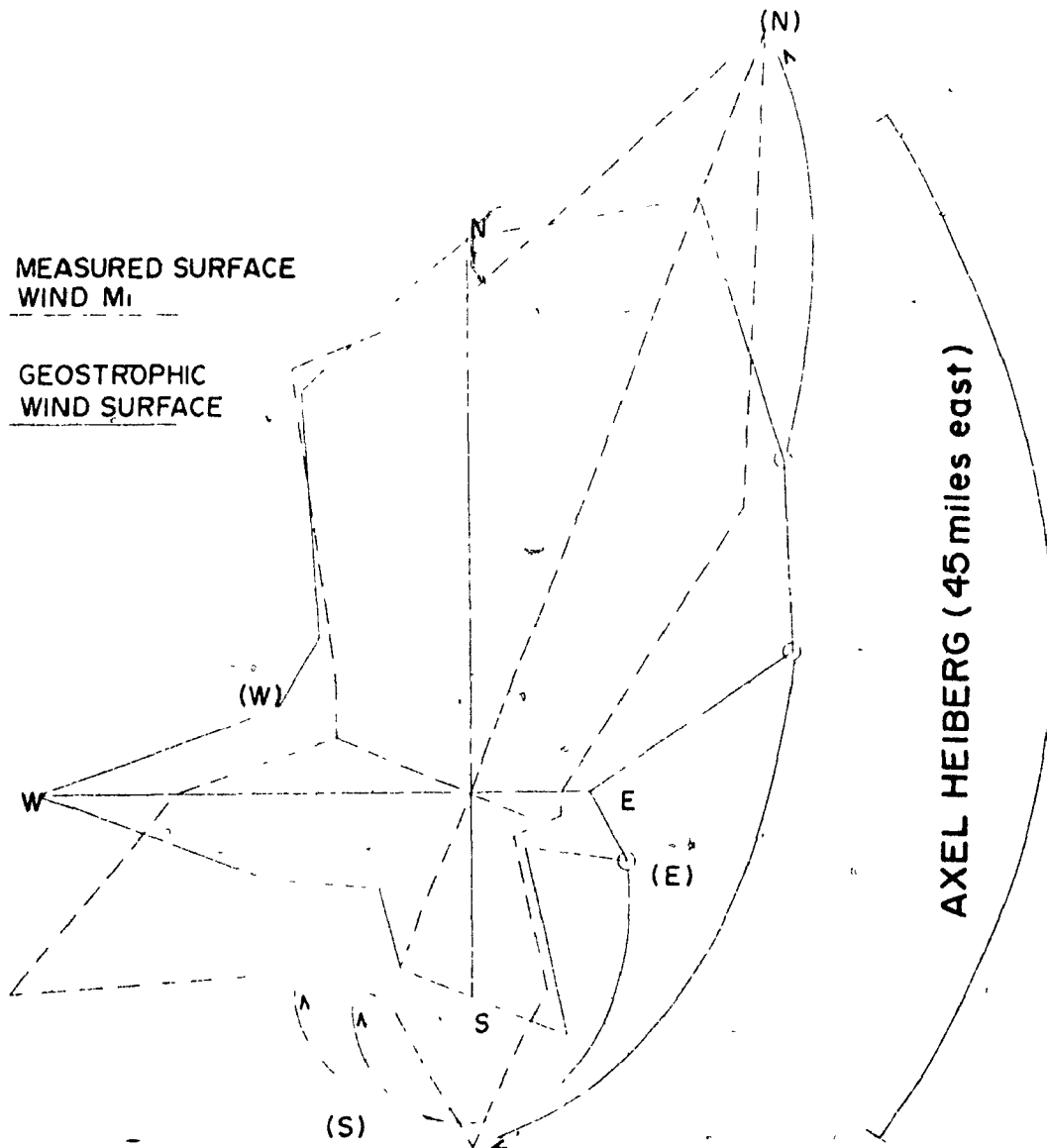


Figure 3: 8b

3: 8 Wind Direction and Synoptic Conditions

In order to interpret the Meighen Island surface wind roses in terms of synoptic conditions it is necessary first to examine the relationship between the direction of surface geostrophic flow and measured surface wind. The direction of the geostrophic flow was extracted from synoptic maps once a day for the six years. Figure 3:8a shows the frequency distribution of the deviation of the actual surface wind direction from the surface geostrophic flow. Surface winds tend to deviate 20 to 40 degrees towards low pressure, due to the effect of surface friction.

Roses of geostrophic and actual wind direction are combined in Figure 3:8b. The surface rose has been rotated clockwise one compass point (ca. 22°). The topography of the Islands, as it relates to Meighen Island is represented by the peripheral shading. The general fit of the two roses is good. Closer examination of the data showed that geostrophic flow from the eastern sector was deflected by Axel Heiberg Island as indicated by the arrows in the diagram. There is a 40 degree deviation between geostrophic and measured direction for flow from the western sector which it will be seen (I 1:2) is most frequently associated with the weak anticyclonic flow of Type III circulations.

With the exception of eastern sector flow, which is deflected around Axel Heiberg Island, the surface wind direction on Meighen Island is directly related to the synoptic pattern. At Isachsen and Eureka local topography has a greater effect on the wind direction.

Roses of surface geostrophic flow, surface wind direction and temperature for individual years at Main Ice are shown in Figures 3:8c and 3:8d.

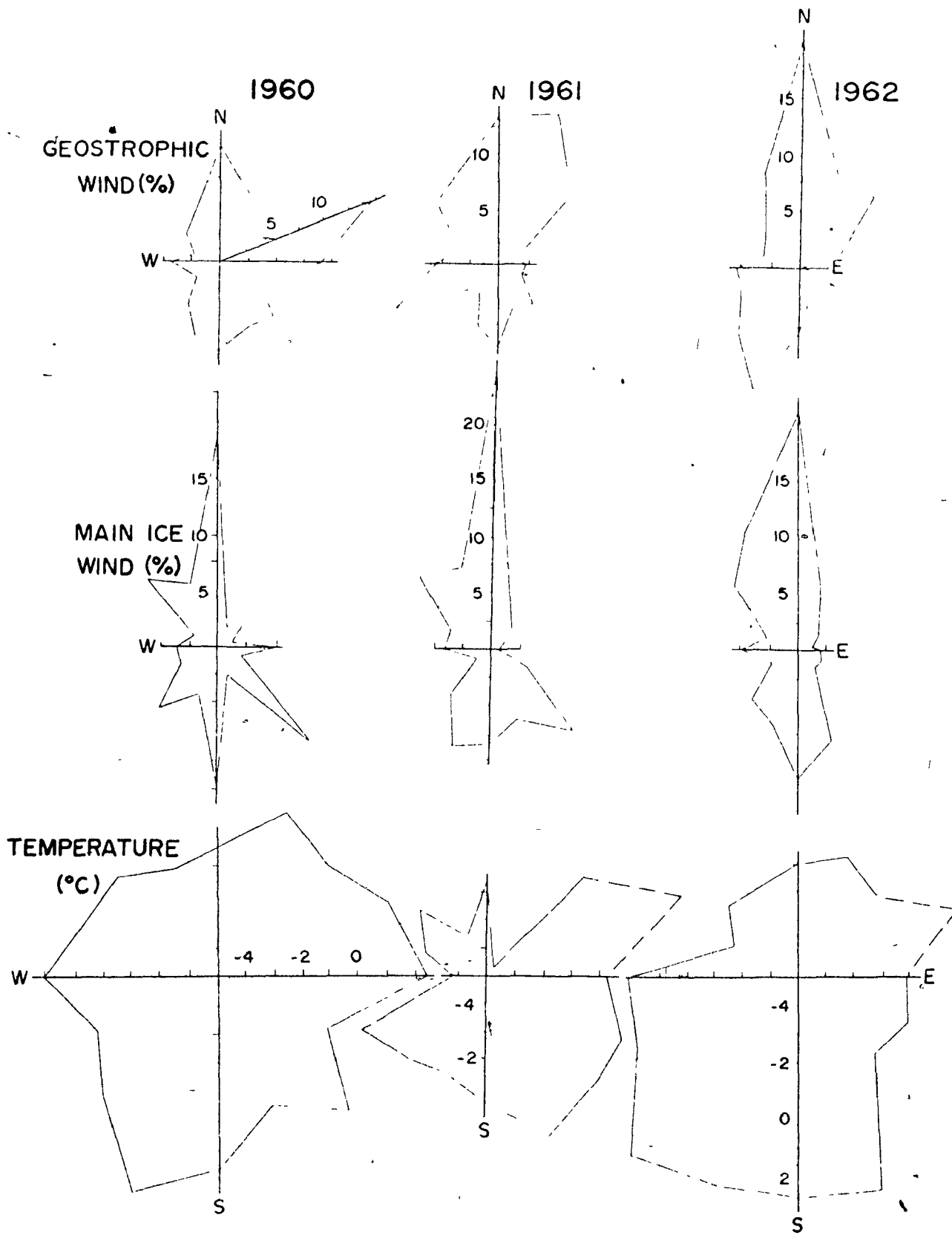


Figure 3: 8c

3: 8.1 1960

The outstanding feature of the 1960 geostrophic rose is the high frequency of ENE flow. This was associated with Type III circulation, which in that year was characterized by motion of ridges across the Islands from the Polar Ocean to Greenland and by a low tracking south of the Queen Elizabeth Islands from Baffin Bay. This flow was deflected by Axel Heiberg Island to produce a maximum of SE'lies and above freezing temperatures on Meighen Island. Type III circulation is also responsible for the S'lies. Temperatures during these S'lies and SSW'lies were well above freezing.

3: 8.2 1961

The geostrophic and surface roses in 1961 have a decided N'ly maximum as a result of frequent dominance of Type I circulation from the Polar Ocean. Temperatures with this Polar Ocean flow were below -1°C . Geostrophic S'lies prevail in advance of the Type II frontal systems (above 0°C temperatures) and shift to WSW'lies in the rear of the cold front (below -1°C temperatures).

3: 8.3 1962

The frequent, well developed Type III circulation of 1962, combined with several cases of Type I Polar Ocean flow, result in strong maxima of N'ly and S'ly flow. Mean temperatures well below 0°C accompany N sector winds, while $+3^{\circ}\text{C}$ averages result from S and SW sector winds.

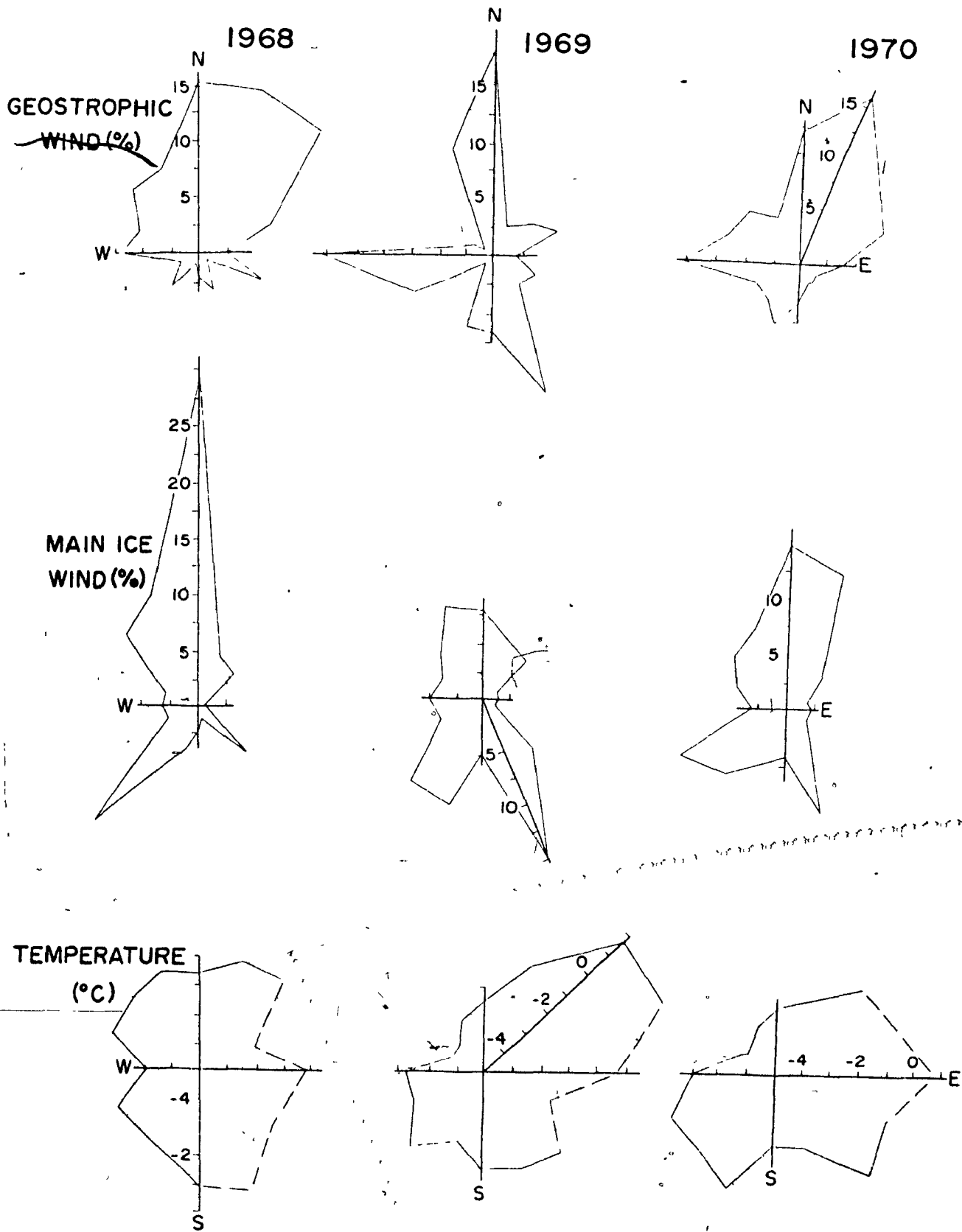


Figure 3: 8d

3: 8.4 1968

In 1968 complete dominance of the circulation by Type I produced the highest frequency of N'lies experienced in the six years. Only the S, SSE and NE winds accompanying brief periods of Type III flow of the a and b types resulted in temperatures near freezing. Cyclonic activity associated with the Type II circulation in late August accounts for some SW and most of the SE winds.

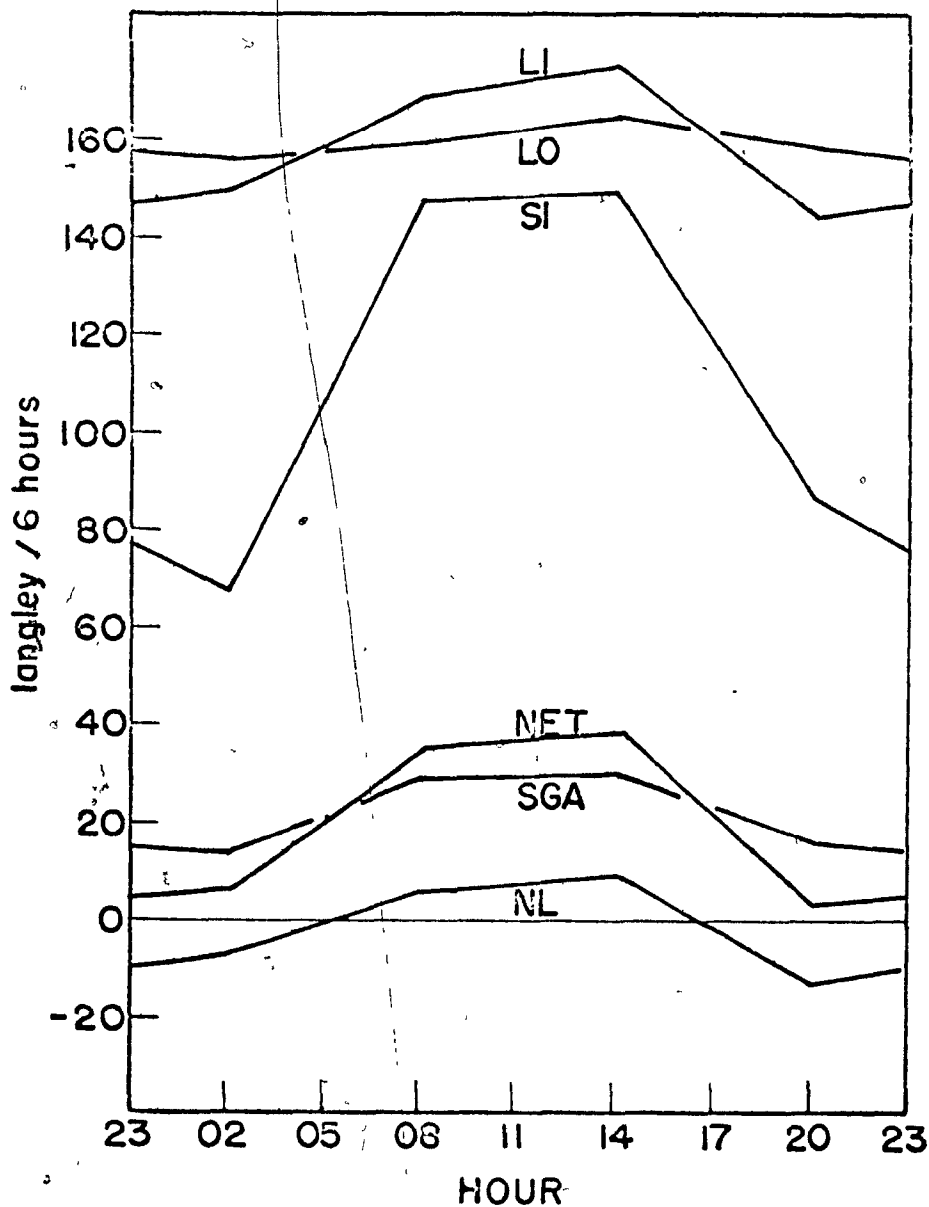
3: 8.5 1969

The predominance of Type II cyclonic flow was obvious from the wind roses for 1969. In fact, the rose for July (see Figure 2:4b) showed no appreciable N'lies. In August, $+2^{\circ}\text{C}$ temperatures resulted from a Type III Case b situation where NE'ly winds at the surface were accompanied by S'ly flow at upper levels.

3: 8.6 1970

The Polar Ocean northerlies again dominated in 1970. The transition Type IV circulation accounted for a portion of the SW'lies and some of the warm temperatures. As in 1969, NE'ly winds at the surface were associated with warm air advection in the lower troposphere. A Type III situation at the end of August, and the SSE winds associated with it did not result in significant warming as the season was well advanced by that time.

DIURNAL SUMMER SEASON MEANS OF
SURFACE RADIATION COMPONENTS (MAIN ICE)



SI - solar incoming radiation
 LI - long wave incoming radiation
 LO - long wave incoming radiation
 NL - net long wave radiation
 NET - net total radiation
 ALB - albedo
 SGA - solar absorbed radiation

Figure 4: 1

CHAPTER 4

MEASURED RADIATION COMPONENTS

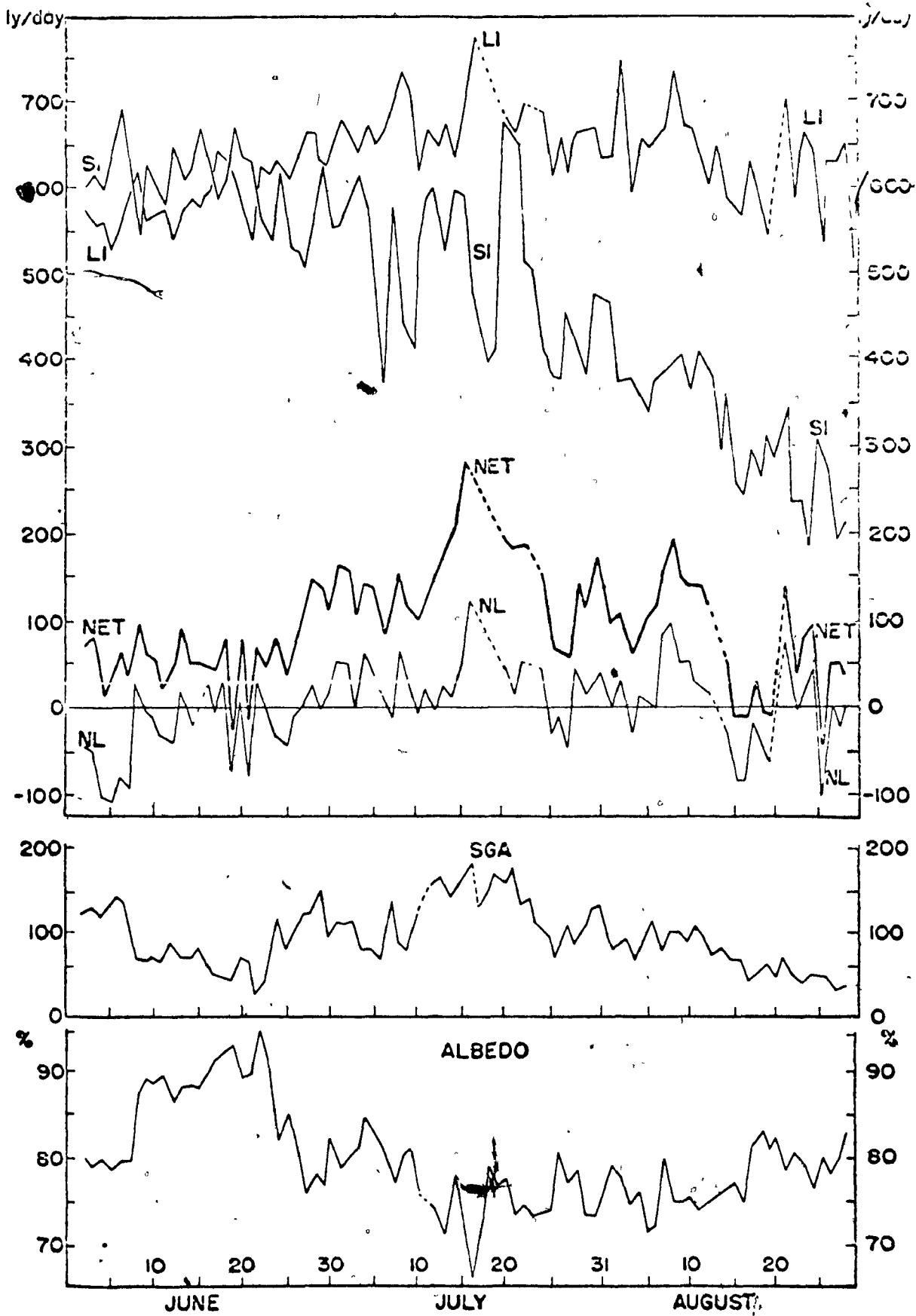
The radiation measurements used in this chapter are from Main Ice for the years 1969 and 1970. Daily totals of the incoming radiation components were obtained from the Belfort pyr heliograph and Davos pyr radiometer traces. Daily values of albedo and long wave outgoing radiation were calculated from spot measurements.

4:1 Diurnal Variations of the Radiation Components

Figure 4.1 shows the mean diurnal six-hour values of the measured radiation components for 1970. From the short wave incoming curve it can be seen that there is no radiation night at these latitudes in June, July or August. The solar radiation actually absorbed at the surface averages ca. 80 ly/day due to the very high albedo. The relationship of long wave incoming to long wave outgoing radiation illustrates a common feature of arctic ice-climates. The ice and snow surfaces, due to their maximum possible surface temperature of 0°C , are often colder than the overlying air. Any appreciable cloud cover in the warm air will result in higher values of long wave incoming than of long wave outgoing radiation at the surface. The warmer and more moist the air, the more positive will be the net long wave balance. The mean diurnal total net radiation on Meighen Island in 1970 was never negative, due to relatively high long wave incoming values.

4:2 Daily Totals of Radiation Components

Daily totals of the radiation components shown in Figure 4:2 also reflect these arctic radiation climate characteristics. Long wave incoming



SI - solar incoming radiation
 LI - long wave incoming radiation
 LO - long wave incoming radiation

NL - net long wave radiation
 NET - net total radiation
 ALB - albedo
 SGA - solar absorbed radiation

Figure 4: 2 Daily Totals of Radiation Components; 1970

radiation exhibits a gentle rise in mid-summer while insolation falls off rapidly after June. The importance of albedo is seen in the curve for solar radiation absorbed at the surface. The decrease of albedo with advancing season somewhat compensates for the rapid decline of the solar incoming radiation. Positive net long wave balances are found in all months, and reach a maximum in mid-summer. The net total radiation, it can be seen, is very sensitive to changes of net long wave radiation, the latter being considerably more variable than the absorbed solar radiation. In general, long wave incoming radiation appears to be the critical component of the radiation balance, in the absence of violent albedo changes.

4.3 The Influence of Weather on the Radiation Components

The spot radiation measurements from Main Ice for 1969 and 1970 were used in this section. Each spot measurement consisted of consecutive readings of each component, repeated two or more times in an attempt to simulate simultaneous readings. When sky conditions were changing rapidly, as in the case of ragged fog or low stratus accompanied by strong winds, it was very difficult to ensure that the readings were representative. For this reason, as well as to account for occasions when a malfunction of the sensor or recorder was suspected in the field, a dependability factor was attached to each spot radiation observation. While in section 4:3.1 all observations were included, in section 4:3.1-5 only those observations were used which had no obvious inaccuracies. The measurements of long wave outgoing radiation have not been discussed as they did not appear to be adequately accurate.

At the time of the radiation observations several additional parameters were recorded. These included:

the sky cover;

the type of cloud and/or fog over the sun,

whether the sun was not visible, dimly visible or brightly visible through the cloud and/or fog;

weather and obstructions vision (including rime) and

snow surface conditions.

In an attempt to understand the factors which govern the radiation climate of Meighen Ice Cap, the radiation components were related to various weather elements and to these additional parameters. The seasonal and diurnal variations were eliminated from the short wave incoming radiation by expressing the measured values as percent of the clear sky value. A clear sky value was calculated for each spot measurement from the Isachsen upper air sounding and Main Ice weather observations using the adapted version of the Vowinckel-Orvig programme EBBA discussed in Chapter 6. Incoming long wave radiation is also presented as percent of clear sky incoming long wave radiation. It should be noted that the clear sky values do not represent true clear sky conditions as they were calculated using the actual Isachsen upper air sounding and Main Ice screen temperature. This distinction is particularly important in the case of long wave radiation where temperature and moisture content are critical. In effect, the clear sky values represent the actual conditions with the cloud removed, and incoming components expressed as percent of clear sky values indicate the influence of cloud and fog on the components. Hereafter measured solar incoming (long wave incoming) radiation as percent of clear sky will be referred to simply as percent solar incoming (long wave incoming) and abbreviated to % SI (% LI) in diagrams and figures.

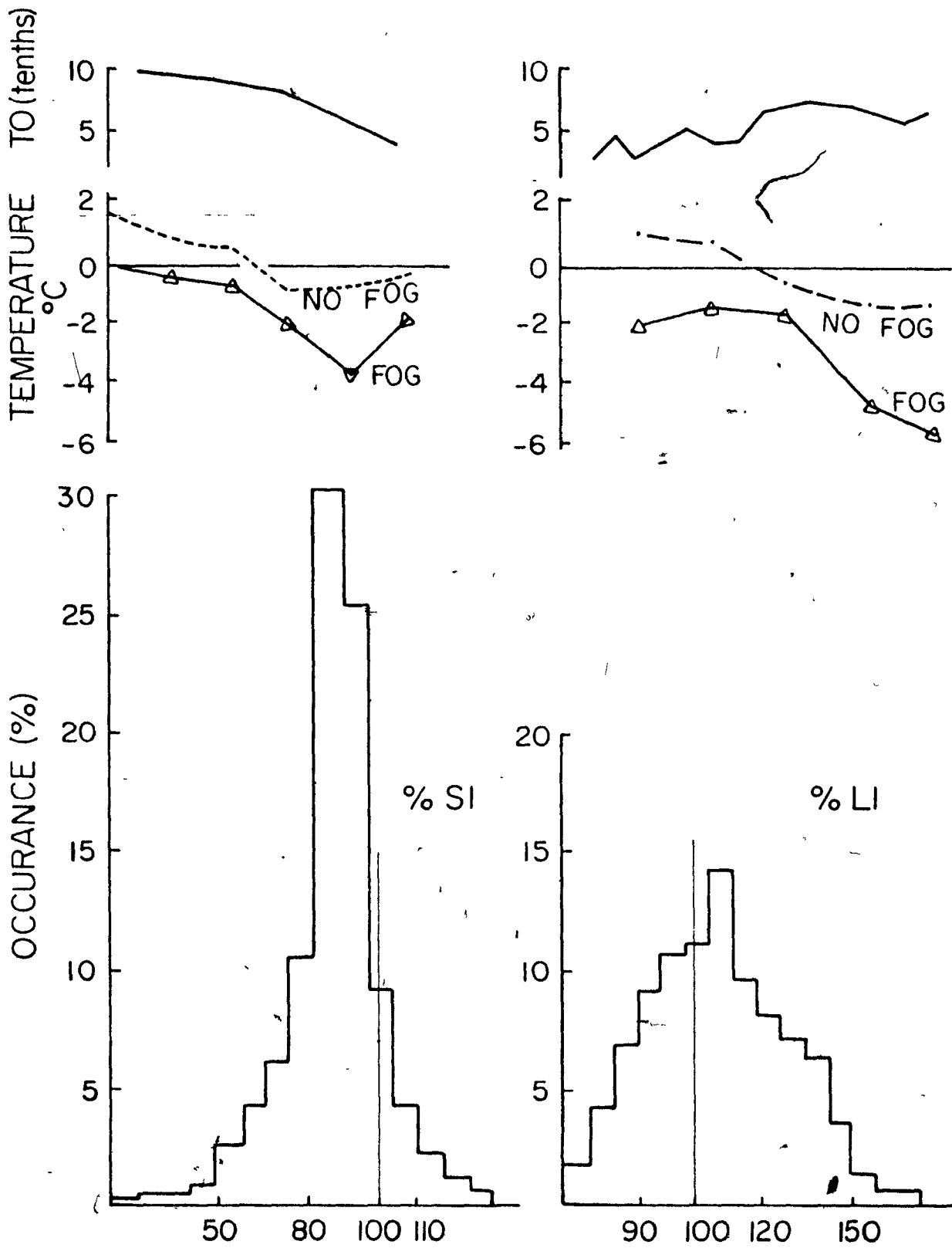


Figure 4: 3.1 Frequency Distribution of Percent Solar and Long Wave Incoming Radiation and Relation to Temperature and Cloud Opacity.

4:3.1 Percent Solar and Long Wave Incoming

Figure 4:3.1 shows the frequency distribution of solar and long wave incoming and their relation to temperature and total cloud opacity (for fog this refers to the portion of the fog through which one cannot see). Percent solar incoming has a flat distribution, peaking around 65 to 70 percent, while long wave incoming peaks more sharply around 125 percent.

Below 100 percent the percent solar incoming increases with decreasing temperature (the colder fog and cloud being more transparent to insolation) and, particularly above 70 percent, the percent solar incoming decreases with decreasing opacity. Low opacities and warm temperatures accompany solar incoming percents over 100. Multiple reflection between snow and cloud accounts for some of these greater than 100 percent values, but it is likely that the nonventilated Kipp and Zonen solarimeters would be subject to overheating on clear warm days. Long wave incoming percents under 100 also occur with low opacities and warm temperatures. Long wave radiation is obtained by subtraction of measured incoming short wave from measured all wave radiation, and the all wave instrument would not be subject to heating from trapped long wave radiation under the dome. The low long wave incoming percents are probably largely a result of heating of the solarimeters.

4:3.2 Radiation Components and Sky Cover

Tables 4:3.2 a and b show the mean values of incoming radiation components along with temperature and albedo for sky cover conditions at the time of the radiation measurements. Only conditions with either fog alone or cloud alone have been used here, and classes were com-

Table 4: 3. 2a

Short Wave Radiation and Sky Cover

No. of Observations	RZI (%)	ALD (%)	T (°C)
24	32 ⊕ _M	X 80	-X _{6,9} -2.9
49	53 ⊖ _L	-X _{6,9} 79	-X _{1,5} -1.7
328	X 57	77 ⊕ _{LM}	X -1.5
43	70 ⊕ _{L, M}	77 ⊖ _L	-1.3 ⊖ _L
24	-X _{6,9} 78	76 1, 2 MH	- .4 ⊕ _{LM}
11	81 ⊕ _H	75 clear	1.1 clear
13	-X _{1,5} 90	-X _{1,5} 72	1.4 3, 5 LM
3	102 clear	71 ⊖ _H	1.4 ⊖ _M
26	107 3, 5 LMH	71 ⊕ _M	b.8 ⊕ _H
16	126 1, 2 MH	69 3, 5 LMH	2.2 1, 2 MH

Legend

X	obscured 10 tenths
-X	partially obscured 6-9 tenths 1-5 tenth
⊕	overcast 10 tenths
⊖	broken 6-9 tenths
3, 5	3-5 tenths
1, 2	1-2 tenths
L	low
M	middle
H	high

bined where there was no significant physical difference between the classes and the means were similar. Totally obscuring fog accounted for more than half the cases and did not break down on the basis of vertical visibility into the fog.

The first portion of Table 4:3.2a shows the mean solar incoming percents for sky conditions. With the exception of the extremely low percentage for overcast middle cloud, which is a result of nimbostratus and rain, the values for cloud are comparable to those obtained by other investigators (see for instance Vowinckel and Orvig, 1962; and Haurwitz, 1945). Percent solar incoming radiation decreases with increasing cloud amount and decreasing cloud height (again with the exception of overcast middle cloud). With fog the measured solar radiation varies from 60 to 90 percent of clear sky values. This represents a range of approximately 80 ly/day in absorbed solar radiation in July. The percentages for fog are higher than those for low cloud for opacities greater than 6/10, i. e., the fog depletes less than the cloud. For opacities less than 6/10, the relationship is reversed. To understand this it must be remembered that the fog actually covers the whole sky though much of it does not obscure the sky while cloud (with the exception of thin cirrostratus) usually covers only slightly more of the sky than the opacity indicates. The solar radiation reaching the surface through fog is mainly diffuse, while a considerable portion of that with low cloud opacities will be direct radiation. This accounts for the reversal of the cloud-fog relationship in two ways. The multiple refraction between the snow surface and cloud base would be more effective with direct radiation. Probably more significant is the fact that heating of the nonventilated solarimeter dome would be more serious with direct than diffuse radiation.

Table 4: 3. 2b

Long Wave Radiation and Sky Cover

	RLI (%)		ZLI (%)		T (°C)
	129	⊕ _L	.470	⊕ _M	-X _{6,9} -2.9
X	129		.457	⊕ _L	-X _{1,5} -1.7
-X _{6,9}	129		X .453		X -1.5
	129	⊕ _L	.451	⊕ _L	-1.3 ⊕ _L
	124	clear	.445	clear	- .7 ⊕ _L
	124	⊕ _M	-X _{6,9} .444		.4 ⊕ _{MH}
	121	⊕ _{MH}	.433	⊕ _{MH}	1.1 clear
	115	3,5 LMH	.410	3,5 LMH	1.4 3,5 LMH
-X _{1,5}	114		-X _{1,5} .392		1.4 ⊕ _M
	107	1,2 MH	.388	1,2 MH	2.2 1,2 MH

Legend

X	obscured 10 tenths
-X	partially obscured 6-9 tenths 1-5 tenth
⊕	overcast 10 tenths
⊙	broken 6-9 tenths
3,5	3-5 tenths
1,2	1-2 tenths
L	low
M	middle
H	high

Table 4:3.2b shows the mean long wave incoming as percent of clear sky for various sky conditions. Fog and low cloud with opacities greater than 6/10 result in a 30 percent increase in longwave radiation over that from the same upper air sounding and no cloud. There appears to be no variation due to opacity in this range. The clear sky value should be disregarded as it is obviously in error (only 3 observations) though the values for low opacities seem quite reasonable. The higher the cloud the less is its effect on long wave incoming radiation. Whereas low and middle cloud could be combined in the case of solar radiation, there is a significant difference between low and middle cloud for long wave incoming, but middle and high cloud were similar in the long wave case. The measured mean values of incoming long wave radiation (ly/min) are shown in the third portion of Table 4:3.2b, to provide additional information on the relationship of long wave incoming radiation to sky condition. The thick warm nimbostratus shows the highest measured incoming long wave radiation. There is a .01 ly/min (14 ly/day) difference between totally obscuring fog and 6-9/10 fog not seen in the percent values.

The means of short wave surface albedo show that although fog transmits more solar radiation, it also results in high surface albedo and thus a decrease of solar radiation absorbed at the surface. The means of temperature (Tables 4:3.2 a and b) with sky condition indicate that fog occurs at colder temperatures than cloud, and explains further some of the variations in incoming short and long wave radiation.

In order to make a rough estimate of the net radiation absorbed at the surface for various sky conditions, the long wave outgoing radiation has been estimated by using σT^4 of the screen temperature reduced to

Table 4: 3. 2c

Estimated Net Radiation and Sky Cover

	NET (ly/day)	
	70	⊕ _M
-X _{1,5}	75	
	75	1, 2 MH
X	85	
	90	⊕ _L
	112	⊕
-X _{6,9}	115	

For Legend see Table 4: 3. 2b.

0°C for positive temperatures, and a clear sky short wave radiation of 600 ly/day, representative of late July values, has been assumed.

Table 4:3.2c shows estimates of solar radiation absorbed at the surface, net long wave radiation and net radiation obtained in this manner. Though the values must be treated with caution they show several interesting things. (Clear sky values are not included due to the small and unreliable sample.) The overcast middle cloud results in the lowest net incoming value due to the excessive depletion of short wave radiation. Totally obscuring fog and overcast low cloud exhibit similar net values as the higher albedo experienced in fog (due to riming of the surface, see 4:4) overrides the effect of lower depletion of insolation in fog. Considerably higher values of net incoming radiation are obtained for fog and cloud with opacities of 6-9/10 cover over those

Table 4: 3. 3

Radiation Components and Sky Condition over the Sun

No. of Observations	RZI %		ALD %		T °C		RLI %		ZLI %						
13	46	As	F	92	Ci	F	-3.2	As	BS	132	.460	As			
44	52	St	F	91	As	BS	-2.7		F	131	As	.455	Sc		
45	55	Ac	BS	88		F	-2.4			130	Sc	F	.452		
7	BS	57		F	83	Sc	F	-1.9	Sc		129	St	BS	.451	
320	F	57		F	81	Ac	F	-1.7	St	F	128	St		.450	St
8	FV	59	St	F	80		F	-1.5		F	128		F	.448	Sc
24	F	60	Ac	F	79	St		-1.3	Sc	F	127	Sc	F	.448	Ac
14	F	63	Sc		77	St		-1.2	St	F	125	Ci	F	.448	Ci
3	F	68	As		77	Sc	F	-1.2	Ci	F	125	Ac		.447	Ac
33		72	Sc		74	none	F	-.8	Ac	F	125		F	.446	St
63	F	82		F	73			.2	Ac		123	Ac	F	.443	As
4	F	86	Ci		73	As		.4	none		123	As	F	.434	
28		93	Ci		73	Ac		.4	As		118	Ci		.428	Ci
59		110	none		70	Ci		1.7	Ci		112	none		.398	none

TABLE 4: 3. 4

Short wave incoming and Sun's Visibility

Sun	RLI	T
not visible	56	-1.2
dimly visible	74	-1.7
brightly visible	100	.7
clear	111	.3

with 10/10 cover, due largely to the decreased solar radiation depletion. When the fog opacity drops below 5/10, the increase in insolation cannot compensate for the decrease in long wave incoming, resulting in a net balance even smaller than for totally obscuring fog. Three to five-tenths cloud gives the largest value of net incoming radiation due to the combined effects of low depletion of solar incoming, multiple reflection (and/or instrument heating), low albedo and warm temperatures, with a significant amount of cloud reradiating at these temperatures. When the cloud amount drops to 2/10 or less, the drop in long wave incoming radiation overcomes the high insolation values.

It appears from these estimated values that the largest net incoming radiation balances accompany broken or thin broken cloud and fog (ca. 3-9/10 opacity).

4:3.3 Radiation Components and Sky Conditions over Sun

Table 4:3.3 shows the mean values of the incoming radiation components, temperature and albedo associated with the type of fog and cloud over the sun at the time of the radiation measurements. The thick middle clouds show up mainly as alto stratus (nimbostratus). The most striking feature of the insolation table is that stratocumulus depletes considerably less than stratus. This does not appear to be a temperature effect but rather a function of the cloud amounts associated with these types.

4:3.4 Solar Incoming Radiation and Sun's Visibility

The sun's visibility through the cloud or fog (Table 4:3.4) gives additional information for solar incoming radiation. Essentially it

Table 4: 3.5

Radiation Components and Weather

No. of Observations	RZI			Albedo			RLI			ZLI			T		
		(%)		(%)			(%)			(ly/mm)			(°C)		
13		31	L	F	90	BS	F, BS	135		F	.478	L	F	-3.9	BS
43	F	43	L	F	82	S		132	S		.476	L		-3.9	S
6	F	51	Z, S		81	Z	F	130	S	F	.454	Z, S	F	-3.5	S, Y
8	BS	53	S	F	80	Z, S	F	130	L	F	.450	BS	F	-2.9	Y
17		55	S	F	79	L	BS	131	S	F	.450	S	BS	-2.6	S
45	F	56	Z	F	78		F	129	Z, S	BS	.447	S	F	-2.0	S
101	F	62	S		78	S		127	Z	F	.447			-1.7	Z
11	F	63	BS	F	77	Y	F	126			.443	Z	F	-1.2	
160	F	67		Fbnk	76		F	126	Y		.435	S	F	-.9	Z, S
80	F	68	Y	F	75	Y, S	F	125	S, Y	F	.435	Y	Fbnk	-.1	
16	F	72	S, Y		74	L		125	L		.434	none	F	.6	L, S
118		77	none		73	none		120	none	Fbnk	.425			.8	none
42	Fbnk	97		BS, S	67		Fbnk	119		F	.421	S, Y		1.4	L

F = fog, BS = blowing snow, S = snow, Y = rime,
Z = freezing precipitation, L = liquid precipitation

estimates the density or thickness of the fog through which the solar radiation passes before reaching the surface. Although the visibility of the sun is not given in the synoptic code, the condition of "sun dimly visible" is given in the aviation weather reports. Combining this with records of hours of bright sunshine, kept at most stations, could provide information similar to sun's visibility for regular stations.

4:3.5 Radiation Components and Precipitation Type

Table 4:3.5 shows means of various radiation parameters with the type of precipitation (including rime) accompanying fog and fogless conditions. As would be expected, fog with rime (indicating low temperatures) depletes least, followed by fog alone. Precipitation accompanying fog has higher mean values of solar incoming radiation and of long wave incoming radiation than that with fogless conditions. In general, only light precipitation was experienced with fog and this was likely often falling from the "fog" itself and not from a layer above, the fog in this case being low Polar Ocean stratus or stratocumulus which had run into the ice cap (see I 1:3). As would be expected, short wave depletion and long wave back radiation both increase from snow through freezing precipitation to liquid precipitation.

4:4 Radiation Component Wind Roses

In order to examine the variation of radiation components in the large group of completely obscuring fog, radiation wind roses have been constructed for observations with 10/10 fog (Figure 4:4). It can be seen that both incoming short and long wave radiation are largely temperature dependant and the long and short wave radiation complement

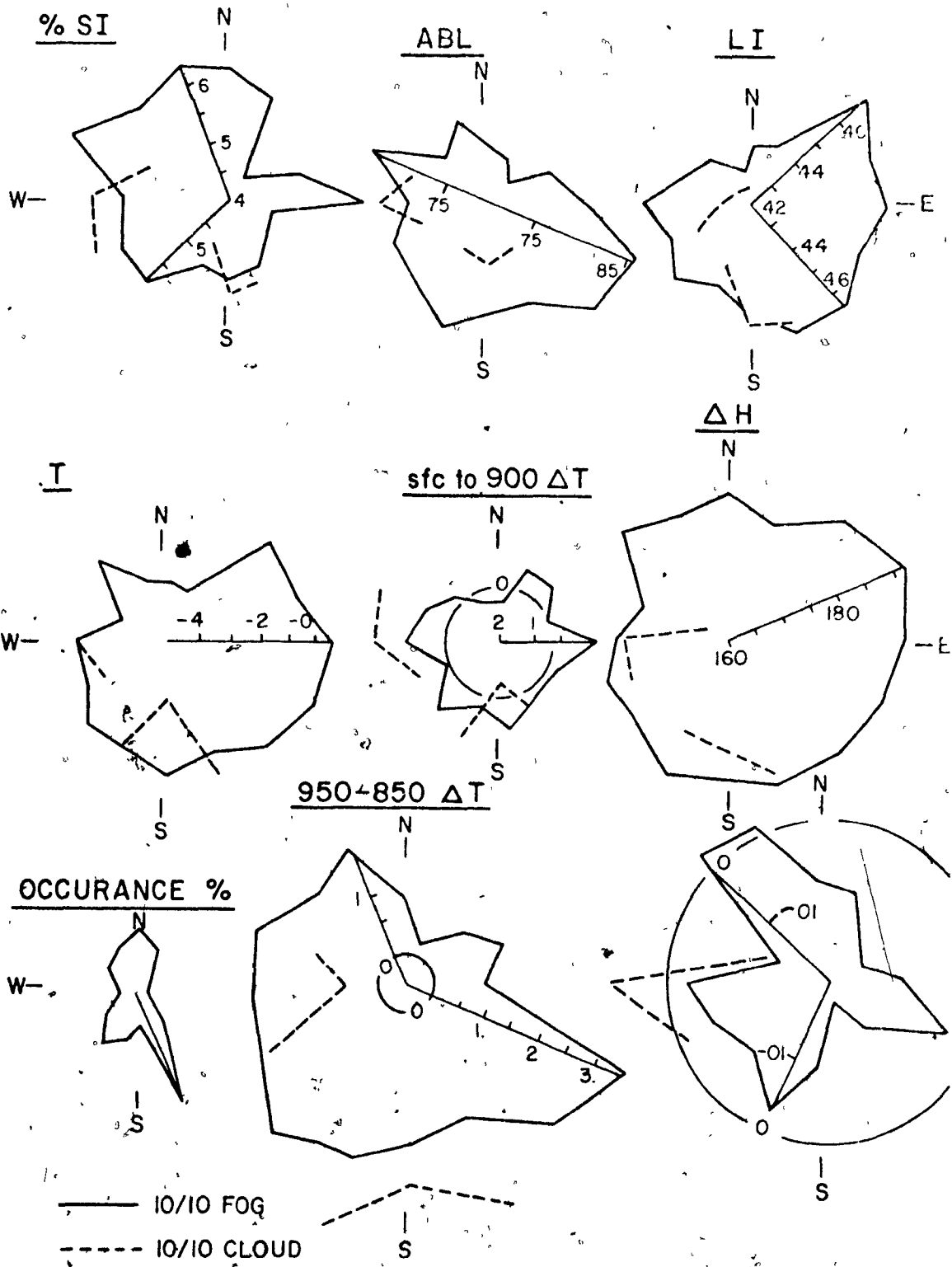


Figure 4: 4 Radiation Component Wind Roses

each other in most cases. N and NW'ly fogs tend to be transparent to insolation but reradiation is low. Fogs with NE'lies (and to some extent SE'lies) reradiate strongly due to warm temperatures but also deplete solar radiation strongly. Solar radiation albedo is low with winds from the NE sector suggesting these conditions occur late in the season. The decrease in insolation with season tends largely to compensate for this decrease in albedo.

The means of the radiation components and climatic elements for 10/10 low cloud have been included in the roses where there were a significant number of observations. In general the low cloud values resemble those of fog. Means of these components for 10/10 middle cloud on the other hand were considerably different (in most cases being off-scale in the roses as presented and thus not plotted).

Comparing the roses for the surface to 950 mb and 950 to 850 mb temperature difference shows that inversions are most common with N sector winds in fog and that with NW'lies the inversion tends to be lower than with NE'lies.

The final diagram in Figure 4:4 was obtained by subtracting measured long wave incoming radiation from σT^4 of the screen temperature and indicates the difference between screen temperature and the effective radiating temperature of the fog. Reference to Figure 5:2 .2d of the temperature slope in the lowest meters of the atmosphere shows that slight lapse conditions accompany NE'lies in fog while strong inversions are experienced in the lowest meters with NE'ly winds. As a result there is little difference between screen temperature and fog radiative temperature with NW'lies but screen temperatures are 1 to 2 deg C lower than the effective radiative temperature of the fog with NE'lies.

TABLE 4: 5a

<u>SURFACE TYPE</u>	<u>ALBEDO (%)</u>	<u>SKY CONDITION</u>	<u>ALBEDO (%)</u>
Wet new snow	83	Totally obscured fog	79
New snow	82	Partially obscured 6- 9/10 fog	77
Wet powder	82	Partially obscured 1 5/10 fog	74
Iced powder	80	Cloud 6-10/10	74
Rimed	79	Cloud 0- 5/10	73
Packed powder	79		
Drifting powder	78		
Frozen granular	74		
Wet granular	73		

SUN'S VISIBILITY

Not visible	80
Dimly visible	77
Variable	73
Brightly visible, Clear	72

SKY OVER SUN

Fog	80
Fog and cloud	79
Low cloud	79
Middle cloud	75
High cloud or clear	71

TABLE 4: 5b

	<u>No. of Observations</u>	<u>Mean (per cent)</u>
Wet mud	21	8.7
Dry mud	36	11.9
Dirty Glacier Ice	15	17.8
Superimposed Glacier Ice	28	33.1
Shallow Water Puddles	13	33.8
Deep Water Puddles	9	36.7
Blue Granular Snow	15	50.4
White Granular Snow	53	58.6
Granular Snow (Crust)	20	66.8
Rimed Surface	15	67.7
New Snow	30	78.2
<u>Total number observations</u>	<u>255</u>	

(After Goodall, 1971)

The underestimate of radiation temperature in the case of SSE'lies is not easily explained and probably results from a combination of inversion and lapse conditions in the lower atmosphere.

The radiation characteristics of fog accompanying NE'lies (and in some cases SSE'lies) tend to be most similar to those expected from usual radiation as advection fogs.

4:5 Surface Albedo

Tables 4:5a and 4:5b show the mean albedo for various surface types on Meighen Ice Cap from 1969 and 1970 and from Goodall (1971) in 1971. The Goodall values are consistently lower than the 1969-70 means as the 1971 melt season was earlier and considerably warmer than either the 1969 or 1970 season, and the observations began in late June in 1971.

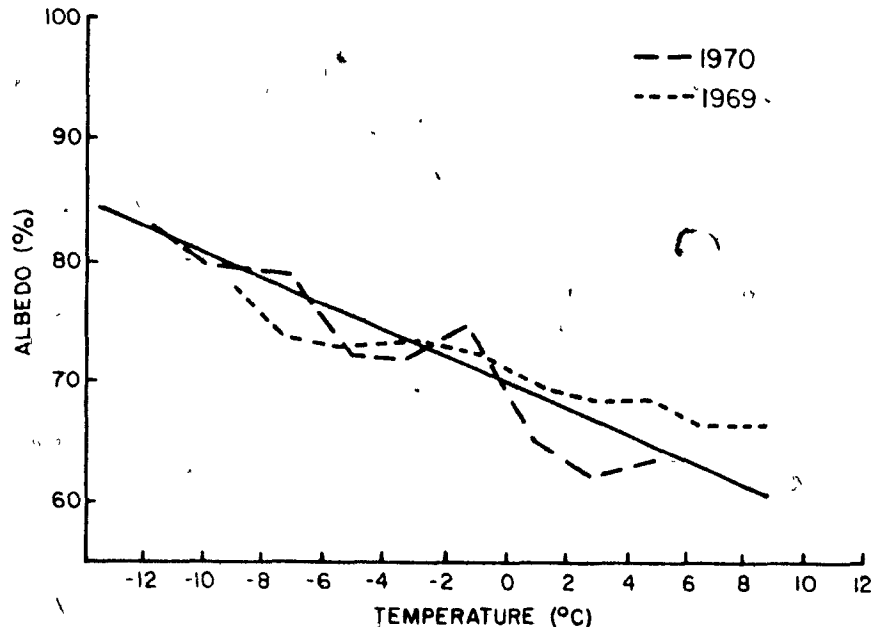


Figure 4: 5a Mean Albedo in Temperature Intervals

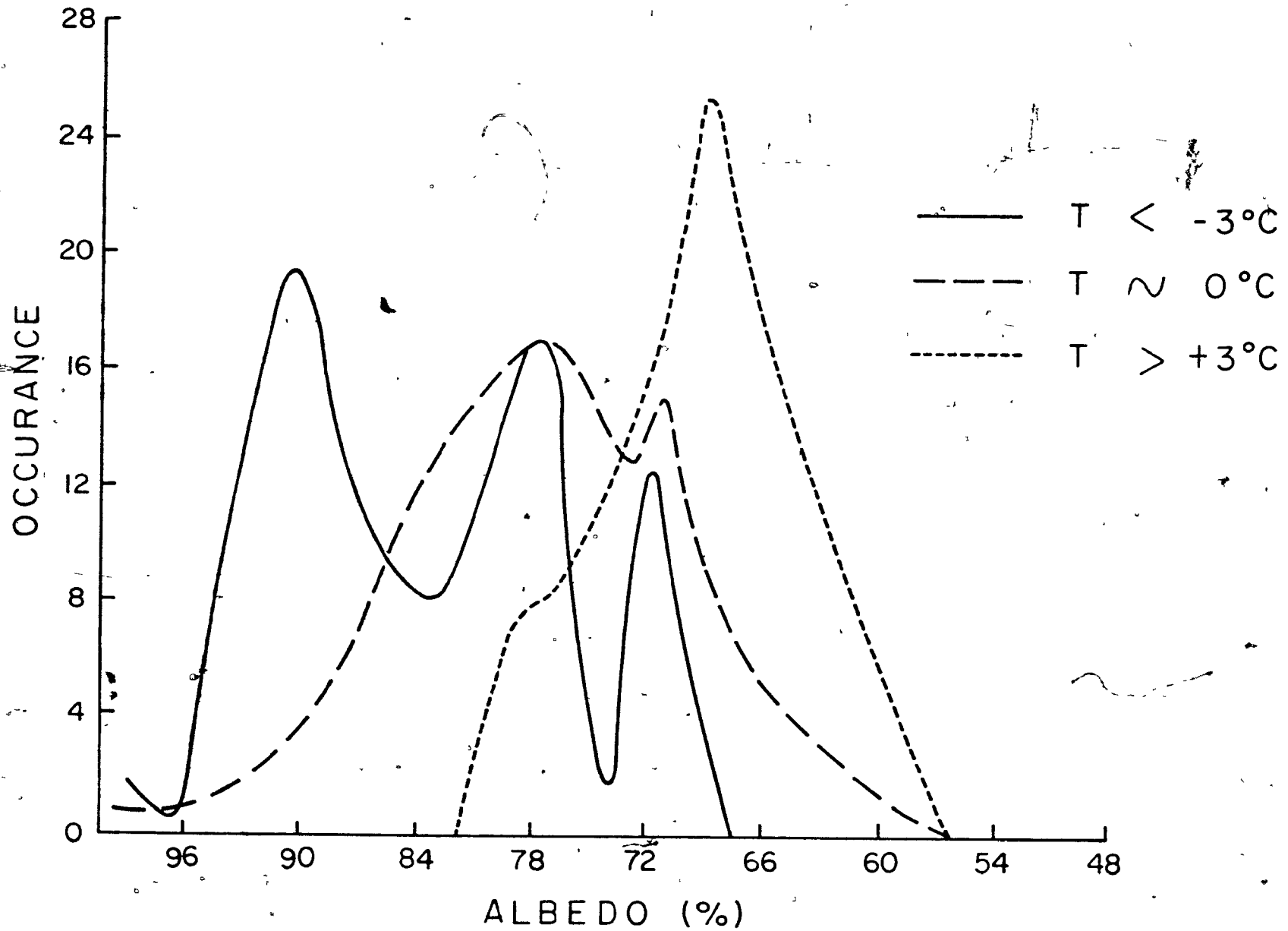


Figure 4: 5b Frequency Distribution of Albedo within Temperature Intervals

The variation of albedo with sky condition and weather has been shown in previous sections of this chapter and is summarized in Table 4:5a. The albedo is highest in totally obscuring fog, when the sun is not visible, and lowest on clear days. These differences result from variations in the amount of direct and diffuse radiation as well as from differences in surface type and temperature.

There is a general decrease in albedo with increasing temperature (see Figure 4:5a). Figure 4:5b of frequency distribution of albedo within temperature intervals shows that there is considerable variation within a temperature interval due to varying surface types. At all temperatures there is a peak between 69% and 75% albedo, related to granular snow, and another around 78% resulting from rimed surfaces and new snow. In the case of temperatures below -2°C there is a third peak, probably due to cold new snow.

Solar angle also effects the surface albedo of direct radiation, particularly when the surface is wet (albedo increasing with decreasing solar elevation as over a water surface).

Based on the observed variations of albedo with various parameters, a method was obtained to extend the albedo measurements to regular three-hourly observations. The method involved modifying the mean albedo for the reported surface type by temperature, cloud amount, fog amount and solar elevation. Albedo values obtained in this manner were generally within 5% of the measured values. The daily means of "observed" albedo used in Chapter 6, are a combination of these calculated albedos and the actual measured values.

CHAPTER 5

SENSIBLE AND LATENT HEAT FLUXES

5:1 Temperature, Humidity and Wind Speed Profiles - Theory

In order to evaluate the sensible and latent heat components of the surface energy balance, an expression must be found for the variation of wind, temperature and humidity with height in the lowest meter of the atmosphere. The transfer coefficients for momentum, heat and water vapour are often assumed to be equal. In this case only the wind profile is necessary to obtain the coefficients for the sensible and latent heat equations. The form of the wind profile depends largely on the stability conditions prevailing in the lowest meters of the atmosphere and on the nature of the surface.

Original studies of sensible and latent heat transfer over glaciers (e.g. Sverdrup, 1936, Wallen, 1948, Orvig, 1954) made use of the power law which has the form

$$u = u_1 \left(\frac{z}{z_1} \right)^{1/n} \quad 5:1.1$$

where u, z , and u_1, z_1 are corresponding wind speeds and heights and $1/n$ is the power index. The power index is dependent on the surface roughness and stability and is subject to large variations; nor is it easily explained in terms of a physical process.

Experiments with fluids in pipes suggest the variation of wind speed as the logarithm of height. This logarithmic law has been used with success by many investigators in neutral and near neutral conditions. It has the form

$$u = \frac{u_*}{k} \ln \frac{z}{z_0} \quad 5:1.2$$

where z_0 is the roughness length or height at which the wind speed goes to zero, k is von Karman's constant and u_* is the friction velocity. The logarithmic law is unsatisfactory for non-neutral stabilities.

Numerous attempts have been made to obtain a universal law which would define the variation of wind with height over the range of stabilities normally experienced in the atmosphere. Deacon (1949), for instance, modified the power law by introducing a stability parameter β (1 for neutral conditions, >1 for unstable conditions and <1 for stable conditions) and represented the velocity profile as

$$u = \frac{u_*}{k(1-\beta)} \left(\frac{z}{z_0} \right)^{-\beta} - 1 \quad 5:1.3$$

This has the added advantage over the simple power law of including the roughness length z_0 . The myriad of subsequent formulations, such as those of Monin and Obukhov (1954), McVehil (1964), and Panofsky (1963), are reviewed in Sellers (1965), Grantger and Lister (1965) and Doronin (1969).

In studies of the turbulent transfer, stability is usually discussed in terms of the non-dimensional Richardson number, Ri . Sellers (1965, p. 153) describes Ri as representing "the ratio of the rate at which mechanical energy for the turbulent motion is being dissipated (or produced) by buoyancy forces (free or natural convection) to the rate at which mechanical energy is being produced by inertial forces (forced or mechanical convection)". $Ri < 0$ for unstable conditions and $Ri > 0$ for stable conditions.

For the present study it is desirable to adopt the simplest possible formulation for the variation of wind, temperature and vapour pressure with height. The logarithmic law is preferable to the simple profile

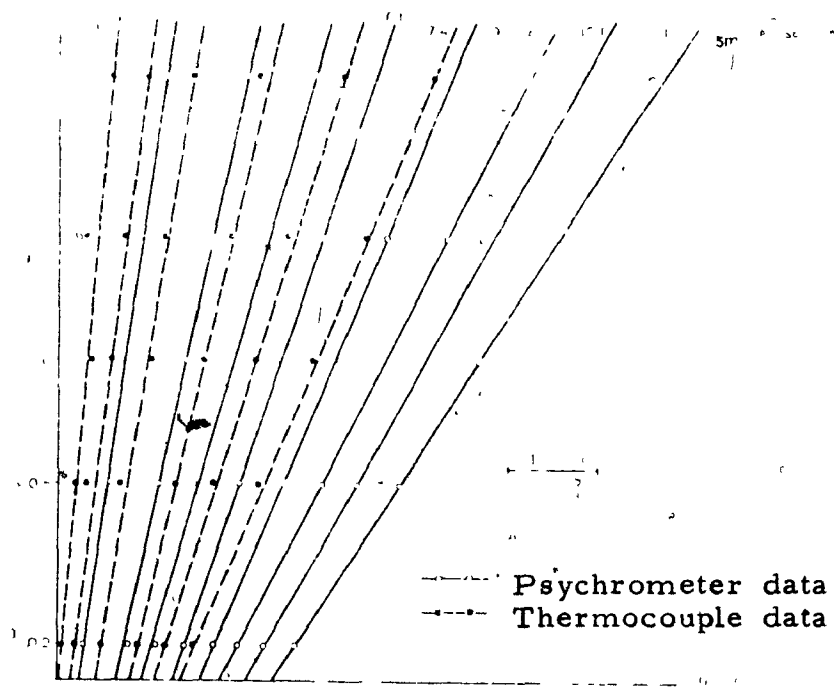


Figure 5: 1a
 Profile of Wind:
 over a snow covered
 ice surface
 (after Doronin, 1969)

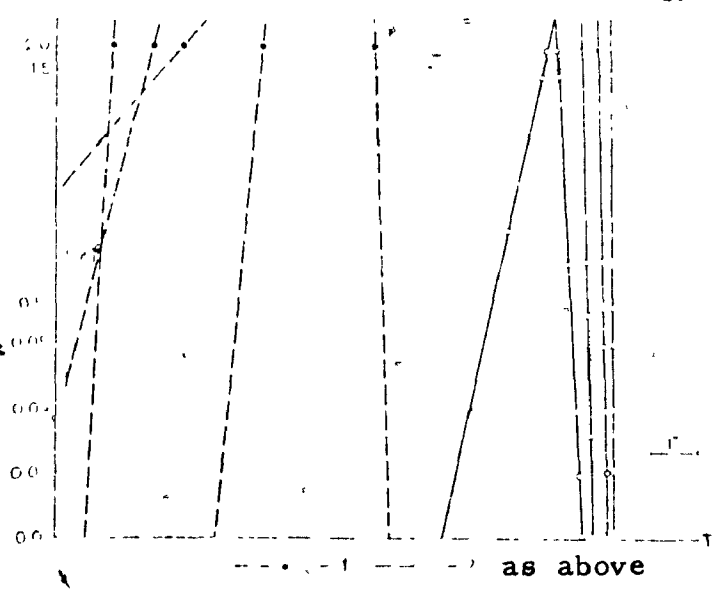


Figure 5: 1b
 Profile of Temperature:
 over a snow covered
 ice surface
 (after Doronin, 1969)

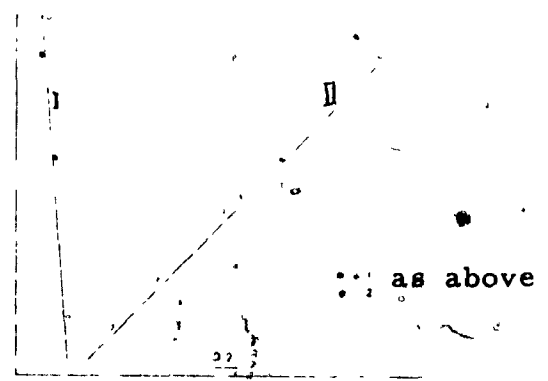


Figure 5: 1c
 Profile of Temperature:
 over a snow-ice surface
 before (I) and after (II)
 a frontal passage (after
 Berlyand, 1956)

law as it has more physical meaning. The range of stabilities over which this law applies appears to vary with author, but there is general agreement that the logarithmic law is suitable for conditions with $+0.0125$ (or $+0.015$) $> R_1 > -0.0125$ (or -0.015). As a strong surface inversion is a frequent phenomenon over most melting snow and ice surfaces, the simple logarithmic law is often unsatisfactory for energy balance studies over glaciers (see for instance Liljequist, 1957 and Holmgren, 1971).

The climate of Meighen Ice Cap has been shown to differ from that of the other glaciers in the Queen Elizabeth Islands (see II 2 and II 3). The principal reasons for these differences are the advection of cool Polar Ocean air over the island and the high frequency of fog on the ice cap. The prevalence of fog limits the formation of stable stratifications over Meighen Ice Cap to the very rare periods of clear weather; unstable stratifications with $R_1 < -0.0125$ are, on the other hand, more frequent. Doronin (1969, p. 14) concludes that over the polar ocean "in the overwhelming majority of cases one may neglect not only the correction for unsteadiness of the process, but also departure of stratification from the neutral state". Vertical profiles of wind and temperature (Figures 5:1 a and b, after Doronin, 1969) from North Pole 4 and 5 in winter and summer show little deviation from a logarithmic profile in the lowest few meters. This was the case in both lapse and inversion conditions, as is further illustrated in Figure 5:1c (after Berlyand, 1956) by the temperature profiles measured before and after a frontal passage at North Pole 4. It seems probable that the logarithmic law will provide a good approximation of the variation of wind and temperature with height in the lowest meters over the surface of Meighen Ice Cap.

Table 5: 2a

Percent Frequency of Mean Deviation from Logarithmic Law

Mean Deviation	(m/sec, °C, mb × 10)													
	from	.0	.3	.7	1.0	1.3	1.7	2.0	2.3	2.7	3.0	3.3	3.7	4.0
to	.3	.7	1.0	1.3	1.7	2.0	2.3	2.7	3.0	3.3	3.7	4.0		
1969														
Wind	28.4	19.6	16.3	12.4	6.7	4.7	3.7	2.5	2.5	.7	.6	.3	1.7	
Temperature	48.4	16.8	12.6	6.4	2.9	1.6	.9	.6	.7	.3	.5	.1	.3	
Vapour Pressure	50.8	23.6	11.0	6.0	2.6	2.2	.6	.3	.9	.1	.0	.0	.9	
1970														
Wind	39.0	22.9	11.7	9.2	6.4	4.1	2.5	.8	.8	.5	.1	.1	1.5	
Temperature	36.5	22.6	12.5	8.1	4.9	4.5	1.9	1.6	.8	1.3	1.3	1.1	2.8	
Vapour Pressure	27.6	20.9	13.6	9.1	5.3	3.7	2.6	1.9	2.7	1.8	1.1	1.1	8.7	

5:2 Measured Profiles

Five-minute wind runs and spot readings of temperature and humidity were made at 30, 90 and 150 cm at Main Ice every 3 hours throughout the 1969 and 1970 field seasons. Similar wind and temperature profiles were taken at North Ice in 1970. The instrumentation used is described in II 1:3. The mercury thermometers from the psychrometers were calibrated, following the 1969 and 1970 seasons by the Physics Division of the National Research Council. The calibration factors did not change significantly between calibrations. The estimated accuracy of the thermometers was $\pm .1$ deg C. An adjustment was made to the temperatures to account for periods when the fan mechanisms in the psychrometers were inoperable.

With the obvious limitations of the instrumentation in mind, the profiles were examined to determine the applicability of the logarithmic law to Meighen Ice Cap conditions. A linear regression line was fitted by the least squares method (Brooks and Carruthers, 1953) to each profile of wind, temperature and vapour pressure (with the logarithm of height). The most satisfactory measure of the goodness of fit proved to be mean deviation of the individual measurements from the regression line.

Table 5:2a gives the percent frequency of the mean deviations from the logarithmic law for wind speed, temperature and humidity profiles. Assuming that mean deviations of .1 deg C and .1 m/sec can be attributed to instrument error, seventy percent of all profiles are logarithmic within the accuracy limits of the instrumentation. Ninety percent of all profiles are within .2 deg C or .2 m/sec of being logarithmic.

Examination of individual wind profiles, having mean deviations greater

Table 5. 20

Mean Deviations from Logarithmic and Power Law

Period	1	2	3	4	5	6	7	8	9
<u>LOG LAW</u>									
Wind m/sec									
M1 1969	.05(1)	.05(1)	.05(1)	.05(1)	.04(1)	.04(1)	.04(1)	.04(1)	.04(1)
M1 1970	.05(1)	.04(1)	.05(1)	.04(1)	.04(1)	.04(1)	.04(1)	.04(1)	.04(1)
N1 1970	--	--	--	.05(1)	.05(1)	.04(1)	.04(1)	.04(1)	.04(1)
Temperature °C									
M1 1969	.08	.04	.03	.05	.04	.04	.04	.05	.05
M1 1970	.07	.05	.04	.06	.06	.04	.04	.05	.05
N1 1970	--	--	--	.10	.10	--	.13	.10	.07
Vapour Pressure mb									
M1 1969	.05	.04	.03	.04	.05	.03	.03	.03	.04
M1 1970	.05	.06	.03	.06	.06	.05	.05	.04	.05
<u>POWER LAW</u>									
Wind m/sec									
M1 1969	.05	.05	.05	.05	.05	.04	.04	.04	.05
M1 1970	.06	.04	.05	.05	.05	.04	.04	.03	.04
N1 1970	--	--	--	.05	.05	.05	--	.06	.03
Temperature °C									
M1 1969	.08	.04	.03	.05	.04	.04	.04	.05	.04
M1 1970	.07	.05	.04	.06	.06	.04	.04	.05	.05
N1 1970	--	--	--	.10	.10	--	.13	.10	.07
Vapour Pressure mb									
M1 1969	.05	.04	.03	.04	.05	.03	.03	.03	.04
M1 1970	.05	.06	.03	.06	.10	.05	.05	.04	.05

* mean as % of mean wind speed

than .1 m/sec, showed that malfunction of one or more anemometer due to icing or riming conditions accounted for most of these deviations. In an attempt to eliminate profiles where large deviations were a result of measuring errors, all profiles occurring with near neutral stability, ($-.0125 < Ri < +.0125$) and having mean deviations greater than .1 deg C or .1 m/sec were discarded. Similarly for all other stabilities, profiles with mean deviations greater than .2 deg C and .2 m/sec were dropped.

Table 5:2b shows ten day means of mean deviation from logarithmic profiles and of mean deviation as a percent of the average 150 cm wind speed, the latter for comparison with Grainger and Lister (1965). In general the wind speed deviations for ten day periods are smaller than the smallest deviations obtained by Grainger and Lister (1965) for any of the laws tested by them (i. e., logarithmic law, power law, Deacon power law, log-linear law or log-cubic law).

Applying a simple power law to the Meighen Ice Cap profiles does not appear to improve the fit for ten-day means. Figure 5:2 shows that logarithmic law is definitely better than the power law under neutral-stable conditions and somewhat better under neutral unstable conditions while in unstable conditions they give quite similar results. Only in the infrequent stable stratifications does the power law appear to fit the measured profiles better than the logarithmic law and here the mean deviations are less than .04 m/sec, well below the accuracy of the instruments. The highest errors occur with unstable conditions which, it will be shown later, occur with light winds and high temperatures. They appear to be a result of a reversal in the sign of the measured gradient above the 90 cm level. The measured profiles appear

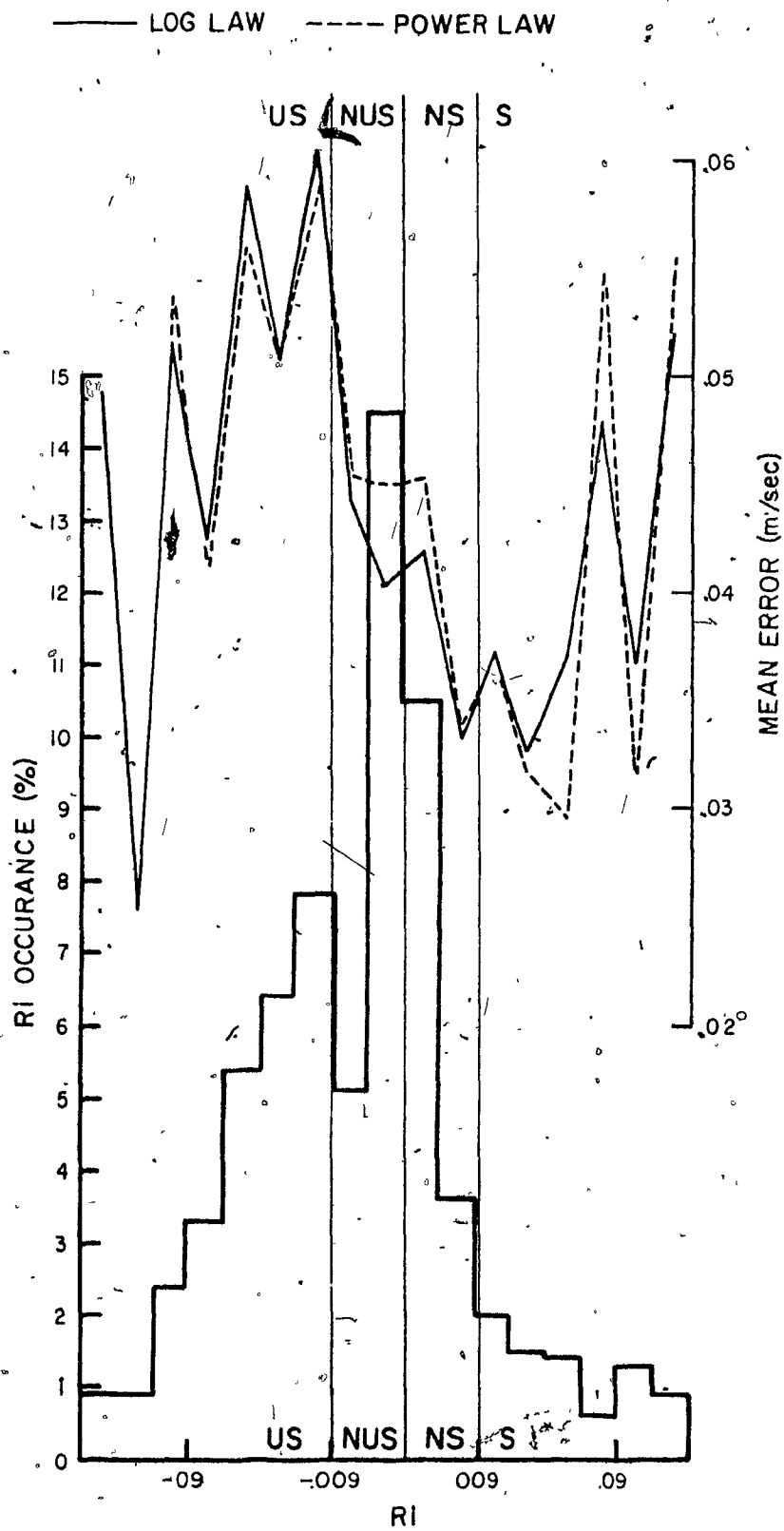


Figure 5: 2 Frequency Distribution of Richardson Number (Ri) and Comparison of Mean Error of Wind Profiles from Log Law and Power Law with Stability

to substantiate the assumption that, in general, the logarithmic law provides a good fit to the wind, temperature and vapour pressure profiles at Main Ice.

5:2.1 Calculation of Ri for 30-90 cm

Assuming logarithmic variation of wind and temperature with height, the Richardson Number can be calculated from the equation

$$Ri = \frac{g}{T} \frac{(T_{90} - T_{30})}{(u_{90} - u_{30})^2} \ln \frac{z_{90}}{z_{30}} \quad 5:2.1$$

where g is acceleration due to gravity, T the mean temperature of the 30 to 90 cm layer, T_{90} , u_{90} and T_{30} , u_{30} are the temperature and wind speed for $z = 90$ cm and $z = 30$ cm.

Referring again to Figure 5:2 it can be seen that near neutral conditions predominate and that these are most frequently slightly unstable. On Devon Ice Cap Holmgren (1971) found lapse conditions only 25% of the time while Keeler (1964) found them to be very infrequent, as did Müller (1967) for Axel Heiberg Island. Further investigations show that the stability distribution in fog is decidedly more negative than with no fog (see Figure 5:1a). Elsewhere, fog is generally associated with stable or near neutral stable conditions; the fog being formed by radiative cooling of the surface, advection of warm moist air over a cold ice or water surface or possibly by orographic uplift and cooling of moist air. In all these cases the air mass is cooled from the bottom which often results in inversion conditions. The Meighen Ice Cap fogs are of a different nature. They are generally accompanied by strong winds and are colder than the snow surface, resulting in lapse conditions in the first meter. This suggests that the fog is

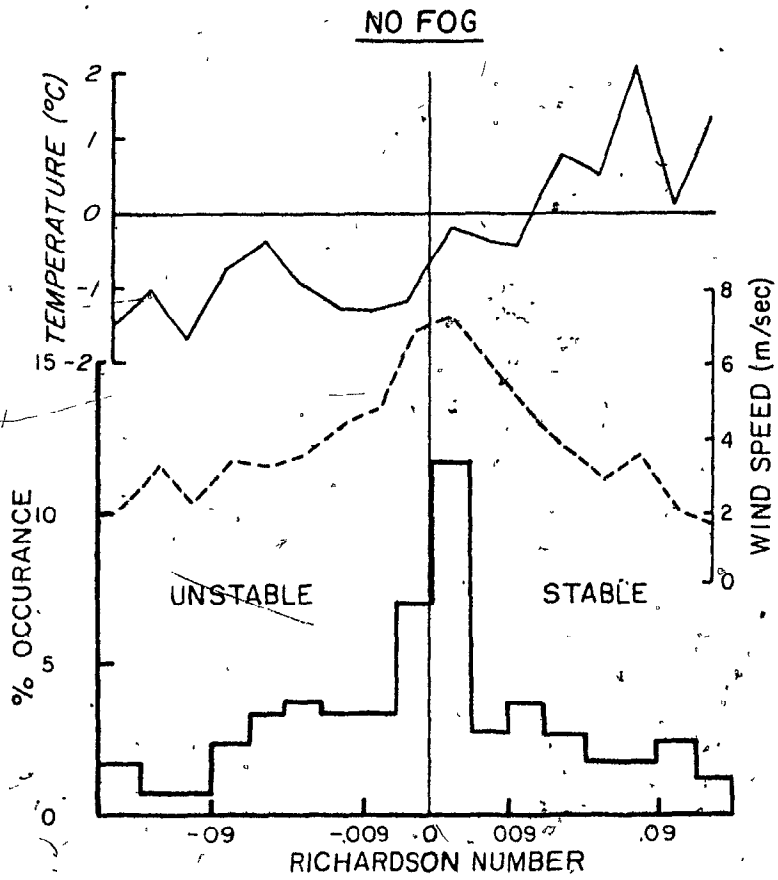
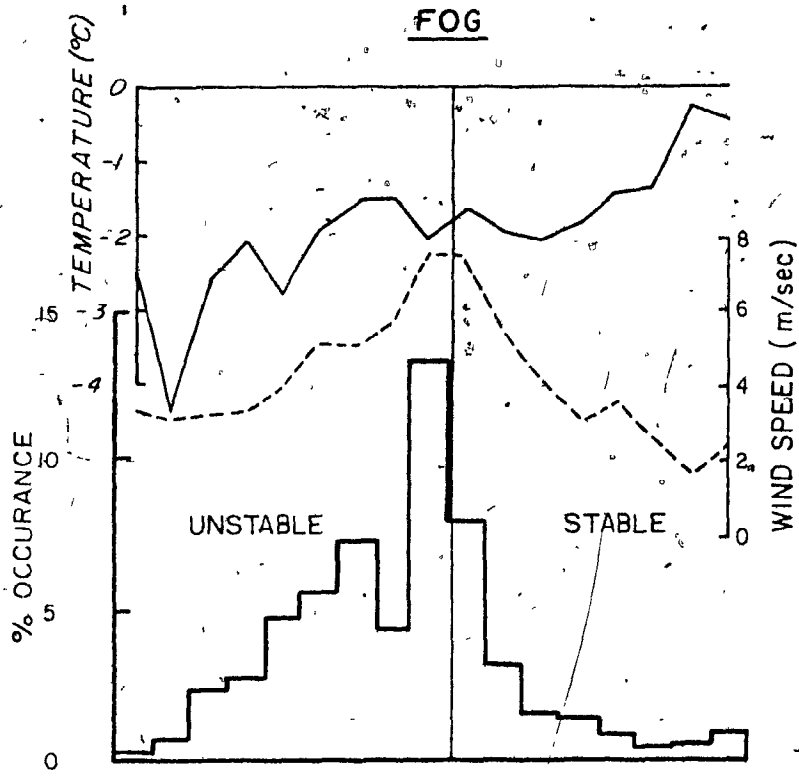


Figure 5: 2.1a Frequency Distribution of Richardson Number (Ri) for Fog and No Fog and Variation of Temperature and Wind Speed with Stability

Table 5: 2.1a

Richardson No. (Ri) and Sky Cover		Stability
Ri		
-0.200	$\oplus, -\ominus_H$	unstable
-0.025	$\ominus, \oplus, \oplus_L$	"
-X		"
X ₂		"
-0.020		"
-0.020	$-\ominus_M$	"
X _{1,2}		neutral unstable
-0.004		" "
-0.000	\ominus_H	" "
.004	\oplus, \oplus_M	neutral stable
.037	\ominus_H	stable
.048	\ominus_M	"

actually low stratus or stratocumulus cloud formed over the cool Polar Ocean and blown against the ice cap (800 ft amsl), appearing to be fog to the Main Ice observer. Figure 5:2.b shows that the distribution of Richardson number for observations where North Land reported cloud while Main Ice reported fog, is very similar to that for all observations of fog at Main Ice. Further discussion of this assumption can be found in I.

Figure 5:2.b also shows that the non-neutral stabilities are largely a result of low wind speeds (see equation 5:2.1) and that stable conditions accompany warm temperatures, while slightly unstable or very unstable conditions accompany cold temperatures.

Table 5:2.1a of mean Richardson numbers with various sky conditions show that middle cloud and small amounts of high cloud results in positive (stable) means and that thick fog produces less instability than thin fog or low cloud.

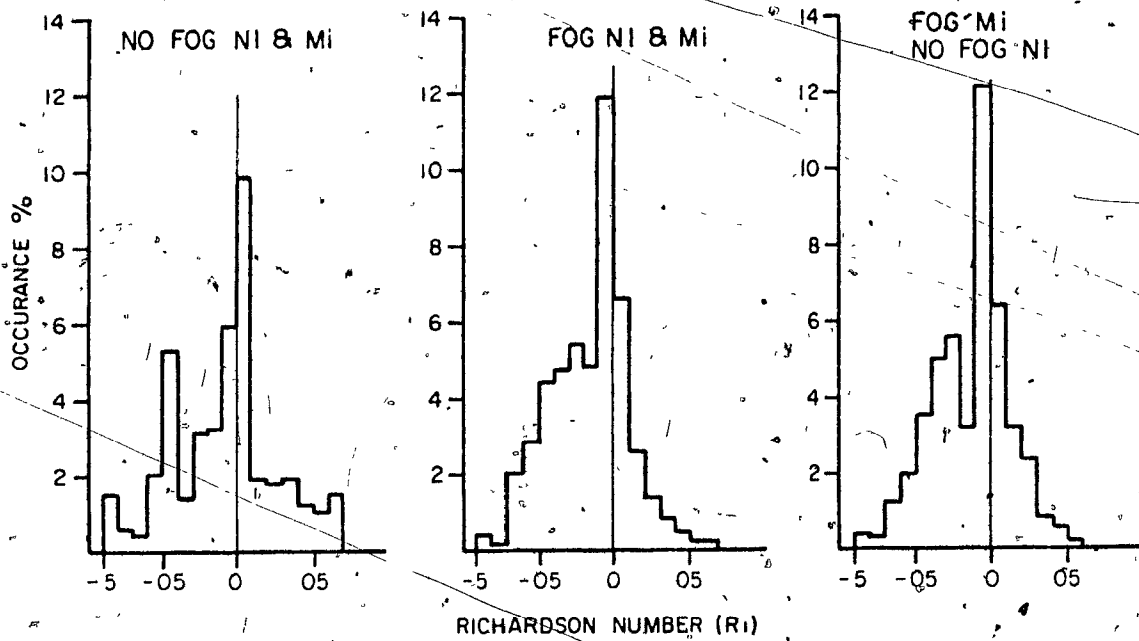


Figure 5: 2.1b Frequency Distribution of Richardson Number² for conditions of 1) No Fog at Mi or Ni; 2) Fog at Mi and Ni; 3) No Fog at Ni but Fog at Mi.

Table 5 2.1b

Ten-Day Means of Richardson Number (Ri)

Period	1	2	3	4	5	6	7	8	9
Mi 1969	-.011	-.020	-.048	-.081	-.023	-.009	-.013	.017	.090
Mi 1970	--	-.058	-.003	-.026	-.061	-.006	-.020	-.065	-.018
Ni 1970	--	--	--	-.022	-.016	-.137	--	-.033	-.077

Table 5: 2. 2a

Wind Speed Power Law Indices (1/n) for Various Periods

Ten Day Period	1	2	3	4	5	6	7	8	9
Mi 1969	.22	.16	.15	.15	.14	.16	.15	.18	.20
Mi 1970	.15	.12	.13	.18	.19	.35	.17	.17	.20
Ni 1970	--	--	--	.17	.14	.18	--	.18	.13

Period*	1	2A	2B	3A	3B	4	5A	5B	6	7	8
Axel Heiberg Lower Ice 1961 **	.23	.21	.22	.18	.23	.20	.40	.11	.31	.11	.18

* See Havens 1965 for details of periods

** After Havens 1965 p. 26

Table 5 2. 2b

Profile Parameters (U*, slope of T, slope of e)

Period	1	2	3	4	5	6	7	8	9
U*									
Mi 1969	26.5	21.2	39.6	31.9	27.3	29.5	34.1	28.2	21.5
Mi 1970	29.4	27.7	29.3	26.1	33.4	18.8	26.9	31.4	24.3
Ni 1970	--	--	--	24.9	27.9	14.3	--	28.6	16.1
Slope of T									
Mi 1969	-.03	-.08	-.09	-.17	-.14	.002	.05	.12	.33
Mi 1970	-.17	-.16	-.08	-.22	-.11	.02	-.07	-.10	-.04
Ni 1970	--	--	--	-.23	-.121	-.20	--	-.21	.08
Slope of e									
Mi 1969	.11	-.08	-.06	-.03	-.12	-.09	.07	-.01	.05
Mi 1970	.05	-.05	-.05	-.08	-.42	-.03	.05	-.06	.03

* See Table 5. 2. 3b for periods.

RICHARDSON NUMBER

- FOG
- - - NO FOG

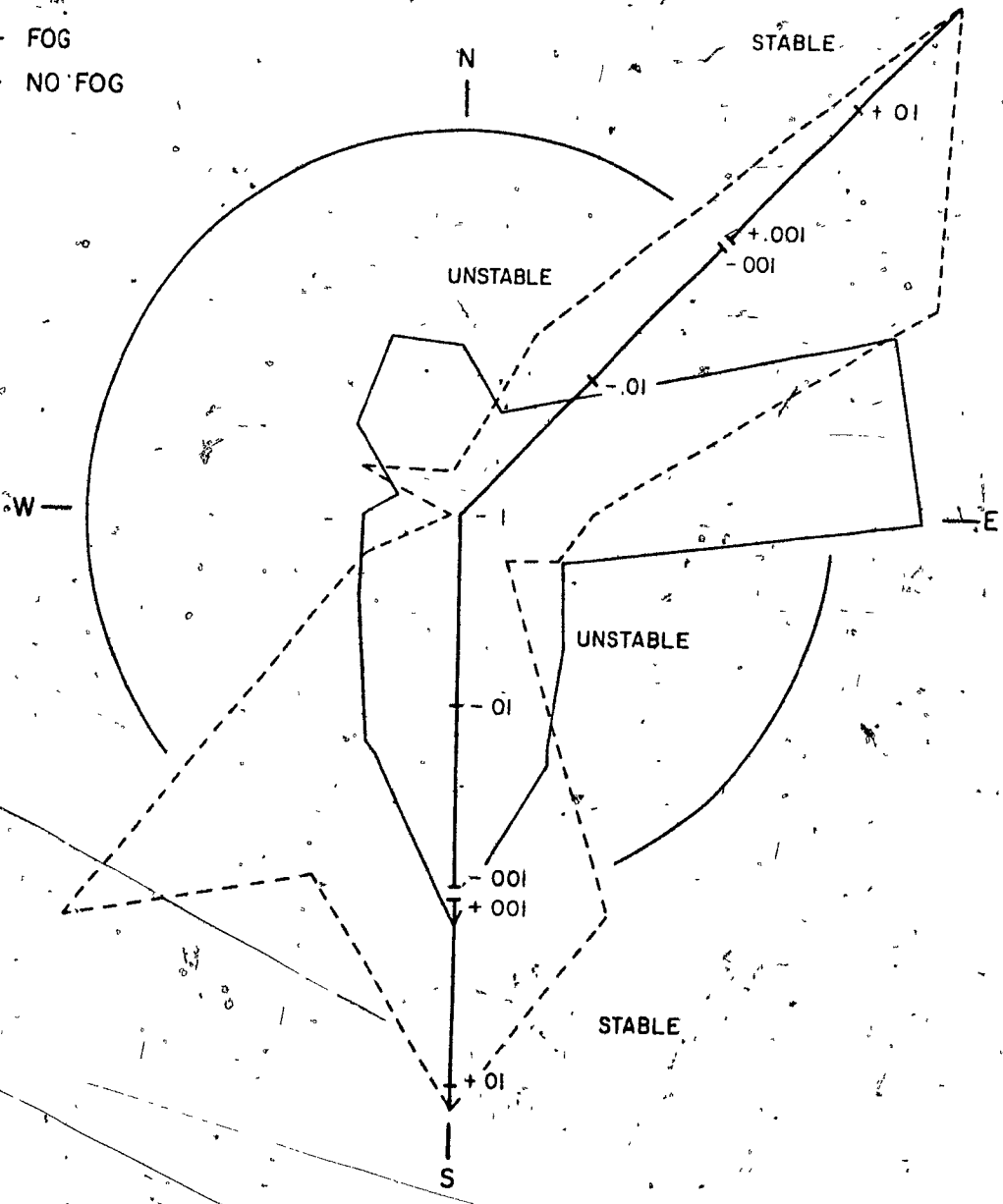


Figure 5: 2.1c Roses of Richardson Number (Ri) for Fog and No Fog

In order to relate stability conditions to the synoptic situation the mean values of Richardson number with wind direction for fog and no fog are plotted in Figure 5:2.k. In fogless conditions NE and SSE through SW winds are most stable, these wind directions representing Island (Type III) circulation and baroclinic (Type II) circulation; while Polar Ocean (Type I) circulation results in unstable conditions. In fog, stable conditions suggesting "real fog", as opposed to cloud at the surface, are experienced with the NE and S winds of Island circulation. Polar Ocean northerlies tend to be near neutral unstable while westerlies are most unstable.

Table 5.2.lb of ten-day means shows positive mean Richardson numbers only during the last two periods in 1969, when Type III circulation resulted in unseasonably warm conditions.

5:2.2 Profile Slopes

The friction velocity was obtained from the slope of the regression line for the wind profiles. Table 5:2.2b gives the ten-day means of friction velocity which lie within the range of those found by other investigators. Table 5:2.2a contains ten-day means of the power law index $1/n$, calculated from the Meighen Ice Cap profiles and those found by Havens (1965) for Axel Heiberg in 1962. The Meighen Island indices are generally lower (n is higher) than the Axel Heiberg values.

The frequency distribution of the slope of the temperature profile is shown in Figure 5:2.2a. The absence of a secondary maximum for strongly negative slopes suggests that the secondary maximum for unstable Richardson numbers is largely a wind speed phenomenon. Further relating the temperature profile slopes to Richardson Number, through

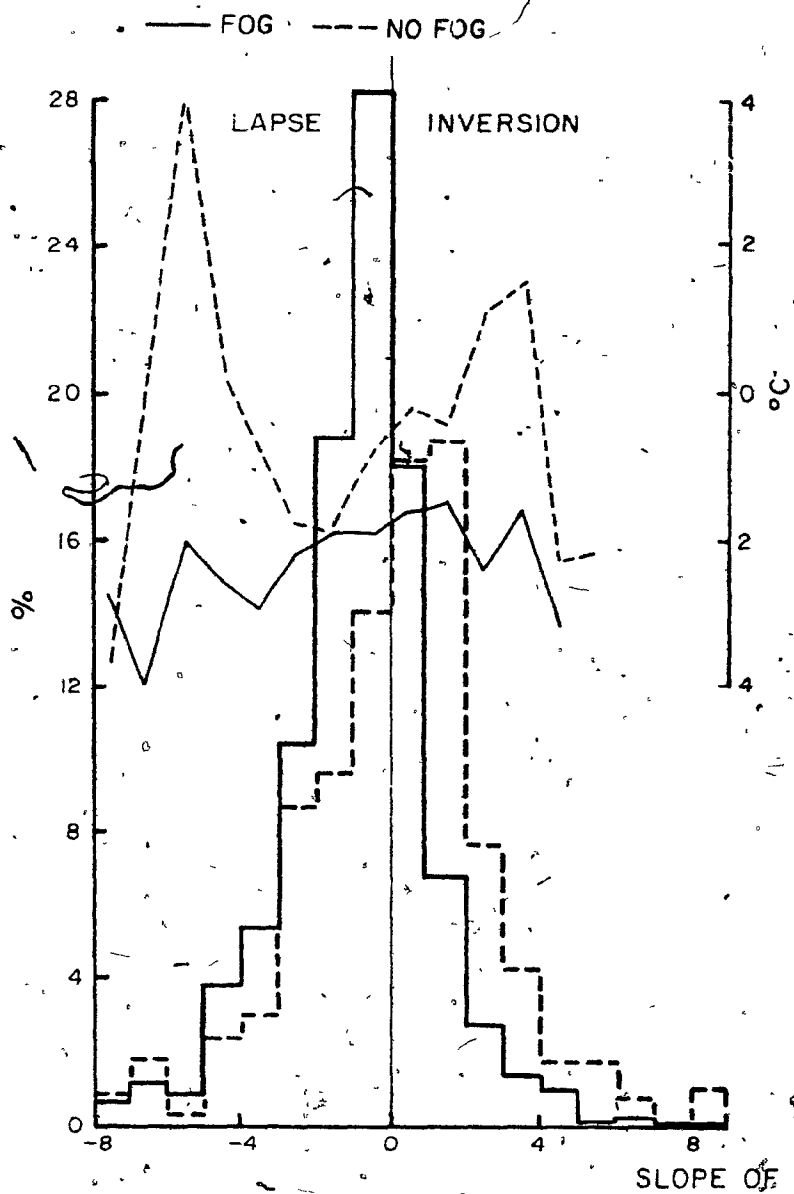


Figure 5: 2.2a

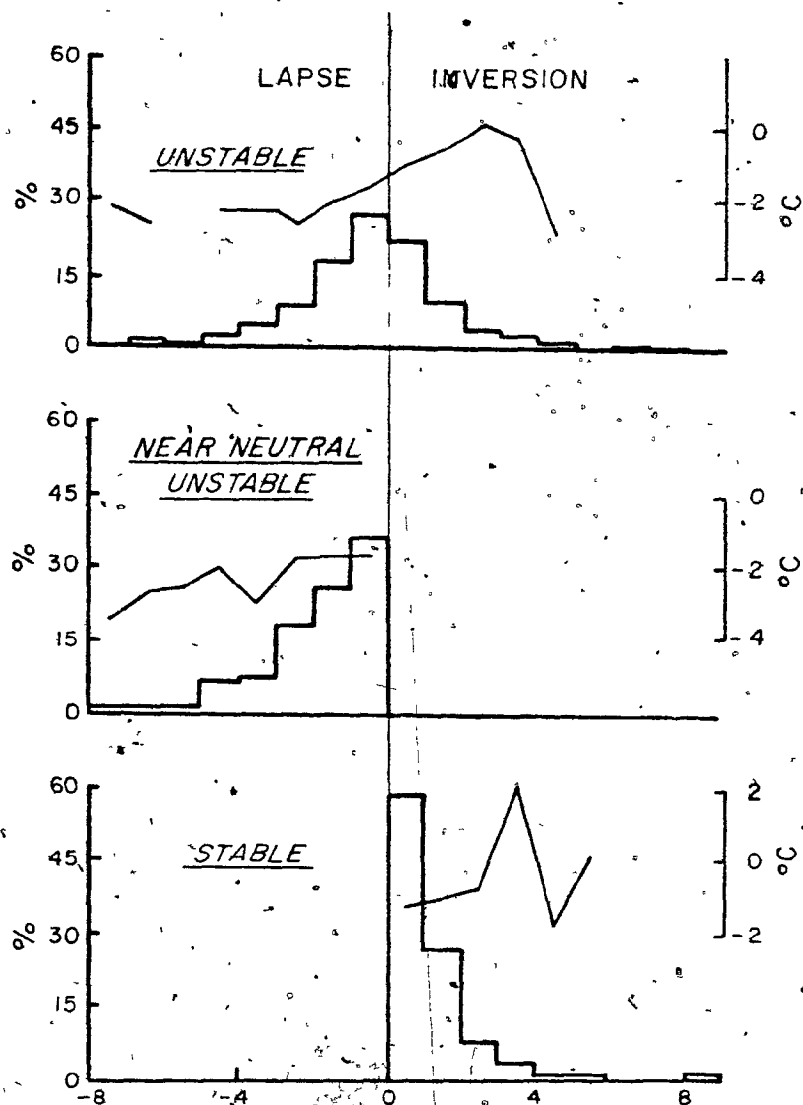


Figure 5: 2.2b

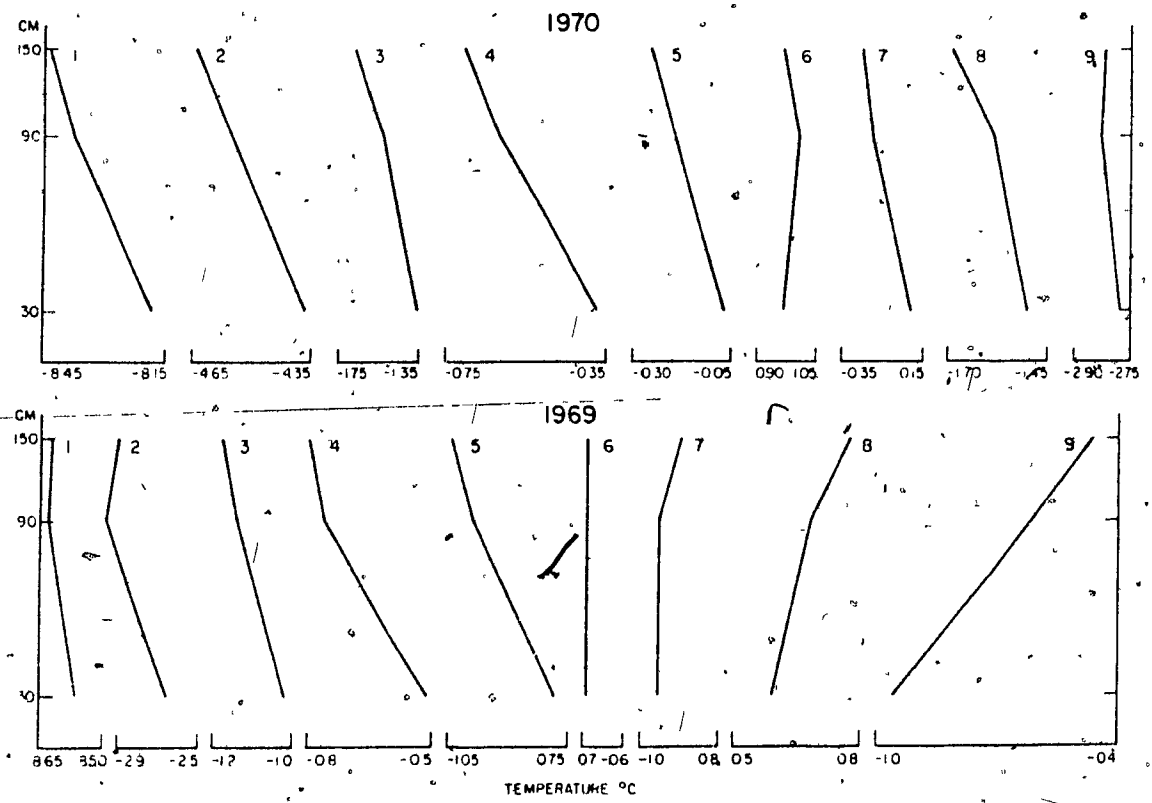


Figure 5: 2.2c / Ten-day Means of Temperature Profiles

Figure 5:2.2a, shows that positive slopes occur with unstable Richardson numbers. This discrepancy results from the fact that the Richardson numbers were calculated using 30 and 90 cm heights while the slope is the best fit regression line through the 30, 90 and 150 cm temperatures. When the temperature profile is negative between 30 and 90 cm and positive from 90 to 150 cm, negative Richardson numbers and positive slopes could be obtained. Comparing ten-day means of Richardson number (Table 5:2.1 a) and temperature profile slope (Table 5:2.2b and Figure 5:2.2c), it can be seen that period 7 in 1969 has a positive mean slope and a negative mean Richardson number, and that the mean temperature profile has the described shape. These cases of a near isothermal first meter, changing to an inversion by screen level, may represent the

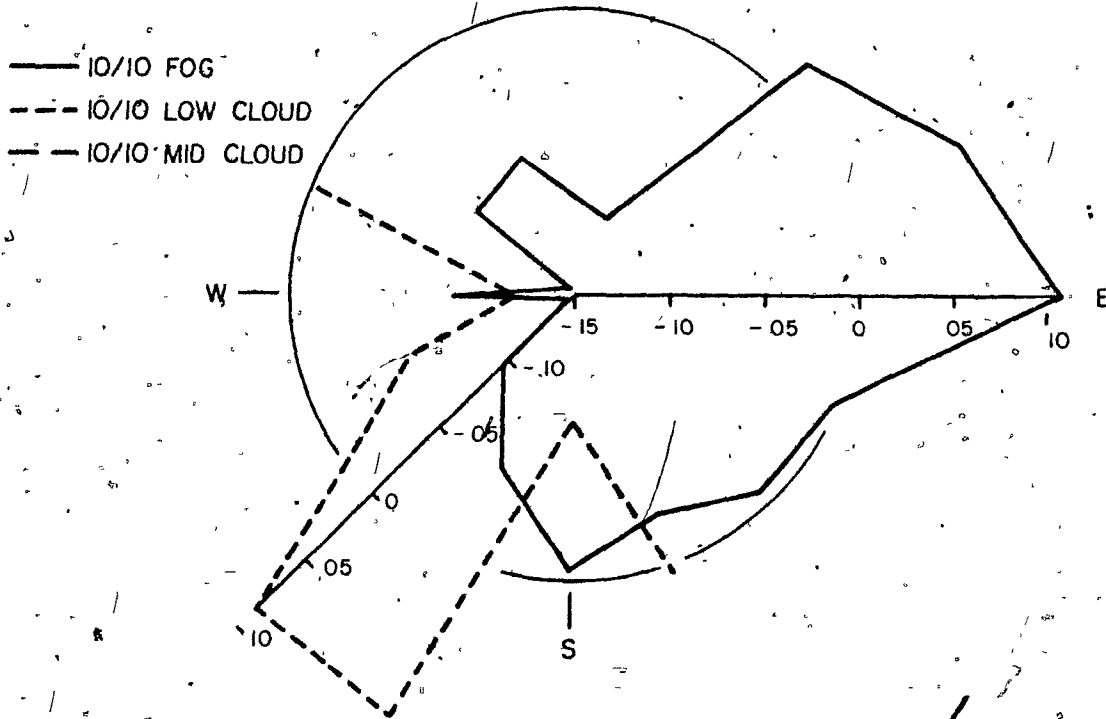
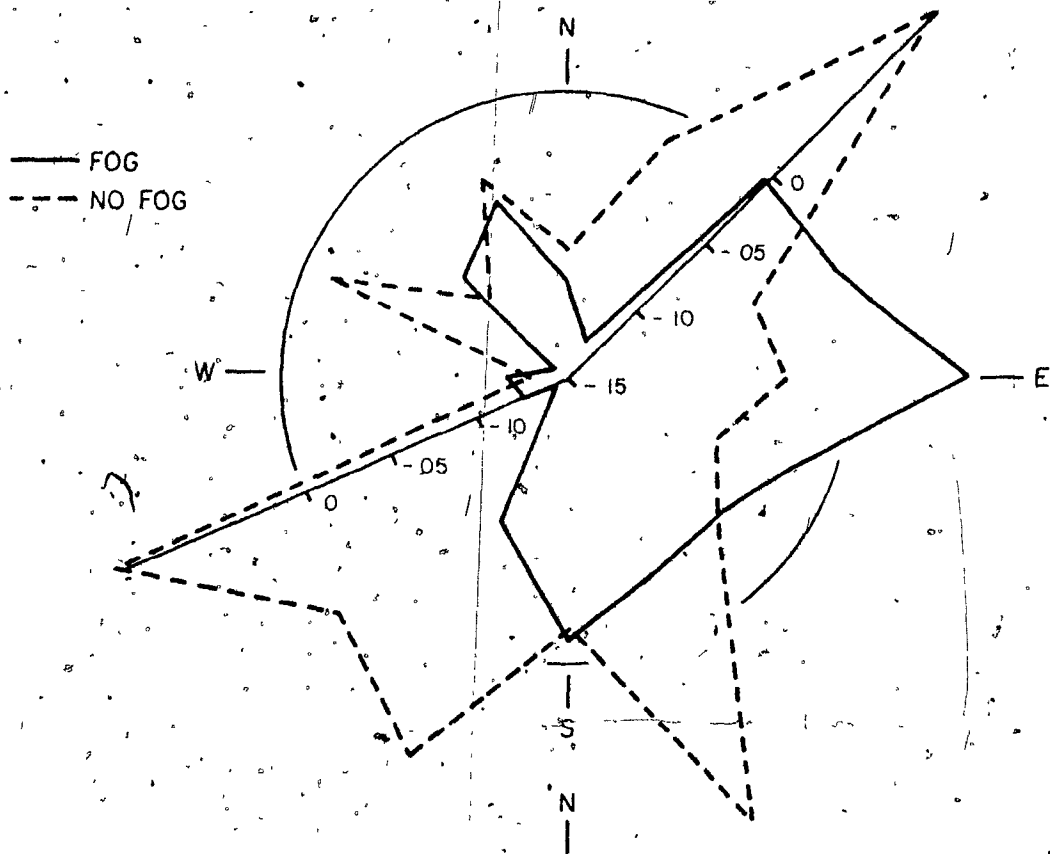


Figure 5: 2.2d Roses of Temperature Profile Slope

transition from lapse to inversion conditions accompanying the advection of warm air over the ice cap.

With negative Richardson numbers there is a tendency towards stronger negative slopes at lower temperatures.

Means of temperature slope with wind direction, Figure 5:2.2d, show positive slopes in fog with NE through E winds only, while the strongest negative slopes accompany W'lies. With no fog, the strongly positive peaks in the SSE and WSW, not seen in the Richardson number rose, suggest the influence of cases with lapse in the first meter and inversion above. It may be inferred from the lack of similar peaks in the roses of temperature slope for 10/10 fog, low cloud and middle cloud that these reversing profiles tend not to occur with overcast conditions.

The frequency distribution of vapour pressure profile slopes with fog (see Figure 5:2.2e) is similar to that of temperature, as would be expected considering that the vapour pressure must be very close to the saturation vapour pressure at all levels in the fog. With no fog the humidity profile is bimodal with a positive and a negative maximum, in contrast to the single positive maximum of the temperature slope. There is a tendency towards more positive slopes with higher vapour pressures in fogless conditions.

Comparing Figure 5:2.2f of humidity slope wind roses with that of temperature (Figure 5:2.2d) it can be seen that for fog the shapes are similar, except in the W'ly sector where the humidity slopes are almost positive while the temperature slope is decidedly negative. W'lies in fog are accompanied by cold temperatures (see Figure 4:4), suggesting that the near positive vapour pressure slopes may reflect

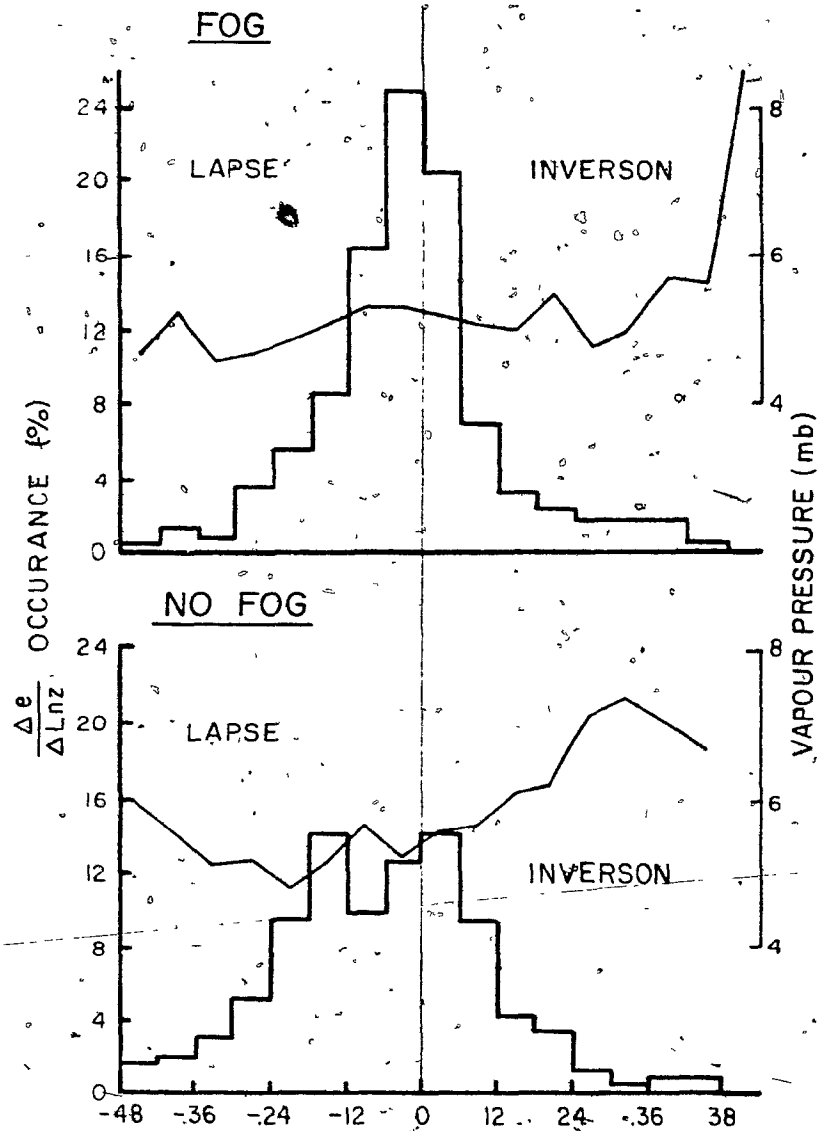


Figure 5: 2.2e

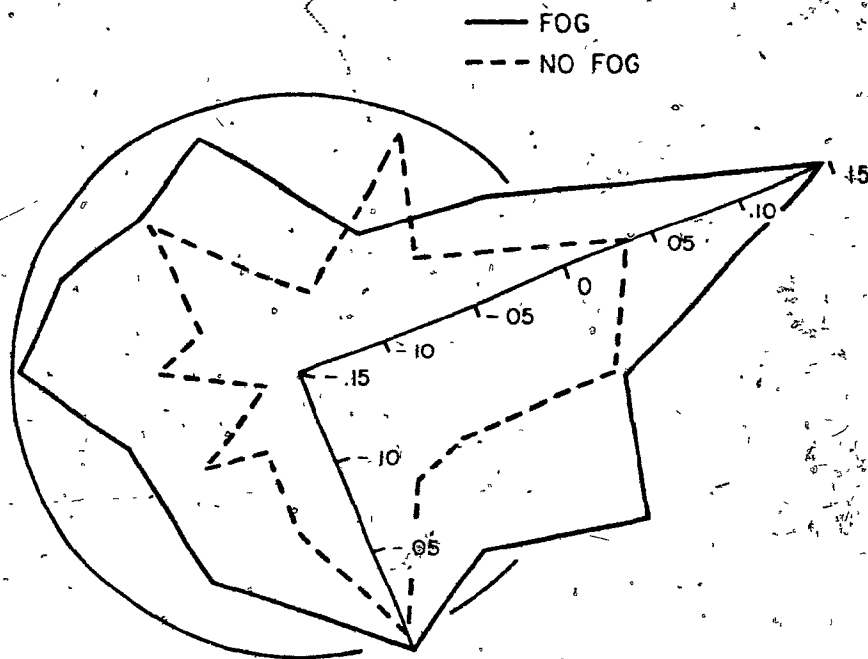


Figure 5: 2.2f

Table 5:2,3a

Surface Roughness (Zo) for Various Snow and Ice Surfaces

Surface Description	Location	Zo (cm)	Reference
Melting snow, Isachsen Plateau		.23	Sverdrup, 1936
Pre-melt season snow		.012	Liljequist, 1957
Pre-melt season snow		.01	Rusby, 1961
Ablation zone, Greenland Ice Cap		.1-.6	Ambach, 1963
Ablation zone ice, Sverdrup Glacier		.34-.52	Keeler, 1961
Ablation zone, Lower Ice White Glacier		.002-3.5	Müller, 1965
Ice with cryoconite holes,	"	1.6	" "
Smooth slippery ice,	"	.002	" "
From snow to firn to smooth ice, Storglaciaren		.01	Granger-Lister, 1965
Frozen ice dammed lake melting, NE Greenland		.04	" " "
Coarse snow with sustrug, spring, Britannia Glacier		1.1	" " "
Undulating wet snow, mid-season,	"	.68	" " "
Bare hummocked ice, end season,	"	.58	" " "
early season, Lower Station	"	.40	" " "
mid-season,	"	.50	" " "
late season,	"	.57	" " "
Pre-melt season snow, Antarctic		.014	Lalrymple et al, 1960
Snow November, North Pole 5		.064	Doran, 1969
Snow July-August, North Pole 4		.033	" "
Fine-grained frozen snow, spring, Devon Ice Cap		.011	Holmgren, 1971
Relatively, fine-grained melting snow	"	.071	" "
Large melting ice grains (2-3 cm diam.)	"	.13	" "
Thin-cover of new snow on superimposed ice	"	.05	" "

Table 5: 2. 3b

Ten Day Means of Surface Roughness (Zo)

Period	1	2	3	4	5	6	7	8	9
Mi 1969	1.29	.45	.16	.22	.16	.27	.35	.77	1.50
Ma 1970	.73	.11	.19	.90	.84	3.70	.62	.68	1.44
Ni 1970	--	--	--	.48	.11	1.28	--	1.51	.21

Period 1 = 1 - 10 June
 Period 2 = 11 - 20 June
 Period 3 = 21 - 30 June
 Period 4 = 1 - 10 July
 Period 5 = 11 - 20 July
 Period 6 = 21 - 30 July
 Period 7 = 31 - 9 August
 Period 8 = 10 - 19 August
 Period 9 = 20 - 29 August

74

the fact that the lowest levels are saturated with respect to ice while the screen level is saturated with respect to water.

The vapour pressure profile rose for fogless conditions shows a reversal of the fog-fogless relationship of the temperature slope. The humidity profiles for no fog are generally more negative than either the temperature profiles or the fog humidity profiles, due to drying out with increased distance from the snow surface in the absence of fog. These conditions are particularly well developed with SW through WSW winds. In the case of NE and SSE winds, the air at screen levels appears to be more moist.

5:2.3 Surface Roughness z_0

The surface roughness z_0 was evaluated for each wind profile from the intersection of the regression line with the $u = 0$ axis. Frequency distributions (Figure 5:2.3) of $\log z_0$ show wide variation of z_0 as was also noted by Havens (1965) and Holmgren (1971). The majority of the values lie between .0016 and 1.6 cm, with a maximum between .1 and .4 cm. This is consistent with the findings of other investigators as shown in Table 5:2.3a. Ten-day means of z_0 for Main Ice and North Ice are shown in Table 5:2.3b. The relatively large spring values of z_0 correspond well with those from Britannia Glacier and probably result from presence of sustrugi.

The values of surface roughness averaged as $\log z_0$ for surface types, are shown in Table 5:2.3c. The rather low z_0 found for packed powder snow is probably a reflection of the strong winds which create this type. Iced powder and new snow agree well with the pre-melt season snow values shown in Table 5:2.3a. Wet granular corresponds

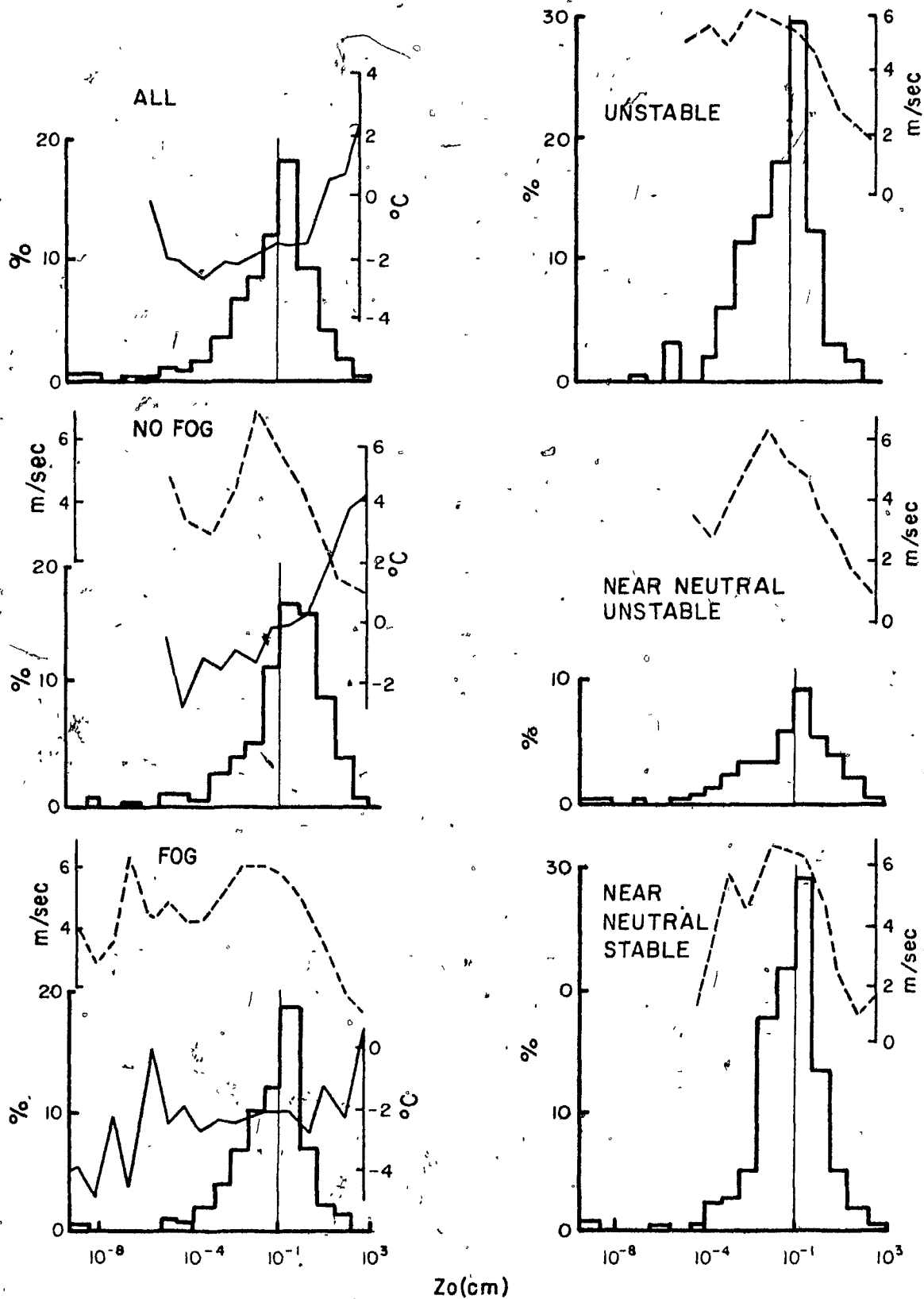


Figure 5: 2,3 Frequency Distributions of Surface Roughness (Z_0) and Variation of Temperature and Wind speed with Z_0 .

Surface Roughness and Surface Type			
Surface Type	Z_0 (cm)	No Fog	Fog
		Z_0 (cm)	Z_0 (cm)
Dry granular snow	.129		.129
Wet granular snow	.083	.242	.033
Rimed surface	.043	.455	.024
Wet powder snow	.021	.060	.012
Wet new snow	.016	.031	.015
Frozen granular snow	.013	.040	.006
New snow	.011	.090	.006
Drifted powder snow	.008	.091	.004
Iced powder snow	.008	.019	.007
Packed powder snow	.003	.002	.004

with Holmgren's melting snow and dry granular with his large melting ice grains.. Rimed surfaces due to the rime flowers which can be several centimeters long, fall between snow and granular snow.

Referring to the second and third columns of Table 5:2.3c and to Figure 5:2.3, it can be seen that fog consistently decreases the surface roughness, due largely to a lack of ^{extreme} high values of z_0 in fog. The Figure also shows that z_0 tends to increase with increasing temperatures and to decrease with increasing wind speed down to z_0 's of .01 cm at least. Fog keeps the temperature down, decreases solar radiation, almost eliminates direct solar radiation (which is responsible for differential melting due to colour or albedo differences) and is normally on Meighen accompanied by strong winds on Meighen Ice Cap.

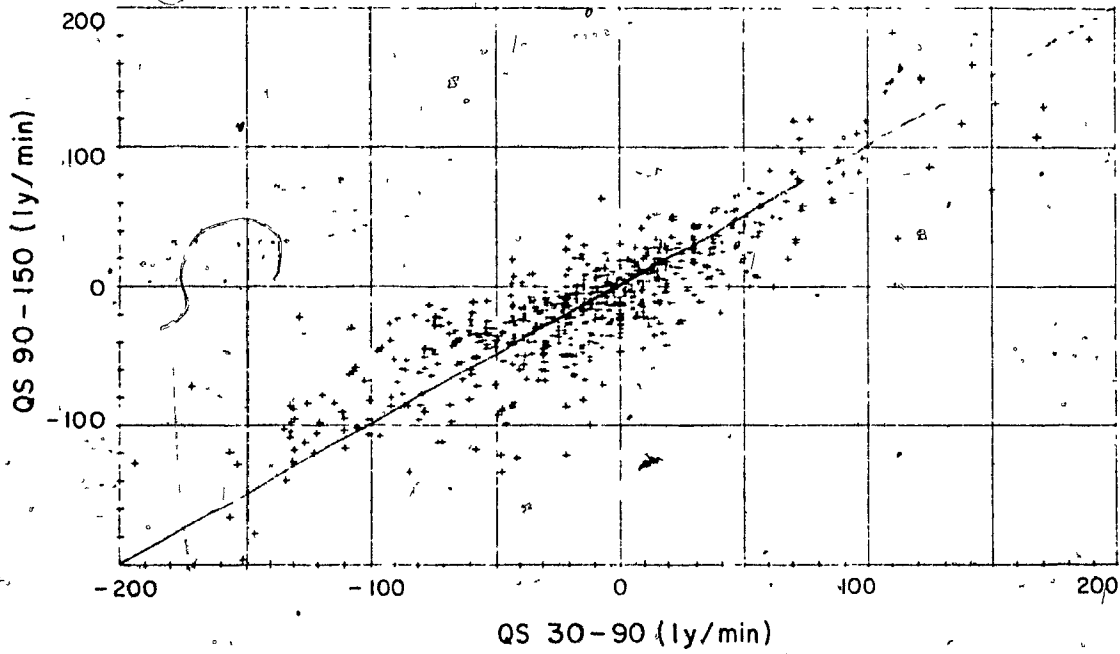
Table 5:2.3d further illustrates the effect of weather on the values of z_0 . The right hand portion of Figure 5:2.3 indicates that stability conditions do not appreciably effect the distribution of surface roughness.

Table 5: 2. 3d

Surface Roughness (Z_o) and Weather

	Z _o (cm)		T (°C)
Fbnk	.226		- .1
F	.114	L	+ .8
	.071	none	+ .8
	.068	L	+1.4
	.052	Z	-1.7
F	.019		-1.2
	.017	S	-3.9
	.015	BS	-2.6
F	.013	BS	-3.9
F	.013	Z, S	+ .9
F	.009	S	-2.4
F	.006	Y	-2.9
F	.003	S, Y	-3.5
F	.003	Z	-1.5

QS 90-150/QS 30-90 Mi 1969 & 1970



QL 90-150/QL 30-90 Mi 1969 & 1970

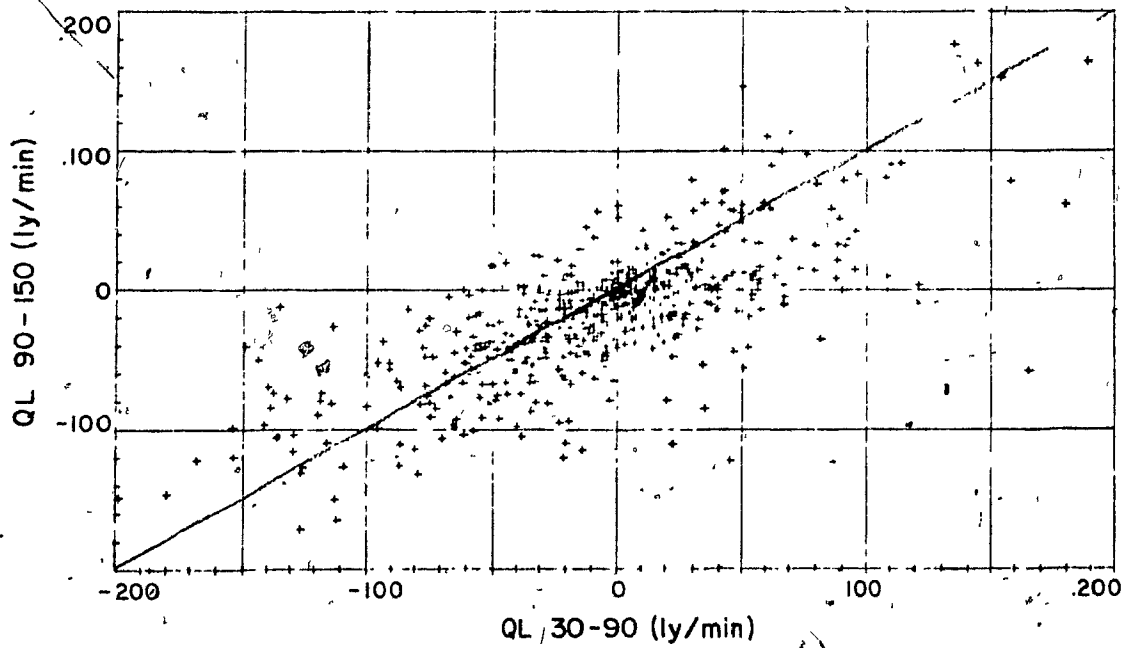


Figure 5: 4

5:3 Sensible and Latent Heat - Theory

As discussed by Sellers (1965) the molecular transfer of momentum, heat and water vapour in the laminar layer immediately next to the surface can be estimated by the turbulent transfer of these quantities in the first one meter of the atmosphere (thus ignoring advection in this layer). Assuming the profiles of temperature, wind and vapour pressure are logarithmic with height up to one meter (see 5:1) and that the eddy conductivities of momentum, heat and vapour pressure are equal, the fluxes of sensible and latent heat from the surface can be calculated from the equation (Sellers, 1965)

$$Q_S = \rho C_p k^2 \frac{\Delta u \Delta T}{(\ln z_2/z_1)^2} \quad 5:3.1$$

$$Q_L = .622 \rho L k^2 \frac{\Delta u \Delta e}{(\ln z_2/z_1)^2} \quad 5:3.2$$

where ρ and C_p are the density and specific heat of air, L is the latent heat of vapourization, k is von Karman's constant, and u , T , and e are the wind, temperature and water vapour pressure at heights z_1 and z_2 .

5:4 Sensible and Latent Heat from Measured Profiles

Equations 5:3.1 and 5:3.2 were applied to measurements of wind, temperature and humidity at 30 and 90 cm and at 30 and 150 cm. Figure 5:4 shows the relationship of the fluxes calculated using 30 and 90 cm (first meter) to those using 30 and 150 cm (screen level). For sensible heat the relationship is quite good, screen level calculations showing slightly less variation than those using the first meter. The relationship for latent heat is not as good, the screen level calculations being generally too low or too negative. The discrepancy can be as much

QL/QS, 90-150cm, MI 1969 & 1970

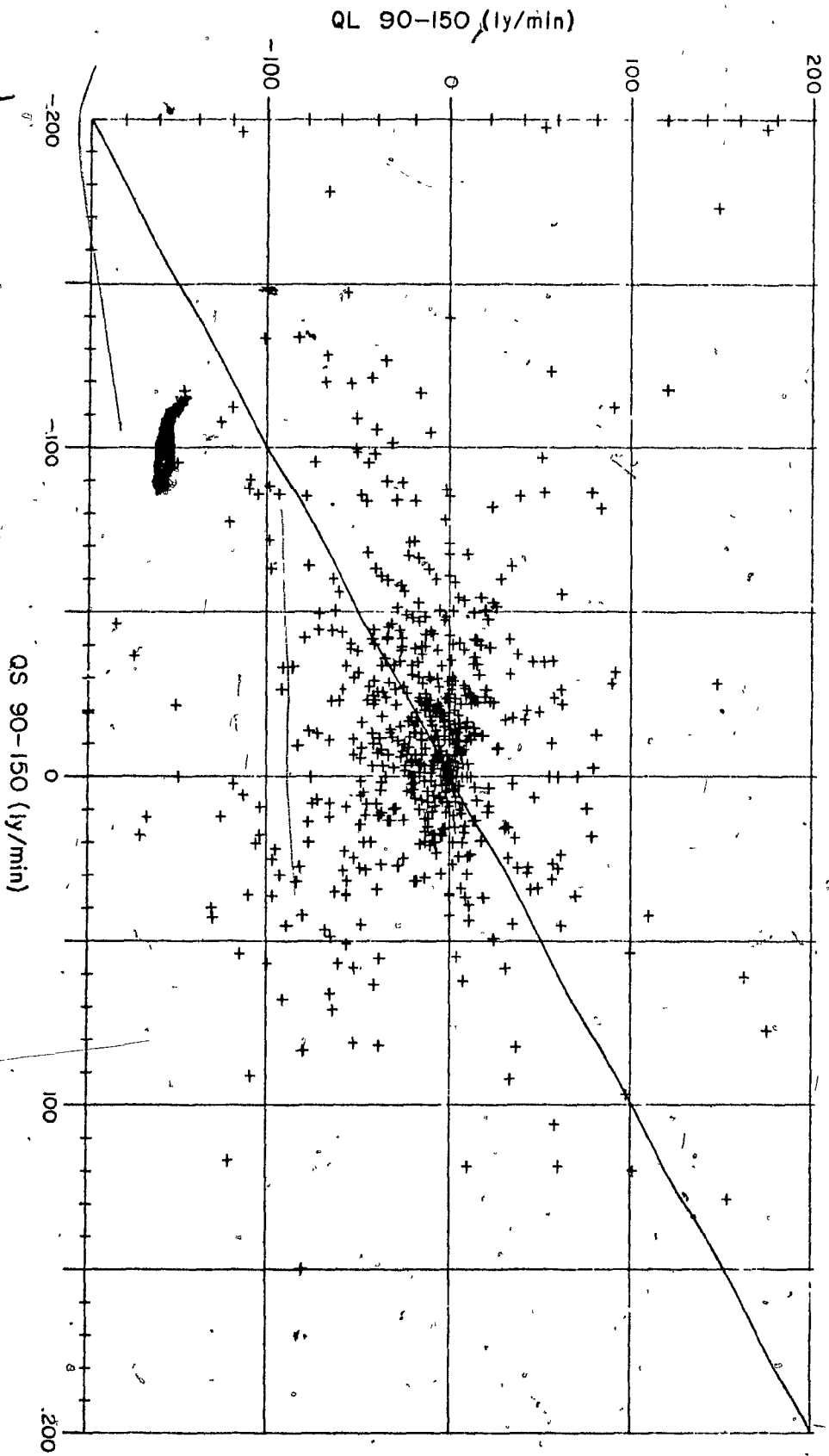


Figure 5: 4. 1a Relationship of QS to QL

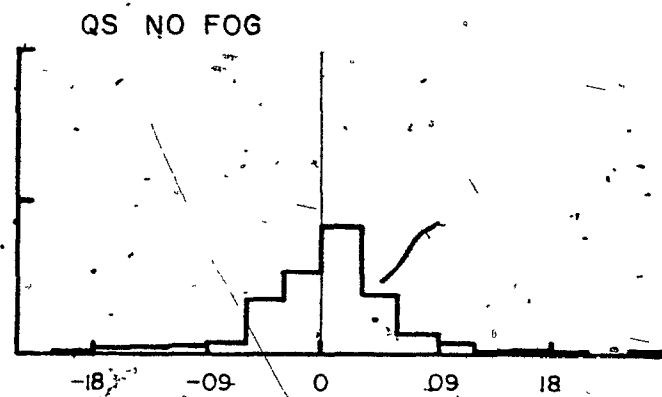
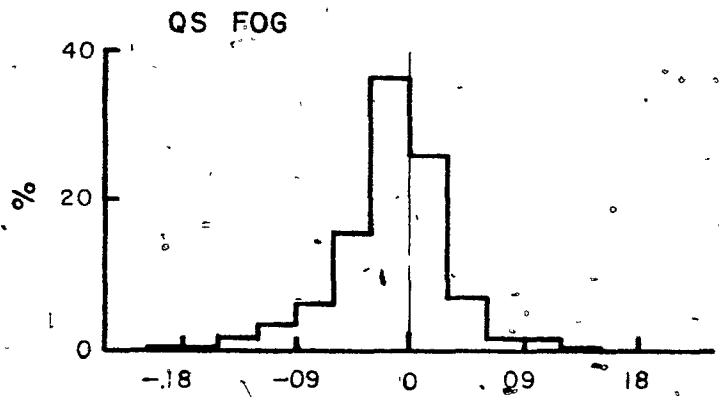
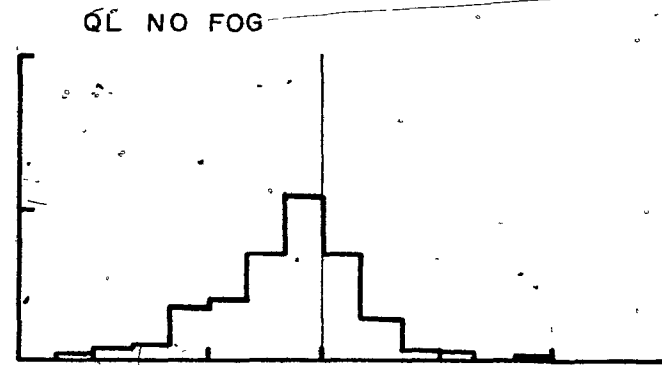
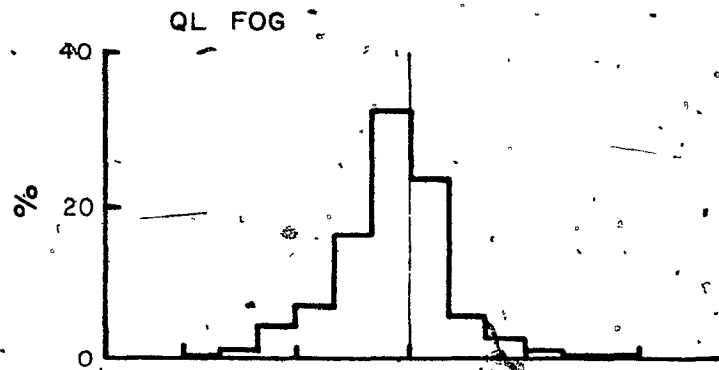


Figure 5: 4. 1b Frequency Distribution of QS and QL

as 20 ly/day. In the following discussions the screen level values have been used as these data are normally available.

5:4.1 Relationship of Sensible to Latent Heat

Figure 5:4.1a shows little relationship between sensible and latent heat fluxes. This is due to the differences in slope of the temperature and humidity profiles already discussed in Section 5:2.2. The frequency distribution of sensible and latent heat for fog and fogless conditions in Figure 5:4.1b exhibit the same tendencies as the slope distributions. Most of the sensible and latent heat values lie between -86 and 86 ly/day.

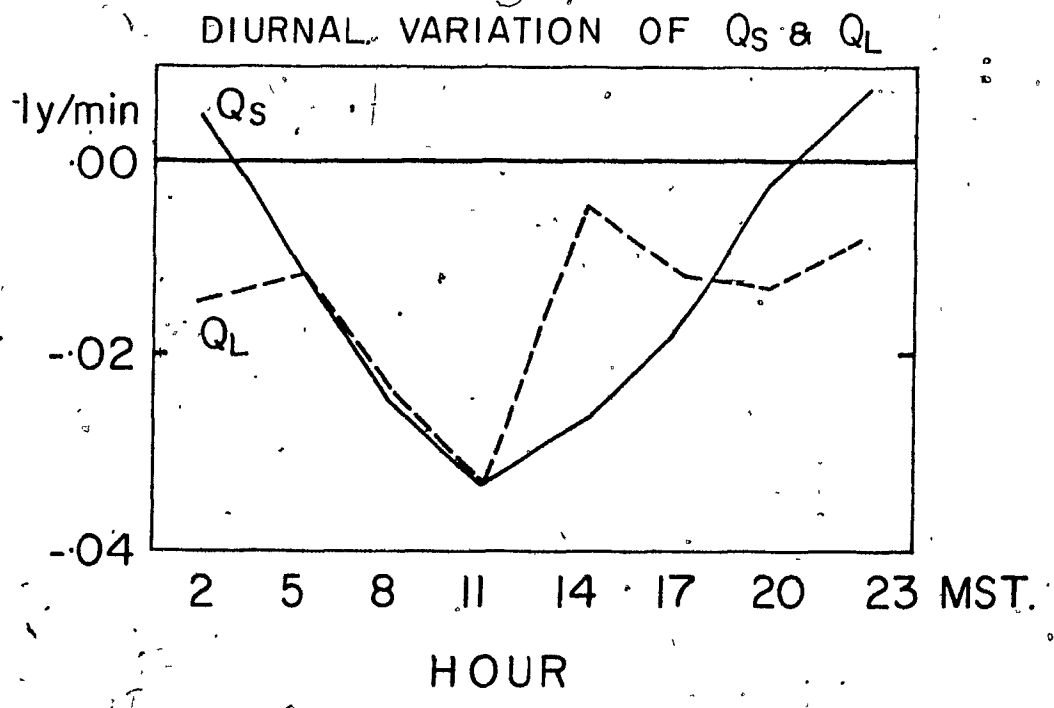


Figure 5:4.2

5:4.2 Diurnal Variation of Sensible and Latent Heat Flux

Figure 5:4.2 shows diurnal averages of sensible and latent heat flux in 1970. Both are most negative at mid-day with only sensible heat averaging slightly positive at night.

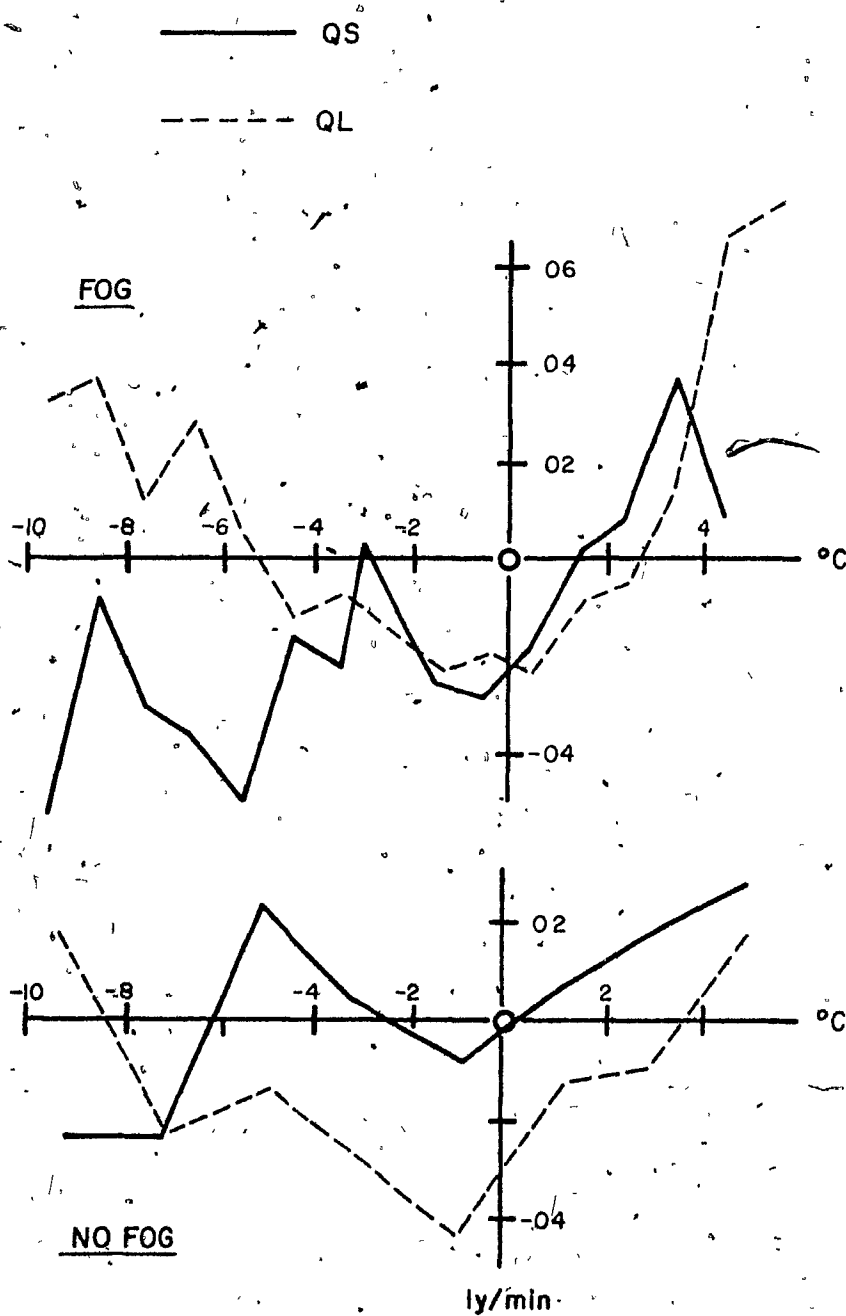


Figure 5: 4.3a Variation of QS and QL with Temperature for Fog and No Fog.

5:4.3 Relationship to Temperature and Wind Direction

The sensible and latent heat fluxes are most strongly negative at temperatures between -2 and 0°C and with northerly winds. Positive values predominate above 3°C and with NE through E winds (see Figure 5:4.3a and b).

In fog the mean values of sensible and latent heat for temperature intervals between -5°C and 3°C are quite similar but the shape of the curves with temperature tend to be opposite. At lower and higher temperatures sensible heat is considerably more negative than latent heat. The wind roses suggest that the cold W'lies which resulted in negative temperature slopes and near positive vapour pressure slopes account for the difference at lower temperatures.

With no fog and temperatures between -6°C and 4°C , latent heat is consistently $.03$ ly/min (40 ly/day) more negative than sensible heat.* At very high temperatures the difference decreases as the humidity slope also becomes positive, possibly reflecting the slightly more moist NE'ly winds. At very low temperatures both fluxes are negative or latent heat becomes positive as the air is almost saturated due to the low temperatures and/or the effect of saturation with respect to ice in the lower levels.

Sensible heat values with fog are generally more negative than fog-less conditions, except perhaps at very low temperatures. Latent heat fluxes are more positive in fog than in no fog, except at near freezing temperatures.

* As Q_S varies from positive to negative while Q_L is consistently negative, the Q_L/Q_S relationship is not constant.

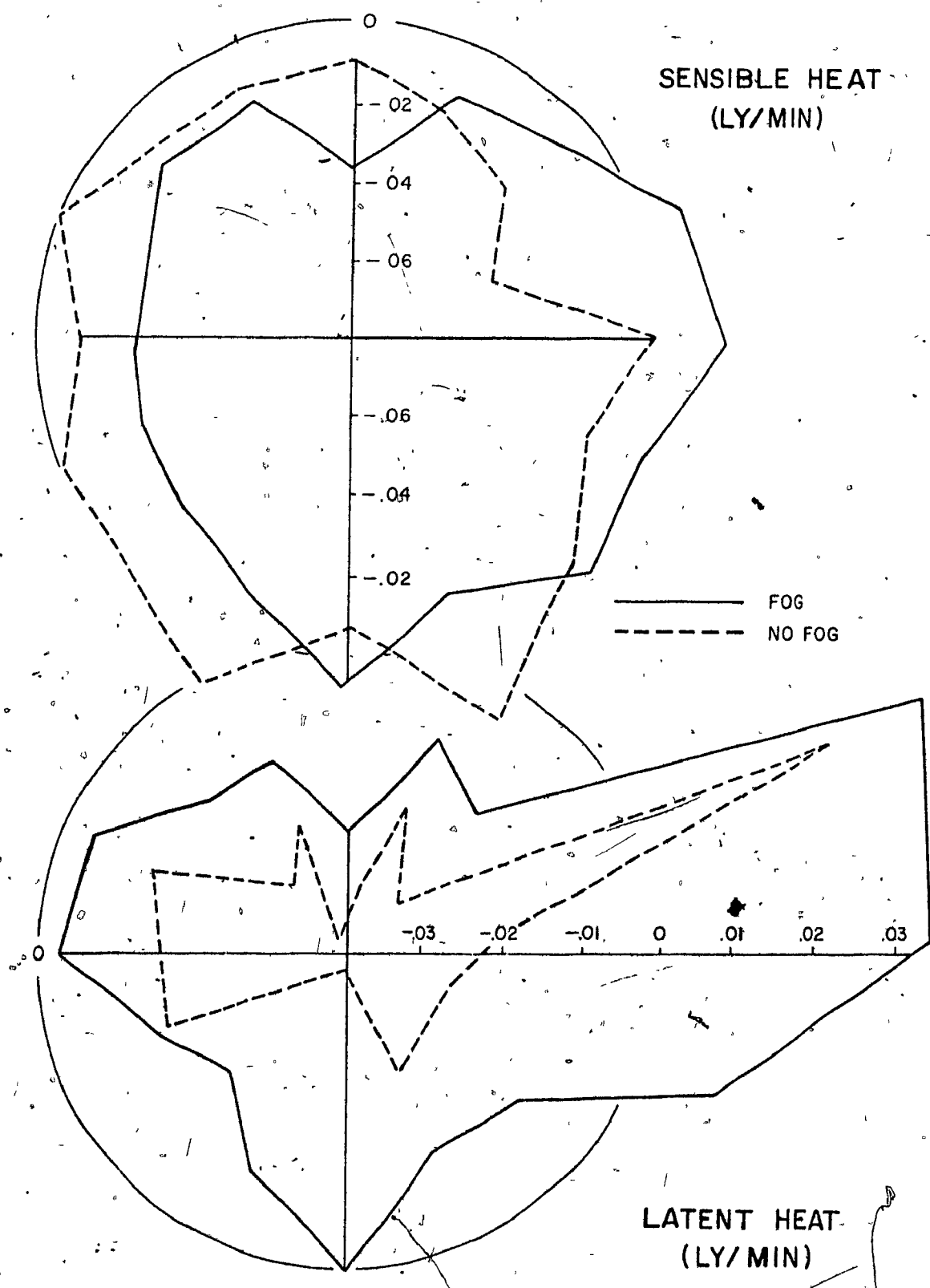


Figure 5: 4.3b Roses of QS and QL

CHAPTER 6

CALCULATED ENERGY BALANCE COMPONENTS

6:1 EBBA

In order to extend the energy balance calculations to cover the six years for which meteorological data is available from Meighen Island, the energy budget programme EBBA (Vowinckel and Orvig, 1972) has been used. The approach of EBBA is to assume "that the surface temperature is unknown, but that all the processes are known" (Vowinckel and Orvig, 1972, p. 5). "An initial estimate of surface temperature is made and all the energy balance terms calculated. From the imbalance in these terms a new surface temperature estimate is arrived at. This process is repeated until the desired degree of accuracy is obtained.

The programme has the following form:

"1) One large umbrella programme, EBBA, determines the main DO loops and decides the sequence in which the major subroutines are called, In addition, it reads in all basic information in the form of tables, and it carries out the necessary summations. Finally, it writes the results.

2) Subordinated to EBBA are the main subroutines which do or instigate the calculations of the different energy budget terms." (Vowinckel and Orvig, 1972, p. 3).

The flexibility of this arrangement allowed EBBA to be adapted to the problem of the surface energy balance of Meighen Ice Cap. For details of the methods and assumptions involved in EBBA reference should be made to "EBBA, An Energy Budget Programme" (Vowinckel and Orvig 1972). Only the modifications made to the programme are

Table 6: 2

Example at Upper Air Sounding Set Up (2300 MST, 7 July 1970)

Press mb	Ht m	Ht m	Temp °C	TD °C	T-TD °C	Level
150	13220		-42.3	-54.0	11.7	1
200					10.0	2.2
250					10.0	2.1
300	8595	1542	-53.2	-64.9	11.7	2
350					10.0	3.3
400					7.9	3.2
450					8.9	3.1
500	5117	869	-27.7	-39.4	11.7	3
550					20.0	4.3
600					14.3	4.2
650					22.5	4.1
700	2610	627	-11.5	-31.7	20.2	4
750					14.3	5.2
800					22.5	5.1
850	1107	501	-6.2	-17.3	11.1	5
875	885	222	-8.8	-16.6	7.8	6
900	663	222	-11.4	-15.9	4.5	1
916	532	131	-10.6	-15.3	4.7	8
930	413	119	-9.9	-14.8	4.9	9
942	313	100	-9.3	-14.3	5.0	10
951	237	76	-8.6	-13.5	4.9	11
958	163	74	-6.1	-9.5	3.4	12
965	96	67	-3.8	-5.9	2.1	13
970	44	52	-2.1	-3.1	1.1	14
975	3	41	-.7	-.9	.2	15
975	.5	2	-.6	-.8	.2	16
975	0	0	-.6	-.8	.2	17

discussed in this chapter. The Meighen Island version of EBBA will henceforth be referred to as MIEBA.

6:2 MIEBA

MIEBA was designed to accept three-hourly surface weather observations (AES card 1), daily climate information (AES card 4) and twelve-hourly upper air data for 50 mb levels (AFS card 5). The upper air observations from Isachsen 300 miles to WSW of Meighen Island were used in the calculations.

The basic calculations were made at three-hour intervals though some terms were evaluated on an hourly basis and others only daily. In the case of 1960 and 1962 where only six-hourly observations were available or in the case of a missing observation, the temperature has been interpolated using daily maximum and minimum temperatures. As diurnal variations are small on Meighen Island in summer due to the lack of solar night and to the ameliorating effect of the ice cap, the sounding has not been interpolated and missing values of elements other than temperature were set equal to the subsequent observations.

Table 6:2 illustrates the set up of the upper air sounding for radiation calculations in MIEBA. The atmospheric layers were concentrated below 850 mb due to the importance of these lower levels to the surface budget and the requirement for only a total atmospheric budget.

Above 900 mb the levels were fixed at constant pressure levels while below 900 mb the layers were a fixed percent of the surface to 900 mb pressure difference.

The four layers of cloud were placed in the sounding on the basis of their reported opacity, amount, height and type, and were extended

upward on the basis of the dew point temperature spread. The method of obtaining the cloud sounding was somewhat modified in MIEBA to account for the particular problems encountered on Meighen Island.

The radiation subroutines were adjusted to accept the MIEBA sounding set up. Calculated and measured clear sky values are compared in Appendix I. The amendments made to the short wave radiation subroutines are discussed in Appendix II.

The short wave surface albedo of the snow pack was calculated using the method developed by Petzold (1972). In this model the snow deteriorates on the basis of the temperature and the number of days since a snow fall of 1 cm or more. This basic albedo is then corrected for cloud amount and solar angle and the effects of rain and rime are incorporated. The basic albedo of the glacier ice was taken to be 50%.

The turbulent fluxes were calculated using equations 5: 3.1 and 5: 3.2 when the screen temperature was less than 2°C and by the EBBA subroutine-VERA (see Vowinckel and Orvig, 1972, p. 37, for details) when screen temperatures were 2°C or greater. The surface roughness for the former method was estimated using albedo (an indication of the state of decay of the surface) along with temperature and wind speed.

The heat flux into the snow or ice was obtained, as in EBBA, from the temperature difference between the surface and the first 10 cm of ice or snow. The temperature in the "ground" was adjusted hourly using the EBBA subroutine GAIA (Vowinckel and Orvig 1972, p. 38). The changes made to GAIA and a comparison of measured and calculated "ground" temperatures can be found in Appendix III.

The surface temperature on an ice cap can not rise above freezing.

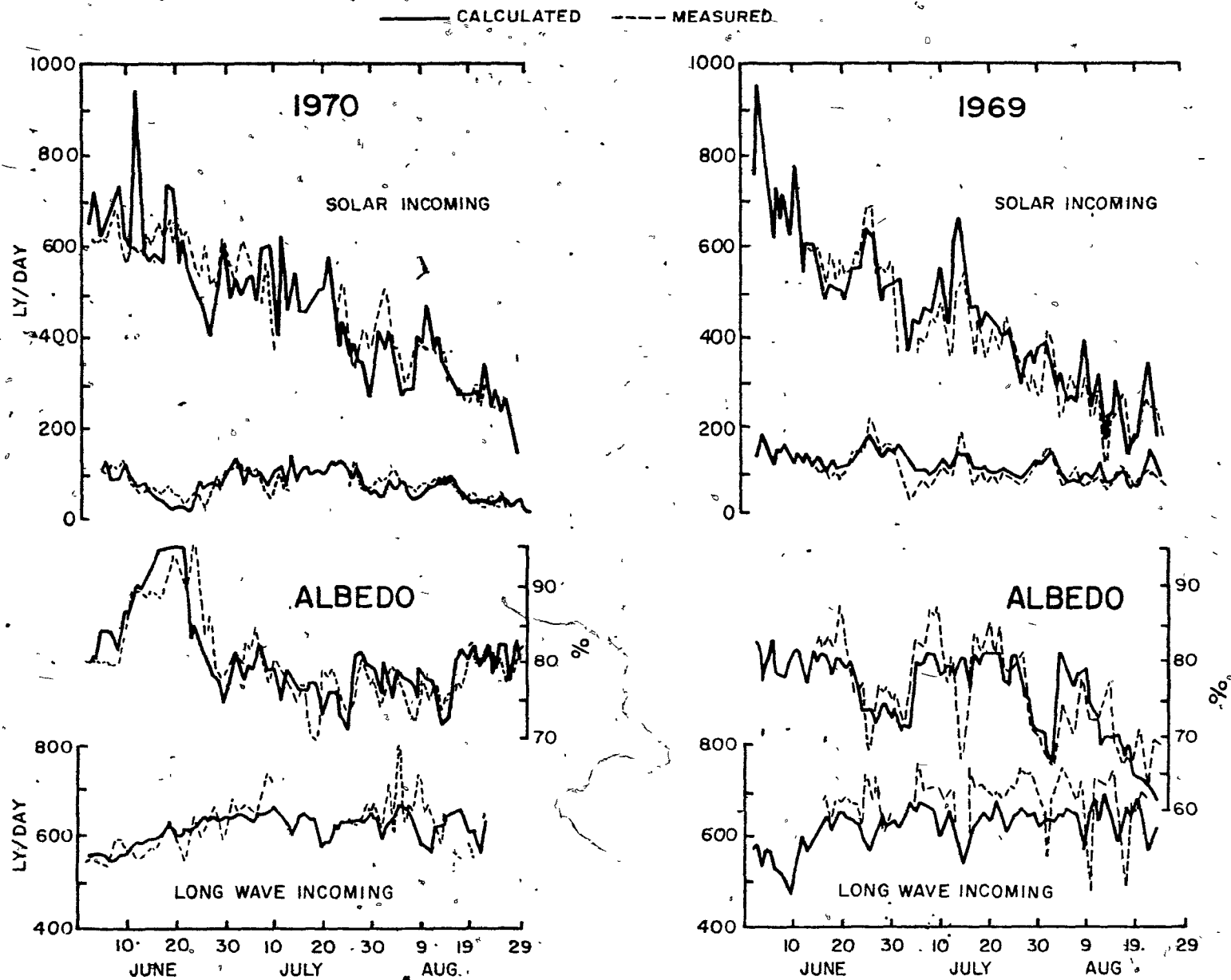


Figure 6: 3 Comparison of Measured and Calculated Radiation Components

If, during the iteration to a balance, the surface temperature reached or exceeded 0°C , the iteration was stopped and the terms recalculated using a surface temperature of 0°C . The imbalance in the energy budget terms was then made available for melting.

6:3 Comparison of Measured and Calculated Radiation Components

The measured and calculated daily totals of incoming short wave radiation, short wave albedo, short wave radiation absorbed at the ground and long wave incoming are plotted in Figure 6:3. The measured values were obtained from continuous records of short and all wave incoming radiation. The "measured" albedo is a combination of measured and calculated values as discussed in 4:5.

Considering the fact that the calculations were made from three-hourly cloud observations there is quite reasonable agreement in the short wave radiation terms.

The long wave radiation curves show greater differences particularly in early August 1970 and during July in 1969. In both cases the calculated values are lower than the measured values. In 1970 the difference is a combination of instrument heating due to clear skies and low wind speeds and of the existence of a stronger low level inversion over Meighen Island than is indicated by the Isachsen upper air sounding. In 1969, though there is the possibility of a calibration problem with the instrument and there was almost constant rain or snow falling during the period, some portion of the difference is probably also a result of underestimating the low level inversion. It appears that the measured values tend to be high due to instrument problems while the calculated values are low as a result of the difference in

the temperatures in the lower troposphere above Isachsen and Meighen Island, the correct values likely lying somewhere between the two curves.

6:4 Errors in Ablation Measurements

The problems of accurate measurement of wasting of snow and ice have been treated in detail by other authors (e. g., Müller and Keeler 1969 and Hubley 1954). On Meighen Island estimates of ablation were obtained from daily measurements of surface lowering. In 1969 and 1970 density measurements were made periodically but were not detailed or frequent enough to produce accurate values of melting.

Probably the most frequent problem in snow melt is the percolation and refreezing of melt water at lower levels in the snow pack or as superimposed ice at the snow-ice interface. The surface in this case lowers considerably faster than mass is lost. The opposite effect is seen when snow or ice melts internally or in holes (due to albedo or density differences) without significant surface lowering. These two effects often combine to produce sudden large surface lowerings which are not a result of melt on that particular day. These differences tend to balance out for longer time periods and are not important when considering the whole melt season.

On Meighen Ice Cap the melt season is not always well defined and the temperature can drop below freezing for hours or days during the melt season. With continual melt and refreezing the snow pack eventually becomes coarse granular slush laced with water puddles and streams. If this does not have a chance to drain off between below freezing periods (as was the case in 1969) slush may remain on the glacier in the liquid or frozen state all summer making accurate ablation

INITIAL AND FINAL SNOW AND ICE PROFILE 1970

1 JUNE

28 AUGUST

EBBA

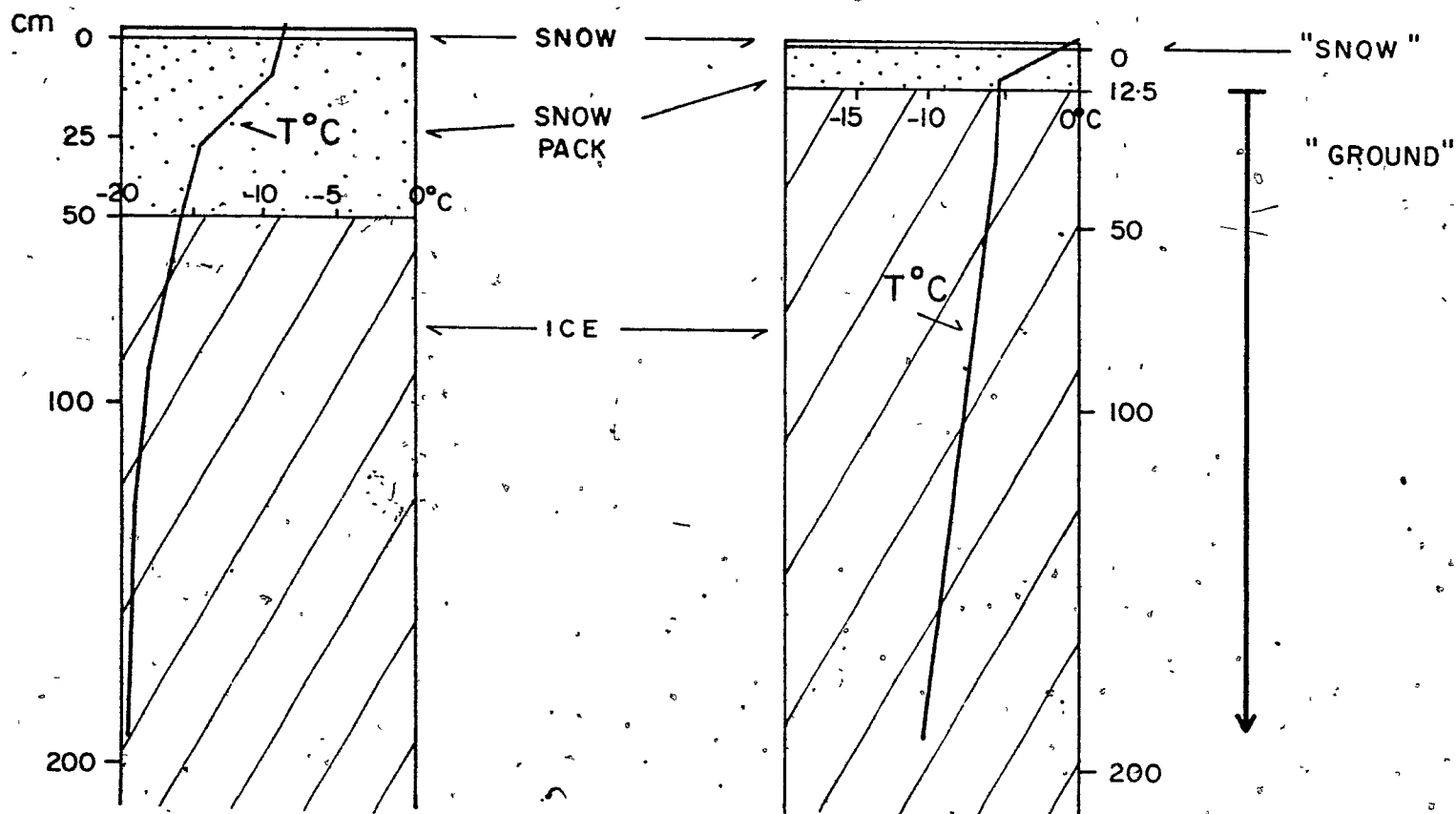


Figure 6: 5

measurements very difficult. This problem is also somewhat alleviated by dealing with longer time periods.

The major difficulty in comparing measured and calculated values of melt on Meighen Ice Cap arises from the fact that significant accumulation can occur during and between melt periods. Snow falling during the summer season is usually accompanied by strong winds in which case the precipitation measured in the rain gauge is almost certainly an underestimate of the real amount. Under these conditions the precipitation can be estimated from the surface lowering measurements but there is no way to measure the ablation which may occur along with or between the precipitation periods. Drifting or blowing snow may also result in a gain or loss in the measuring area which is not representative of the general conditions or which masks concurrent ablation.

The effects of underestimating precipitation and ablation due to high winds and drifting do not balance out over the season and are the most serious problems faced in comparing measured and calculated melt at Main Ice on Meighen Ice Cap over short or long periods.

6:5 Modeling Run Off.

Figure 6:5 shows the initial snow and ice profile for 1970. The winter snow pack was considered to be part of the "ground" in terms of EBBA. This snow pack was assumed to have a density of .32 gm/cc. On 1 June it was assumed that this snow pack was topped by 2 cm of snow having a density of .3 gm/cc. This initial layer and subsequent snow accumulation were treated as snow in terms of EBBA.

If heat was available at the surface for melt the temperature of the first 10 cm of "ground" was brought to 0 deg C and then the snow

was allowed to melt, followed by the snow pack and finally the glacier ice. Melt from the snow was allowed to percolate into the snow pack and was held there available for refreezing until the end of the glaciological day (0630 MST) at which time it became runoff. Similarly melt from the snow pack or glacier ice was available for refreezing until the end of the glaciological day. At the end of each day half the melt water still available was allowed to run off. The remaining half was stored in the snow pack or on the glacier and could be refrozen the following day. Half of this stored melt was allowed to run off each following day, unless refreezing took place. When the stored runoff became less than 1 cm it was all allowed to run off. If the depth of the snow and snow pack was greater than 10 cm or the temperature was below -1°C any rain which fell was also held in the "ground" available for freezing.

If there was runoff from the snow pack or glacier ice the "ground" levels were adjusted so that the first level was still 10 cm. below the surface. If snow pack was still present the conductivity and specific heat profiles were adjusted to account for the relative upward movement of the snow-ice interface. The temperature in the interface layer was adjusted to compensate for the change in heat content due to the change in specific heat.

6:6 Comparison of Measured and Calculated Melt

Daily values of measured and calculated melt for the six years are shown in Figure 6:6. The measured values of ablation were not adjusted for precipitation as the accuracy of the precipitation measurements was too variable. Instead, days on which precipitation or accum-

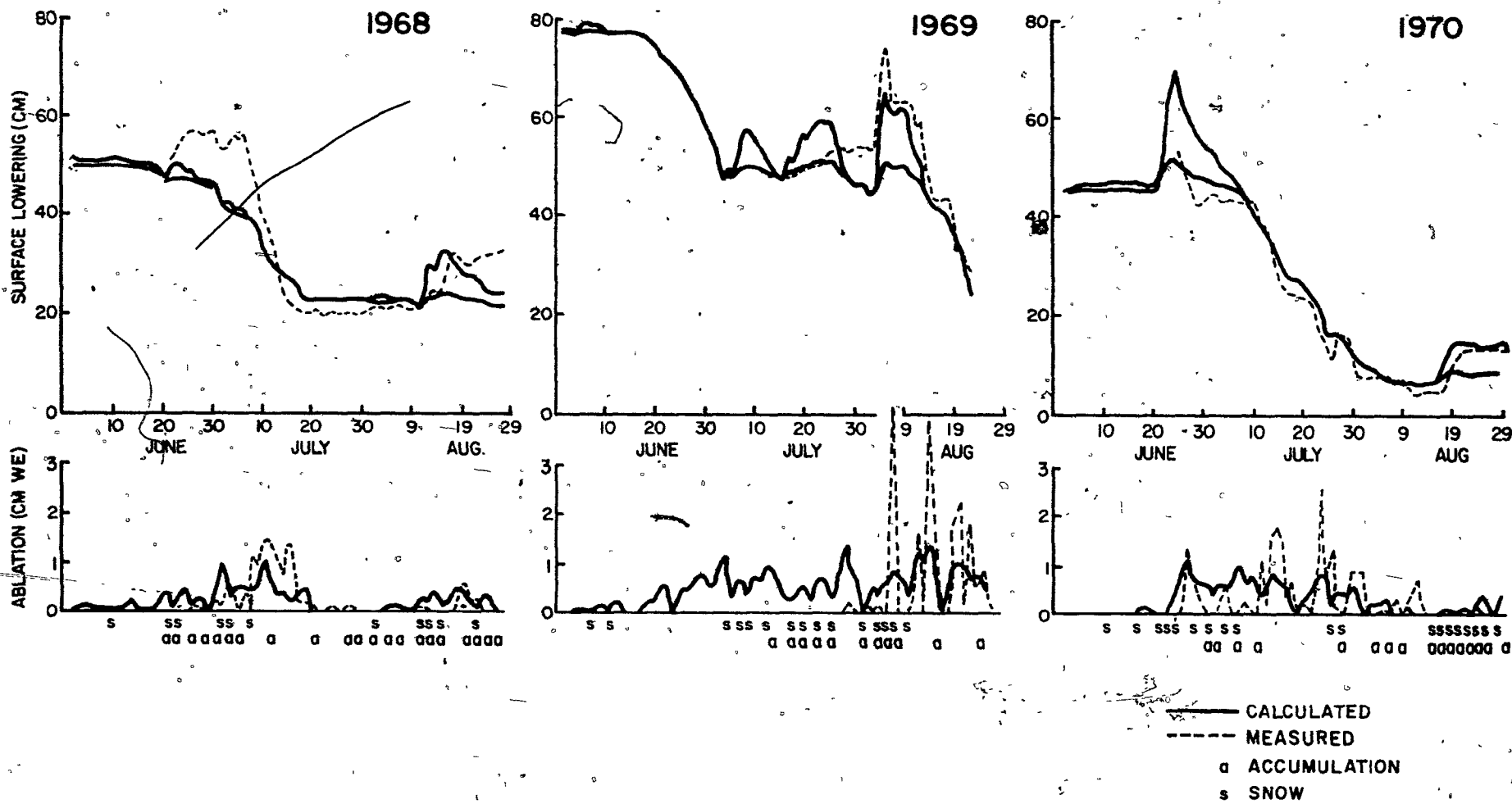


Figure 6: 6 Measured and Calculated Melt

ulation was recorded have been indicated below the plot. During periods of precipitation the calculated level of the surface is given for snow of density .3 gm/cc and for snow of density .1 gm/cc.

As discussed in 6:4 measured values of ablation tend to show much sharper variations than the heat available for melt would indicate, due to percolation refreezing and differential melting. On many occasions when net accumulation was observed the calculated values suggest there was also significant ablation. All the important differences between the measured and calculated values of melt can be explained in terms of the problems involved in measuring total daily melt.

The plots of surface height emphasize the characteristics of the melt regime of the various years.

6: 6.1 1970

In 1970 accumulation in form of hard packed snow dominated in June. The most significant melt took place before the end of July, and by mid-August accumulation in the form of light new snow had taken over. The measured and calculated plots of surface level show good agreement all season.

6: 6.2 1969

Ablation began early in 1969 and by the end of June the surface had lowered more than 20 cm. During July and early August ablation continued, but this was more than compensated by precipitation. In mid-August ablation took over again and over 50 cm of snow pack was lost. The freeze-up did not begin until the last few days in August. Comparison of measured and calculated melt is almost impossible during the mid-season accumulation period due to the difficulties in obtaining representa-

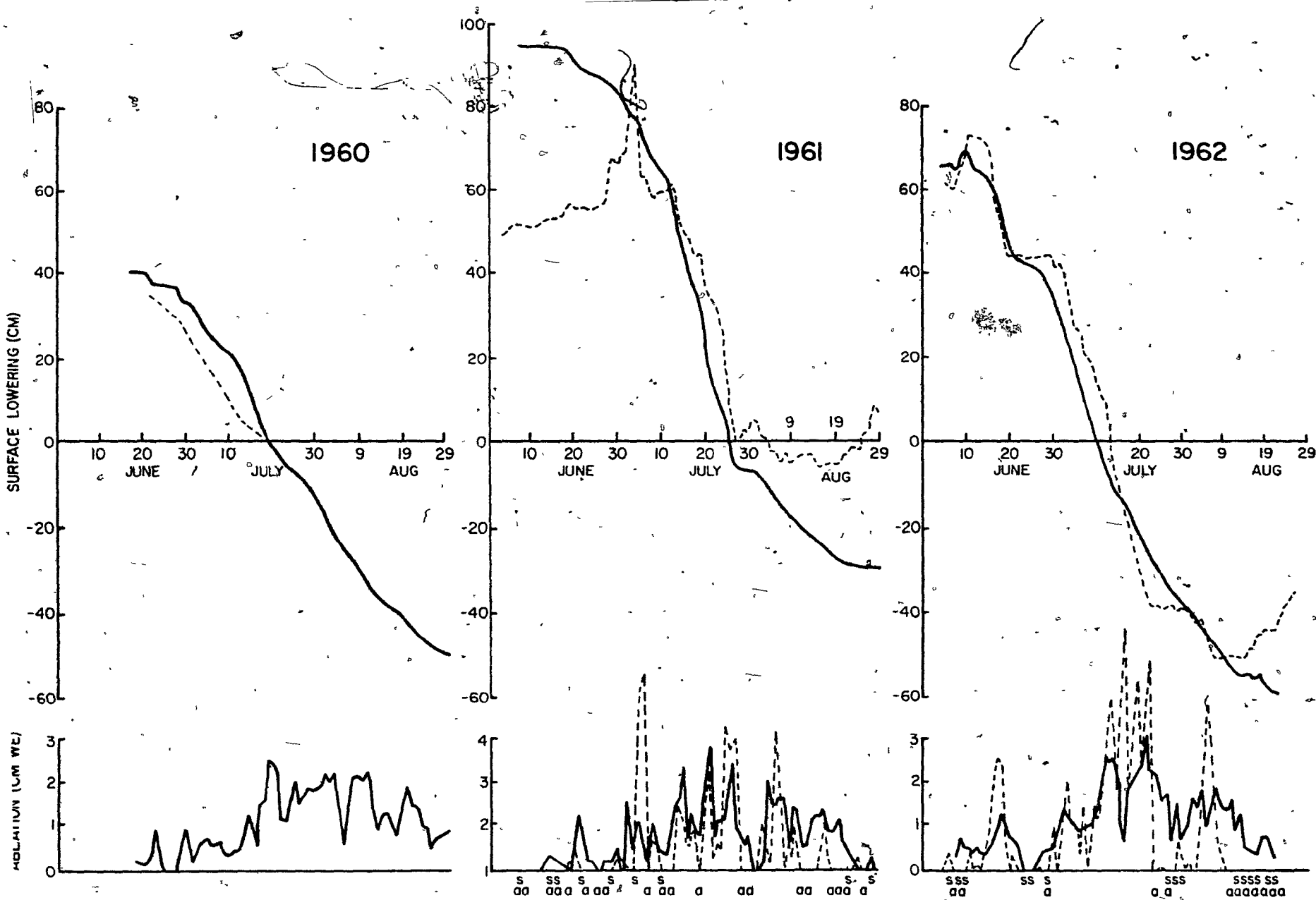


Figure 6: 6 cont'd

tive daily values of total ablation, and to the problems of, percolation and refreezing of melt water in the slush and of the formation of large puddles and slush streams in the sampling area. Once ablation takes over in August there is good agreement between measured and calculated melt.

6: 6.3 1968

A period of measured accumulation in late June did not show up in the precipitation measurements. There was little change in the measured surface level until early July though the calculations indicate melt had begun. During the first 15 days of July the surface lowered sharply as a result of melt which had begun in late June. This was followed by 20 days when both ablation and accumulation were almost zero. In late August melt began again, but accumulation of new snow more than compensated for the loss. Precipitation was considerably underestimated in 1968, but the general characteristics of the measured and calculated curves coincide.

6: 6.4 1962

Melt began early in 1962 and continued throughout the season. Glacier ice was reached in early July. The measured and calculated curves agree well during the melt season. In late August significant accumulations were measured, but these did not show up in the precipitation measurements. During this period, the calculated values of ablation may be too high as the measured precipitation was not sufficient to cover the ice surface in terms of the model, and thus the calculated albedo was quite possibly too low.

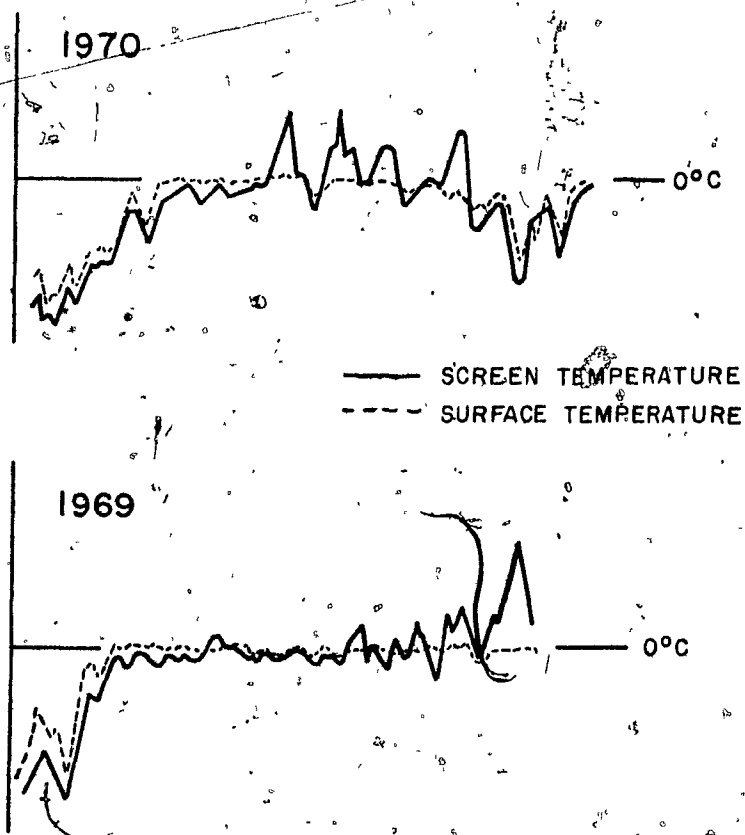


Figure 6: 7 Daily Mean Surface and Screen Temperatures.

6: 6.5 1961

During the middle of the season, when ablation dominates, the measured and calculated surface levels agree well. Glacier ice was reached in late July. Considerable amounts of accumulation were recorded at the beginning and end of the season in 1961, but these were accompanied by unusually strong winds (see Figure 2:4a) and do not show up in the precipitation measurements. As in 1962, the calculated ablation values late in the season may be too high due to an underestimate of surface albedo.

6: 6.6 1960

In 1960 melt began early and continued until the end of August. Glacier ice was reached in mid-July. The weekly measurements of surface lowering show the same slope as the calculated ablation curve. There appears to have been little accumulation during the summer season of 1960.

The calculated values of melt appear to be consistent with the measured ablation for periods when ablation dominates, and in most cases the calculated values are a better estimate of total daily melt than can be obtained from surface lowering and precipitation measurement.

6: 7 Calculated Surface Temperature

Figure 6: 7 of mean daily surface and screen temperature shows that until the screen temperature rises above freezing it is consistently lower than the surface temperature (i.e., there is an inversion in the first meters). The estimates of net long wave radiation made using screen temperature (Chapter 4) will thus always be too positive. In

fact, positive net long wave balances are not very common over the ice cap due to the prevailing unstable fog conditions.

APPENDIX I

Clear sky short and long wave incoming radiation were calculated for the time of the spot measurements of these terms. The calculated clear sky values are compared here with the spot measurements for the few cases of almost clear skies experienced at Main Ice.

Table A: 1

Clear Sky Short and Long Wave Incoming Radiation

Date: Hr	Solar Absorbed		Long Wave Incoming	
	Calculated	Measured	Calculated	Measured
10/8: 14	.570	.577	.365	.435
10/8: 08	.471	.474	.366	.315
10/8: 05	.284	.253	.367	.317
9/8: 20	.200	.205	.359	.376
9/8: 05	.273	.275	.359	.364
20/7: 20	.332	.353	.360	.420

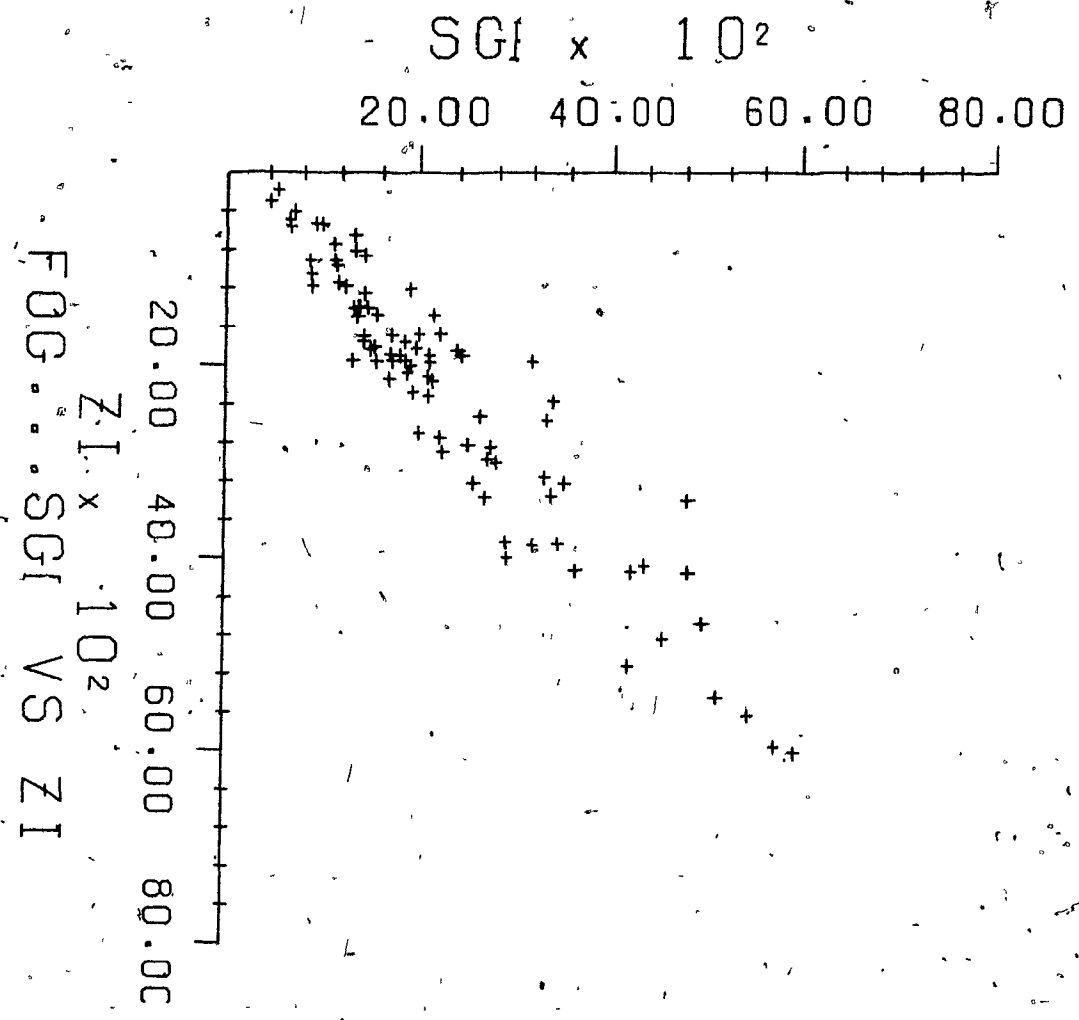
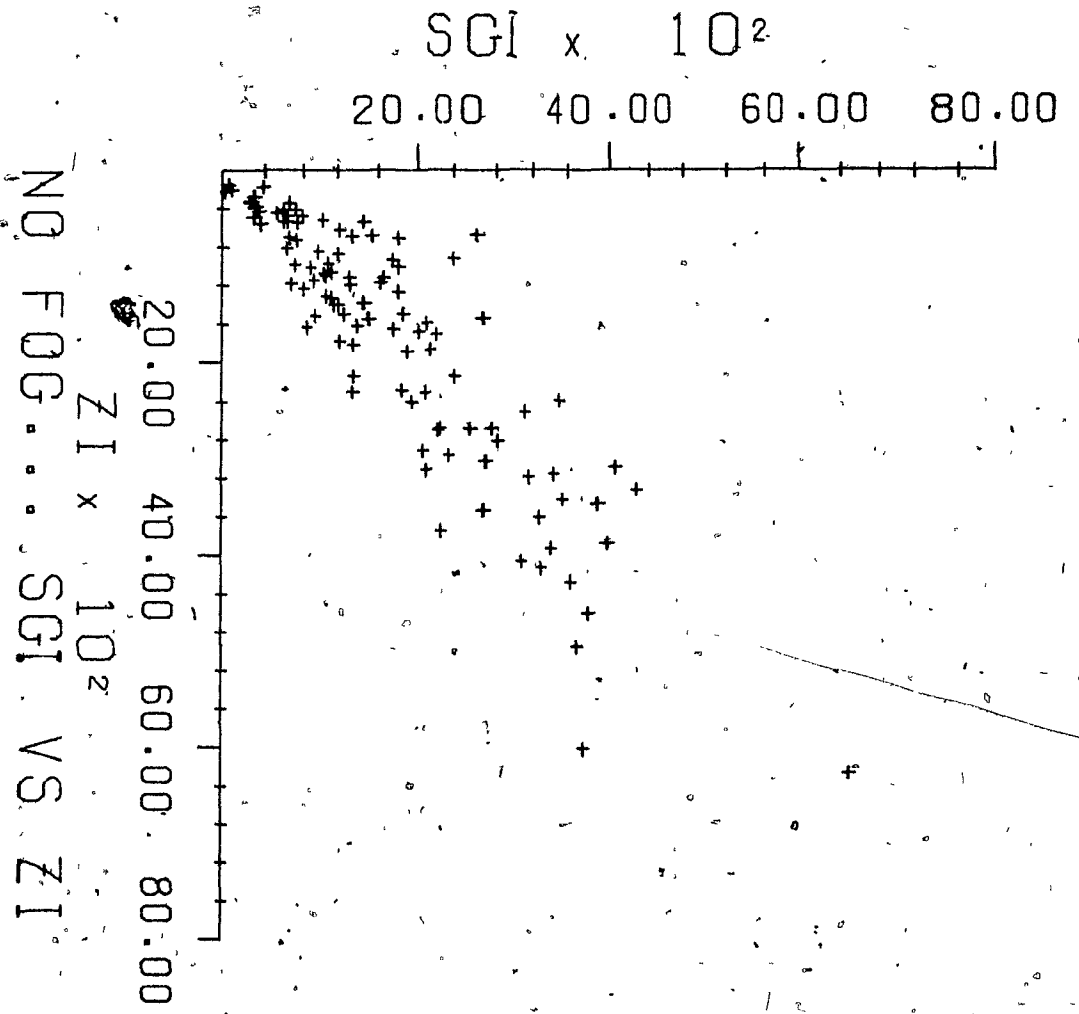


Figure A: 2



APPENDIX II

The formulation for the calculation of cloud top albedo was amended on the basis of Main Ice insolation measurements. For fog the albedo was calculated as a function of screen temperature and solar angle, and for cloud as a function of screen temperature, solar angle, cloud thickness and cloud top temperature. The cloud top albedo was not allowed to become greater than 80% or less than 5%. Calculated and measured values of insolation for overcast skies with fog only and cloud only are compared in the figures.

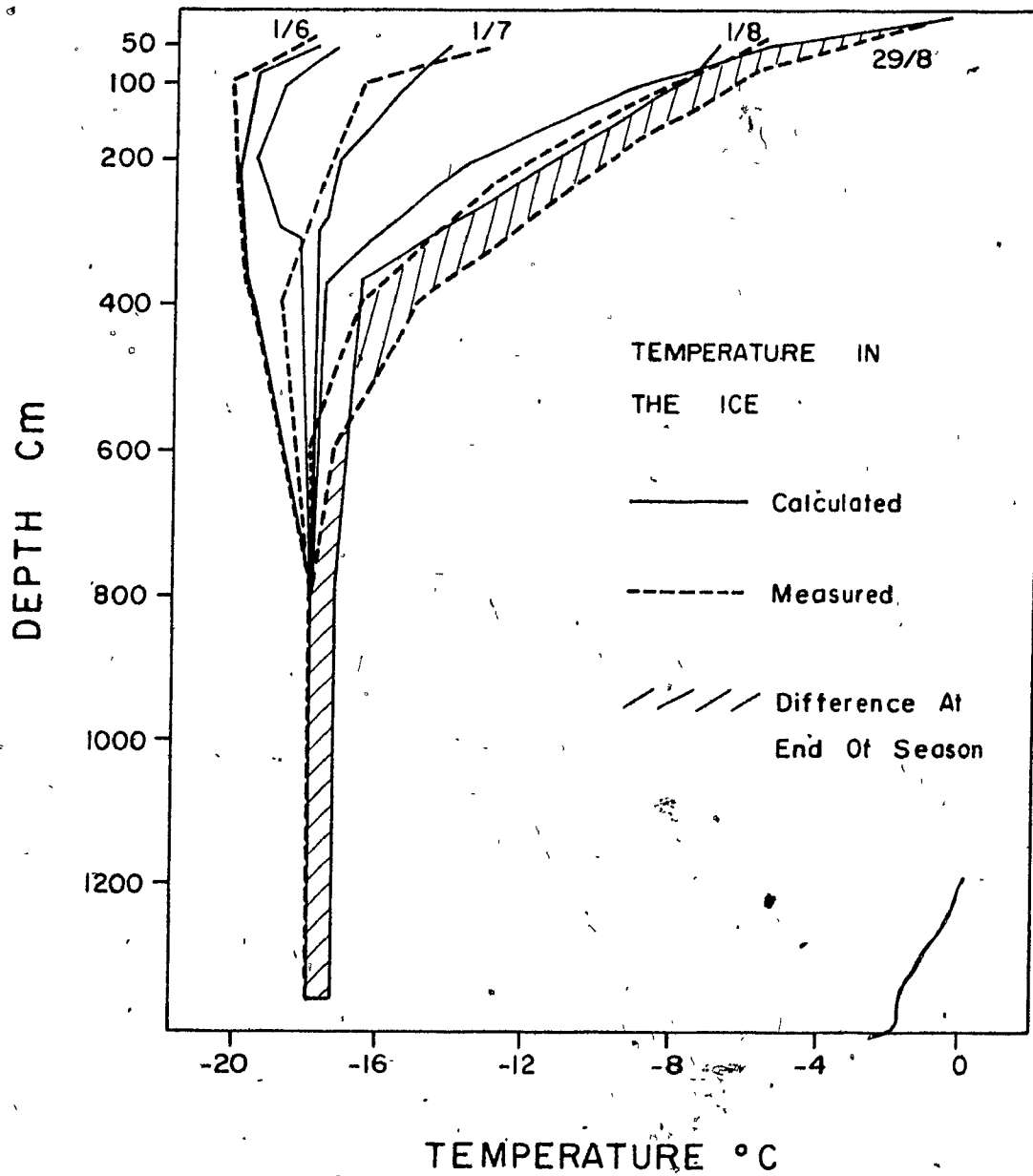


Figure A: 3b

APPENDIX III

The number of "ground" layers was increased from 12 to 20 but this extended calculations only to 400 cm. It can be seen from the ten-day plots of temperature in the ice that the penetration of the annual cycle is at least 800 cm. To compensate for the halving of the penetration depth, the conductivity was also divided by two. The plot of measured and calculated temperature from 1970 shows that the match is not very satisfactory but results in only 129 cal underestimate of the flux into the ground over the whole season. This amounts to 1.4 cal/day and is not very significant in comparison to the other terms.

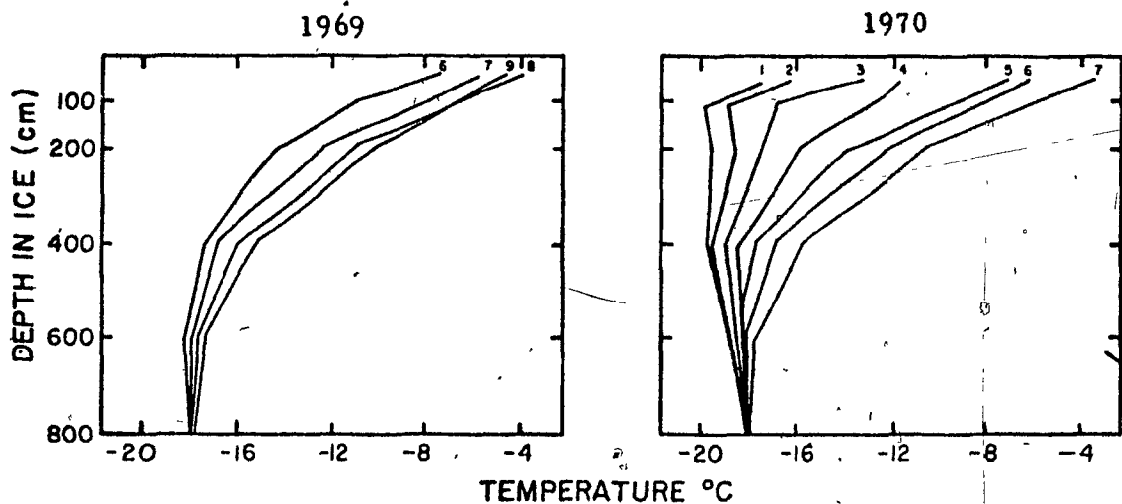


Figure A: 3a Measured Temperatures in the Ice at Ten-Day Intervals (Mi)

REFERENCES

- Adams, W.P., 1966: Ablation and run-off on the White Glacier. Axel Heiberg Island, Canadian Arctic Archipelago. Axel Heiberg Island Research Reports, Glaciology, No. 1, McGill University.
- Ahlmann, H.W., 1935: The Fourteenth of July Glacier. Scientific results of the Norwegian-Swedish Spitsbergen Expedition, 1934. Pt 5. Geogr. Annlr. , Arg. 17, pp 167-218.
- Ahlmann, H.W., 1936: The firn structure on Isachsen's Plateau. Scientific results of the Norwegian-Swedish Spitsbergen Expedition, 1934. Pt 7, Arg. 18, pp 48-73.
- Ahlmann, H.W., 1948: Glaciological research on the North Atlantic Coasts. The Royal Geographical Society, Research Series, No. 1, 83 pp.
- Ahlmann, H.W., and S. Thorarinnsson, 1938: The ablation. Vatnajökull - scientific results of the Swedish-Icelandic investigations 1936-38, Chapter 5. Geogr. Annlr. Arg. 20, pp. 171-233.
- Ambach, W., 1963: Untersuchungen zum energieumsatz in der ablationszone des Grönlandischen Inlandseises. Meddeleser om Grønland, Bd. 174, Nr. 4.
- Andrews, R.H., 1964: Meteorology, No. 1. Meteorology and heat balance of the ablation area, White Glacier, Canadian Arctic Archipelago - summer 1960. Axel Heiberg Island Research Reports, McGill University, Montreal.
- Arnold, K.C. and D.K. MacKay, 1964: Different methods of calculating mean daily temperatures, their effects on degree-day totals in the high arctic and their significance to glaciology. Geogr. Bull., Ottawa, No. 21, pp. 123-129.
- Arnold, K.C., 1965: Aspects of the glaciology of Meighen Island, Northwest Territories, Canada. J. Glaciol., Vol. 5, No. 40.
- Arnold, K.C., 1966: The glaciological maps of Meighen Island N.W.T. Can. J. Earth Sci., Vol. 3, No. 6, Paper No. 19.
- Berlyand, M.E., 1956: Predskaznie- regulirovanie teplavogo rezhima prizemnogo sloya atmosfery (Prediction and Adjustment of the Heat Regime of the Surface Air Layer). - Leningrad, Gidrometeoizdat.
- Brooks, C.E.P. and N. Carruthers, 1953: Handbook of Statistical Methods in Meteorology. Her Majesty's Stationery Office, London. 412 pp.

- Budyko, M.I., 1966: Polar ice and climate; Proceedings of the Symposium on the Arctic Heat Budget and Atmospheric Circulation, The Rand Corporation, Santa Monica, California, RM-5533-NSF, p. 3-22.
- Can. Dept. Transp., Meteorol. Br., 1968: MANOBS, CIR-3450 DBS-30.
- Chizhov, O.P., and V.R. Bazeva, 1970: World Ocean. Problems of Geography, Sci. Publ. Geogr. Soc. U.S.S.R., Volume 84, Moscow, pp. 243-253.
- Dalrymple, P.C., 1961: South Pole Micrometeorology program, 1 Data presentation. Tech. Rep. ES-2, Quartermaster Ras. Center, Natick, Mass.
- Dalrymple, P.C., Lettau, H. and Wollaston, S.H., 1966: South Pole micrometeorology program: Data analysis. Antarctic Research Series, Vol. 9., p. 22.
- Deacon, E.L., 1949: Vertical diffusion in the lowest layers of the atmosphere, Quart. J. Roy. Meteorol. Soc., London Meteorological Office, No. 91.
- Doronin, Yu. P., 1969: Thermal interaction of the atmosphere and the hydrosphere in the Arctic. (Translated from Russian) Israel Program for Scientific Translation, Jerusalem (1970).
- Dunbar, Moira and Greenaway, K.R., 1956: Arctic Canada from the air. Ottawa, Canada. Defence Research Board.
- Fletcher, J.O., 1965: The heat budget of the Arctic Basin and its relation to climate, The Rand Corporation, Santa Monica, California, RM-5793-NSF.
- Goodall, D., 1971: Surface types of Meighen Ice Cap and surrounding land. Unpublished paper for Dept. of Engineering, McGill University.
- Grainger, M.E., and H. Lister, 1965: Wind speed, stability and eddy viscosity over melting ice surfaces. J. Glaciol., Vol. 6, No. 43, p. 101-127.
- Grosval'd and Krenke, A.N., unpublished: Glaciers of Franz Josef Land.
- Hare, F.K. and S. Orvig, 1958: The Arctic circulation, Arctic Meteorology Research Group, Pub. in Meteor, No. 12, McGill University, Montréal.
- Haurwitz, B., 1945: Insolation in relation to cloudiness and cloud density. J. Met., Vol. 2, No. 3, pp. 154-166.

- Havens, J.M., 1964: Meteorology and Heat Balance of the Accumulation Area, McGill Ice Cap. Canadian Arctic Archipelago - Summer 1960. Axel Heiberg Island Research Reports, Meteorology No 2, Montreal, 87 pp.
- Havens, J.M., F. Müller, G.C. Wilmot, 1965: Meteorology, No. 4. Comparative meteorological survey and a short-term heat balance study of the White Glacier, Canadian Arctic Archipelago - summer 1962. Axel Heiberg Island Research Reports, McGill University, Montreal.
- Holmgren, B., 1971: Climate and energy exchange on a sub-polar ice cap in summer: Part A: Physical climatology. Met. Instn. Upps Univ., Meddn Nr 107, pp. 83.
- Holmgren, B., 1971: Climate and energy exchange on a sub-polar ice cap in summer; Part B: Wind- and temperature-field in the low layer on the top plateau of the Ice Cap. Met. Instn. Upps Univ., Meddn. Nr 108, pp. 43.
- Holmgren, B., 1971: Climate and energy exchange on a sub-polar ice cap in summer: Part C: On katabatic winds over the north-west slope of the ice cap. Variations of surface roughness. Met. Instn. Upps Univ, Meddn. Nr 109, Uppsala. 43 pp.
- Holmgren, B., 1971: Climate and energy exchange on a sub-polar ice cap in summer; Part D: On the vertical fluxes of water vapour at Ice Cap Station. Met Instn. Upps Univ, Meddn. Nr 110, pp. 29.
- Holmgren, B., 1971: Climate and energy exchange on a sub-polar ice cap in summer. Part E: Radiation climate. Met. Instn. Upps Univ, Meddn. Nr 111, 111 pp.
- Holmgren, B., 1971: Climate and energy exchange on a sub-polar ice cap in summer; Part F: On the energy exchange of the snow surface at ice cap station. Met. Instn. Upps. Univ, Meddn. Nr 112, Uppsala, 53 pp.
- Hornal, R., 1961: Detailed gravity surveys on Ellef Ringnes and Meighen Islands, Queen Elizabeth Islands, Northwest Territories, 1960. B.Sc. thesis, Queen's University, Kingston, Ontario.
- Hublèy, R.C., 1954: The problem of short period measurements of snow ablation. Journal of Glaciology, Vol. 2, No. 16, p. 437-40.
- Hubley, R.C., 1957: An analysis of surface energy during the ablation season on Lemon Creek Glacier, Alaska. Trans. Am. Geophys. Un, Vol. 38, No. 1, p. 68-85.
- Jackson, C.I., 1969: The summer climate of Tanquary Fiord, N.W.T. Arctic Meteorology Research Group, Pub. in Meteor., No. 95, McGill University, Montreal; 65 pp.

- Keeler, C.M., 1964: Relationship between climate, ablation, and run-off on the Sverdrup Glacier, 1963 Devon Island, N.W.T. Research Paper No. 27, Arctic Institute of North America, Montréal.
- Koerner, R.M., 1968: Fabric Analysis of a core from the Meighen Ice Cap, Northwest Territories, Canada. *J. Glaciol.*, Vol. 7, No. 51.
- Koerner, R.M., 1970: Some observations on superimposition of ice on the Devon Island Ice Cap, N.W.T. Canada. *Geografiska Annaler* 52. A. 1 p. 57-67.
- Koerner, R.M., 1970: Weather and ice observations of the British Trans-Arctic Expedition 1968-9. *Weather*, Vol. 25, No. 5, p. 218-228.
- LaChapelle, E., 1959: Errors in ablation measurements from settlement and sub-surface melting. *J. Glaciol.*, Vol. 3, No. 26, p. 458-67.
- Lister, H., 1962: Heat and mass balance at the surface of Ward Hunt Ice Shelf, 1960. Arctic Institute of North America, Research Paper No 19, 54 pp.
- Lister, H., and P.F. Taylor, 1961: Heat balance and ablation on an arctic glacier. *Meddelelser om Grønland*, Bd. 158, Nr. 7, 55 pp.
- Liljequist, G.H., 1956: Energy exchange of an Antarctic snow field, Part I A: Short-wave radiation. Norwegian-British-Swedish Antarctic Expedition, 1949-52. Scientific Results, Vol. II, Norsk Polarinstitut, Oslo.
- Liljequist, G.H., 1956: Energy exchange of an Antarctic snow field Part I B: Long-wave radiation and radiation balance. Norwegian-British-Swedish Antarctic Expedition, 1949-1952, Scientific Results. Vol. II, Norsk Polarinstitut, Oslo.
- Liljequist, G.H., 1957: Energy exchange of an Antarctic snow field Part I C: Wind structure in the low layer. Norwegian-British-Swedish Antarctic Expedition, 1949-1952. Scientific Results, Vol. II, Norsk Polarinstitut, Oslo.
- Liljequist, G.H., 1957: Energy exchange of an Antarctic snow field Part I D: Surface inversions and turbulent heat transfer. Norwegian-British-Swedish Antarctic Expedition, 1949-52. Scientific Results, Vol. II, Norsk Polarinstitut, Oslo.
- MacKay, D.K. and K.C. Arnold, 1965: Access to Meighen Island, N.W.T., Arctic, Vol. 18, No. 3.
- McKay, G.B. Findlay and H. Thompson, 1969: A climatic perspective of tundra areas. International Union for Conservation of Nature and National Resources, pp. 10-33.

- Maykut, G.A. and N. Untersteiner, 1969: Numerical prediction of the thermodynamic response of Arctic sea ice to environmental changes. The Rand Corporation, Santa Monica, California, RM-6093-PR.
- McVehil, G.E., 1964: Wind and temperature profiles near the ground in stable stratification. *Quart. J. Roy. Meteorol. Soc.*, No. 90: pp. 136-46.
- Monin, A.S. and A.M. Obukhov, 1954: Dimensionless characteristics of turbulence in the surface layer, *Akad. Nauk. SSSR. Geofis. Inst. Turdy* 151, pp. 163-87.
- Müller, F. and N. Roskin-Sharlin, 1967: A high arctic climate study on Axel Heiberg Island, Canadian Arctic Archipelago - Summer 1961. Axel Heiberg Research Reports, Meteorology, No. 3, McGill University, Montreal, 81 pp.
- Müller, F. and C.M. Keeler, 1969: Errors in short-term ablation measurements on melting ice surfaces. *J. Glaciol*, Vol. 8, No. 52, p. 91-105.
- Ommanney, C.S.L., 1969: A study in glacier inventory, the ice masses of Axel Heiberg Island, Canadian Arctic Archipelago. Axel Heiberg Res. Rep. *Glaciol*, No. 3, McGill University, Montreal.
- Orvig, S., 1951: The climate of the ablation period on the Barnes ice cap in 1950. *Geogr. Annlr. Bd.* 33 (3-4).
- Orvig, S., 1954: Glacial meteorological observations on ice caps in Baffin Island. *Geogr. Annlr. Bd.* 36, pp. 197-311.
- Orvig, S., 1970: Climates of the Polar Regions, Elsevier Publishing Company, Amsterdam, 368 pp.
- Panofsky, H.A., 1963: Determination of stress from wind and temperature measurements. *Quart. J. Roy. Meteorol. Soc.* 89: 85-94.
- Paterson, W.S.B., 1967-1971: Polar Continental Shelf Project, Dept. of Energy, Mines and Resources - Mass Balance Studies. Ice.
- Paterson, W.S.B., 1968: A temperature profile through the Meighen Ice Cap, Arctic Canada. *Int. Ass. Sci. Hydrol.*, Publ. No. 79.
- Paterson, W.S.B., 1969: The Meighen Ice Cap, Arctic Canada: accumulation, ablation and flow. *J. Glaciol*, Vol. 8, No. 54, pp. 341-352.
- Petzold, D., 1971: Study of upper winds over Meighen Island. Unpublished term paper, McGill University, Montreal.
- Petzold, D., 1972: A Method of calculating albedo of snow surfaces. Unpublished paper for the Dept. of Geography, McGill University, Montreal.

- Rae, R.W., 1951: Climate of the Canadian Arctic Archipelago, Canada Department of the Environment, Toronto, 90 pp.
- Reed, R.J., and R.K. Surface, 1959: Arctic weather studies: summer season. Dept. of Meteorology and Climatology, University of Washington, Scientific Report, No. 5, 47 pp.
- Reed, R.J., and R.K. Surface, 1959: Arctic circulation studies, Dept. of Meteorology and Climatology, University of Washington, Final Report, 56 pp.
- Rusin, N.P., 1961: Meteorological and radiational regime of Antarctica. (Translated from Russian) Israel Program for Scientific Translations, Jerusalem.
- Savile, D.B.O., 1961: The botany of the northwestern Queen Elizabeth Islands. Can. J. Bot., Vol. 39, No. 4, p. 909-42.
- Savile, D.B.O., 1972: Microclimate and plant growth at Isachsen and Mould Bay. Arctic, Vol. 24, No. 4, pp. 306-307.
- Sellers, W.D., 1965: Physical Climatology. The University of Chicago Press, Chicago, pp. 272.
- Stebelsky, I., 1962: A microclimatological study in the Canadian Arctic. Unpublished B.A. thesis, University of Toronto.
- Stefansson, V., 1939: The problem of Meighen Island. Privately printed for Mr. Joseph Robinson, New York.
- Stefansson, V., 1942: Choosing sites for Arctic Stations. New York.
- Stefansson, V., 1944: The Friendly Arctic. New York.
- Sverdrup, H.U., 1935: The Ablation on Isachsen's Plateau and on Fourteenth of July Glacier in Relation to Radiation and Meteorological Conditions. Geogr Annlr., Arg. 17. pp. 145-66.
- Sverdrup, H. U., 1936: The eddy conductivity of the air over a smooth snow field. Geofys. Publ., Vol. 11, No. 7, pp. 5-49.
- Sverdrup, H.U., 1936: Results of the Meteorological Observations on Isachsen's Plateau. Geogr Annlr, Arg 18, pp. 34-47.
- Thorsteinsson, R., 1961: The history and geology of Meighen Island, Arctic archipelago. Geol. Surv. Can. Bull. 75.
- United States Navy, 1952: Study and Research-Arctic Weather, Task 3, Fourth Quarterly Progress Report.
- Untersteiner, N., 1961: On the mass and heat budget of arctic sea ice, Arch. Meteorol. Geophys. Bioklimatol., A, 12, 151-182, 1961.

- Untersteiner, N., 1966: Calculating the thermal regime and mass budget of sea ice, Proceedings of the Symposium on the Arctic Heat Budget and Atmospheric Circulation, The Rand Corporation, Santa Monica, California, RM-5233-NSF, p. 203-314.
- Vowinckel, E., and S. Orvig, 1962: Relation between solar radiation income and cloud type in the Arctic. J. Appl. Met. Vol. 1, No. 4, pp. 552-559.
- Vowinckel, E., and S. Orvig, 1966: The heat budget over the Arctic Ocean, Arch. Meteorol. Geophys. Biokl. Ser. B, 14, pp. 303-325.
- Vowinckel, E., and S. Orvig, 1967: Climate change over the Polar Ocean. I: The radiation budget. Arch. Met. Geoph. Biokl. Ser. B, 15, pp. 1-23.
- Vowinckel, E., and S. Orvig, 1969: Climate change over the Polar Ocean. II: A Method for Calculating Synoptic Energy Budgets. Arch. Met. Geoph. Biokl., Ser. B, 17, pp. 121-146.
- Vowinckel, E., and S. Orvig, 1969: The energy budget of an Atlantic cyclone. Arch. Meteor. Geophys. Biokl. Ser. B, 17, pp. 147-174.
- Vowinckel, E., and S. Orvig, 1971: Synoptic heat budgets at three polar stations. J. Appl. Met. Vol. 10, No. 3, p. 387-396.
- Vowinckel, E., and S. Orvig, 1972: EBBA- An Energy Budget Programme. Arctic Meteorology Research Group, Pub. in Meteor., No. 105, McGill University, Montreal, 50 pp.
- Wallén, C. C., 1948: Glacial-meteorological investigations on the Karsa glacier in Swedish Lappland 1942-1948. Geogr. Annlr. Arg. 30, Ht. 3-4, pp. 451-672.